A STUDY ON THE APPLICABILITY OF DISTINCT ELEMENT METHOD TO EPS BLOCK FILL

November 1996

by

Toshiyuki Takahara

①

A STUDY ON THE APPLICABILITY

OF DISTINCT ELEMENT METHOD TO EPS BLOCK FILL

November 1996

by

Toshiyuki Takahara

Contents

Contents

Introduction

Introduction

1. General Introduction

Numerical calculation methods are the powerful tools in geotechnical engineering area, because of the nonlinear and irrecoverable mechanical behavior of soils and the complex boundary conditions to be dealt in this area. Out of many numerical methods FEM (Finite Element Method) is the most popular method due to its wide applicability to various types of materials and phenomena; many problems related to geotechnical engineering have been solved with proper modifications to FEM. As FEM was, however, originally developed for continuum bodies, its limitations in analyzing discrete media becomes sometimes severe obstacles for finding reasonable answers; well cracked rocks are typical discrete media and even soils must be dealt as discrete media from microscopic point view. To solve the problems related to discrete media and to grasp the characteristic behavior of soil and soil structures, some numerical calculation methods were recently proposed, and DEM (Distinct Element Method) is one of these methods. DEM was proposed by Cundall originally for failure behavior of rock and deformation behavior of granular materials, and the applicability of DEM is being proved in many branches in geomechanics as well as in engineering.

Reinforced soil and light weight fill are new trends in geotechnical engineering in Japan, and many promising construction methods which are based on the developments of new materials and new concepts. The EPS (Expanded Poly-Styrole) fill construction method is one of the popular construction methods of light weight fill, where fills are constructed by stacking up the light weight EPS blocks whose density is only a few hundredths of water. This method is used for embankments on soft ground and backfills of bridge abutments, and effective on the reduction of self weight of the fills and the suppression of earth pressure on retaining structures. As well as the other methods EPS construction method was not founded on the sound mechanical concepts; the mechanical behaviors of

assemblies of EPS is not fully investigated. Stress propagation and deformation properties of EPS block fill are still not well clarified. The EPS block fill may be considered to behave as a continuum in a certain condition, and the fill is usually modeled and analyzed as a continuum media. Actually constituent EPS blocks seem, however, to possess sufficient freedom and behave as individual units when the fill is subjected to external agencies; not only the mechanical properties of individual EPS blocks but also the interactions between the blocks such as contact, separations and slips at the interfaces between blocks will play an important role. For establishment of rational design specification of EPS block structures, their intrinsic mechanical behaviors such as load-deformation behaviors and vibration behaviors, must be understood.

The aim of the present study is to clarify the applicability of Distinct Element Method to static and dynamic problems in geotechnical area. EPS block fill was selected as a typical discrete materials, and its mechanical behaviors were examined in several series of laboratory model tests including shaking table tests. The following mechanical behaviors of EPS fills with different internal structures were focused:

- Load propagation properties and stress concentration properties
- Deformation properties
- Vibration properties

In the discussion on the observed mechanical behaviors, the following factors were considered and their effects on the above listed mechanical behaviors were carefully investigated:

- Internal structures formed with the shape of EPS blocks and their arrangement
- Distortion of internal structures induced by differential settlement of foundation
- Fasteners which arranged at interfaces between EPS blocks
- Surcharge which changes mechanical properties of interfaces

The applicability of DEM to the quantitative simulation of discrete body was evaluated with comparisons with FEM and other linear elastic models.

2. Brief review of Previous Studies

2.1. Distinct Element Method

Cundall (1971) originally proposed DEM for the collapse of rock mass, and Cundall and Strack (1979) extended the DEM to the microscopic behavior of granular materials, where discs or spheres were incorporated and the applicability of DEM to granular materials was investigated by comparing the calculation results with experimental results of photoelastic model. In the framework of this type of DEM dynamic behaviors of the discrete bodies were dealt, and explicit numerical scheme with central difference scheme was used for numerical calculations.

Granular element method, one kind of DEM, was proposed by Kishino (1989), where quasi-static deformation behaviors of granular materials were focuses. In this method an iterative process was employed, where the calculation of the contact stiffness matrices and the cancellation of the applied force vectors were employed to derive the static equilibrium state. In original DEM dealing with dynamic problems and even quasi-static problems, the damping components must be considered; on the other hand, in the concept of granular element method, acceleration and velocity components were neglected.

Miura (1993) investigated efficiency of calculation schemes in DEM on dynamic and static problems. And it was suggested that in DEM analysis for static problems static calculation schemes in which acceleration and velocity components were neglected are effective compared with the dynamic calculation scheme, and either of two types of calculation routines should be employed depending the amount of unbalanced resultant forces; in a routine local stiffness matrix for each distinct element is solved in turn,

and in another routine global stiffness matrix for whole assembly system is solved.

In the present study, both static and dynamic DEM were prepared and used for calculations of static and dynamic behaviors, respectively.

2.2. Static Behavior of EPS Block Structures

A series of prototype loading tests was carried out by EPS Construction method Development Organization (EDO, 1989), as a result they showed the efficiency of concrete slab overlying the EPS fill on dispersion of the applied load. The laboratory of Hokkaido Development Bureau (1995) investigated the load propagation properties of EPS fill with high stiffness EPS blocks (XPS), where the effectiveness of concrete slab and the high stiffness blocks on the dispersion of stress was demonstrated. By their investigations the reduction of earth pressure on retaining structures by using EPS blocks was demonstrated, because EPS block fill can keep their whole formation by themselves. The vertical distribution of stress and strain was simulated by FEM, and it was validated that assembly of EPS blocks can be modeled as a continuum media even under limited condition.

Noto, et al. (1992) investigated the reduction properties of earth pressure on under ground structure in EPS fill. It was found that EPS fill was available for reduction of dead load; however, for active load sometimes the load was propagated directly to the structure through EPS block fill body. In this study the mechanical behavior of EPS block fill was introduced as a typical discrete material.

Although there are some other research works besides those cited in this section, only the analogy of observed behaviors with predicted behaviors was introduced, where stress distribution and some other properties were analyzed with linear elasticity by FEM or Boussinesq's formulae.

2.3. Dynamic Behavior of EPS Block Structures

Goto, et al. (1989) carried out a series of model tests with small EPS

block structures on a shaking table to investigate the seismic stability of EPS fills. As a result it was found that in low frequency, the EPS block structures became unstable against vibrations, as the height of EPS block structures was getting high. And the efficiency of fasteners for stability was confirmed only in high frequency region.

Tamura, et al. (1989) also conducted a series of model tests on a shaking table; test fills of 120 cm in height were shook in various surcharge conditions. They showed that the vibration properties of EPS fill were strongly influenced by the surcharge, because the friction properties were changed by reduction of the amount of gaps between EPS blocks.

Murata, et al. (1989) investigated the resonant property of prototype EPS fill enclosed by precast panel, where the importance of rocking vibration was demonstrated.

Ministry of construction (1993) examined the stability of EPS fill during vibration experimentally and analytically; the simple estimation method of resonant frequency and modification method of finite element were proposed. And the importance of surcharge stress and rocking vibration were suggested.

3. Composition of the Present Thesis

Present thesis consists of 4 parts. The composition of the thesis is as follows:

Part 1. Numerical Analysis Methods

In Part 1 the numerical calculation methods employed in the present study were introduced: Distinct Element Method (DEM) and Finite Element Method (FEM). Two versions of DEM were prepared; one is for static problems such as load propagation and deformation behaviors of EPS block fill, and the other is for dynamic problems such as vibration behavior of EPS block fill. Calculation schemes for both versions are explained in two chapters. Modeling of EPS blocks and fasteners are explained as rigid

bodies with springs at contact points. FEM was also used as a contrast with DEM, however the FEM was for linear elastic body in 2-dimensional, the calculation results by FEM were used to investigate the influence of modeling whether discrete or continuum media. Program codes for both DEM and FEM were prepared and examined by the Author.

Part 2. Static Behavior of EPS Block Fill

Static mechanical behavior of EPS block fill is investigated experimentally and analytically, and the applicability of DEM to static mechanical behavior of the fill is examined in Part 2.

In Chapter 1 load propagation characteristics of model EPS fills with different internal structures are examined; the internal structures are controlled with arrangement of EPS blocks and intentionally induced distortion. Testing apparatus and method for model EPS fills are described and the experimental results are introduced. By examined the observed behaviors, the properties of EPS block fills as a discrete body are revealed. Test results are simulated by DEM and FEM; the calculation results by both numerical methods are comparatively examined and the applicability of DEM is evaluated.

In Chapter 2 the deformation properties of model EPS fills with different internal structures are investigated. Testing method and measuring method of deformed fills with image processing technique aided by computer are introduced. Observed deformation behaviors are examined and the features of EPS block fills as a discrete body are revealed. Test results are simulated also by DEM and FEM; the calculation results by both numerical methods are comparatively examined and the applicability of DEM is evaluated.

In Chapter 3 the load propagation properties of many prototype size models of EPS fill are simulated by DEM; the internal structures of model fills are characterized with aspect ratio of EPS block and vertical joints. By examining the simulation results, the effects of internal structures are reexamined. And based on the discussions, a simple estimation method of load propagation properties is proposed.

In Chapter 4 the EPS fills subjected to differential settlement of foundation are investigated analytically. Characteristic behavior of the EPS fills with distorted their internal structures induced by the differential settlement are simulated by DEM. And the guide lines for the remarkable stress concentration due to differential displacement are presented.

The controllability of load propagation properties in EPS block fill is the subject of Chapter 5. Since the experimental and analytical results obtained in this part show the significant effects of internal structures on load propagation properties, the possibility of load propagation control is investigated experimentally and analytically. As a result of the examination, the possibility of control of load propagation and suppression of stress concentration is presented quantitatively.

Part 3. Dynamic Behavior of EPS Block Fill

Vibration behavior of EPS block fills is investigated experimentally and analytically, and the applicability of DEM to dynamic mechanical behavior of EPS block fill is examined in Part 3.

In Chapter 1 testing apparatuses including shaking table are presented. The preparation method of model fills, the installation method of measuring devices on the models and surcharging method, are shown. Testing programs are presented, where the surcharge, acceleration amplitude and frequency are varied parametrically. Measured behaviors are analyzed with an aid of Fourier analysis method, and the amplification factor are presented as a function of frequencies. As a result of the discussion, the effects of internal structure, surcharge and fastener are examined.

In Chapter 2 the model EPS fills tested in Chapter 1 are analyzed with three elastic models: modified elastic beam model, continuous stratified layer model and stratified layer model with slip element. Based on analytical results by these elastic models, the stiffness variation properties of whole EPS block fill is examined, then the useful ideas for the simulations of vibration behavior by DEM are extracted. Finally the simulation results by DEM are compared with observed vibration behaviors;

the applicability of DEM to dynamic problems is evaluated.

Part 4. Conclusions

In chapter 1 the results of experimental and analytical study on the static behaviors of EPS block fills, which are presented in Part 2 of the present thesis, are summarized. The significant effects of internal structure in EPS block fills on its load propagation and deformation properties are emphasized.

In chapter 2 the results of experimental and analytical study on the vibration behaviors of EPS block fills, which are presented in Chapter 3, are summarized.

Part 1. Numerical Analysis Method

Chapter 1. Distinct Element Method

1.1. Introduction

In the present study, several series of laboratory tests are carried out to make clear the mechanical properties of EPS fill, the laboratory tests can be distinguish by their objectives; only static phenomena are concerned in load propagation tests and deformation tests introduced in Part 2, on the other hand, dynamic behaviors are concerned in the vibration tests introduced in Part 3.

The original DEM was proposed by Cundall (1971) to simulate dynamic behaviors of discontinuous media. On the other hand, the static DEM was proposed by Kishino (1989) and Miura (1991), where acceleration and velocity components of elements are neglected, and the static equilibrium position of the elements are determined by iterative computation scheme. In quasi-static problem such as load propagation test and deformation test, the static DEM was adopted. On the other hand, in dynamic behaviors observed in vibration tests, the dynamic DEM similar to the original was adopted.

As a common part between static and dynamic DEM, quadrilateral elements as well as circular or rectangular elements are incorporated to the both DEM computer codes developed by the Authors, which analyze the discrete objects in 2-dimensional plane condition.

The EPS model fills prepared for load propagation test in Part 2, Chapter 2 are shown in Photos. 1.1 (a), (b) and Figs. 1.1 (a), (b), the corresponded initial arrangements of distinct elements are shown in Figs. 1.2 (a), (b). The black circular targets in Photos-1.1 (a), (b) were set up for the measurement of individual EPS blocks with image processing technique. The shaded blocks in Figs. 1.1 (a), (b) were fixed with adhesive agent, five steel plates of 22 kg each are placed on the surface of the EPS model fills for dead load as shown in Photos-1.1 (a), (b) and Figs 1.1 (a), (b). The fasteners made of steel were used in prototype construction of EPS block fill for ensuring the consistency of whole fill

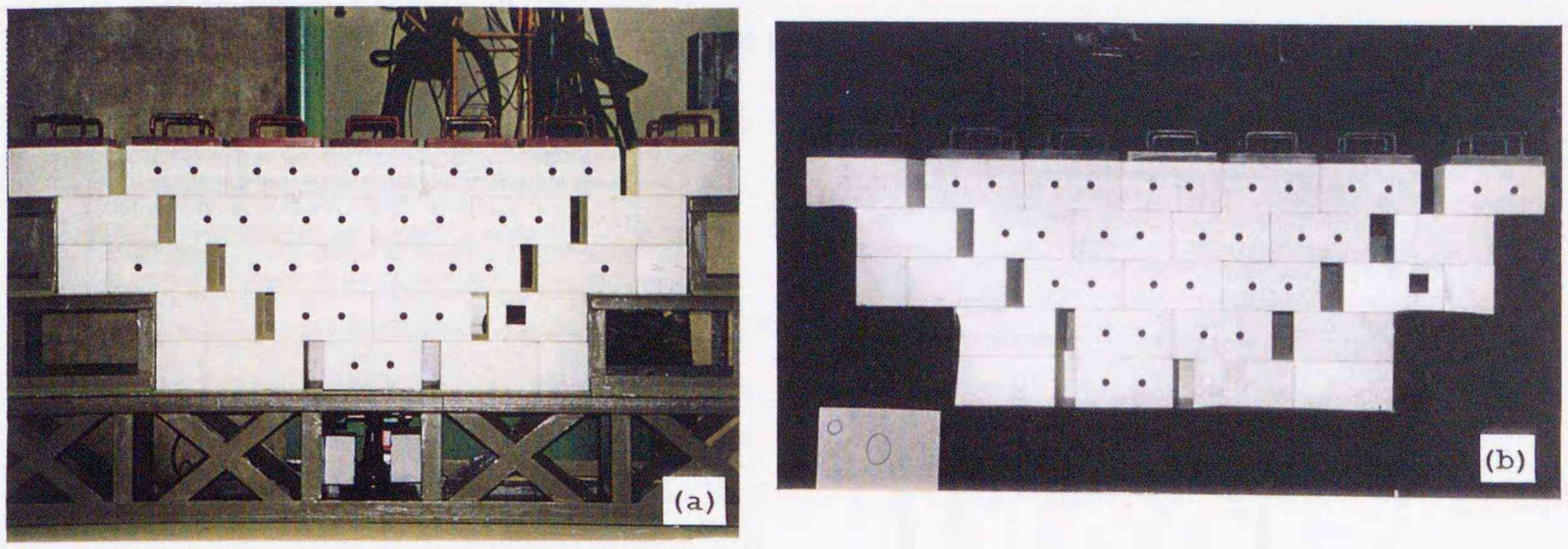

Photos. 1.1 (a), (b). Prepared EPS model fills for load propagation test; (a) symmetrical model fill, (b) asymmetrical model fill.

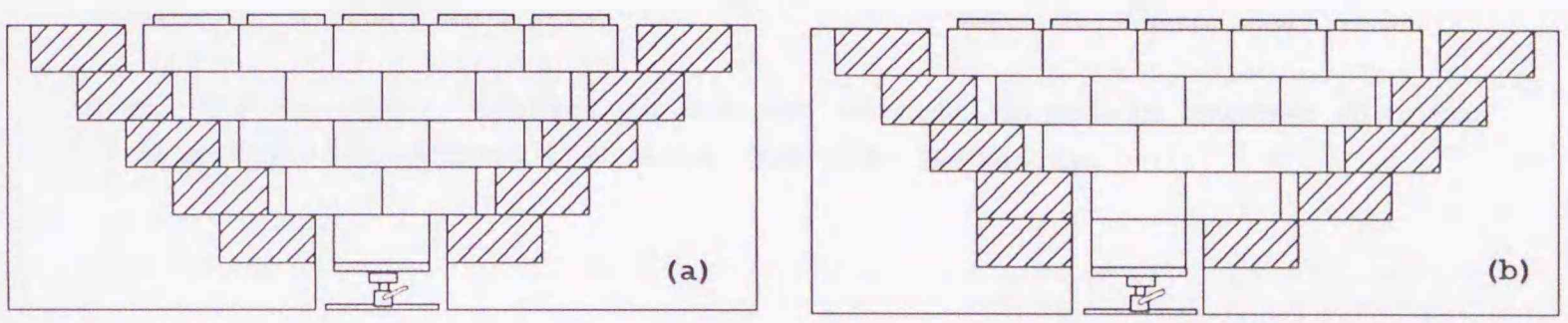

Figs. 1.1 (a), (b). Prepared EPS model fills for load propagation test; (a) symmetrical model fill, (b) asymmetrical model fill.

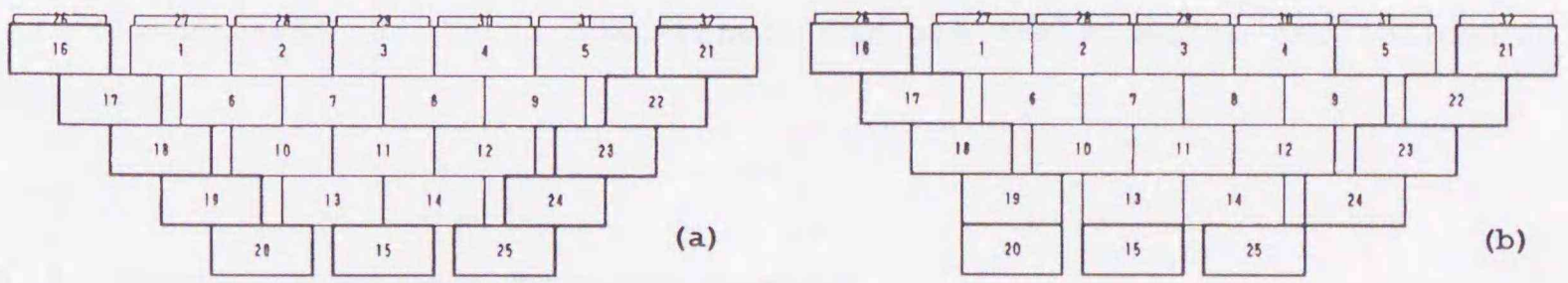

Figs. 1.2 (a), (b). Arrangements of distinct elements; (a) symmetrical model fill, (b) asymmetrical model fill.

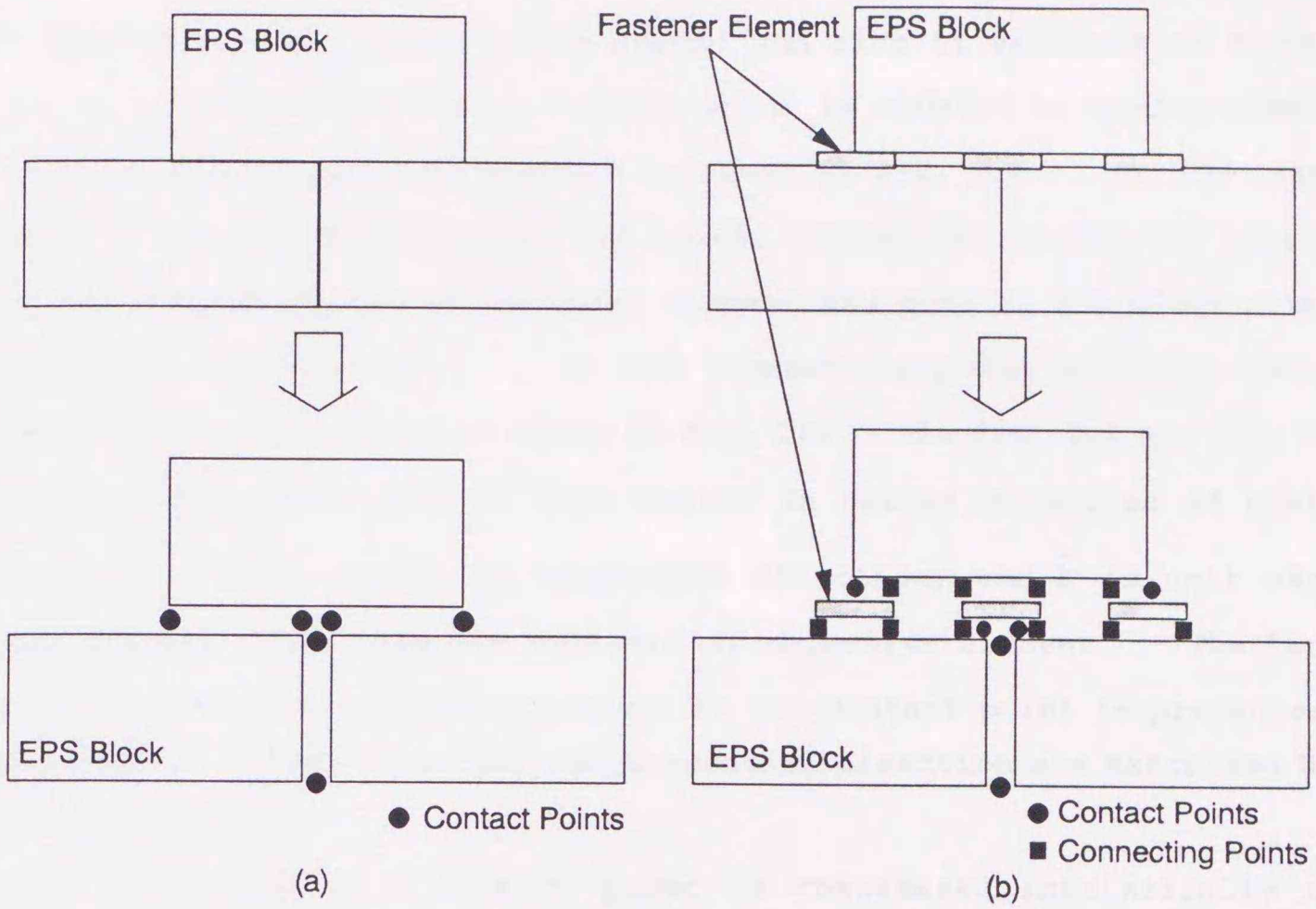

Figs. 1.3 (a),(b). Contact points and connecting points between distinct elements; (a) without fasteners, (b) with fasteners.

during assembling EPS blocks. Fig. 1.3 shows the fastener used in model test.

In the initial arrangements of distinct elements shown in Fig. 1.2 (a) and (b), though the shown arrangements are for the case without fasteners, EPS blocks, loading plates for dead load and fasteners were modeled as rectangular elements.

The details of static and dynamic DEM are explained in the following sections.

1.1. Static Distinct Element Method

1.1.1. Contact Points and Contact Forces

In the framework of static DEM, each of elements is modeled as a rigid body and its deformation is expressed by the overlap and stiffness of springs assigned at contact points. The contact points between EPS blocks

were supposed to generate between corner and side of elements as shown in Fig. 1.3 (a); the mechanism at contact point is modeled by spring element, no-tension element and slip element as shown in Fig. 1.4. In the case of connection between fastener and EPS block, connecting points are supposed to appear between corner of fastener element and side of EPS block element as shown in Fig. 1.3 (b). At the connecting point slippage between elements is not considered as shown in Fig. 1.5. In Fig. 1.4 and Fig. 1.5, the indicated symbol of $\vec{n}$ is unit vector in normal direction of contact surface, $\vec{t}$ is unit vector in tangential direction, and $\vec{e}$ is unit vector toward contact point from the centroid of objective element. The length from the centroid of objective element to the contact point is presented as r, the contact forces in normal and tangential direction are expressed by f_n and f_t respectively.

The mechanism at a contact point is considered intrinsically non-linear as represented by case B in Fig. 1.6; however, as shown in Fig. 1.7, stiffness of spring per unit depth in normal direction k_n was calculated by

$$k_n = \frac{bc}{a} E \tag{1.1.1}$$

where a is height of EPS block, b and c are width and depth of EPS block, respectively. This variable spring coefficient is determined so that rigid body-spring system attains the same deformation as the elastic body, as shown in Fig. 1.7.

From the preliminary parametric calculation, stiffness of spring in tangential direction: k_t was assumed to be $k_n/10$ with regarding the effective convergence during iterative calculation.

1.2.2. Connecting Points with Fasteners

Stiffness of spring for fastener element: k_f is determined from the results of the element tests on the shearing resistance at the interface between fastener and EPS block described in Part 2, Chapter 2. The test device and its results are shown in Figs. 1.8 (a), (b) and Fig. 1.9, respectively; one cubic EPS block is stacked between two confining plates set up two steel fasteners, the EPS element is supported by the two fasten-

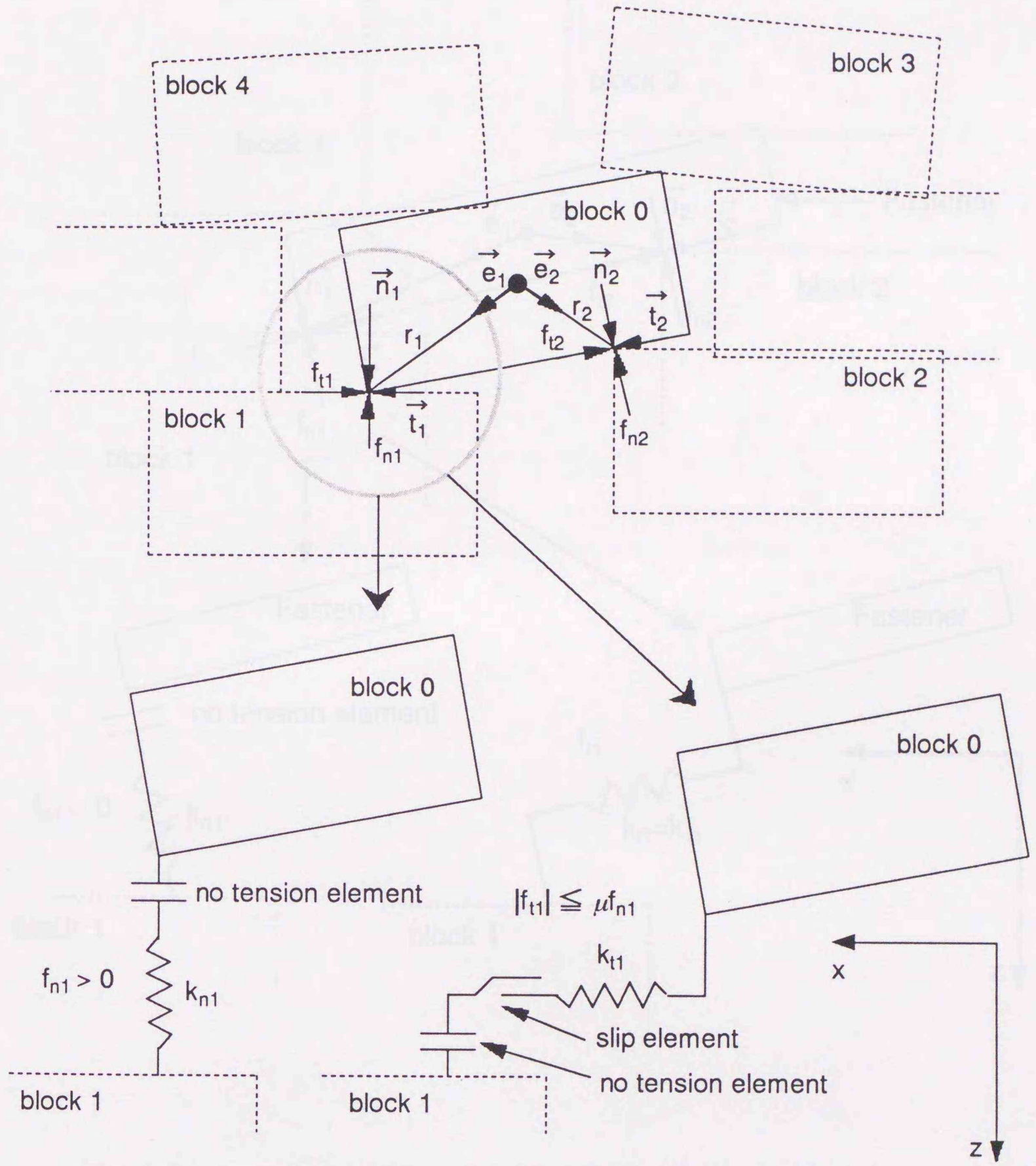

Fig. 1.4. Contact points modeled by springs and no-tension element and slip element.

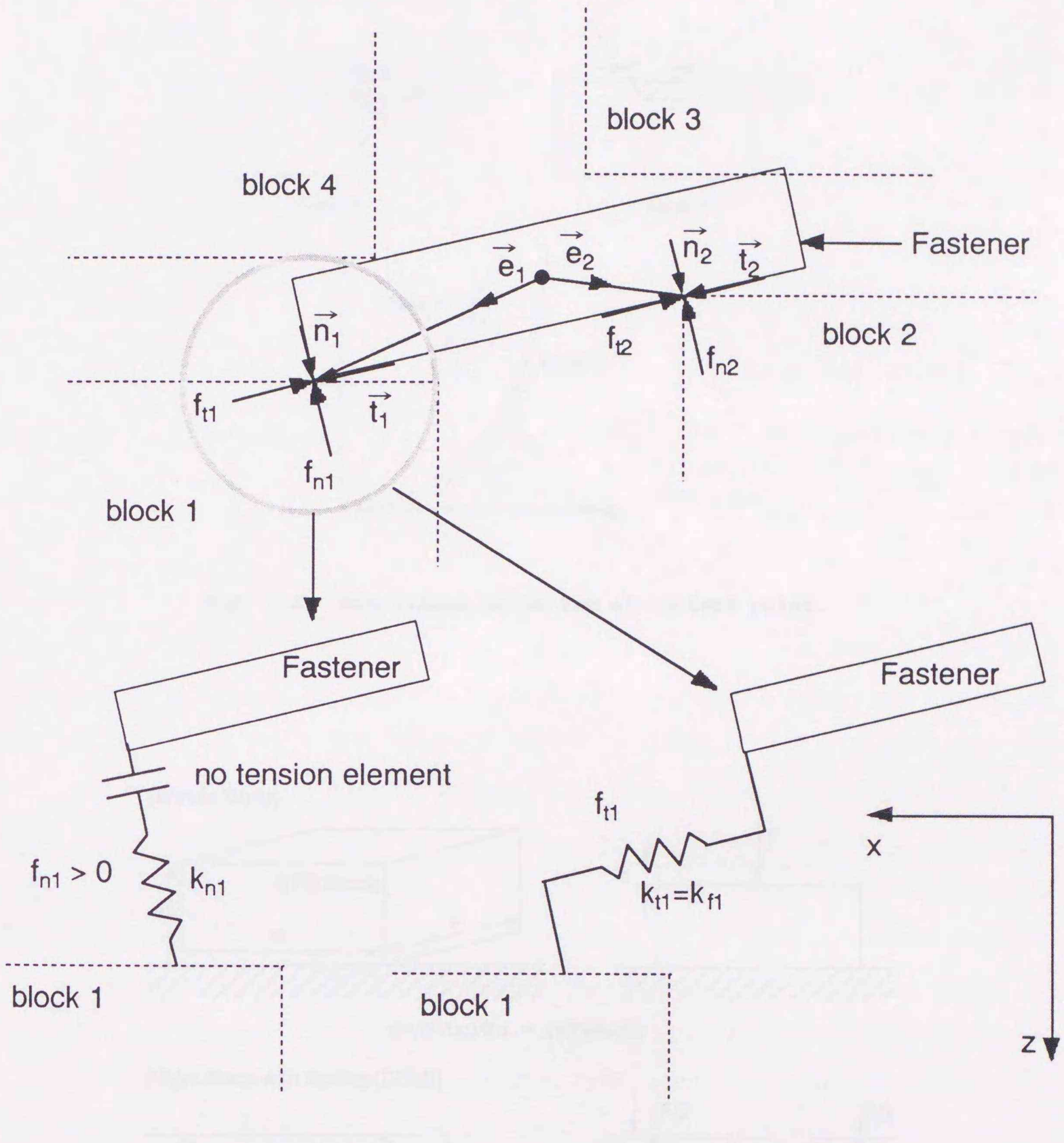

Fig. 1.5. Connecting points modeled by springs and no-tension element.

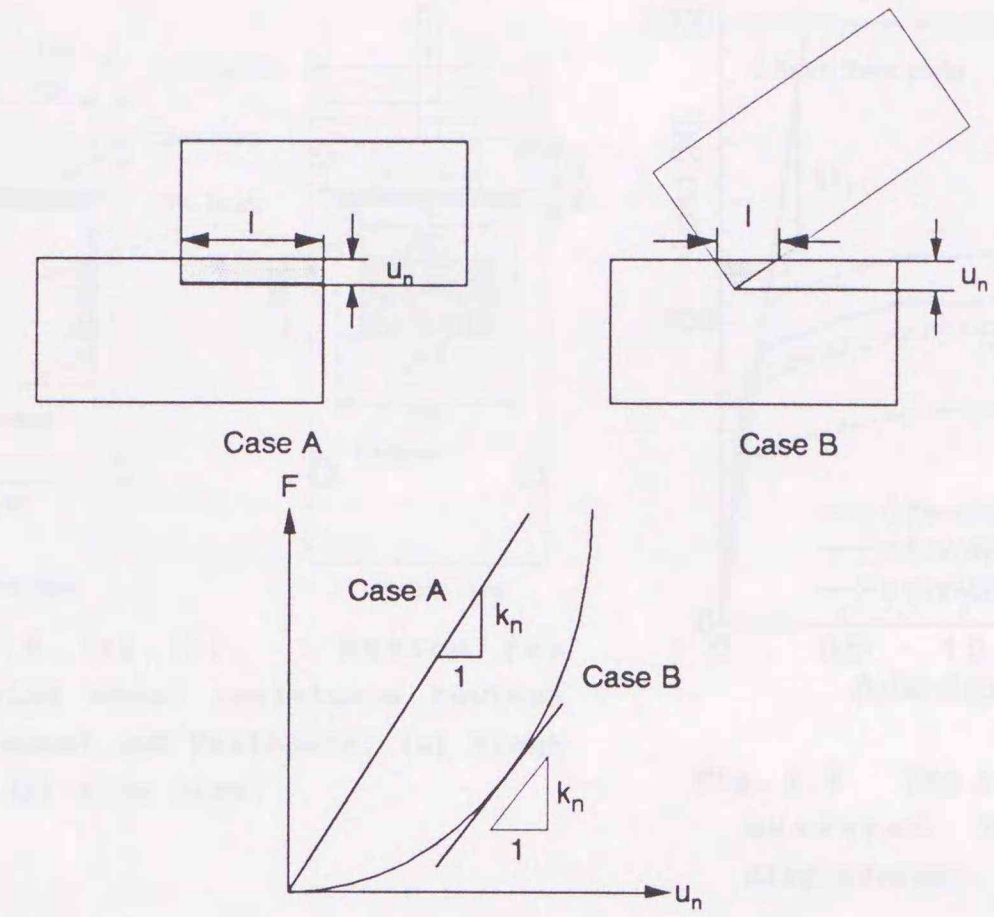

Fig. 1.6. Non-linear mechanism at contact point.

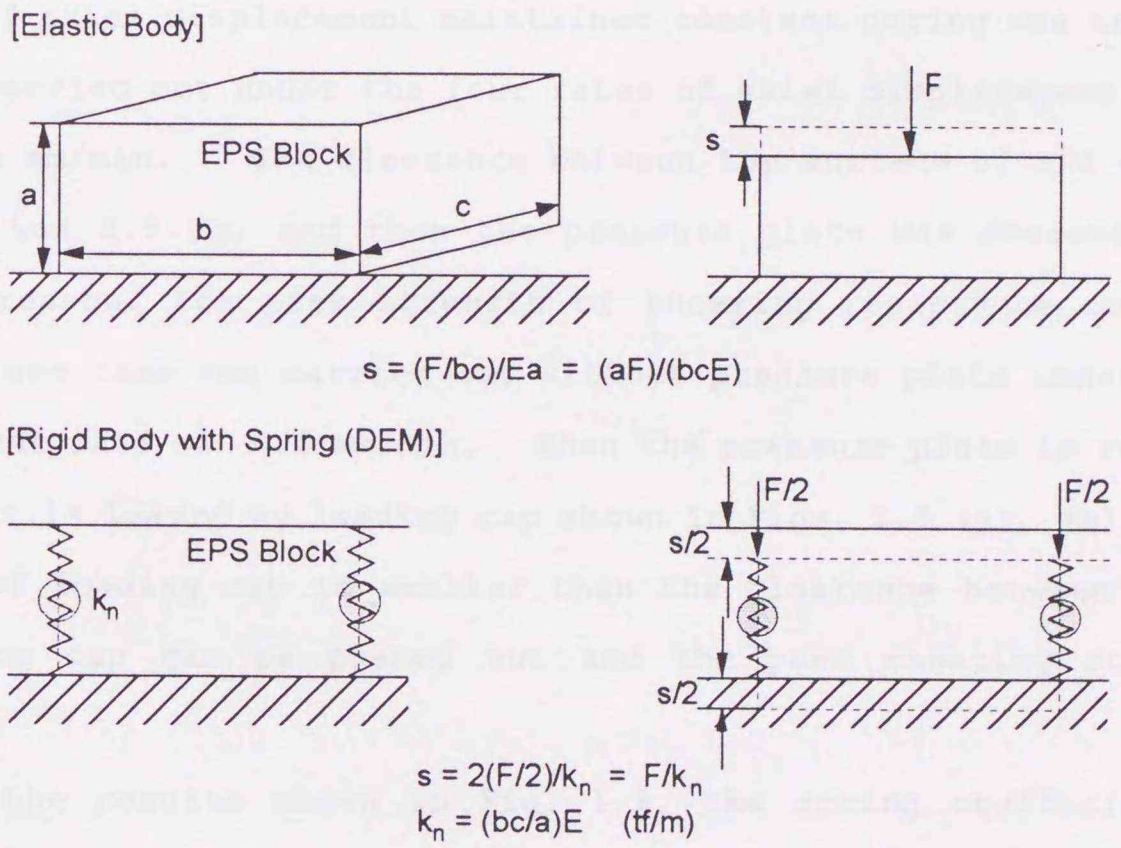

Fig. 1.7. Definition of stiffness of normal spring: k_n.

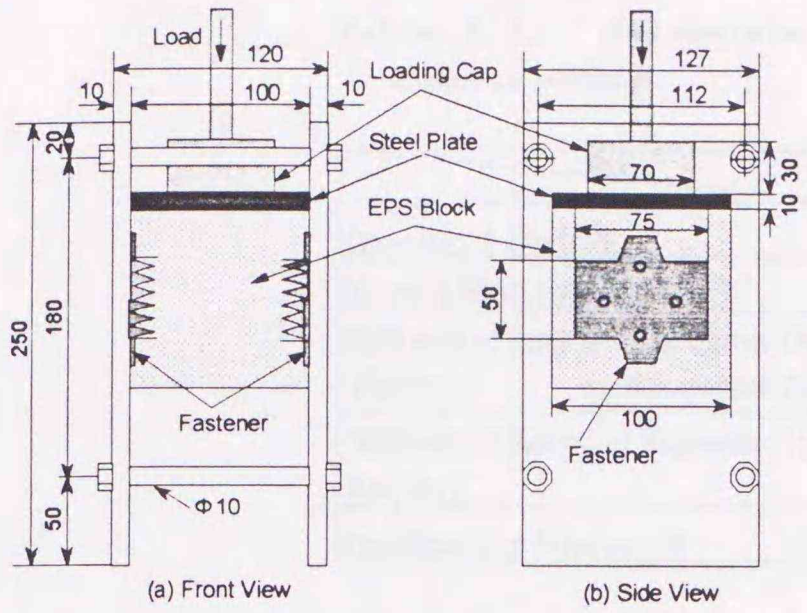

Figs. 1.8 (a),(b). Device for measuring shear resistance bewteen EPS element and Fasteners; (a) front view, (b) side view.

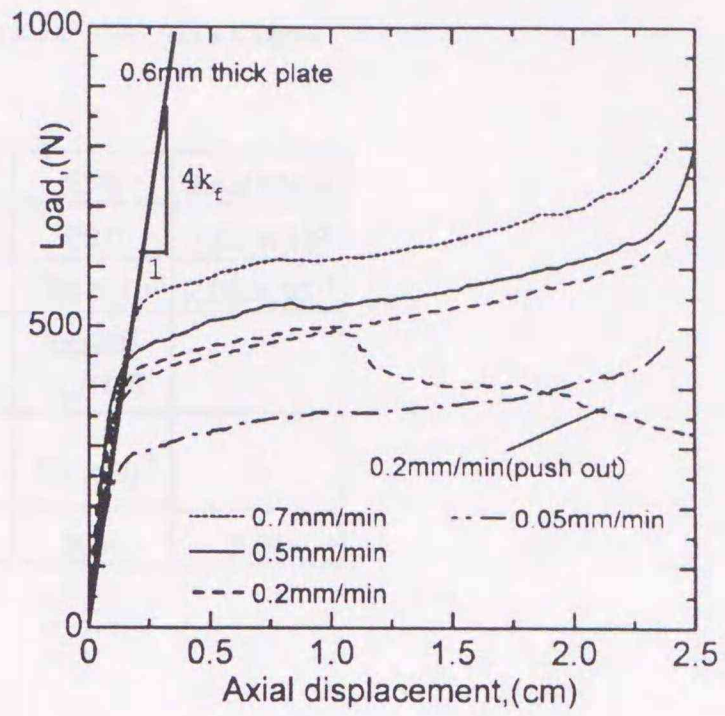

Fig. 1.9. The relationship between measured load and Axial displacement.

ers. The pressure plate shown in Figs. 1.8 (a), (b) was loaded with load cell and attachment in various loading rate and the shearing resistant force was measured. The test condition was plane stress condition, and the rate of axial displacement maintained constant during one test. This test was carried out under the four rates of axial displacement: 0.7, 0.5, 0.2, 0.005 mm/min. The clearance between top surface of EPS element and fasteners was 2.5 cm, and then the pressure plate was descended 2.5 cm. For this reason, the peek strength of shearing resistance could not be obtained; one case was carried out without pressure plate under the axial displacement rate of 0.2 mm/min. When the pressure plate is removed, the EPS element is loaded by loading cap shown in Figs. 1.8 (a), (b); since the diameter of loading cap is smaller than the clearance between fasteners, the loading cap can be pushed out and the peek shearing strength was measured.

From the results shown in Fig. 1.9, the spring coefficient can be expected 0.25 - 0.3 MN/m. In the load propagation test, however, the fasteners were installed between interfaces of two blocks, then the spring coefficient for one fastener can be thought a quarter of 0.25 - 0.3 MN/m. And since DEM calculation is carried out in 2-dimensional plane condition, the spring coefficient of fastener k_f is determined 0.15 MN/m/m.

Table 1.1. Parameters used in distinct element method.

	EPS	Steel Plate
Density : ρ (kg/m^3)	20.0	7.65×10^3
Young's Modulus : E (N/m^2)	7.84×10^6	2.06×10^{11}
Stiffness of Spring : k_n (Normal Dir.) (N/m/m) k_t (Tangential Dir.)	(bc/a)E k_n/10.0	–
Stiffness of Spring of Fastener : k_f (N/m/m)	1.5×10^5	–
Coefficient of Friction : μ	0.64	0.64

The parameters used in the DEM analysis are listed in Table 1.1, and except for spring coefficient in normal and tangential direction, the used parameters were measured in laboratory tests[1),2)].

1.2.3. Equilibrium Condition

Forces and moment acting on an element $\{F_x \; F_z \; M\}^t$ are given by

$$\begin{Bmatrix} F_x \\ F_z \\ M \end{Bmatrix} = \begin{Bmatrix} 0 \\ \rho g h b \\ 0 \end{Bmatrix} + \sum_{m=1}^{N} \begin{bmatrix} \begin{Bmatrix} n_{xm} \\ n_{zm} \end{Bmatrix} f_{nm} + \begin{Bmatrix} t_{xm} \\ t_{zm} \end{Bmatrix} f_{tm} \\ \left| \left(r_m \vec{e}_m \times \vec{n}_m \right)_y \right| \quad \left| \left(r_m \vec{e}_m \times \vec{t}_m \right)_y \right| \end{bmatrix} \qquad (1.2.2)$$

where

$\vec{n}_m = \left(n_{xm} \; , \; n_{zm} \right)$, $\vec{t}_m = \left(t_{xm} \; , \; t_{zm} \right)$ and $\left| \vec{n}_m \right| = \left| \vec{t}_m \right| = \left| \vec{e}_m \right| = 1$.

The number of contact points and connecting points for an element is designated as *N*; see Figs. 1.4 and 1.5. Then the increments in displacement and rotation $\{\Delta u_x \; \Delta u_z \; \Delta\theta\}^t$ needed to satisfy the equilibrium condition is calculated as

$$\begin{Bmatrix} \Delta u_x \\ \Delta u_z \\ \Delta\theta \end{Bmatrix} = \left[K\right]^{-1} \begin{Bmatrix} F_x \\ F_z \\ M \end{Bmatrix} \tag{1.2.3}$$

where

$$\left[K\right] = \sum_{m=1}^{N} \left[\begin{Bmatrix} n_{xm} \\ n_{zm} \\ \left(r_m \vec{e}_m \times \vec{n}_m\right)_y \end{Bmatrix} \left\{ n_{xm} \;\; n_{zm} \;\; \left(r_m \vec{e}_m \times \vec{n}_m\right)_y \right\} k_{nm} + \begin{Bmatrix} t_{xm} \\ t_{zm} \\ \left(r_m \vec{e}_m \times \vec{t}_m\right)_y \end{Bmatrix} \left\{ t_{xm} \;\; t_{zm} \;\; \left(r_m \vec{e}_m \times \vec{t}_m\right)_y \right\} k_{tm} \right] \tag{1.2.4}$$

Square matrix $\left[K\right]$ is stiffness matrix. The new position of the element is determined by adding $\left\{\Delta u_x \;\; \Delta u_z \;\; \Delta\theta\right\}^t$ to current displacements and rotation $\left\{u_x \;\; u_z \;\; \theta\right\}^t$.

The above calculation step for an element is applied to all the discrete elements in turn, and this calculation cycle is repeated until the unbalanced resultant forces and moment on each of discrete elements become less than the prescribed boundary value of 9.8 N and 0.27 Nm/m, respectively.

1.3. Dynamic Distinct Element Method

1.3.1. Contact Points and Contact Forces

DEM for dynamic solution developed by Authors is almost same as the static DEM except for including acceleration and velocity components, however, different in assumption of the contact point and contact force. In static DEM for static solution, the contact points are occurred at each corner, and the contact force is proportioned to the overlap, however, it is suggested that the assumption can not express the influence of sharp edge appropriately compared with obtuse edge, in Part 2, Chapter 6. It can be thought that this influence of nonlinear contact must be enlarged in dy-

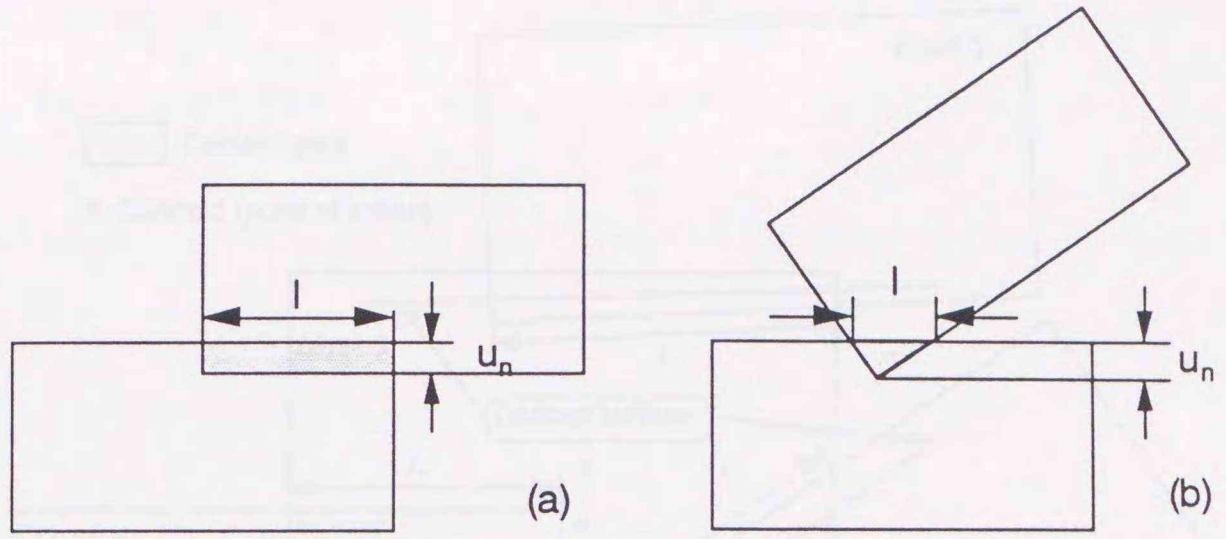

Figs.1.10(a),(b). Infulence of contact area; (a) contact between side and side, (b) contact between corner and side.

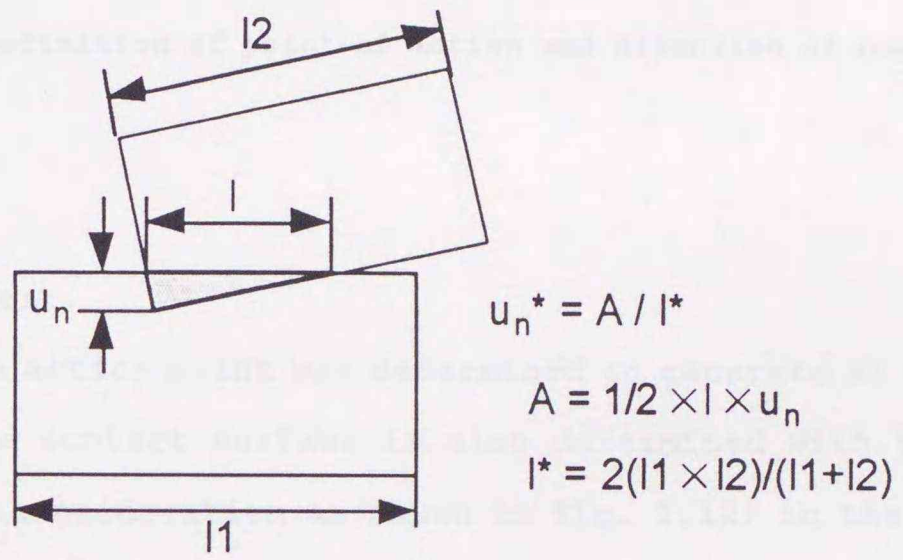

Fig. 1.11. Modification of u_n considering contact area.

namic problem, then new assumptions of contact points and contact forces were adopted for dynamic problem in Part 3.

To consider the influence of the contact area as shown in Fig. 1.10 (a), (b) whose two situations indicate same overlap u_n, the overlap u_n is modified with the contact length l as shown in Fig. 1.11. Stiffness of normal spring k_n and stiffness of tangential spring k_t were determined in same way of the static DEM, but this modification of overlap u_n is equivalent to the modification of the stiffness of normal spring k_n. The overlap in tangential direction was not modified, because its friction mechanism has

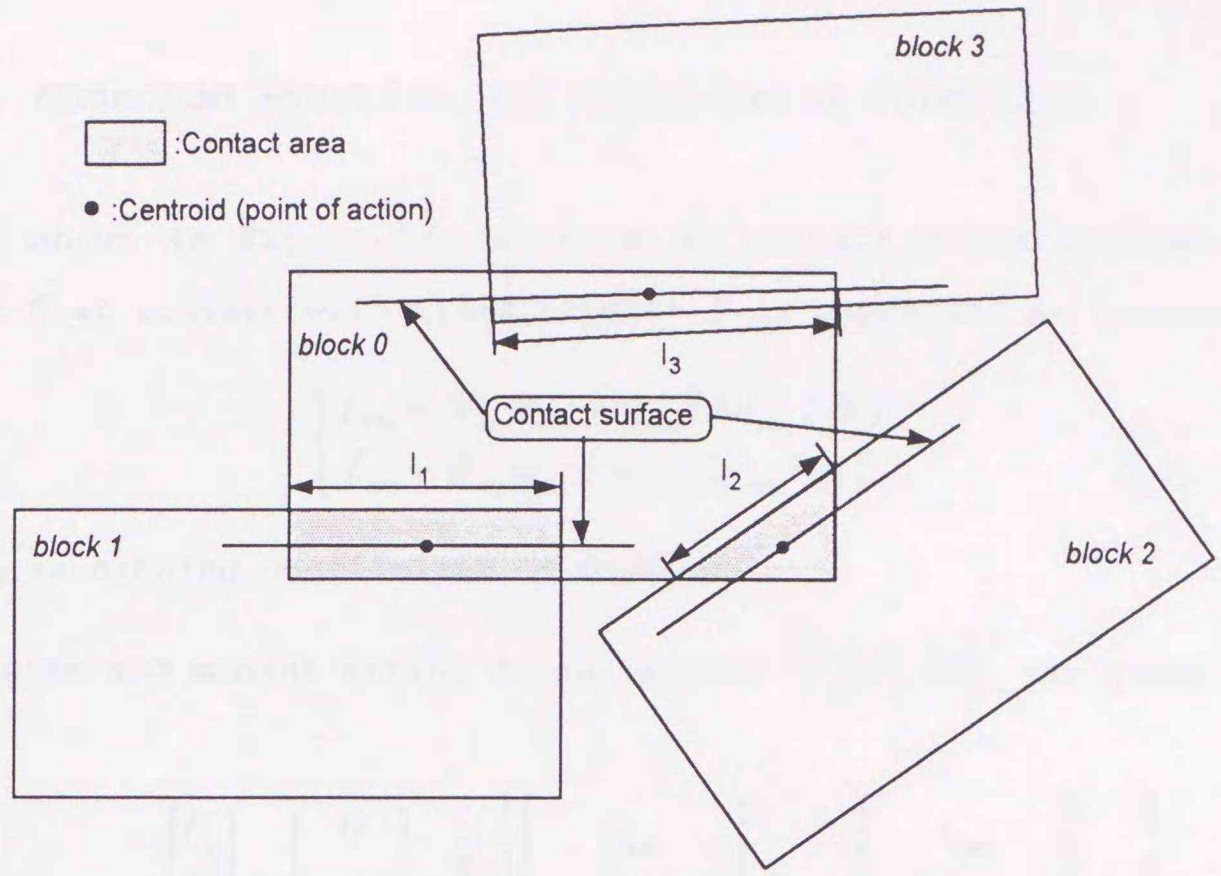

Fig. 1.12. Definition of point of action and direction of contact surface.

not been made clear.

Moreover the action point was determined to generate at the centroid of contact area, the contact surface is also determined with the inclination of elements into consideration as shown in Fig. 1.12; in the cases of block 0 and block 1, and block 0 and block 2, the direction of contact surfaces were same as the static DEM, but different in case of block 0 and block 3 in Fig. 1.12. The contact surface between block 0 and block 3 was determined as the surface which has the average angle of the longer subtense. The mechanism at contact point is modeled by spring, dashpot, no-tension and slip elements in the same way as static DEM shown in Fig. 1.13. For fastener element, the mechanism was same as EPS blocks except that the no-tension element was not used.

1.3.2. Momentum Equation and Equilibrium Condition

As shown in Fig. 1.13, at time t, contact force applied to block element 0 at contact with block element m is expressed as follows;

$$\begin{cases} f_{nm} = k_{nm} u_{nm} + \eta_{nm} (\Delta u_{nm} / \Delta t) \\ f_{tm} = k_{tm} u_{tm} + \eta_{tm} (\Delta u_{tm} / \Delta t) \end{cases} \tag{1.3.1}$$

where η is damping coefficient of dashpot.

Forces and moment acting on an element $\{F_x \; F_z \; M\}^t$ are given by

$$\begin{Bmatrix} F_x \\ F_z \\ M \end{Bmatrix} = \begin{Bmatrix} 0 \\ \rho g h b \\ 0 \end{Bmatrix} + \sum_{m=1}^{N} \begin{bmatrix} \begin{Bmatrix} n_{xm} \\ n_{zm} \end{Bmatrix} f_{nm} + \begin{Bmatrix} t_{xm} \\ t_{zm} \end{Bmatrix} f_{tm} \\ \left(r_m \vec{e}_m \times \vec{n}_m \right)_y \quad \left(r_m \vec{e}_m \times \vec{t}_m \right)_y \end{bmatrix} \tag{1.3.2}$$

where

$$\vec{n}_m = \left(n_{xm} \; , \; n_{zm} \right) , \; \vec{t}_m = \left(t_{xm} \; , \; t_{zm} \right) \text{ and } \left| \vec{n}_m \right| = \left| \vec{t}_m \right| = \left| \vec{e}_m \right| = 1$$

Equ. (1.3.2) is same as indicated in static DEM, the number of contacts points of element is designated as N. Then the acceleration at time t $\{\ddot{u}\} = \{\ddot{u}_x \; \ddot{u}_z \; \ddot{\theta}\}^t$, were determined by

$$\begin{cases} \ddot{u}_x = F_x / m \\ \ddot{u}_z = F_z / m \\ \ddot{\theta} = M / I \end{cases} \tag{1.3.3}$$

where m is mass of element and I is inertia moment.

The increment of acceleration $\{\Delta\ddot{u}\}$ was determined by $\{\Delta\ddot{u}\} = \{\ddot{u}_t - \ddot{u}_{t-\Delta t}\}$, then the increment in velocity and displacement are calculated by means of direct integration method as follows;

$$\begin{cases} \Delta\dot{u} = \dot{u}\Delta t + \alpha \Delta\ddot{u} \Delta t \\ \Delta u = u\Delta t + \frac{1}{2}\ddot{u}(\Delta t)^2 + \beta \Delta\ddot{u}(\Delta t)^2 \end{cases} \tag{1.3.4}$$

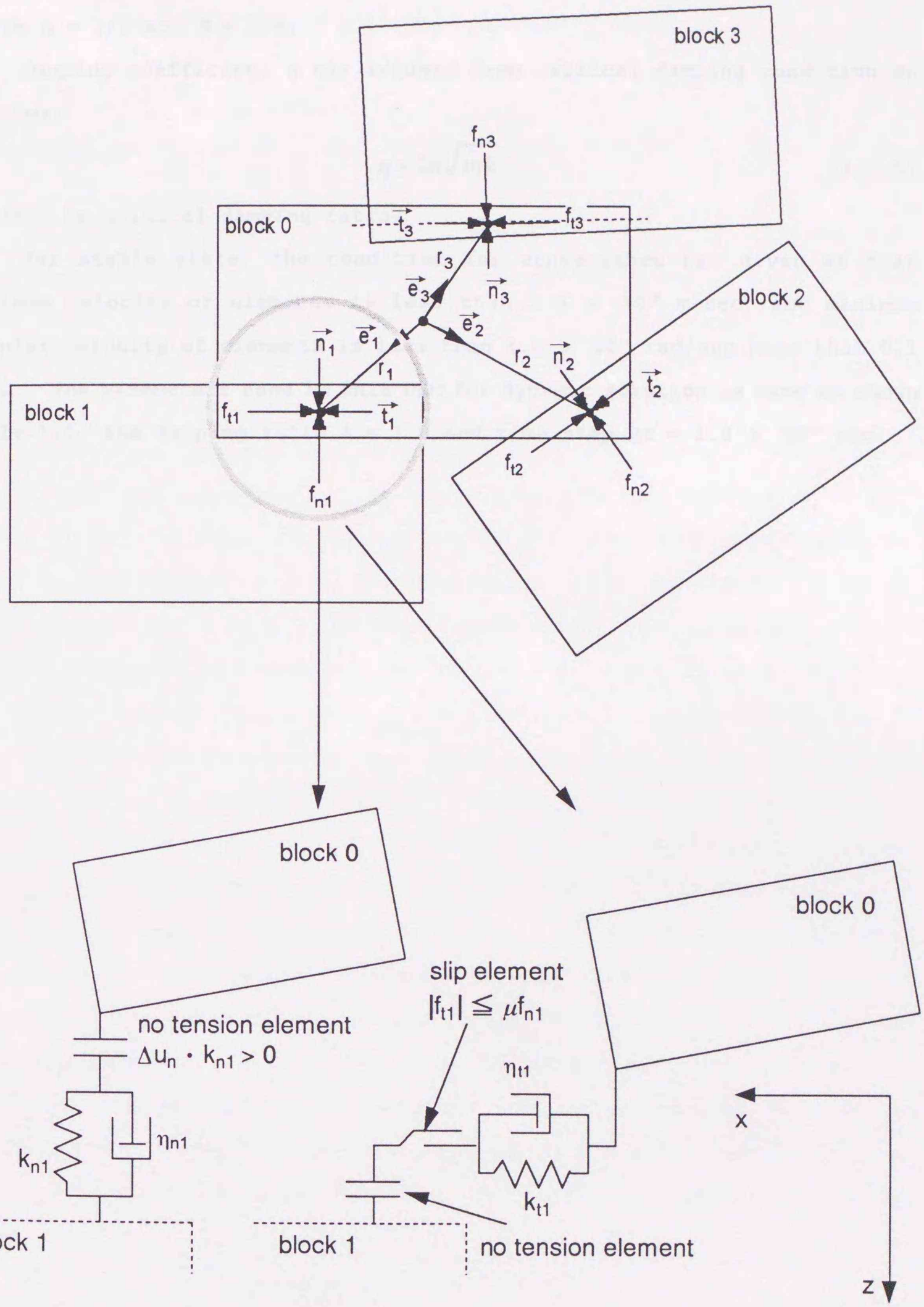

Fig. 1.13. Contact Points modeled by springs, dashpots, no-tension element and slip element.

where α = 1/2 and β = 1/6.

Damping coefficient η was assumed from critical damping condition as follows;

$$\eta = 2h\sqrt{mk} \tag{1.3.5}$$

where h is critical damping ratio.

For stable state, the condition for convergence was given as that maximum velocity of elements is less than 1.0×10^{-8} m/sec, and maximum angular velocity of elements is less than 1.0×10^{-6} rad/sec more than 0.1 sec. The parameters used in this DEM for dynamic solution is same as shown Table 1.1, and damping ratio h = 1.0 and time step $\Delta t = 1.0 \times 10^{-5}$ sec.

Chapter 2.Finite Element Method

2.1 Employed Finite Element Method

Conventional type of FEM for linear elastic body in 2-dimensional condition was used; the computer code was developed by the Authors. Quadrilateral element with four nodes is incorporated, and numerical integration is done at four inner points. All the five model EPS block fills were analyzed in plane stress condition.

To simulate the behaviors of EPS blocks by FEM, certain type of joint element must be introduced. However, even with innumerable joint elements, it will be generally impossible to simulate thoroughly the mechanisms in the interfaces, where the generations and disappearance of contact points frequently occur. In the present study, FEM was simply adopted without joint elements to emphasize the contrast with DEM; model EPS block fills were regarded as a continuum media with uniform properties.

The finite element meshes for the EPS model fills for load propagation test in Part 2, Chapter 2 are shown in Fig. 2.1 (a), (b); these two model fills are for the model fills shown in Figs. 1.1 (a), (b) of Part 1, Chapter 1. In the load propagation test of Part 2, Chapter 2, the five model fills are prepared for model test, the model fills can be distinguish by their silhouettes; one is symmetrical model fill, the other is asymmetrical model fill. If the model fills are same in silhouette, their internal structures are different each other. Since the difference in initial structure of those EPS model fills cannot be taken into consideration in FEM employed in the present study, the finite element meshes are only these two meshes; one is for symmetrical model fills and the other is for asymmetrical model fills.

The mechanical parameters used are listed in Table 2.1.

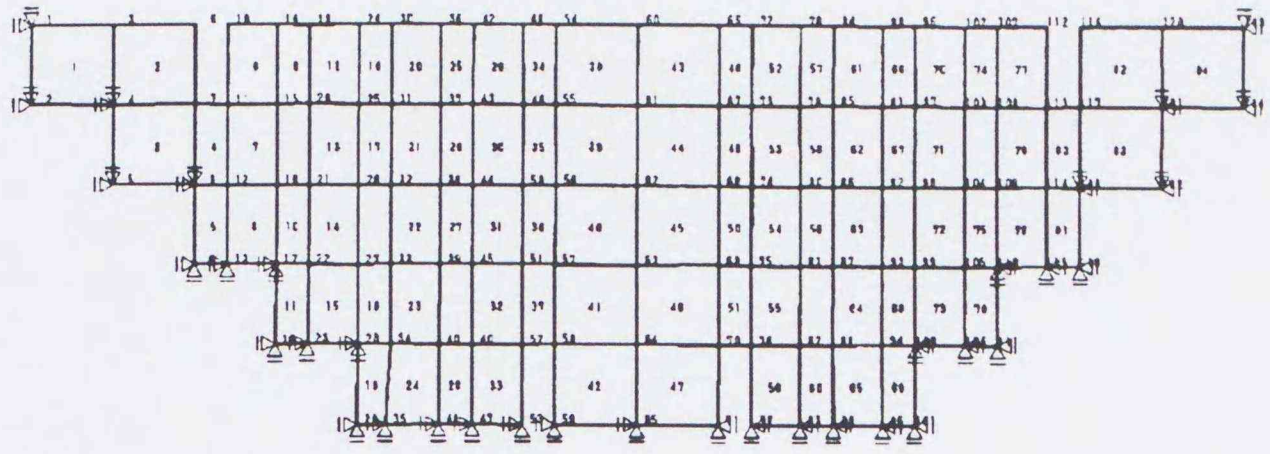

(a) for symmetrical model fills

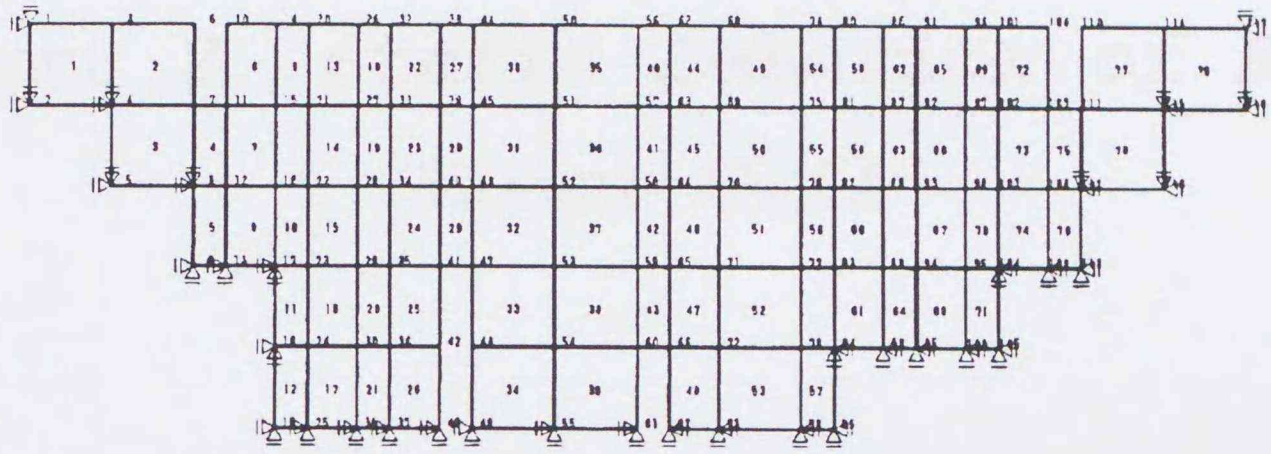

(b) for asymmetrical model fills

Fig. 2.1 (a),(b). Finite element meshes; (a) used for symmetrical model fills, (b) used for asymmetrical model fills.

Table 2.1. Parameters used in Finite Element method.

	EPS
Density : ρ (kg/m^3)	20.0
Young's Modulus : E (N/m^2)	7.84×10^6
Poisson's Ratio : ν	0.01

Part 2. Static Behavior of EPS Block Fill

Chapter 1. Experimental Investigation of Load Propagation Characteristics of EPS Block Fill

1.1. Preparation of EPS Model Fill

To make clear the load propagation characteristics of EPS block fill, a series of load propagation tests were carried out and five different 2-dimensional EPS model fills were prepared for the laboratory tests as shown in Figs. 1.1 (a)-(e).

There are two types of model fills, which can be distinguish by their silhouettes, one is a group of symmetrical pattern model fills (Model-A and Model-B), the other is a group of asymmetrical pattern model fills (Model-C, Model-D and Model-E). In both of the two pattern model fills, their silhouettes are same; Model-A and Model-B have same silhouette and Model-C, Model-D and Model-E have same silhouette respectively, but the internal structures composed of different EPS blocks are not same. In Model-B and Model-D, the fill bodies were separated by vertical continuous joints, and these differences of internal structure were arranged to investigate the influence of internal structures on the mechanical properties of EPS block fills.

Three types of EPS blocks used in the present study are shown in Figs. 1.2 (a)-(c); Type-A block is a quarter of prototype in linear dimension and its width is 25.0 cm, and Type-B block's width is 18.8 cm, Type-C block's width is 12.5 cm. The height and depth of each block are common, and the density of EPS block is 20 kg/m^3. The Young's elastic modulus E and Poisson's ratio n is 7.84 MPa and 0.01 respectively. These value of parameters were defined by laboratory test (EPS Construction method Development Organization (EDO), 1990, EDO, 1993), and the frictional coefficient m between EPS blocks was also measured 0.64. Each blocks has two marks on its front face to determine their displacement and rotation by the image processing method in deformation test (in Chapter 2). In image processing, the position of these two marks was determined and the block type was

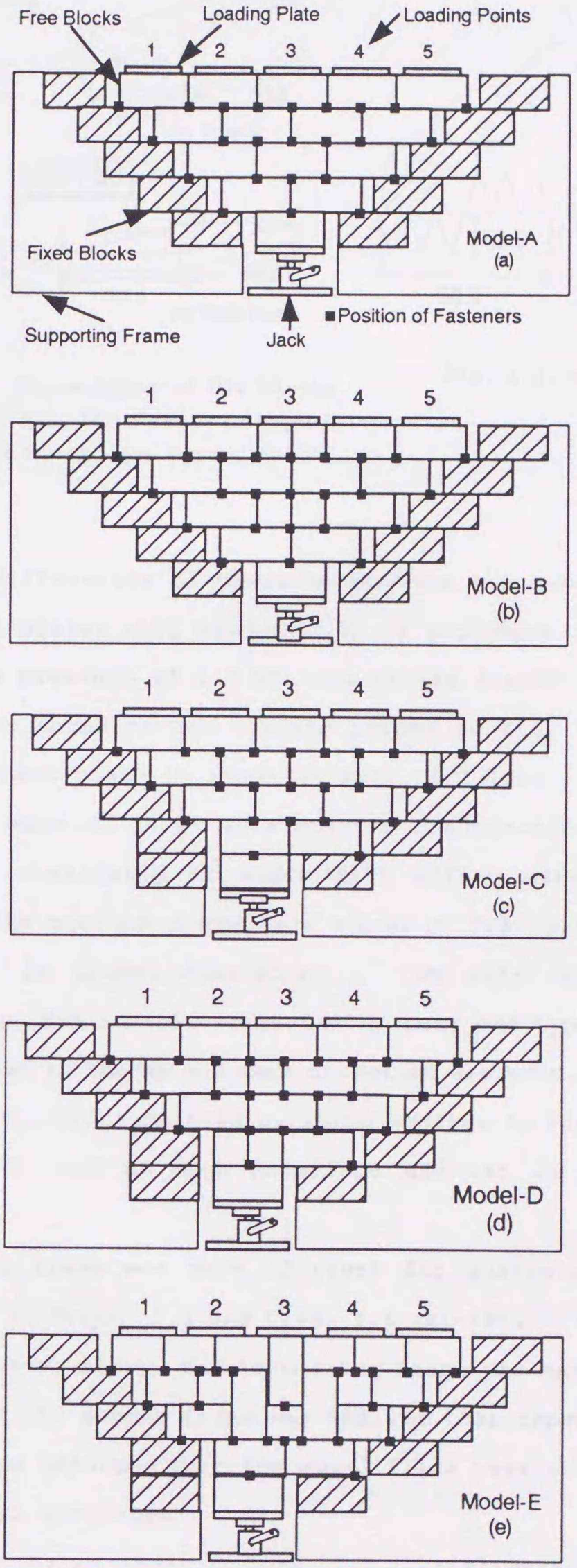

Figs. 1.1 (a)-(e). Prepared EPS model fills and definition of loading points; (a) Model-A, (b) Model-B, (c) Model-C, (d) Model-D, (e) Model-E.

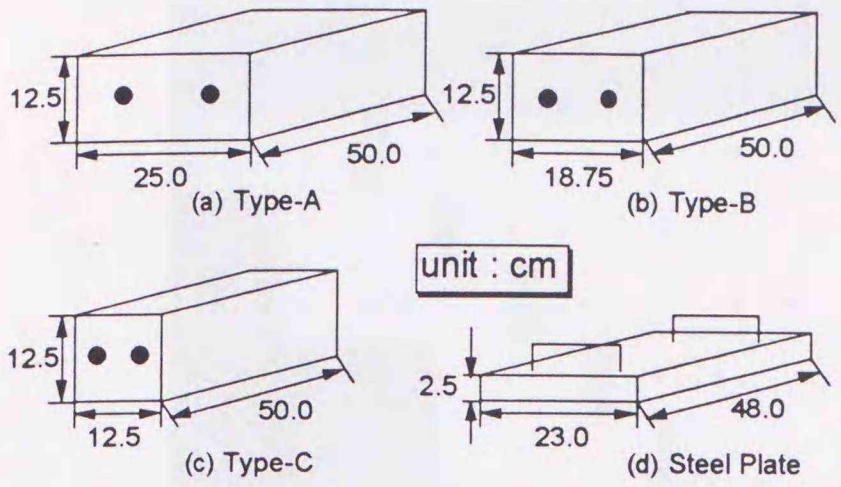

Figs. 1.2 (a)-(d). Three types of EPS blocks and the steel plate for load; (a) Type-A block, (b) Type-B block, (c) Type-C block, (d) steel plate.

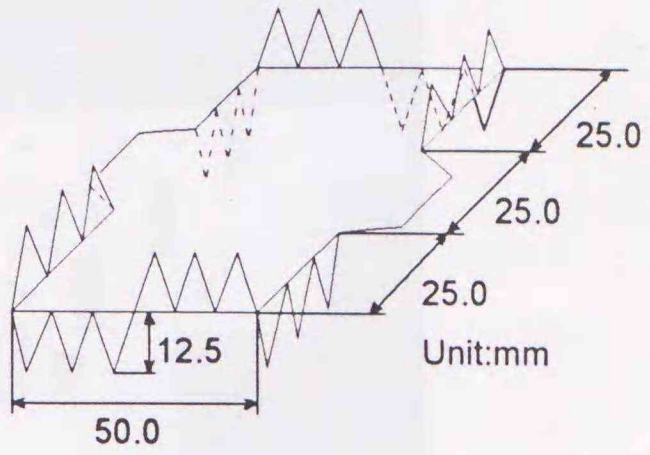

Fig. 1.3. Steel fastener.

derived from the differences of distance between the two marks automatically. The steel plates with weight of 22 kg each were used for applying uniform overburden pressure of 1.7 kPa and single static load of 215.6 N; the static load was moved on the loading points in Fig. 1.1 (a), and the dimension of the steel plate is shown in Figs. 1.2 (d).

The fasteners made of steel were used in constructing EPS block fill for ensuring the consistency of whole fill during assembling. The fastener used in the present study, are shown in Fig. 1.3; it is about a half of prototype in linear dimension. At site, various types of fasteners are using, but in this model tests, only one type fastener which sawlike teeth are set to the up and down direction was used. The fasteners are placed at the positions pointed by solid squares in Figs. 1.1 (a)-(e); single fastener was used at each interface and set in center of depth direction.

The supporting frame was made of steel for guaranteeing sufficient rigidity, as shown in Photo. 1.1 and Figs. 1.1 (a)-(e). At the beginning of this series of model tests, the supporting frame was made of wood. But as the stiffness of the wooden frame was smaller than expected, the wooden supporting frame had deformed when the model fills were subjected to pressure or differential settlement.

The shaded EPS blocks shown in Figs. 1.1 (a)-(e) were fixed EPS blocks which were adhered to the supporting frame with adhesive agent. These fixed blocks were prepared for simplifying the boundary condition. A jack

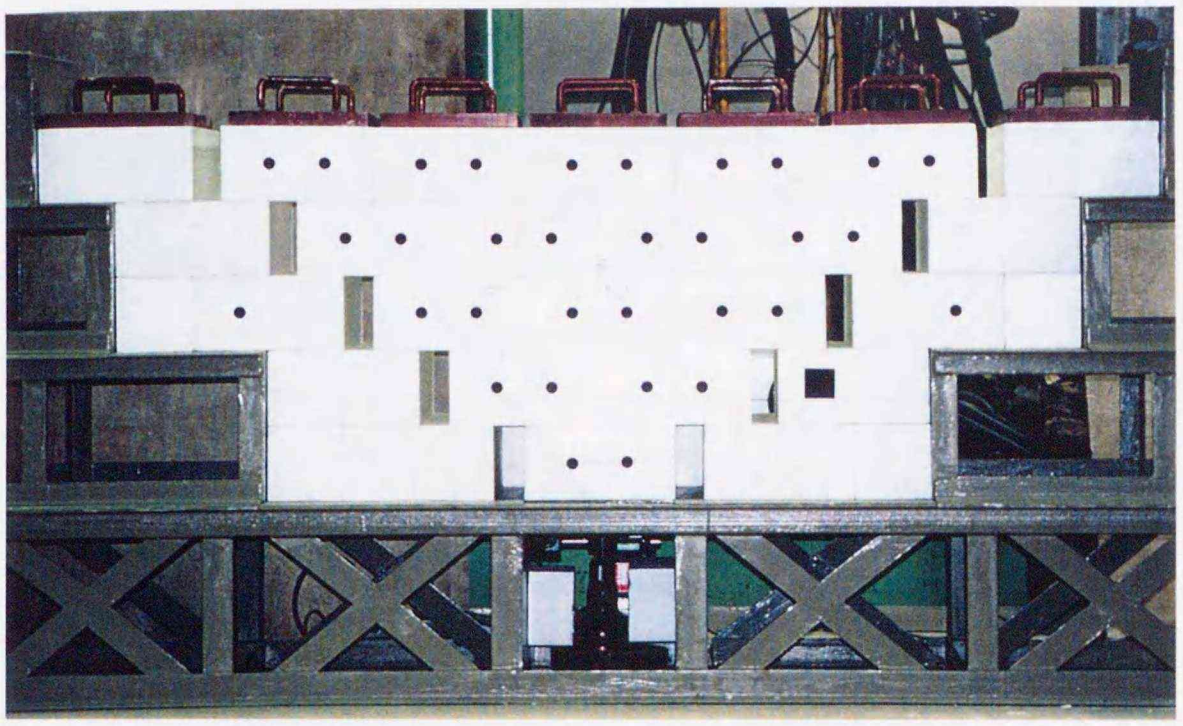

Photo. 1.1. Prepared EPS block fill (Model-A).

which has a steel plate for supporting EPS block was set at the bottom of each model fill, and a load cell with capacity of 4.9 kN and a dial gauge were devised under the supporting plate of jack. Some deformation as differential settlement can be applied by using this jack, and the propagated load from single static load to a bottom EPS block through the fill body, or reaction due to applied deformation were measured by the load cell. The free blocks were stuck up between the fixed blocks and the supporting plate of the jack with or without fasteners shown in Fig. 1.3.

The position of five steel plates for uniform overburden pressure were defined as five loading points as shown in Fig. 1.1 (a), and these loading points show the position for applying the single steel plate for static load.

1.2. Load Propagation Test

At initial condition, the EPS model fill was subjected to uniform overburden pressure of 1.7 kPa by the five steel plates, and the load cell set to the jack was initialized at this condition. Then the single steel plate was placed on each of the five loading points on surface of EPS model fill as static load as shown in Fig. 1.4. At first, the single steel plate was placed at loading point 1, and the propagated load to the plate mounted on the jack was measured by the load cell. Next, the single plate was

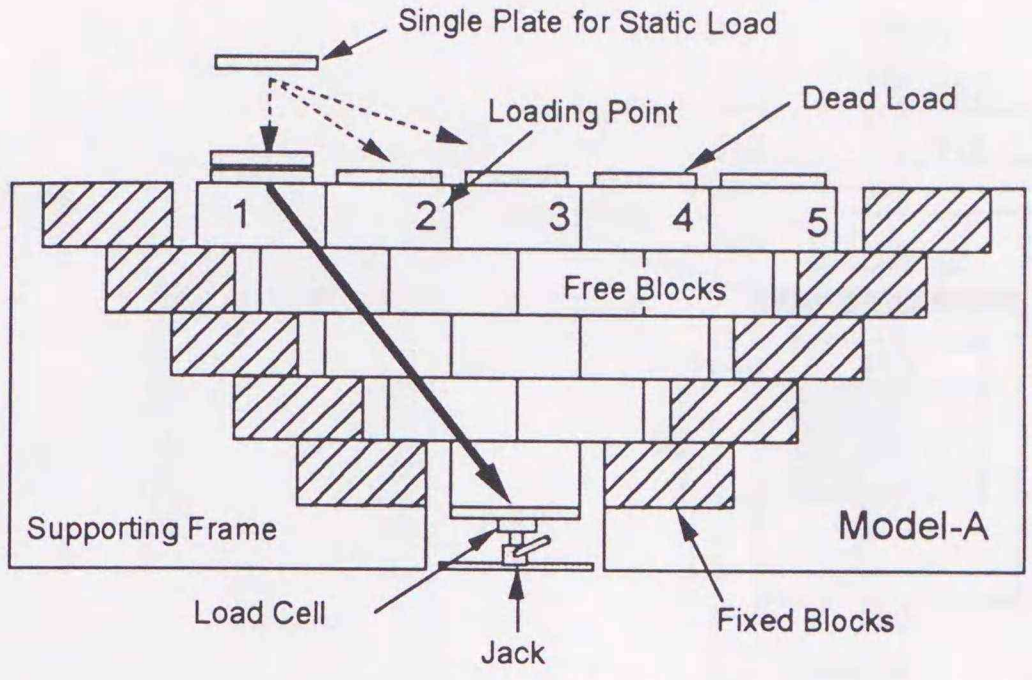

Fig. 1.4. Load propagation test without distortion.

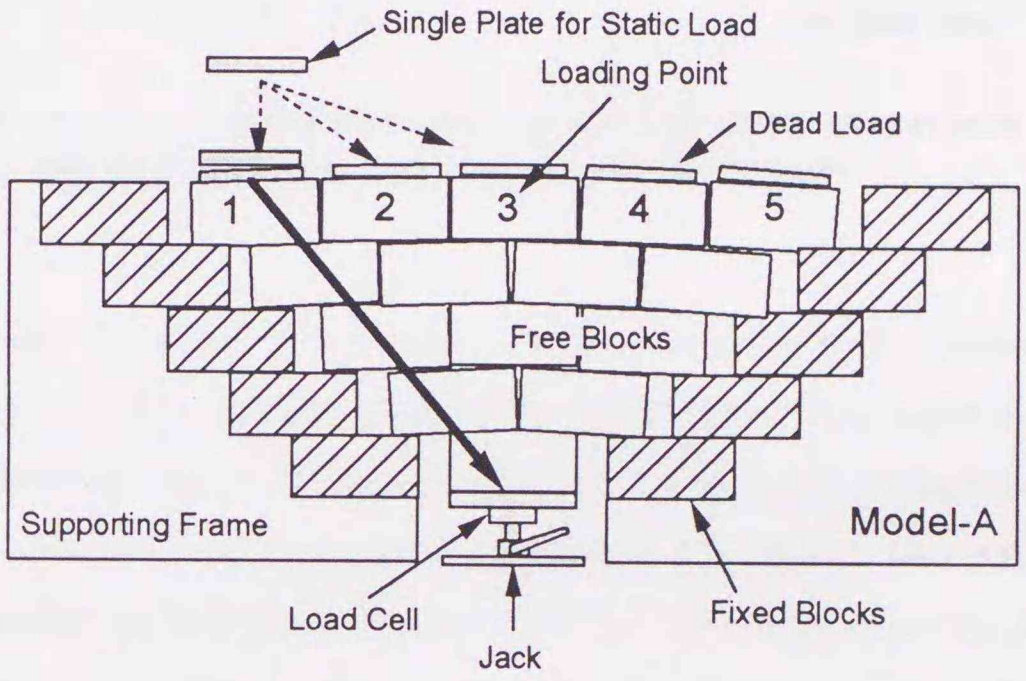

Fig. 1.5. Load propagation test with distortion.

placed at loading point 2, and the propagated load was measured, and this procedure was repeated to loading point 5 over and over. In fact, the order of loading was not from loading point 1 to upward, the loading was carried out in random and several times at each loading point to obtain the average and steady value.

This load propagation tests were carried out in two conditions; the first condition is without distortion due to jack up, and the second one is with distortion due to jack up of 1.0 cm in vertical direction, as shown in Fig. 1.5. The forced displacement of supporting plate of the jack was defined as the vertical displacement of the sprouting plate Δ. In the

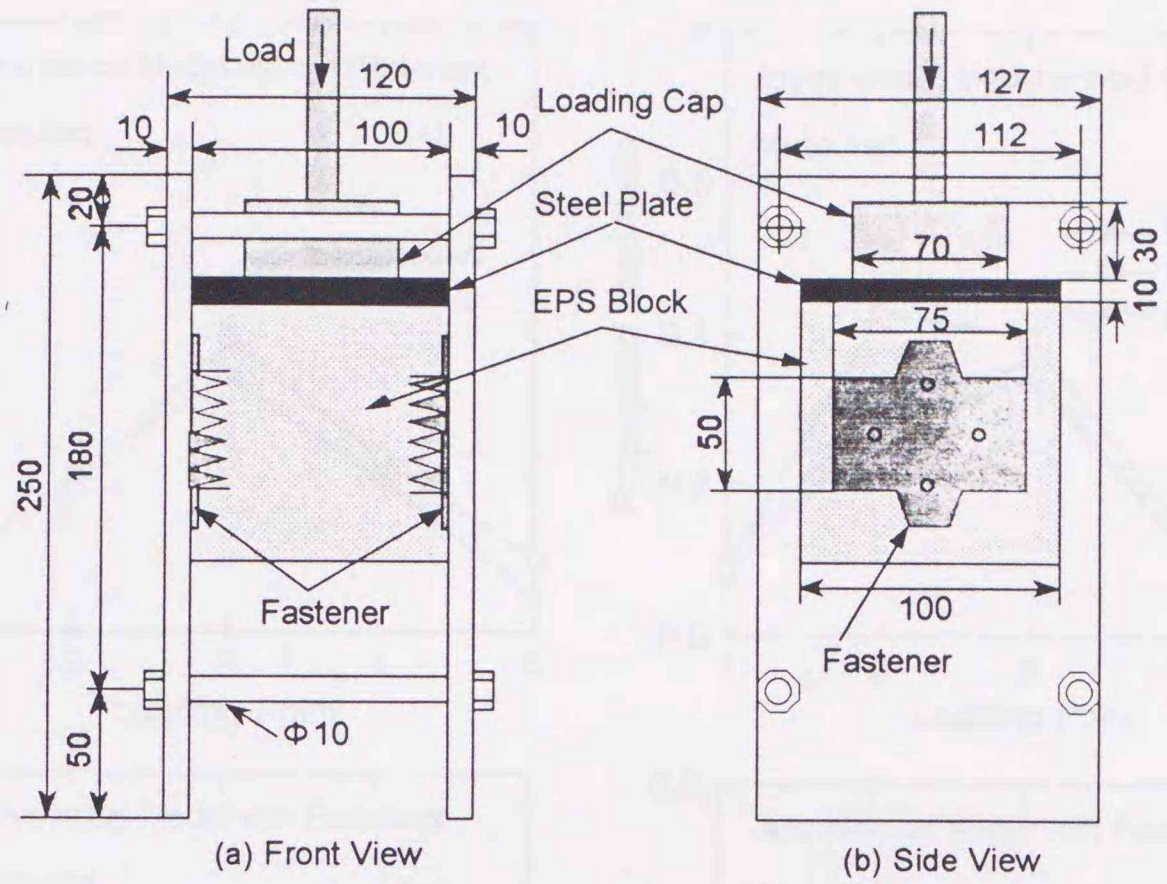

Figs. 1.6 (a),(b). Apparatus for measureing shear resistance between EPS element and fastener; (a) front view, (b) side view.

first condition without distortion, the cases with fasteners fills were also examined. But in the distorted condition, the results of the case with the fasteners were not shown, because remarkable plastic deformation or fracture occurred at interfaces between fasteners and EPS blocks; the reaction measured at bottom supporting plate was significantly unstable and the repeatability of the test results could not be acceptable for discussion. Therefore, the effect of distortion of internal structure on the mechanical properties of EPS block fill was examined only in the tests on model fills without fasteners.

In the distorted condition, even if without fasteners, the propagated load was not steady just after placing single plate, because of sliding between EPS blocks, so the propagated load was monitored in a few minutes for obtaining steady value. In the first condition, without deformation, the propagated load was steady in almost model fills, so the propagated load was measured just after loading.

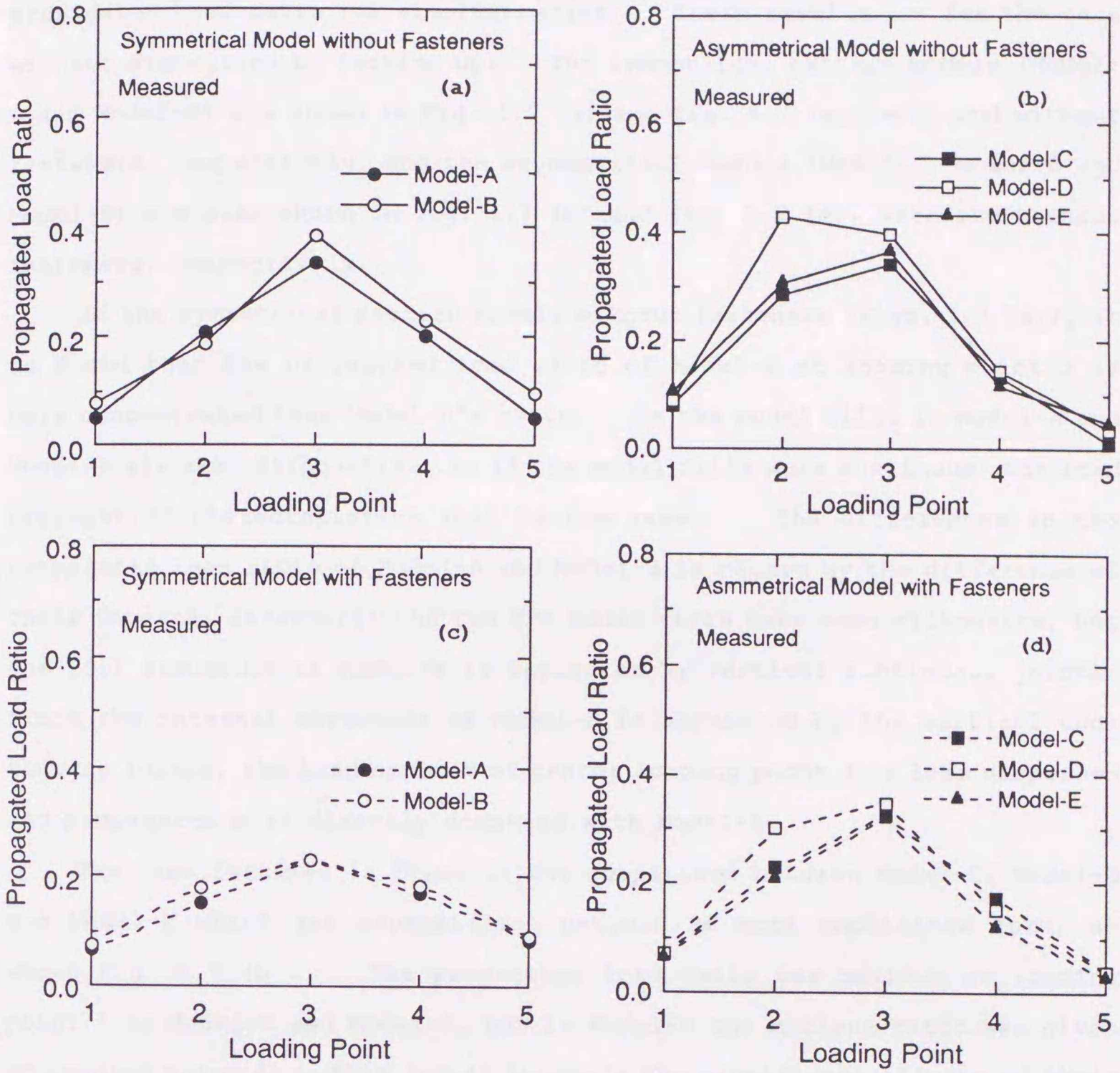

Figs. 1.7 (a)-(d). Load propagation ratio - loading points relationship; (a) Symmetrical model fills without fasteners, (b) Asymmetrical model fills without fasteners, (c) Symmetrical model fills with fasteners, (d) Asymmetrical model fills with fasteners.

1.3. Test Results and Discussion

1.3.1. Undistorted Model Test

Figs. 1.7 (a)-(d) shows the test results on the model fills with and without fasteners; the ratio of the propagated load measured at jack plate to applied load is plotted against the loading points and this plot is a kind of influence line used in structural mechanics. The ratio of the propagated load measured at jack plate to applied load was defined as the

propagated load ratio for simplification. These results are for the case without distortion by jacking up. The symmetrical pattern models (Model-A and Model-B) are shown in Fig. 1.7 (a) and Fig. 1.7 (c), with and without fasteners, respectively, and the asymmetrical models (Model-C, Model-D and Model-E) are also shown in Fig. 1.7 (b) and Fig. 1.7 (d), with and without fasteners, respectively.

In the symmetrical pattern models without fasteners (Figs. 1.7 (a)), it is found that the propagated load ratio of Model-B at loading point 3 is more concentrated than Model-A's ratio. As the model fills in Model-A and Model-B are same silhouettes, so if the model fills were continuum, the load propagation characteristics must become same. The differences in the propagated load ratio of Model-A and Model-B is caused by the difference of their internal structure; the two EPS model fills have same silhouette, but the fill structure of Model-B is separated by vertical continuous joints. Since the internal structure of Model-B is separated by the vertical continuous joints, the load applied at center loading point 3 is less dispersed and propagated more directly downward with Model-A.

The same features is found in the comparison between Model-C, Model-D and Model-E which are asymmetrical pattern in more emphasized form, as shown Fig. 1.7 (b). The propagated load ratio was maximum at loading point 3 in Model-C and Model-E, but in Model-D the maximum ratio was given at loading point 2. This result suggests the significant effects of their internal structures, vertical continuous joints, on load propagation behavior, and the applied static load does not propagate beyond the vertical continuous joints. Moreover in Model-C, Model-D and Model-E, the propagated load ratio at loading point 4 and 5 were extremely small. This indicates that the EPS model fills are not continuum, whether with or without vertical continuous joints. Although the propagated load ratio at loading point 2 and 3 in Model-D were larger than in Model-C, the propagated load ratio at loading point 4 and 5 in Model-D were smaller than in Model-C, this suggests that the vertical continuous joints in Model-D makes the load distribution effect low. This tendency is found between Model-A and Model-B as described previously, the reason for this are being failed the combination of EPS blocks largely by the vertical continuous joints in Model-B and Model-D.

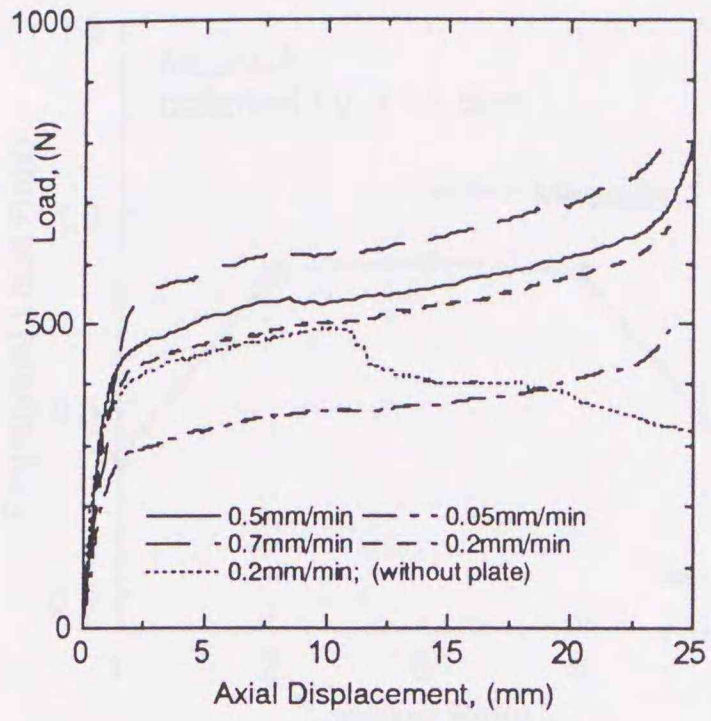

Fig. 1.8. Influence of load rate in shear resistance between EPS element and steel fastener.

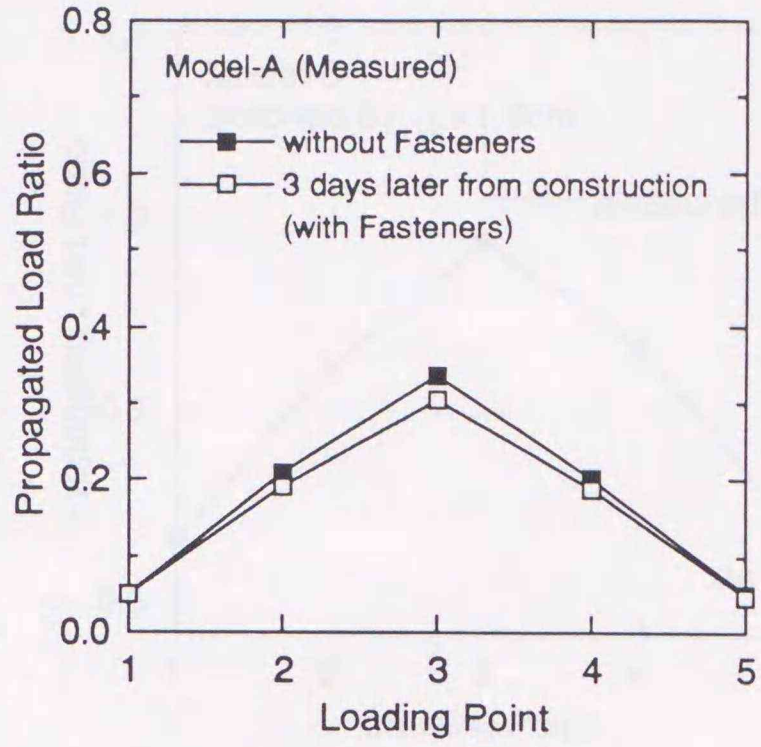

Fig. 1.9. Time effect of EPSmodel fill with fasteners in load propagation cahracteristics.

Shown in Figs. 1.7 (c), (d) are the effect of fastener on the load propagation properties in EPS block fills; the differences between Model-A and Model-B, and between Model-C, Model-D and Model-E become small compared with Figs. 1.7 (a), (b). Especially, in Model-D, the loading point that gives the maximum ratio of propagated load was changed from 2 to 3.

Certainly the fasteners used for fixing EPS blocks, makes the construction process easy and speedy; however, the effect of fastener is not enough for erasing the influence of internal structure. Fig. 1.8 shows the result of the element test for shear resistance between EPS element and fastener; testing method is described in Part 1, Chapter 1. The reaction at load cell is plotted against the axial displacement; this reaction can be thought as the shear resistance force between EPS element and steel fastener. It is found that the shear resistance depends on loading rate strongly; as the loading rate is smaller, the shear resistance is smaller. As time goes by, the effect of fasteners can not be expected, and the effect will be emphasized only during dynamic or fast loading. These load propagation tests for model fills installed with fasteners were carried out just after the fasteners were set up, it can be thought that this situation was the most advantageous condition for the effect of fasteners. In fact, as shown in Fig. 1.9, when the load propagation test was carried out on

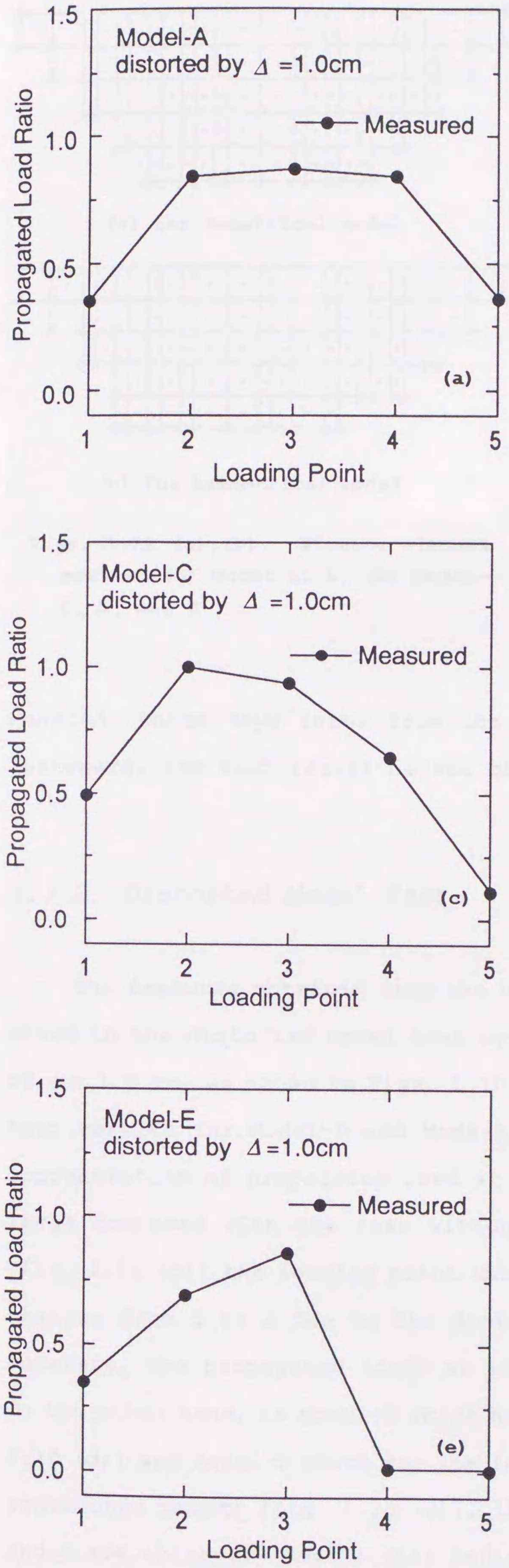

Figs. 1.10 (a)-(e). Propagated load ratio - loading points relationship of disturbed model fills; (a) Model-A, (b) Model-B, (c) Model-C, (d) Mode-D, (e) Model-E.

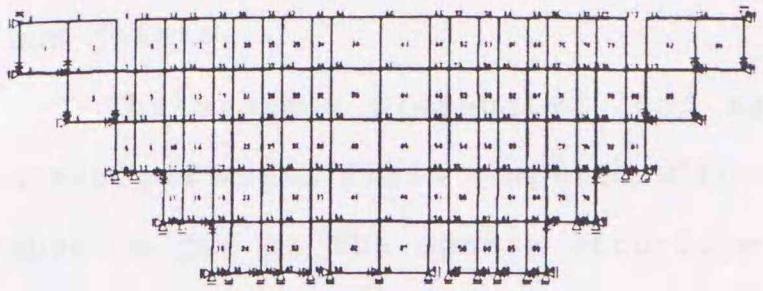

(a) for Smmetrical model

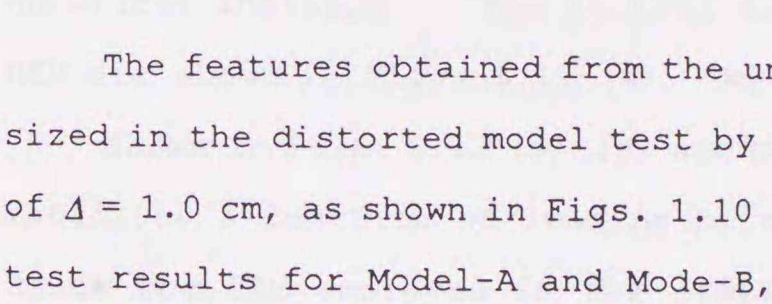

(b) for Asmmetrical model

Figs. 1.11 (a),(b). Finnite element meshes; (a) Model-A, B, (b) Model-C, D, and E

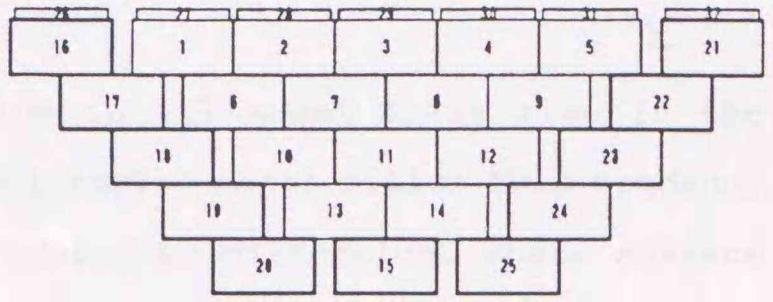

(a) for Model-A

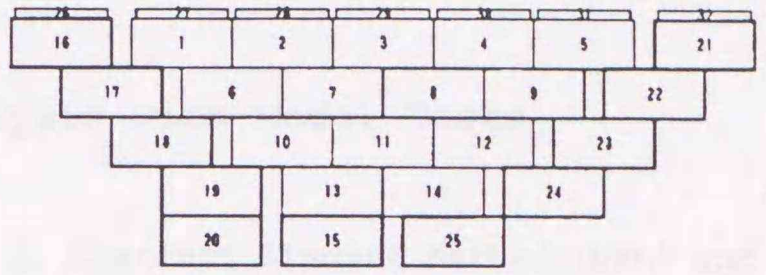

(b) for Model-C

Figs. 1.12 (a),(b). Initial arrangement of distinct elements in DEM; (a) Model-A, (b) Model-C

Model-A, three days later from the constructing the EPS model fill with fasteners, the test result became close to the case without fasteners.

1.3.2. Distorted Model Test

The features obtained from the undistorted model test, was more emphasized in the distorted model test by ascending the bottom supporting plate of Δ = 1.0 cm, as shown in Figs. 1.10 (a)-(e). The comparison between the test results for Model-A and Mode-B, shown in Fig. 1.10 (a) and (b), the concentration of propagated load at loading point 3 in Model-B is getting large compared with the case without distortion. Although in Model-C (Fig. 1.10 (c)) the loading point which gives maximum propagated load ratio changes from 3 to 2 due to the distortion, the form of the whole plot is moderate; the propagated loads at loading point 4 and 5 are not so small. On the other hand, in Model-D which has the vertical continuous joints (Fig. 1.10 (d)) and Model-E which has the internal structure close to the vertical continuous joints (Fig. 1.10 (e)), the propagated loads at loading point 4 and 5 are extremely small; this indicates that the applied static load can not propagate beyond cracks due to the week joint like the vertical continu-

ous joints.

The maximum propagated load ratios in all model fills rise in the distorted model fills compared with undistorted model fills; this tendency must be due to the sparse structure induced by distortion, where surface load is poorly dispersed.

1.4. Comparison of Numerical Analysis with Model Tests

In this study as mentioned in Part 1, Distinct Element Method (DEM) and Finite Element Method (FEM) are adopted as numerical analysis method. The static DEM which the acceleration and velocity components of the element motion are neglected is adopted. And in FEM calculation, since any joint or slip elements were not employed, the difference in internal structure of the fills cannot be taken into consideration in the adopted FEM. So the finite element meshes for this model test are only two meshes: for symmetrical model fills (Model-A and Model-B) and for asymmetrical model fills (Model-C, Model-D and Model-E), as shown in Figs. 1.11 (a), (b), respectively. On the other hand, as DEM can be dealt with discrete objects, the difference in internal structures can be taken into consideration in the numerical analysis. The initial arrangements of Model-A and Model-C for DEM are shown in Figs. 1.12 (a), (b).

Shown in Figs. 1.13 (a)-(e) are measured and calculated propagated load ratios as a function of loading point for model fills without fasteners. Since the FEM employed in the present study, where EPS block fills are modeled as an uniform continuous media, cannot distinguish the differences in internal structures, the calculated propagated load is same for symmetrical model fills (Model-A and Model-B), and also same for asymmetrical model fills (Model-C, Model-D and Model-E). On the other hand, DEM can take account of the influence of internal structures on load propagation properties as obtained by load propagation tests; the propagated load at loading point 3 in Model-B, which has the vertical continuous joints, is less dispersed compared with Model-A, and the loading point which gives maximum propagated load ratio is changed between Model-C and Model-D which has also the vertical continuous joints. And in asymmetrical model fills,

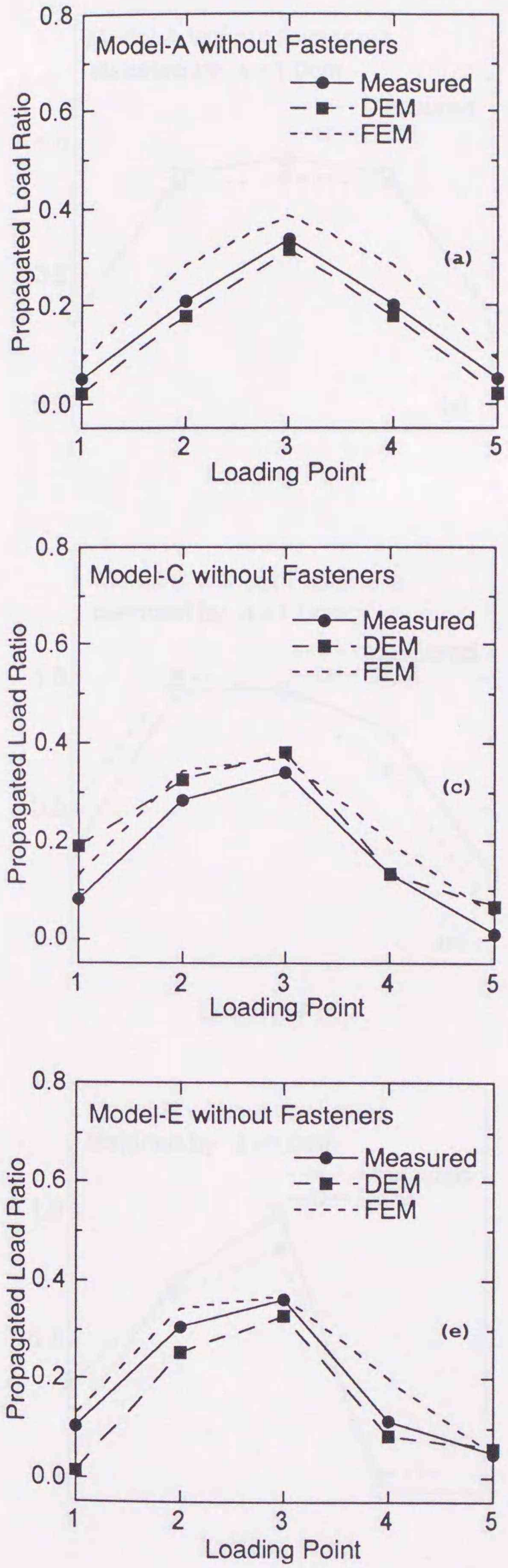

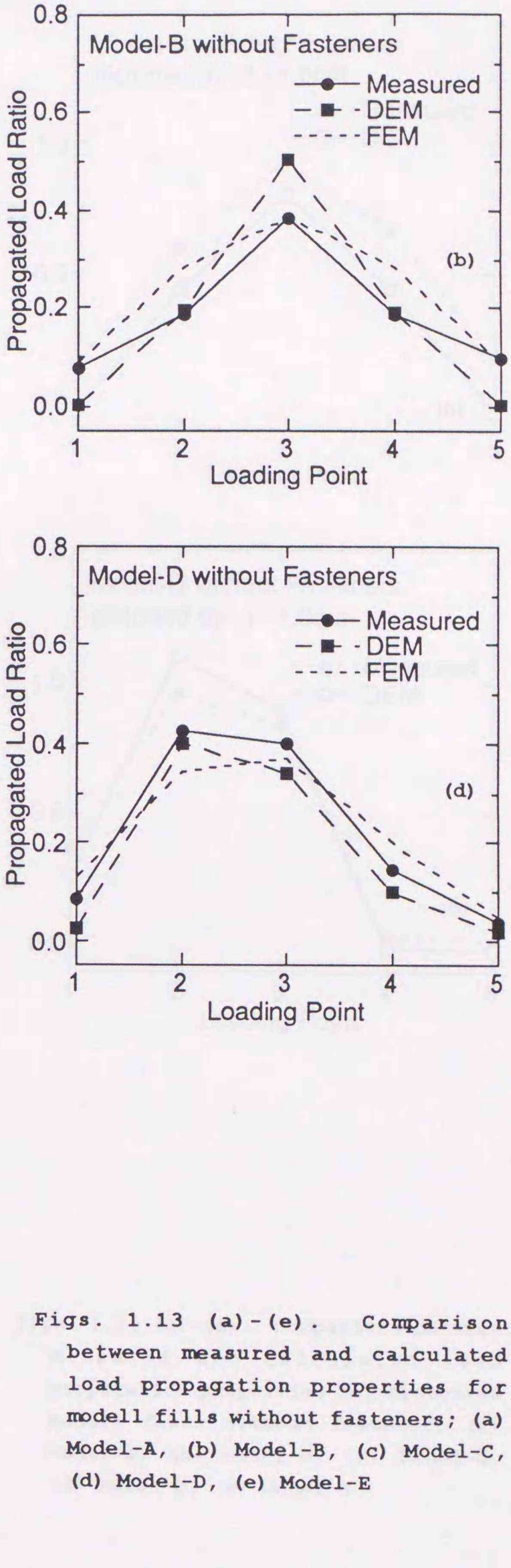

Figs. 1.13 (a)-(e). Comparison between measured and calculated load propagation properties for modell fills without fasteners; (a) Model-A, (b) Model-B, (c) Model-C, (d) Model-D, (e) Model-E

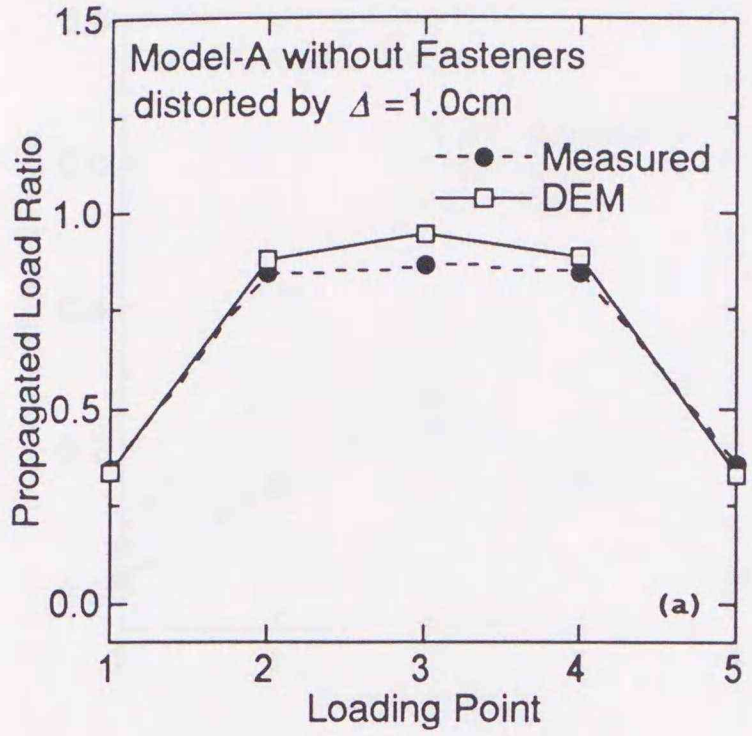

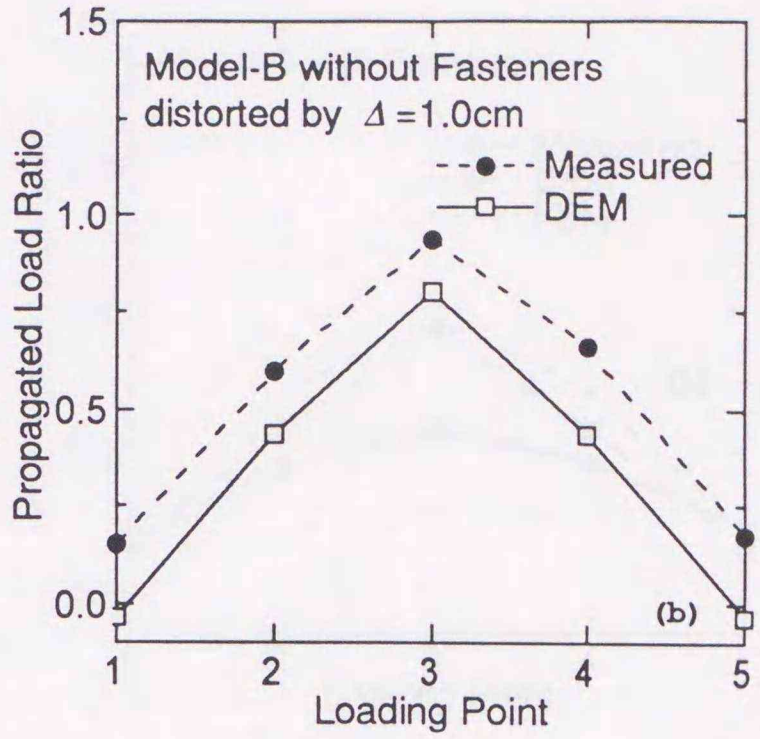

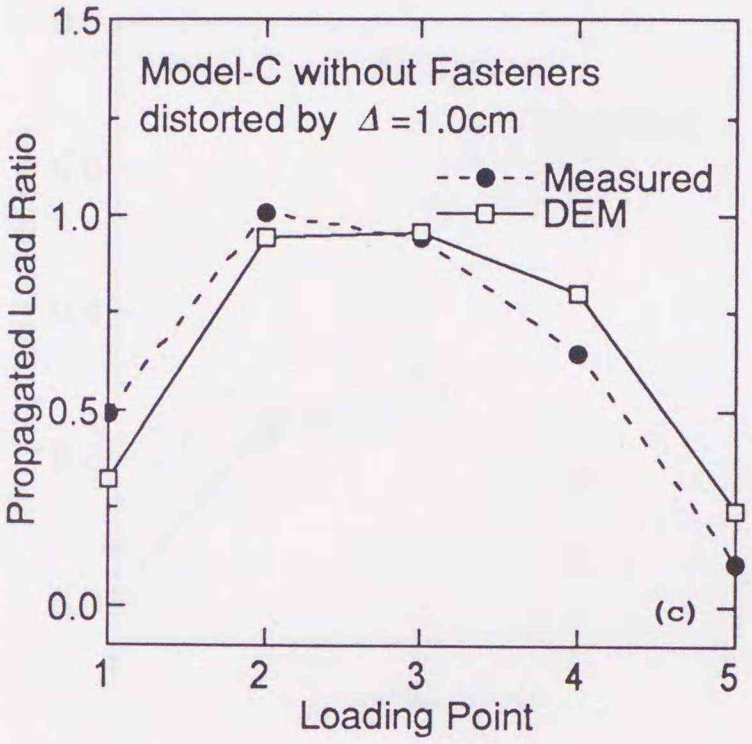

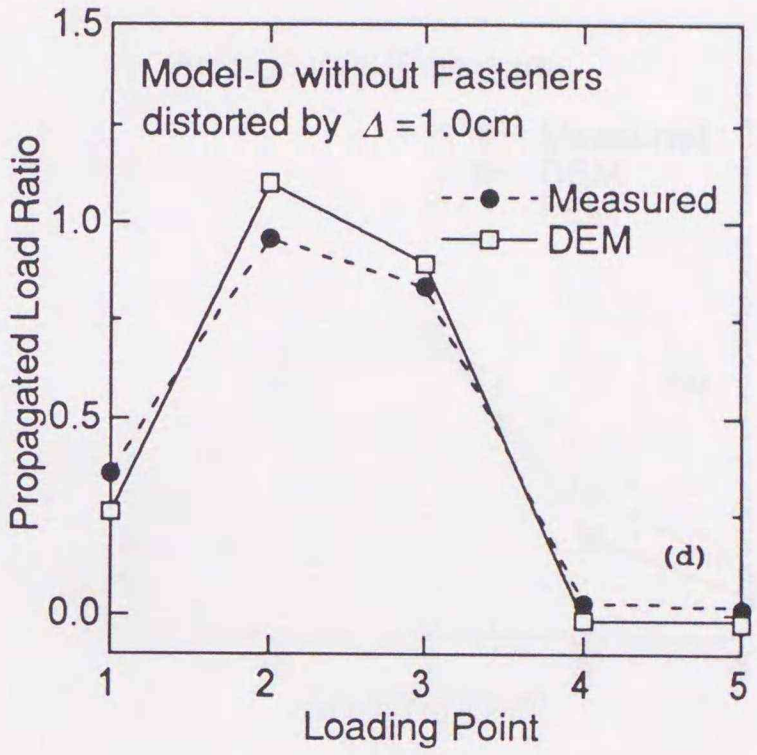

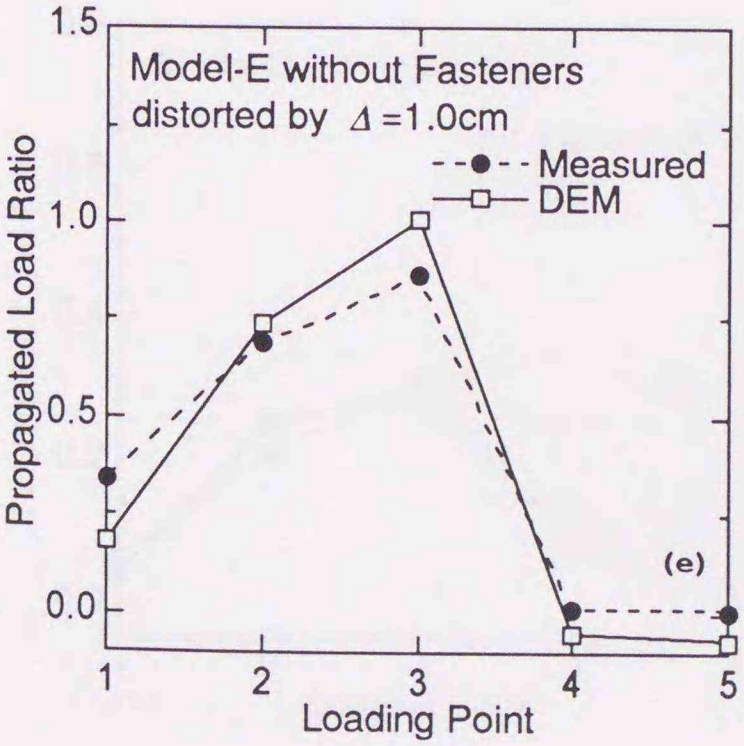

Figs. 1.14 (a)-(e). Comparison between measured and calculated load propagation properties for distorted modell fills without fastener; (a) Model-A, (b) Model-B, (c) Model-C, (d) Model-D, (e) Model-E

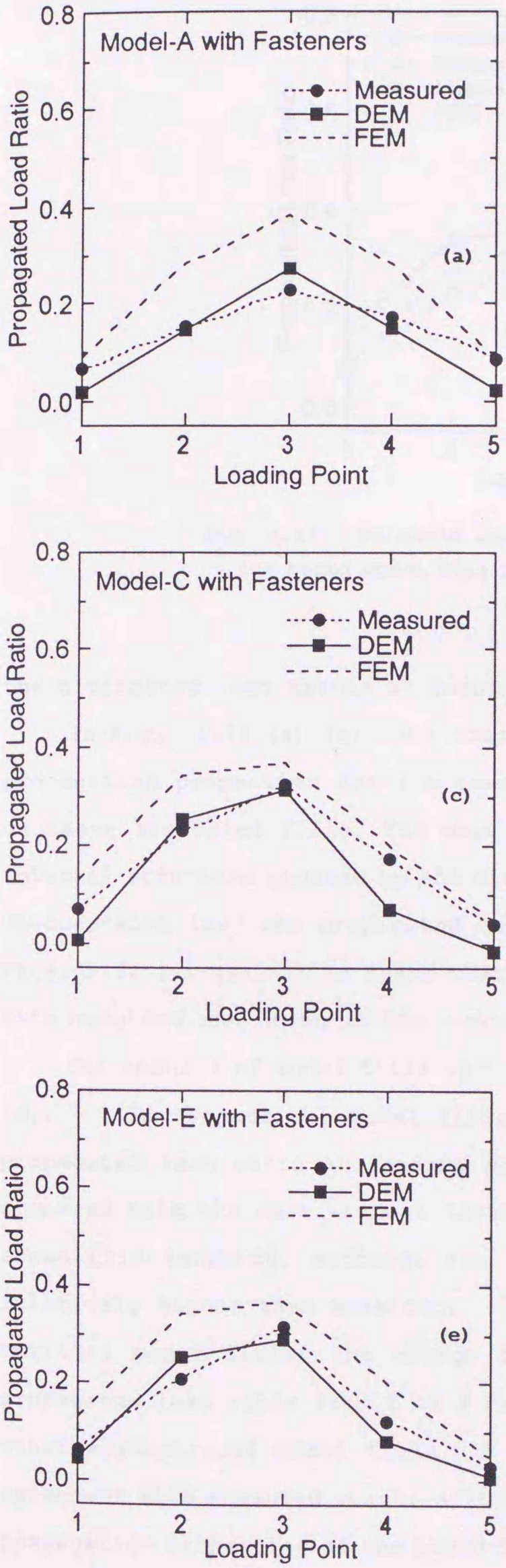

Figs. 1.15 (a)-(e). Comparison between measured and calculated load propagation properties for modell fills wit fasteners; (a) Model-A, (b) Model-B, (c) Model-C, (d) Model-D, (e) Model-E

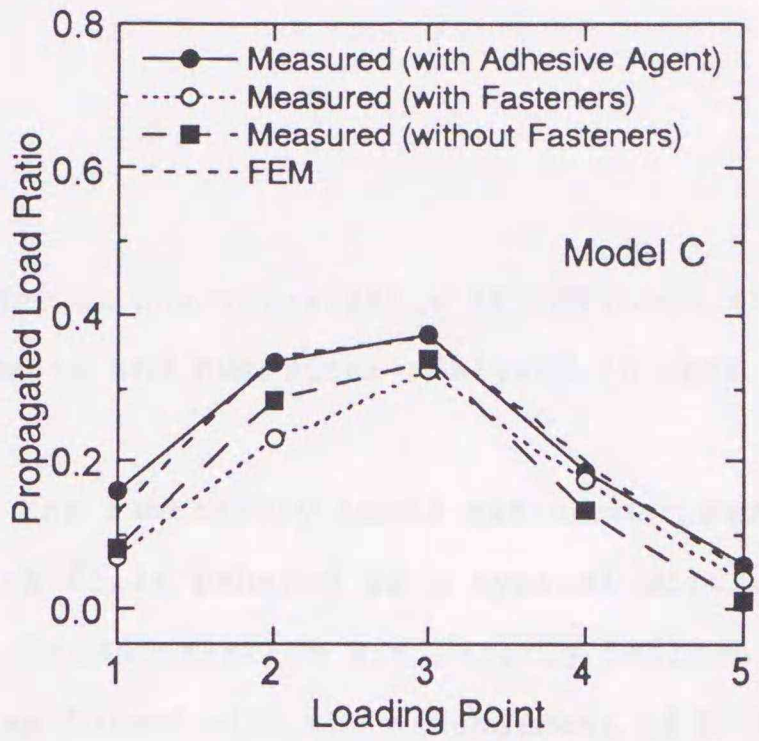

Fig. 1.16. Measured and calculated load propagation of the bound model fill of Model-C.

the propagated load ratios at loading point 4 and 5 are small extremely.

In Figs. 1.14 (a)-(e), the comparison of measured and calculated load propagation properties for the case of distorted model fills are shown. On these distorted fills, FEM were not conducted, because the change in internal structure induced by the distortion cannot be accounted by FEM and unacceptable load was propagated to the bottom EPS block. As shown in Figs. 1.14 (a)-(e), it is found that DEM calculation gives good agreements with measured one, even in the condition with disturbance.

The results of model fills with fasteners are shown in Figs. 1.15 (a)-(e). In symmetrical model fills (Model-A and Model-B), the measured propagated load ratio at loading point 3 in Model-B is relatively small compared with the case without fasteners shown in Fig. 1.15 (b), DEM also shows this tendency, although the quantity of propagated load ratio is relatively higher than measured. And in Model-D which is one of asymmetrical model fills, the change of loading point which gives maximum propagated load ratio from 2 to 3 can be simulated by DEM. Moreover in other asymmetrical model fills, it can be said that the DEM shows good agreement with measured quantitatively. It should be noted that the load propagation properties of the bound EPS block fill where constituent blocks were adhered one another with adhesive agent, is explained by the FEM as shown in Fig. 1.16.

1.5. Summary

The load propagation characteristics of EPS block fill were examined by a series of model tests and numerical analyses in this chapter.

The results of the laboratory tests are summarized as follows:

1) The EPS block fills behaved as a typical discrete media, the load propagation characteristics are largely influenced by their internal structures formed with the arrangement of EPS blocks. The load propagation intensity and the loading point which gives maximum propagated load, were changed with the difference in their internal structures; it was emphasized especially between the model fills with and without vertical continuous joints.
2) The effect of fastener on load propagation properties was recognized just after the application of loads; however, the effect was restricted and the improvement of load propagation properties was diminished under static loading condition or long term lading condition. The EPS model fill which was left for three days after installing fasteners, behaved as the model fill's without fasteners.
3) The load propagation of the EPS block fills which are subjected to distortion behaved in rather different manner with the EPS block fills without the distortion; even the slight distortion as 1.0 cm for the fill with 62.5 cm in height changed strongly the load propagation properties, and even if the disturbance of the EPS block fill is slightly and notable load concentration was recognized.

The results of the comparison of the numerical analysis and the laboratory tests are summarized as follows:

1) DEM shows enough applicability to the EPS block fills in various situation of the model fills; the effects of arrangement of EPS blocks, installation of fasteners and distortion can be explained by the static DEM.
2) FEM could be applied only to the EPS block fill bounded with

adhesive agents which behaved as a continuum media. Even in the case with fasteners, the FEM adopted in the present study could not explain the load propagation properties.

Chapter 2. Experimental Investigation of Deformation Characteristics of EPS Fill

2.1. Deformation Test

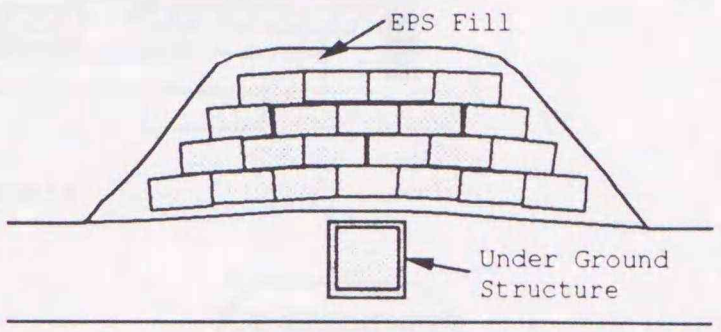

Fig. 2.1. EPS fill constructed on the culvert structure.

The aim of the deformation test is to observe the deformation behaviors of the EPS model fill; the situation of this test corresponds to actual EPS block fill which is suffered from the differential settlement of foundation ground. Of course, as EPS block is light weight material, it is thought that the differential settlement is not occurred frequently. But in situation as shown in Fig. 2.1, the stiff underground structure underlays EPS fill, it can be said that the possibility of occurring differential settlement is not small.

Initially, the EPS model fills were subjected to uniform overburden pressure of 1.7 kPa, and distorted by jacking up and down in vertical direction. At first, the EPS model fills were displaced upward with the step of Δ = 5.0 mm, then returned to original position with step of Δ = 10.0 mm. At each displacement step, the photos were taken and the jack was hold for one or two minutes to measure the load at steady state.

The measurements were carried out on the reaction by the load cell set to the jack, and each displacement of EPS blocks were measured by the image processing technique. This test series was carried out only on model fills without fasteners, due to the previous mentioned reasons in Chapter 1., 1.2. Loading Test.

2.2. Image Processing Method

In deformation test, it is difficult to measure the displacements of

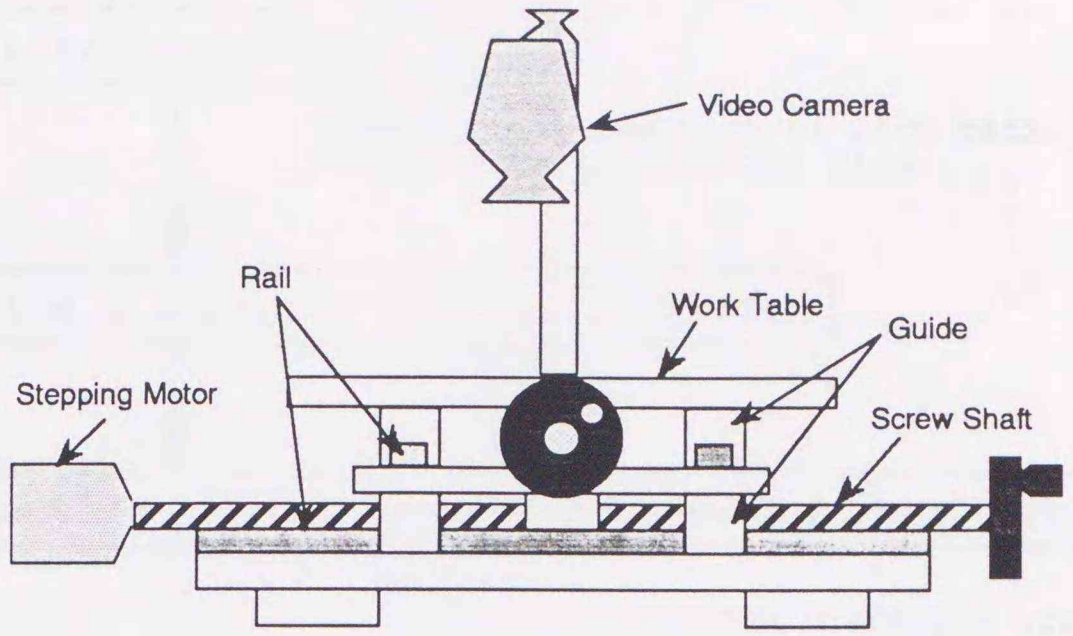

(a) X-Y Table

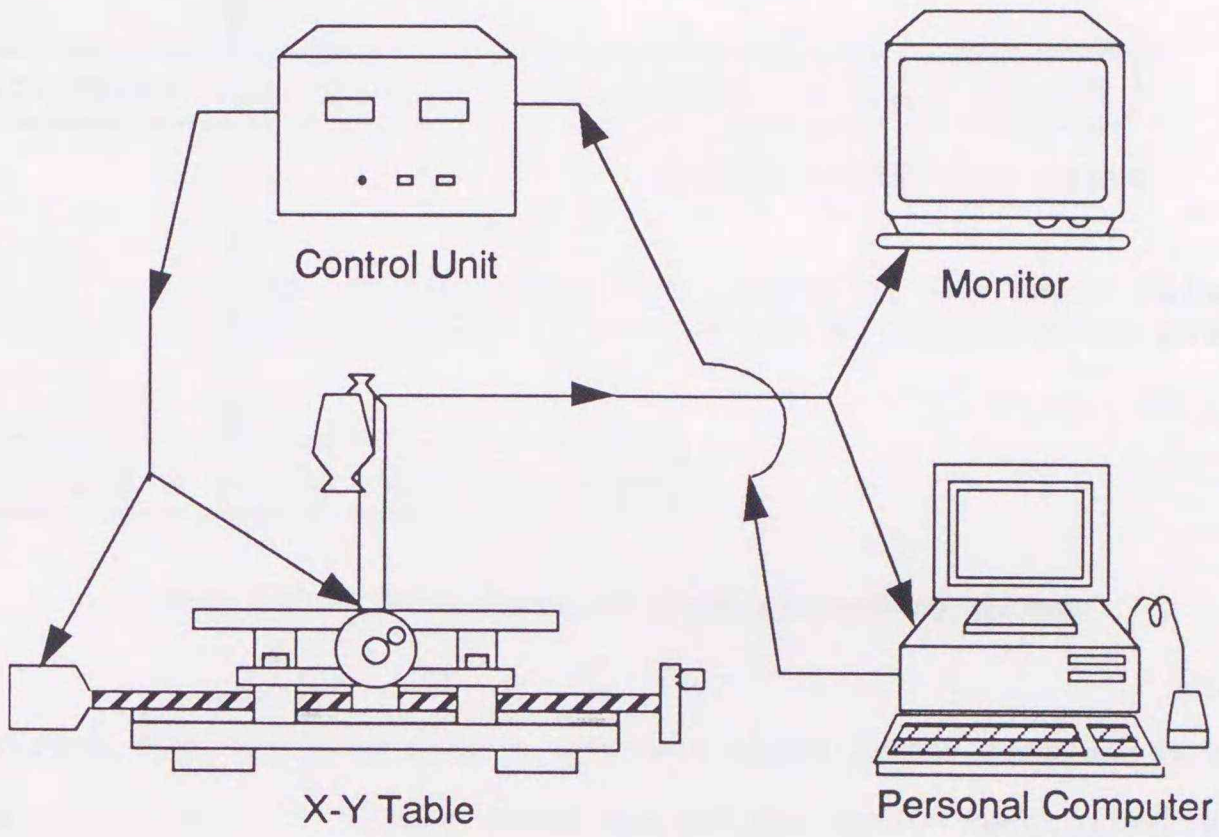

(b) Whole system for image processing

Figs. 2.2 (a), (b). Image processing system for determining the displacements of EPS blocks; (a) X-Y table, (b) whole system for image processing.

each EPS block directly by some gauges which contact to EPS blocks. Then by using the image processing method, the displacements of EPS blocks were measured.

During the deformation tests for investigating the deformation behavior of EPS fills, photos were taken at each step of jacking up and down by optical camera, whose collimating axis was set exactly perpendicular to the front face of the fills. Developed and enlarged photos were put on X-Y

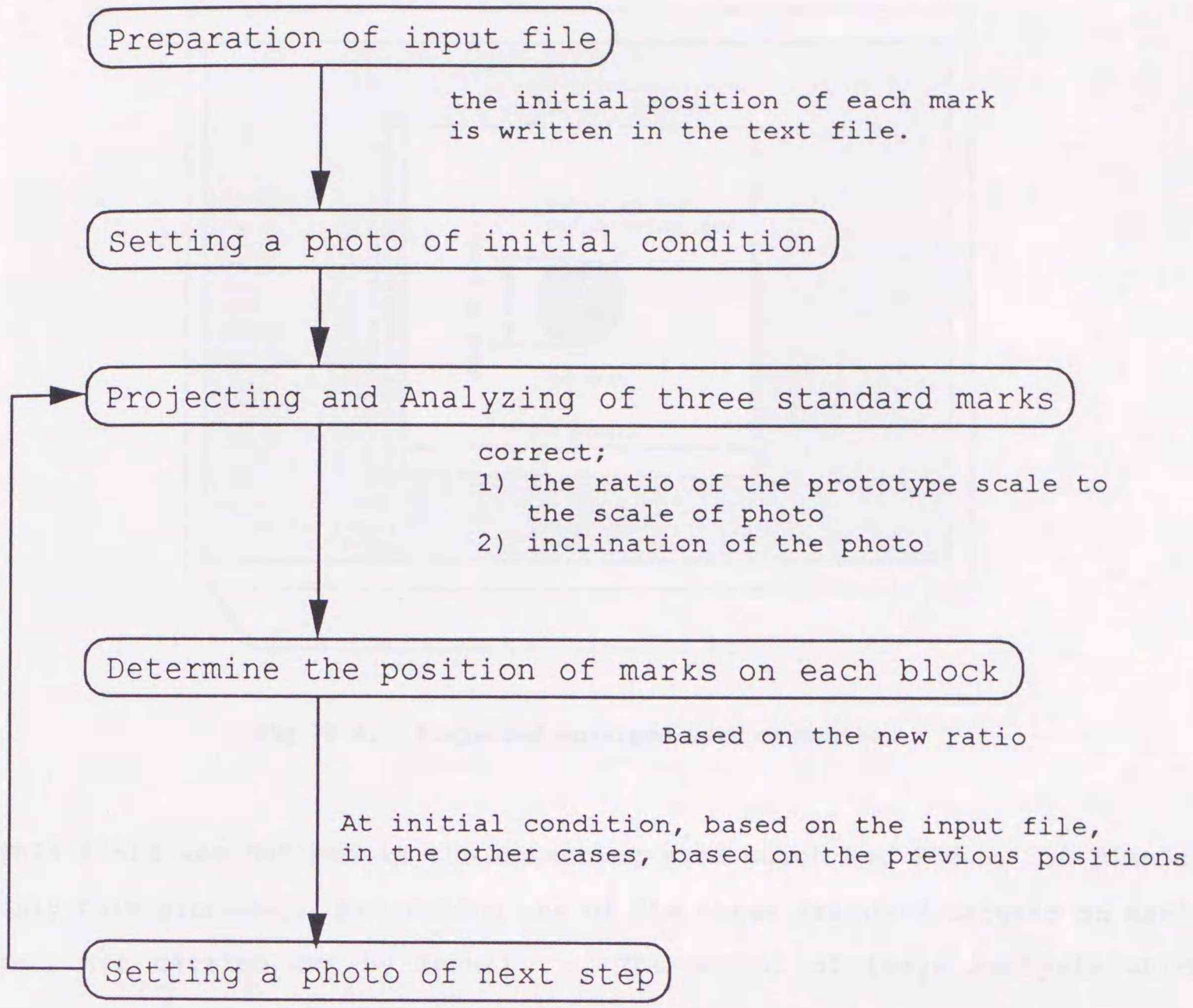

Fig. 2.3. Flow chart of image processing method.

table devising two stepping motors and one fixed video camera, as shown in Figs. 2.2 (a), (b). These stepping motors were controlled by micro computer, and the field of video camera was taken into the micro computer.

On the model fills, three black circular target for reference field were fixed on the supporting frame, and two black targets also set to the front of each EPS block. The positions of each target included the standard targets in initially condition and the approximately ratio of prototype scale to scale in photos, were inputted to the computer code for image processing by the form of text file in advance.

The flow chart of the image processing technique developed for this test is shown in Fig. 2.3. First, one of previous three standard targets was projected by video camera with enlarged, and the field taken into the micro computer was converted to black and white picture by means of the contrast between black targets and white EPS blocks as shown in Fig. 2.4.

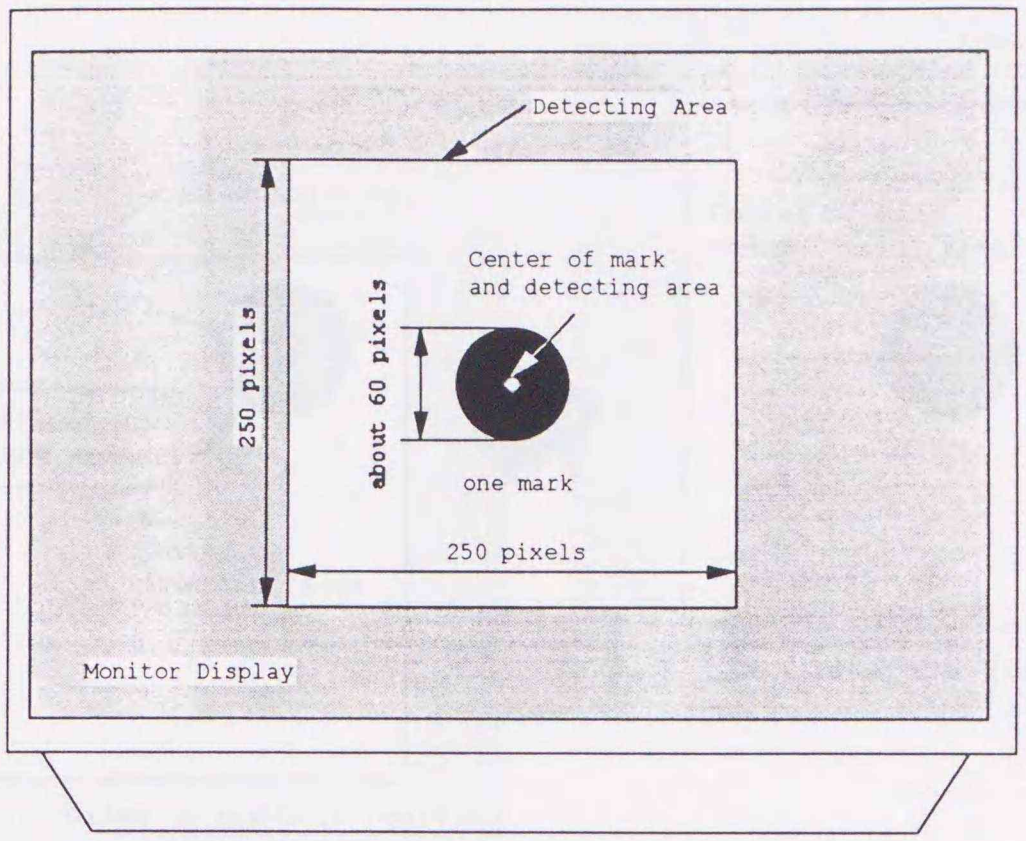

Fig. 2.4. Projected enlarged mark on monitor.

This field was defined as the detecting area which had 250 × 250 pixels, only this procedure, projecting one of the three standard targets on monitor, was carried out by manual. The method of image analysis which convert color image to black and white picture are described later. Then, the center position of the enlarged black target was determined in monitor with computer code; the centroid of the black area was assumed as the center of the target. As this determined position of the centroid was showed in form of coordinates in monitor, when the position of the centroid was not correspond to the center of monitor, the X-Y table was moved so as to adjust it. Then the micro computer make move the X-Y table to the second standard targets, according to the previous input ratio of prototype scale to photo scale. In almost cases, the centroid of second standard target was not correspond to the center of monitor, because the given ratio was approximate value. In this time, the ratio of prototype scale to scale of photo was corrected, based on the measured length of between the first standard target and the second one. In same way, the third standard target was detected by the micro computer, the ratio of prototype scale to scale of photo was corrected once again, and the inclination of the photo against monitor was also detected.

After the EPS model fill was suffered from some distortion, as the

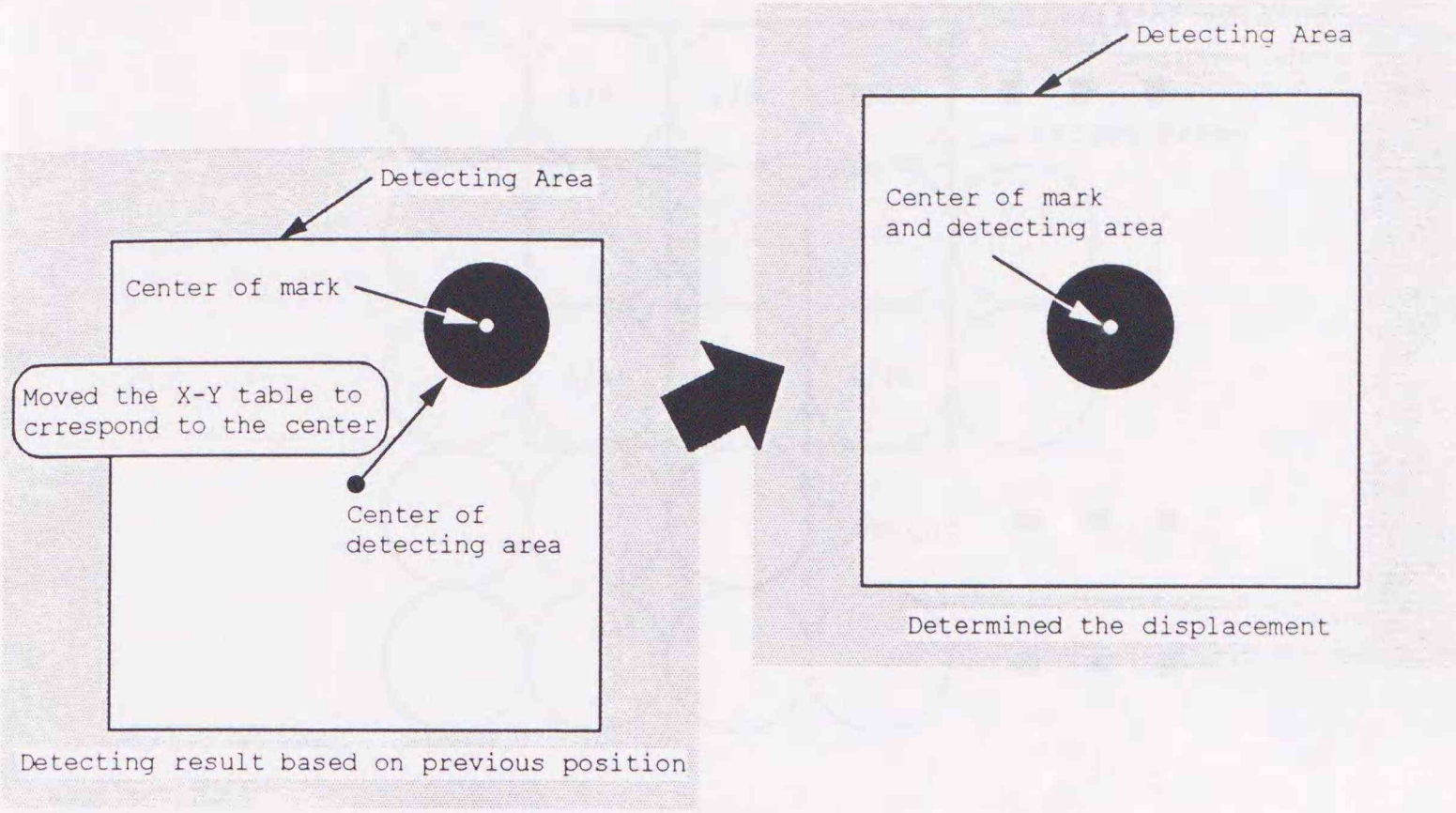

Fig. 2.5. Determination of displacement of target.

displacement of target was small enough to enter the detecting area, the X-Y table was moved to the position of previous displacement step and the centroid was determined as shown in Fig. 2.5. When the whole target did not exist in the detected area, as the determined centroid did not correspond to the center of monitor, the X-Y table was made move so as to fixed it. This procedure was carried out repeatedly, until the determined centroid appears on the center of monitor. And then at the next step, based on this new position, the X-Y table was moved.

In image analysis method which convert the full color field to black and white picture, the local weighted average method was adopted as smoothing method. As the brightness of each pixel of monitor was given, with a determined threshold value, the color of pixels was judged; when the brightness of a pixel was larger than the threshold value, the pixel was identified as a white pixel, otherwise the pixel was identified as a black one. When the convert was carried out without using smoothing method, the shape of targets was sometimes deformed by some noise or difference of lightening. Fig. 2.6 shows the detail of smoothing method.

By using this system, individual targets were taken into the micro

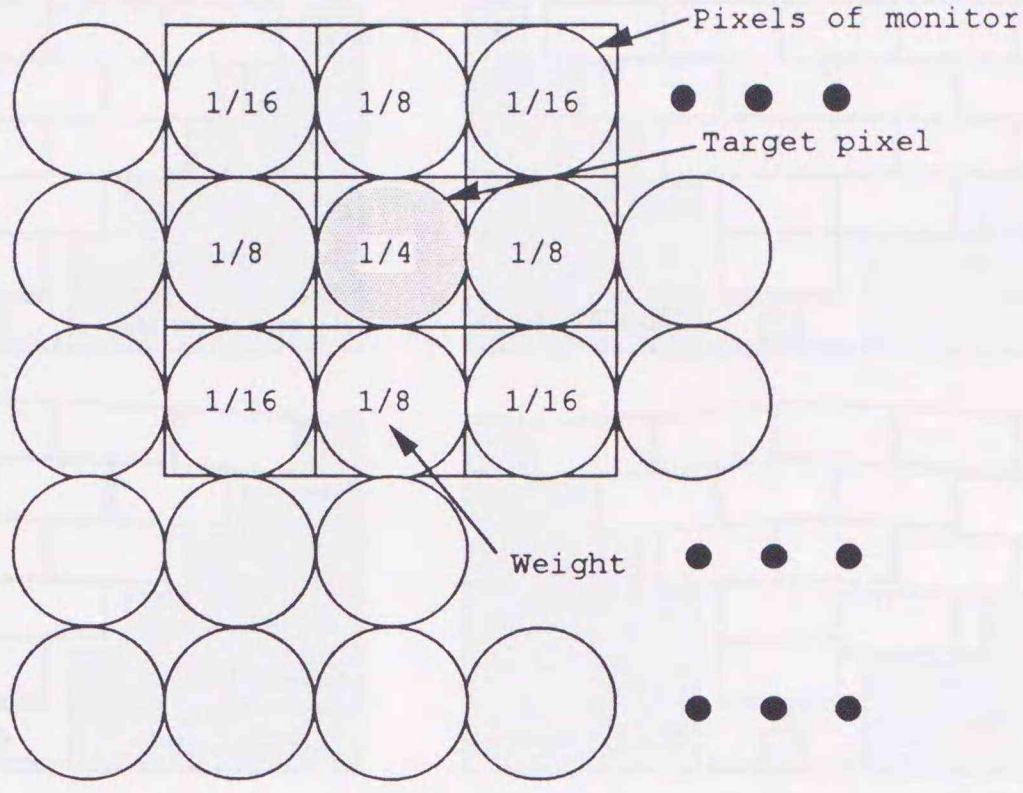

Fig. 2.6. Local weighted average method.

computer with scaling up, and the accuracy of image analysis became high and made it possible to determine the target's position with the accuracy of 2.0 mm.

The measured deformation behavior of the EPS model fill can be represented on computer screen in an animation form; this makes it possible to compare the measured and calculated deformation behaviors in visually.

2.3. Test Results and Discussion

Shown in Figs. 2.7 (a)-(e) and Figs. 2.8 (a)-(e) are the measured deformation behaviors of Model-A and Model-C without fasteners during a single cycle of distortion by vertical displacement of supporting plate; the displacement of each EPS block were determined with previous image processing method. It should be noted that somewhat errors for searching the position of the targets on the block surface are seen in these figures; the error is considered to be at most 2.0 mm.

At even small displacement, the EPS blocks began to separate from adjacent blocks, and gap appeared significantly at most interfaces. At large displacement, sliding of some blocks was observed. The large

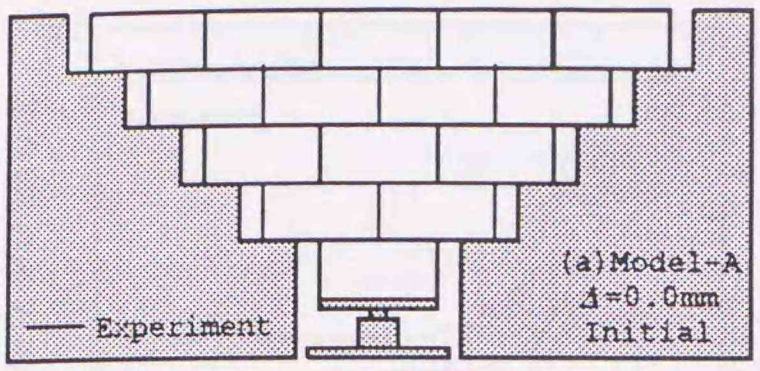

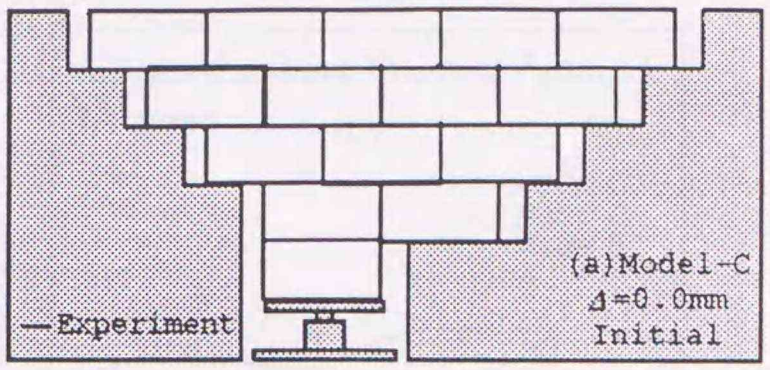

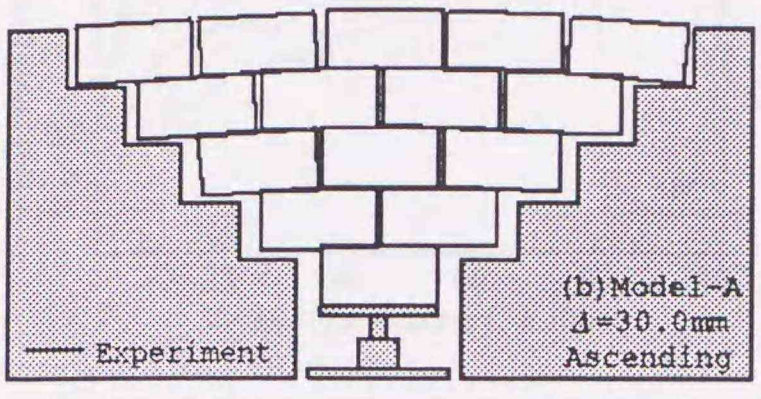

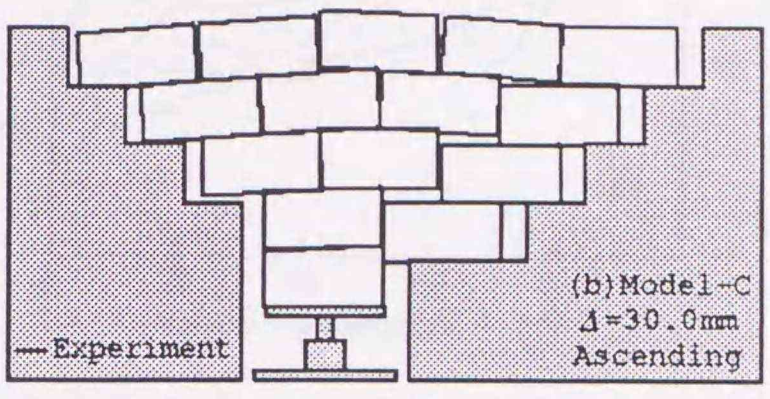

Arch Action

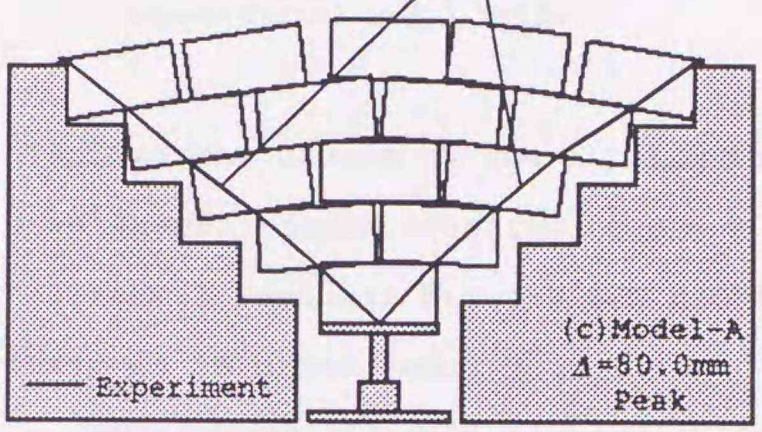

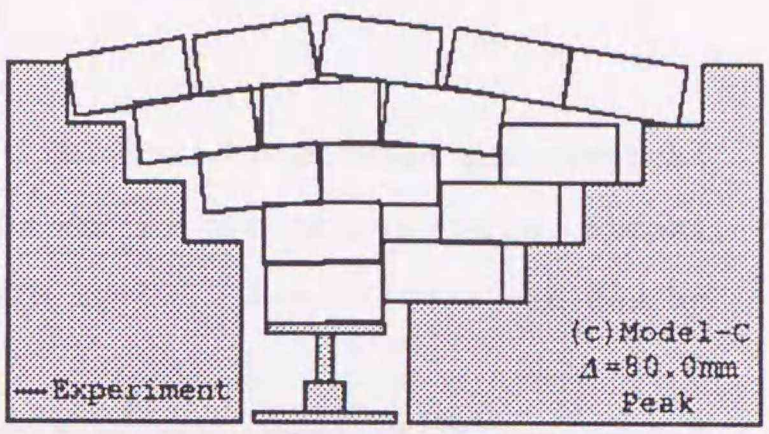

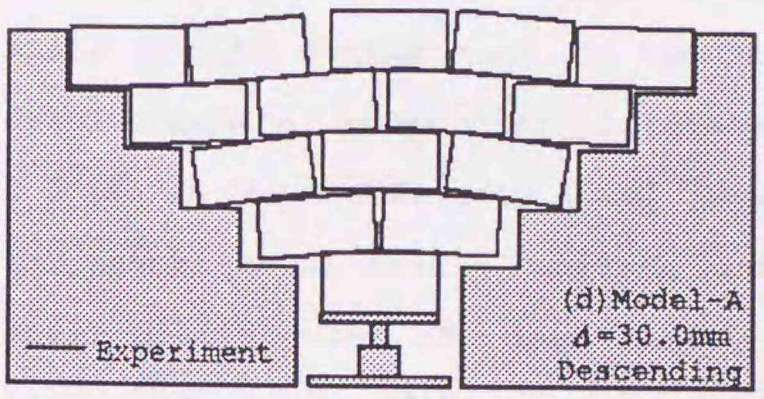

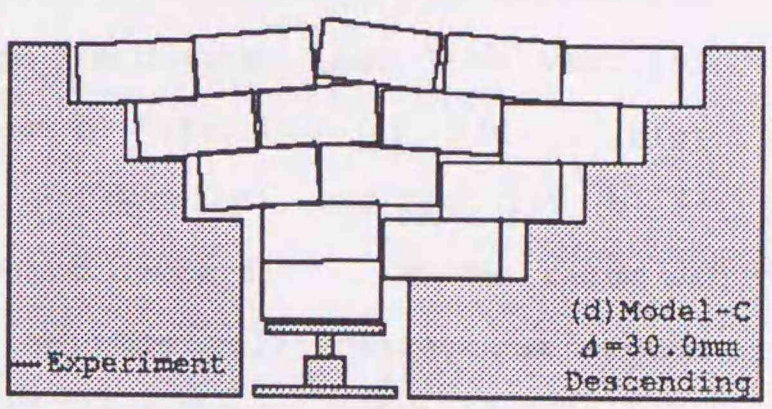

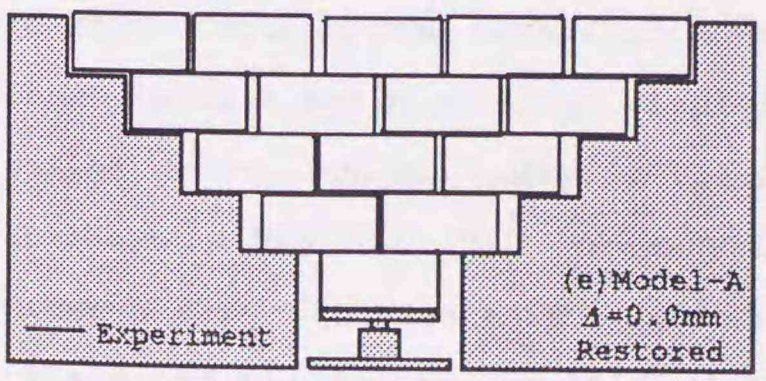

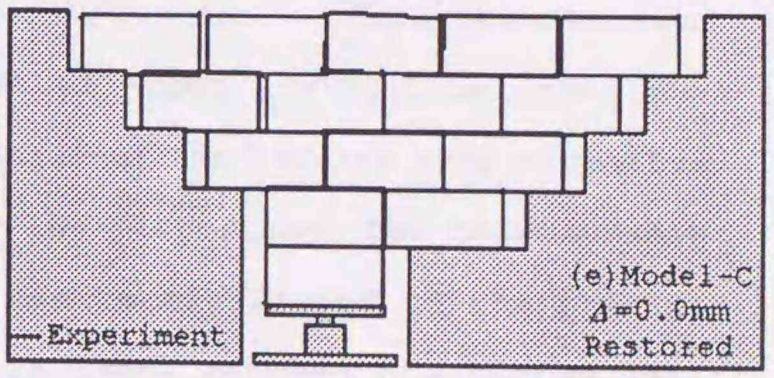

Figs. 2.7 (a)-(e). Observed deformation behavior of Model-A; (a) initial state, (b) ascending (Δ =30.0mm), (c) peak (Δ =80.0mm), (d) descending (Δ =30.0mm), (e) restored.

Figs. 2.8 (a)-(e). Observed deformation behavior of Model-C; (a) initial state, (b) ascending (Δ =30.0mm), (c) peak (Δ =80.0mm), (d) descending (Δ =30.0mm), (e) restored.

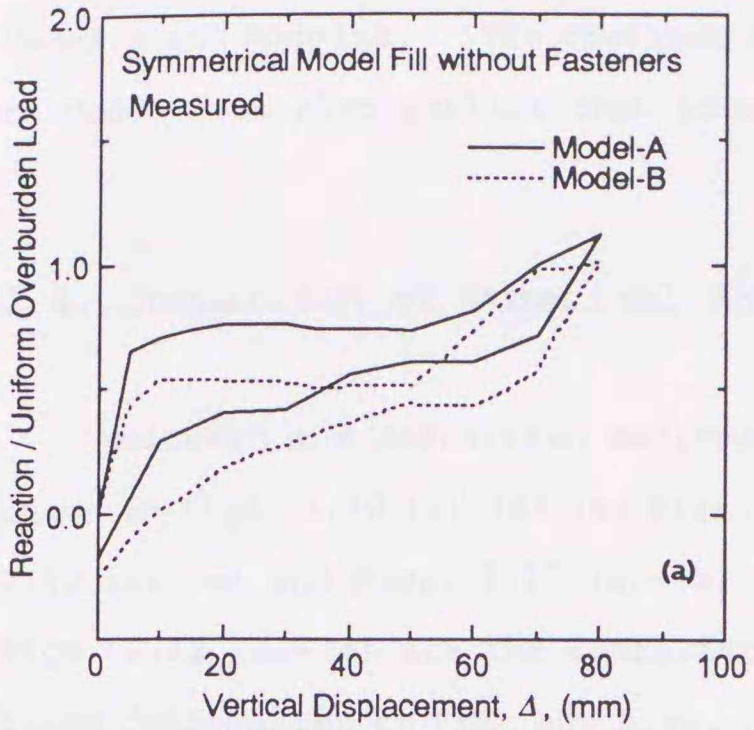

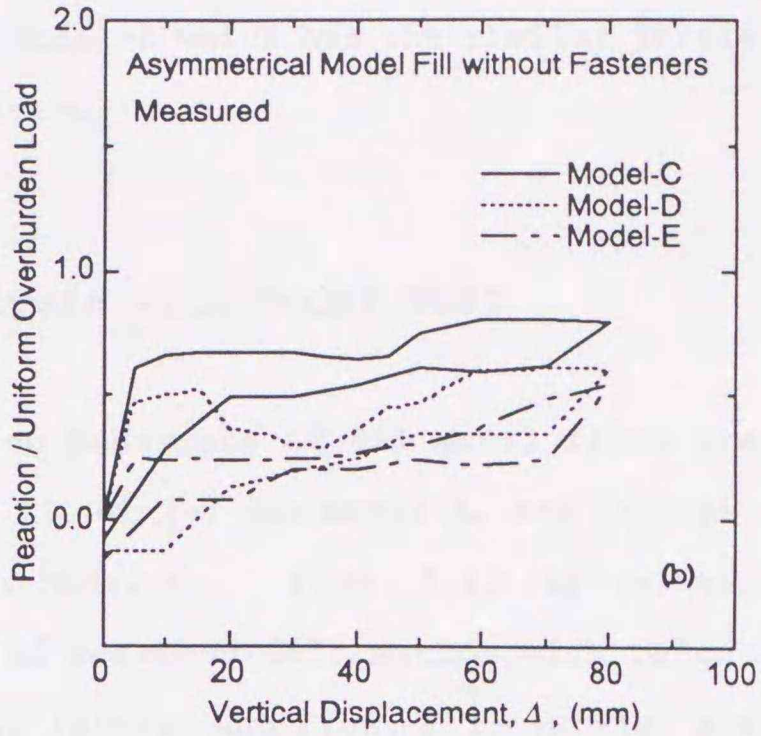

Figs. 2.9 (a), (b). Ratio of reaction to overburden load - vertical displacement for modelfills without fasteners; (a) for symmetrical model fills, (b) for asymmetrical model fills.

displacement caused by the sliding was not recovered even when the vertical displacement Δ was restored to $\Delta = 0$ at the end of distortion cycle, almost horizontal contacts between EPS blocks were lost. Similar feature can be observed in other model fills.

The measured relationships of the ratio of the reaction at supporting plate of the bottom jack to the uniform overburden load with vertical displacement of supporting plate are shown in Figs. 2.9 (a), (b). Fig. 2.9 (a) is for symmetrical model (Model-A and Model-B), and Fig. 2.9 (b) is for asymmetrical model (Model-C, Model-D and Model-E). In the range of small displacement of less than $\Delta = 5$ mm, the relationship was seemed linear; however, after the initiation of gaps between EPS blocks, the reaction force became rather constant or fluctuated. Then the reaction began to rise again at large displacement of about $\Delta = 50.0$ mm; this re-rising in reaction was caused by the formation of the inverse arch structure as shown in Fig. 2.7 (c). In a cycle of the distortion, the relationship draws a part of hysteresis loop, which may be attributed to the partial release of the friction mobilized at interfaces between EPS blocks initially.

In Model-B and Model-D whose internal structures are separated by the vertical continuous joints, the reaction is relatively small compared with

Model-A and Model-B. The reaction in Model-E which has the similar joints to Model-D is also smaller than in model-C.

2.4. Comparison of Numerical Analysis with Model Test

Measured and calculated deformation behaviors of EPS model fills are shown in Figs. 2.10 (a)-(e) and Figs. 2.11 (a)-(e) for model-A, and in Figs. 2.12 (a)-(e) and Figs. 2.13 (a)-(e) for Model-C. Figs. 2.10 (a)-(e) and Figs. 2.12 (a)-(e) are the comparison of measured deformation with calculated deformation by FEM, and Figs. 2.11 (a)-(e) and Figs. 2.13 (a)-(e) are the comparison of measured deformation with calculated deformation by DEM. While the FEM employed in the present study is unable to simulate the separation and contact between blocks, DEM can simulate the displacements of individual blocks during distortion with sufficient accuracy as shown in the figures. As shown in Figs. 2.10 (a)-(e) and Figs. 2.12 (a)-(e), in FEM analysis, the deformation of bottom block is too large to accept it, and the top blocks of the model fills are not so rise. On the other hand, DEM is able to express the slide of side blocks to fixed blocks and the remaining of the gaps at restored position.

Shown in Figs. 2.14 (a)-(e) are comparisons of the measured and calculated relationship of the ratio of reaction to overburden load with vertical displacement: Δ for all the model fills. FEM predicts only linear relationships; however, DEM is able to predict the nonlinear hysteretic relationship and gives good agreement with the measured relationships.

On deformation properties as well as load propagation properties, the good applicability of DEM to EPS block fills are confirmed in comparison with FEM.

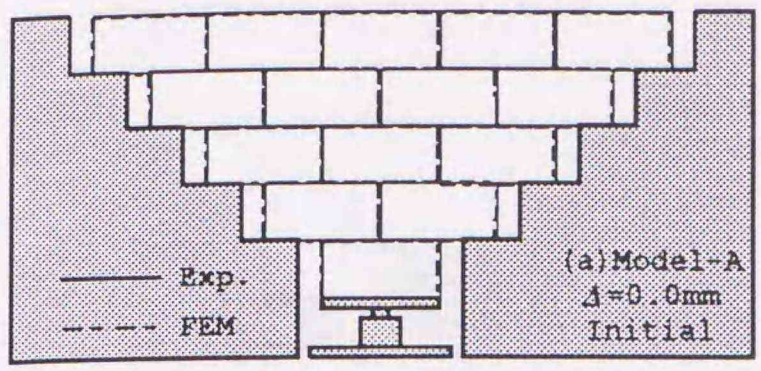

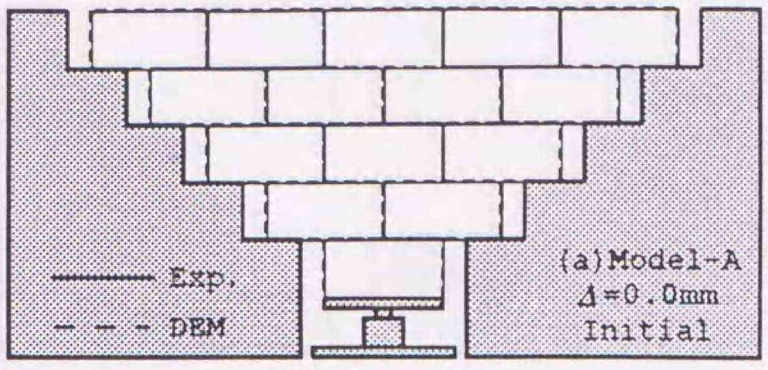

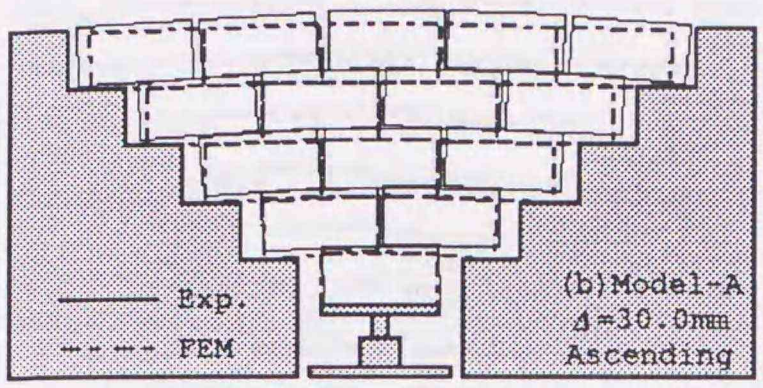

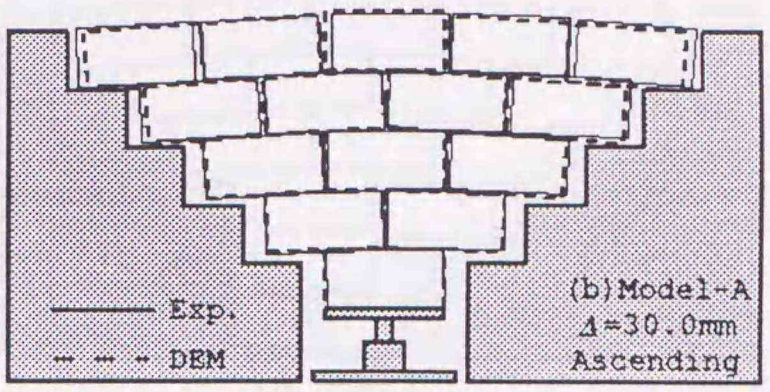

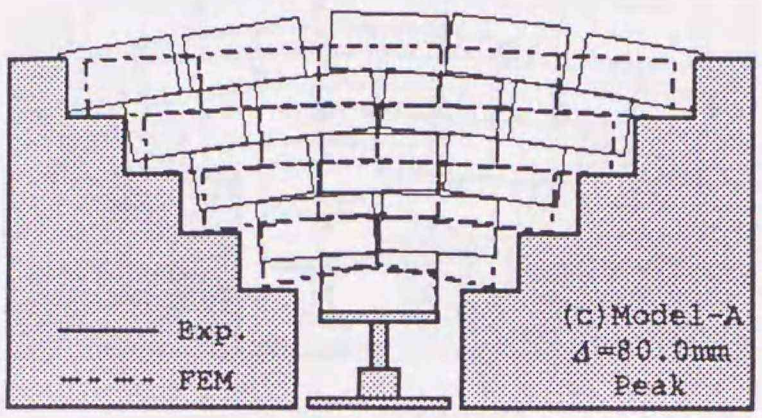

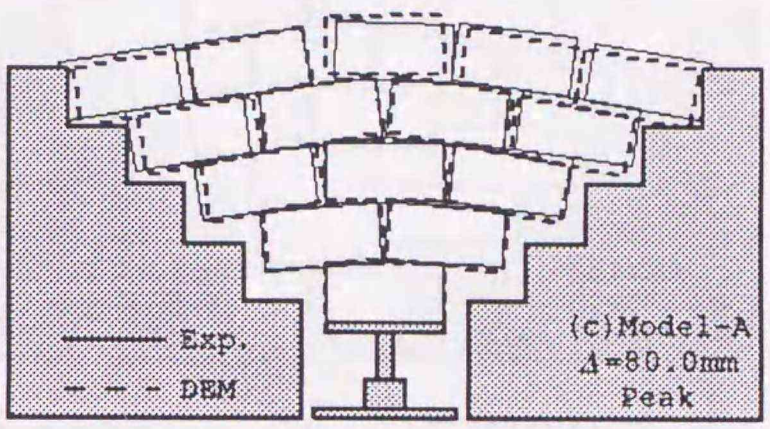

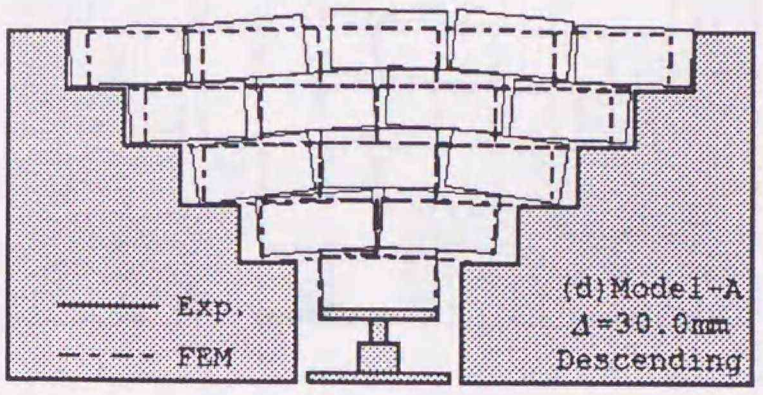

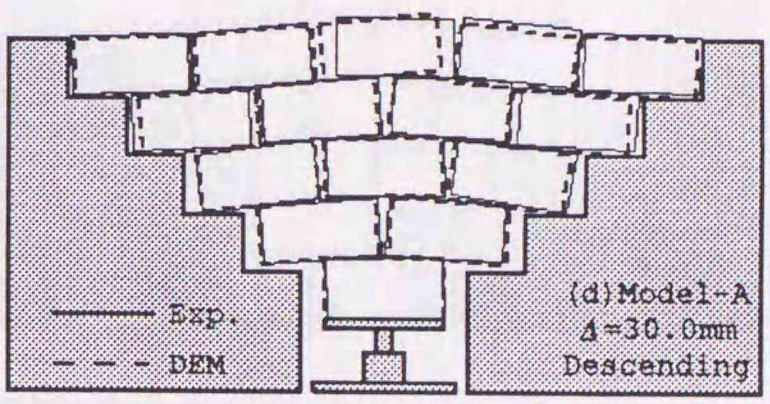

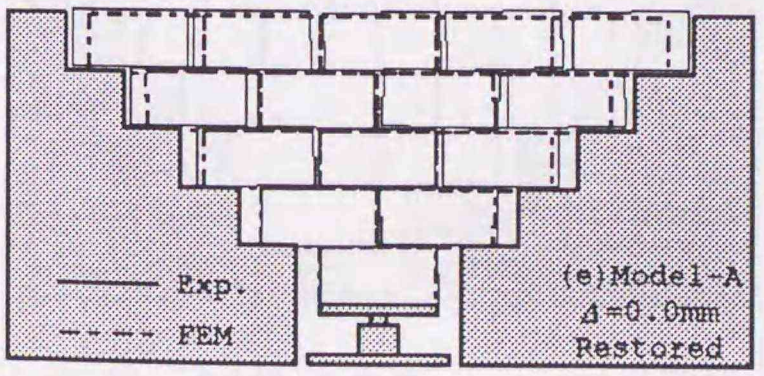

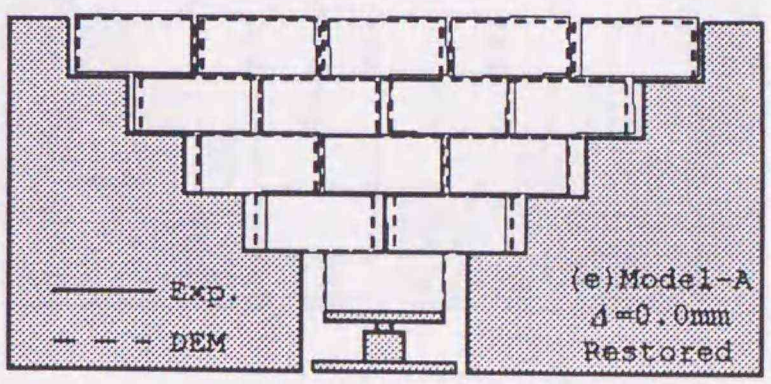

Figs. 2.10 (a)-(e). Comparison between measured and calculated deformation behaviors by FEM for Model-A; (a) initial state, (b) ascending (Δ =30.0mm), (c) peak (Δ =80.0mm), (d) descending (Δ=30.0mm), (e) restored.

Figs. 2.11 (a)-(e). Comparison between mesured and calculated deformation behaviors by DEM for Model-A; (a) initial state, (b) ascending (Δ =30.0mm), (c) peak (Δ =80.0mm), (d) descending (Δ =30.0mm), (e) restored.

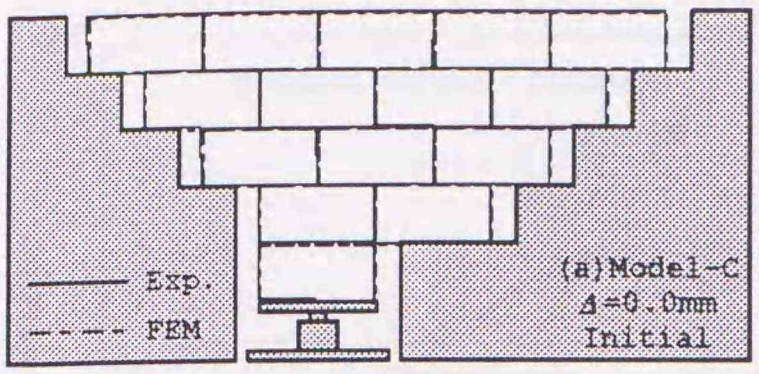

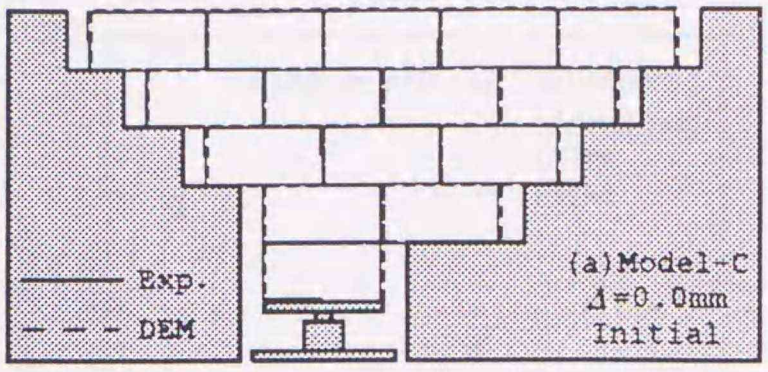

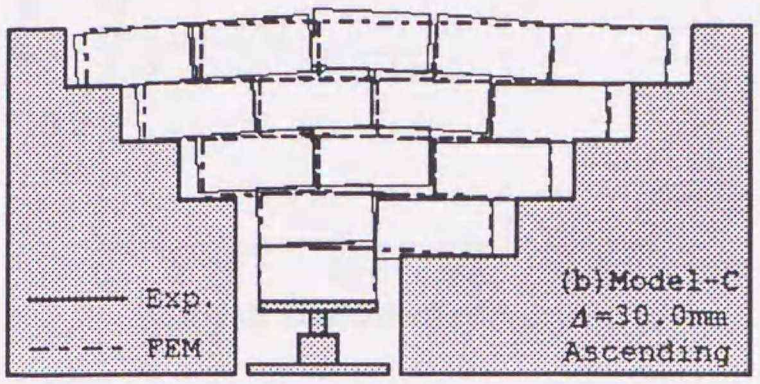

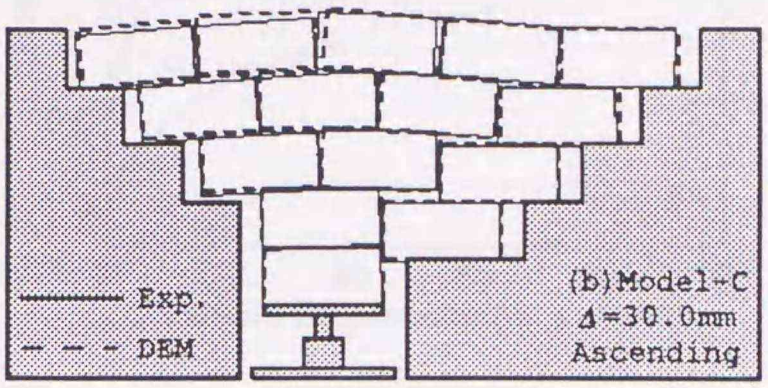

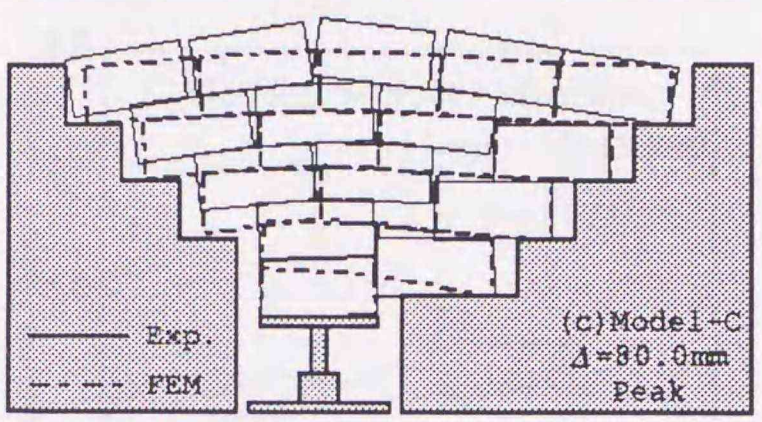

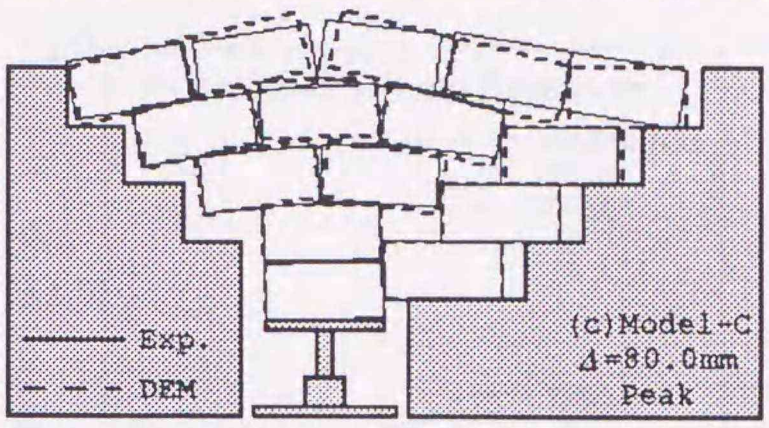

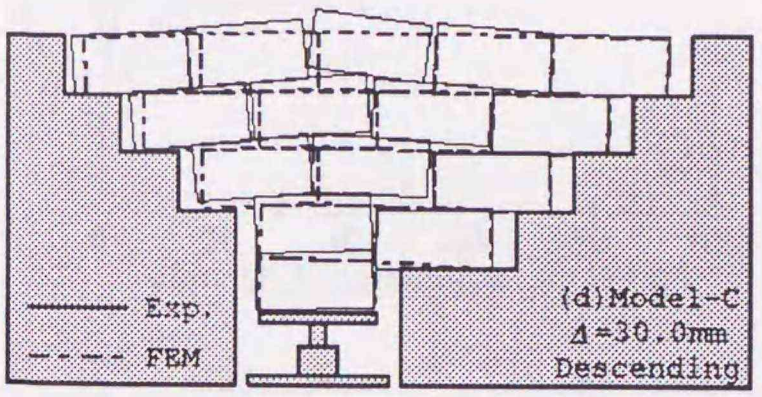

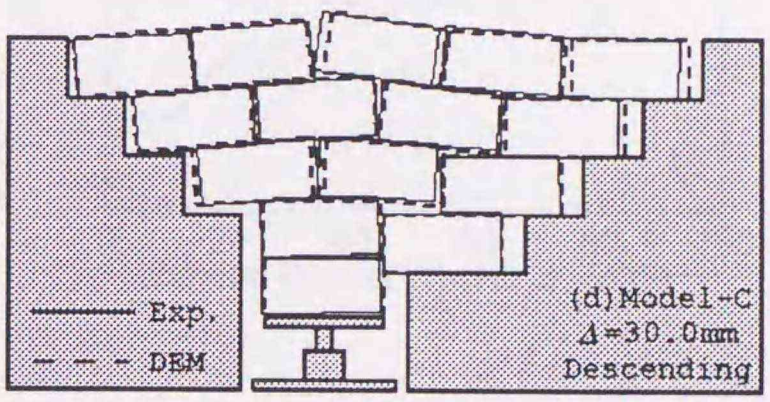

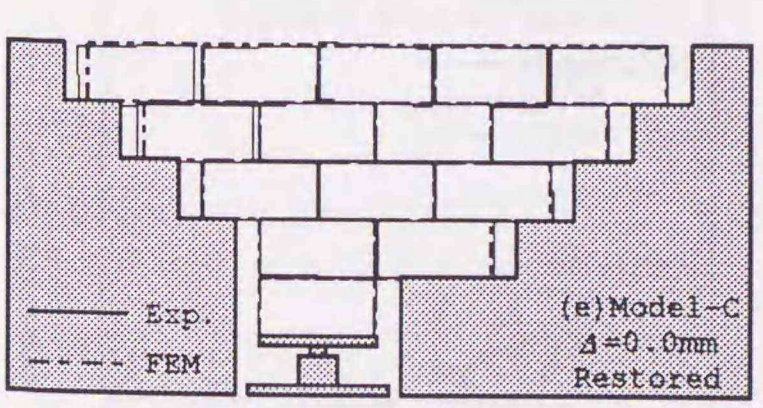

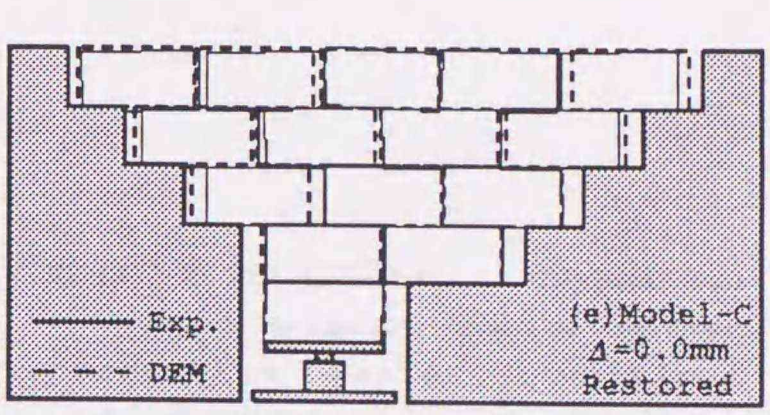

Figs. 2.12 (a)-(e). Comparison between measured and calculated deformation behaviors by FEM for Model-C; (a) initial state, (b) ascending (Δ =30.0mm), (c) peak (Δ =80.0mm), (d) descending (Δ=30.0mm), (e) restored.

Figs. 2.13 (a)-(e). Comparison between mesured and calculated deformation behaviors by DEM for Model-C; (a) initial state, (b) ascending (Δ =30.0mm), (c) peak (Δ =80.0mm), (d) descending (Δ =30.0mm), (e) restored.

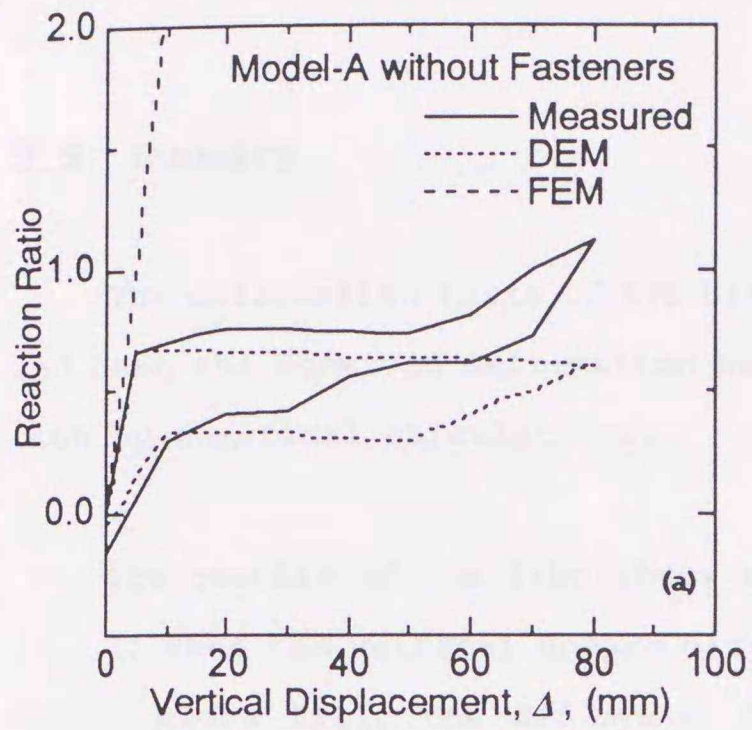

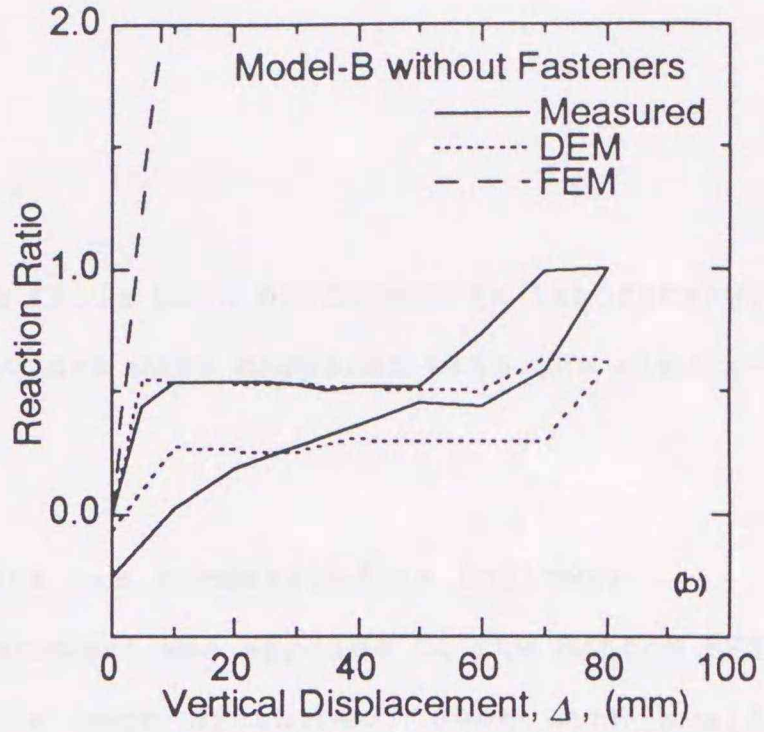

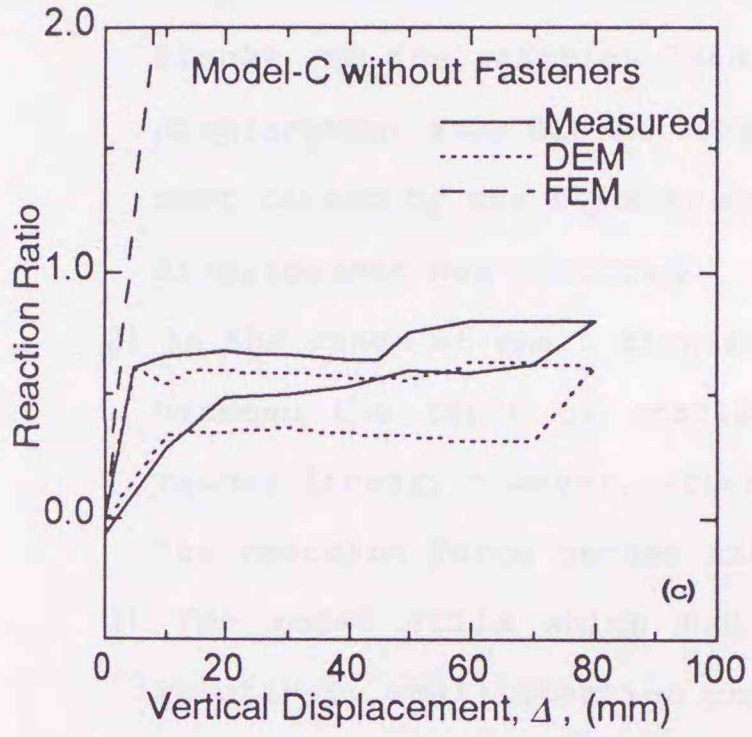

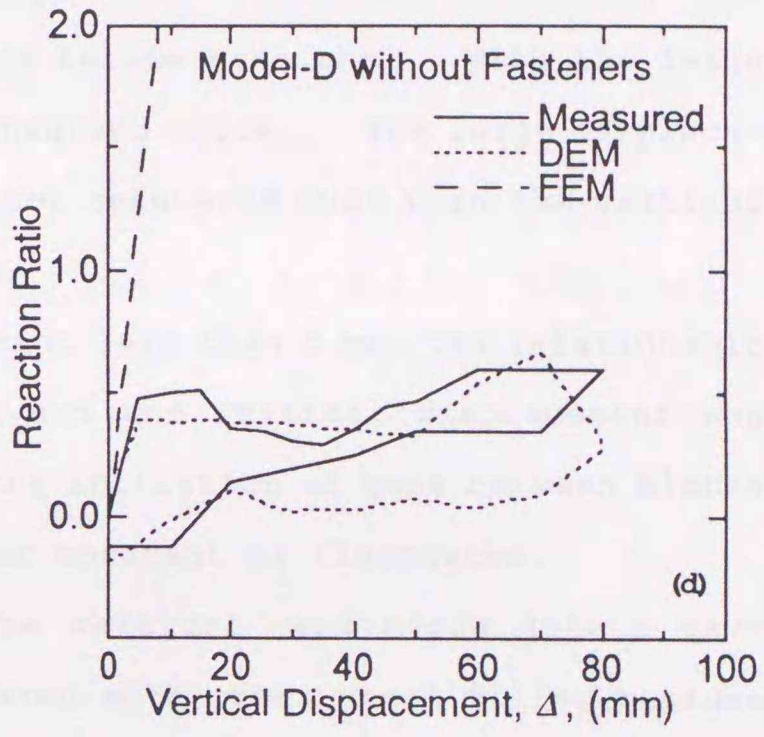

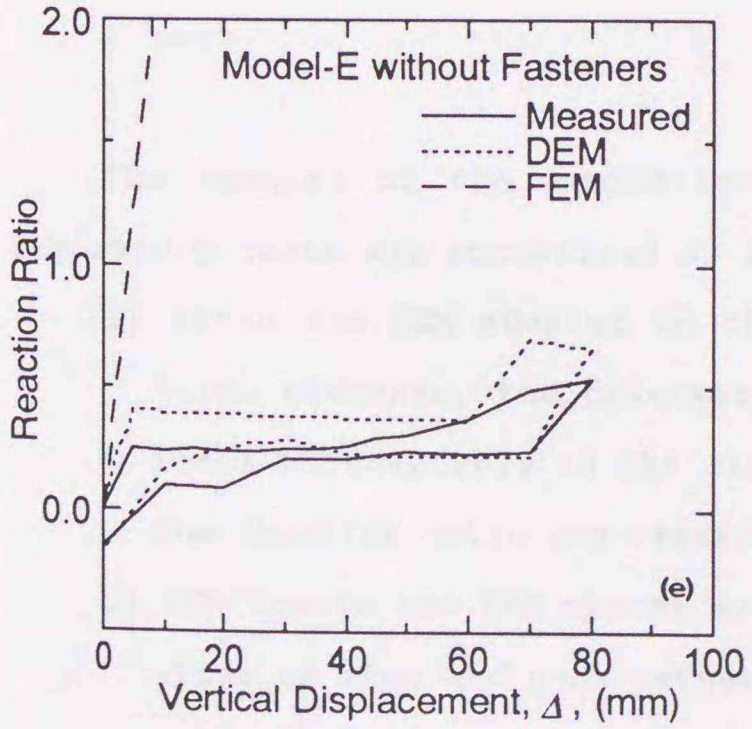

Figs. 2.14 (a)-(e). Comparison between measured and calculated reaction ratio - vertical displacement Δ relationships for the model fills without fasteners; (a) Model-A, (b) Model-B, (c) Model-C, (d) Model-D, (e) Model-E

2.5. Summary

The deformation tests of EPS block fills were performed in laboratory, and then the observed deformation behaviors were compared with the simulation by numerical calculations.

The results of the laboratory tests are summarized as follows;

1) When the vertical upward displacement was applied to the bottom EPS block fill, the EPS model fills were disturbed; even with small displacements the significant gaps which was enough to separate EPS blocks and the reaction load was became constant. With the large displacement some blocks were observed slide. The large displacement caused by the sliding was not recovered even when the vertical displacement was restored.
2) In the range of small displacement less than 5 mm, the relationship between the ratio of reaction and the vertical displacement was rather linear; however, after the initiation of gaps between blocks the reaction force became rather constant or fluctuated.
3) The model fills which had the vertical continuous joints gave relatively small reaction compared with other model fills, because their fill bodies were separated at early step of vertical displacement.

The results of the comparison of the numerical analysis with the laboratory tests are summarized as follows;

1) Since the FEM adopted in the present study considers no slip or joint elements, the deformation is concentrated at the bottom EPS block unacceptably in the simulation, and the relationship between the reaction ratio and vertical displacement showed only linearity.
2) DEM treats the EPS blocks as individual elements, and can take the slide of side and gaps between EPS blocks. The simulation by DEM is in good agreement quantitatively with the measured behaviors, in the relationships between reaction and vertical displacement.

Chapter 3. Estimation Method of Propagated Stress Distribution in EPS Fill

3.1. Objectives and Overview

As the forms of model fills in Chapter 2 and Chapter 3 were only inverse triangles, the examination of the mechanical behavior of prototype EPS block fills was some what limited. In Chapter 2 and Chapter 3, however, the applicability of DEM to EPS block fill has already been confirmed, then the mechanical behavior of EPS block fill were investigated by DEM analytically in this chapter.

The aim of this chapter is to make clear the stress distribution properties due to line load on horizontal foundation, and the simple estimation method of the stress distribution is proposed. In Chapter 5, the load concentration characteristics in EPS block fill subjected to foundation differential settlement are examined analytically.

3.2. Simplified EPS Fill

One of the prepared numerical analysis models for DEM is shown in Figs. 3.1 (a), (b), and the definition of the thickness H, width W of EPS block fill and the aspect ratio r (width w / height h) of cross section of EPS block which constitutes the EPS block fill are indicated. In all model fills, the height h of one EPS block is 0.5 m in common.

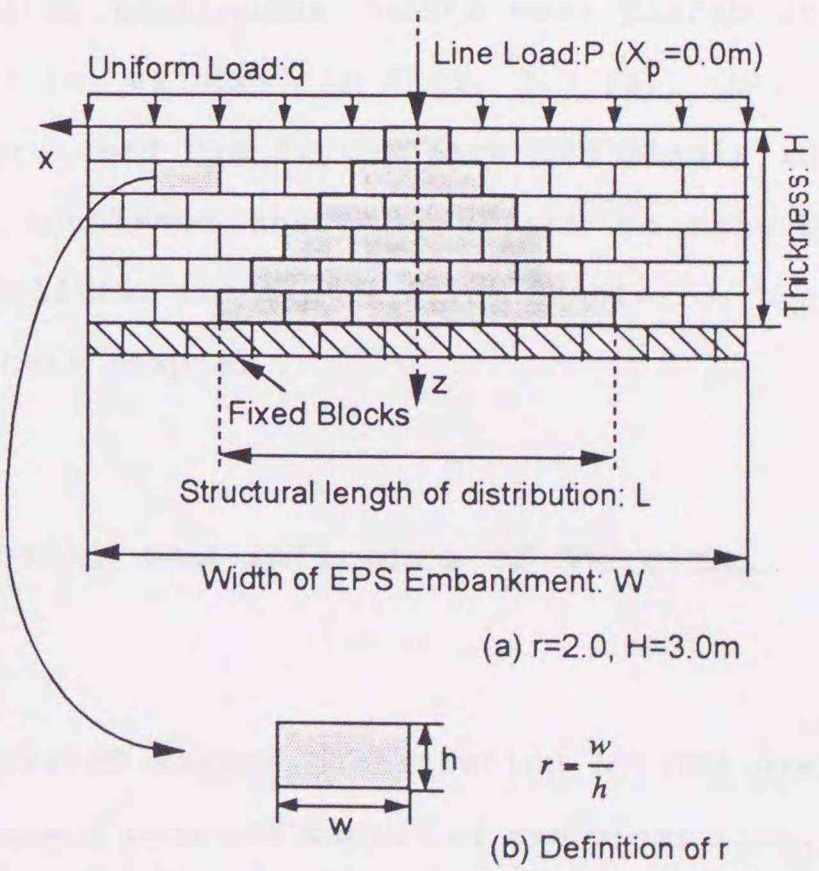

Figs. 3.1 (a), (b). Idealized EPS model fill; (a) Model of r=2.0 and H=3.0m, (b) definition of block aspect ratio: r.

At initial condition, uniform

stress q (9.8 kPa/m) were applied on the surface of all the EPS model fills, then the line load P (9.8 kN/m) were applied to the top-center block of EPS model fills. The shaded blocks placed at bottom line in Fig. 3.1 (a) are fixed, and the propagated stress only by line load P to these fixed blocks were assumed as the propagated stress p to foundation.

The thirty-five model fills are prepared in total, the basic models are five models which have different aspect ratio r (1.0, 1.5, 2.0, 3.0, 4.0), and each basic model have three different thickness H = 1.0, 1.5, 2.0, 2.5, 3.0 m. The model fill r = 1.0 is composed of square section EPS blocks, as the value of r gets large, the section of constituent EPS blocks of model fill was made oblong so as to eliminate the effect of the boundary. Since the size of prototype EPS block is 0.5 × 1.0 × 2.0 m, the aspect ratio r is 1.0 / 0.5 = 2.0 or 2.0 / 0.5 = 4.0; for this reason the aspect ratio was determined so as to cover this range.

The basic models whose thickness H is 3.0 m are shown in Figs. 3.2 (a)-(e), and the fill width W is 10.0 m in common except for the model fill of r = 4.0 whose fill width W = 20.0 m; the fill width was determined so as to be longer enough than the structural length of distribution L.

Moreover, each basic model of H = 3.0 m has two variations which have vertical continuous joint, the examples of model fill of r = 2.0 are shown in Figs 3.3 (a), (b). The vertical continuous joints were placed at distance of w or 1.5 w from center line, as shown in Figs. 3.3 (a), (b).

Although the steel fasteners are used for fixing each EPS blocks in situ construction, it was already confirmed that the effect on stress propagation characteristics was very little in Chapter 2 and Chapter 3, the fastener elements were not used in this chapter.

3.3. Stress Distribution Properties and Influence of Vertical Continuous joint

In Figs. 3.4 (a)-(c) the calculated stress distribution by DEM are plotted against the horizontal distance X from the center of EPS block fill. Although DEM can gives only force of each element, in this chapter the force is translated to stress with dividing by the block width. Though obtained

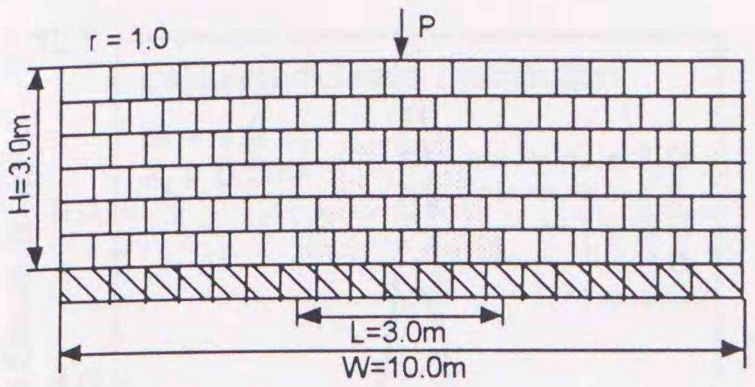

(a) Model-A (r=1.0, H=3.0m)

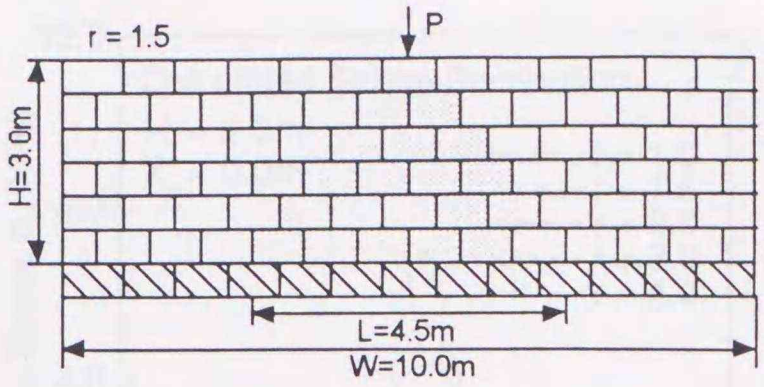

(b) Model-B (r=1.5, H=3.0m)

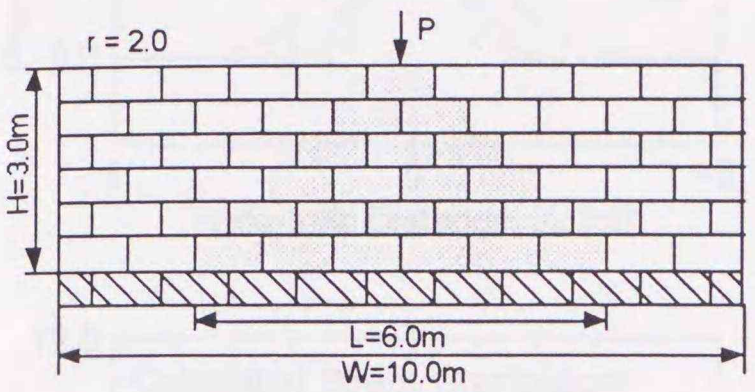

(c) Model-C (r=2.0, H=3.0m)

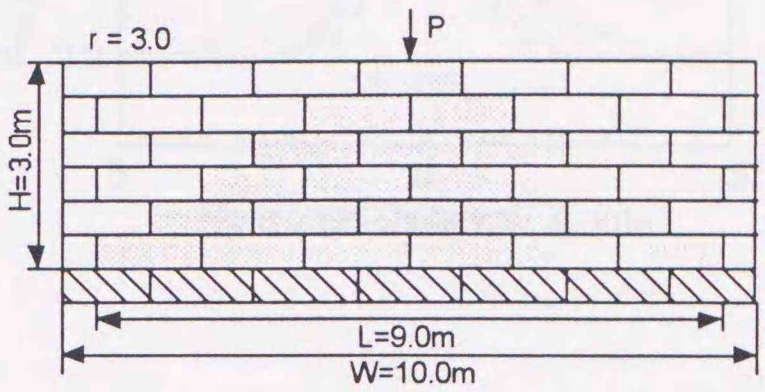

(d) Model-D (r=3.0, H=3.0m)

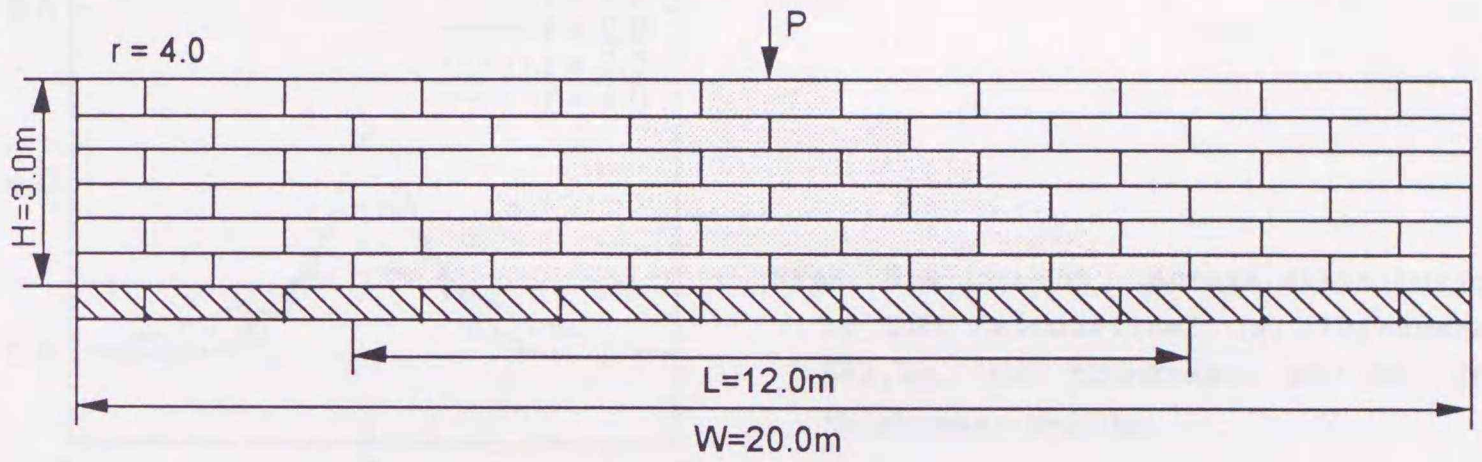

(e) Model-E (r=4.0, H=3.0m)

Figs. 3.2 (a)-(e). Basic model fill of H=3.0m; (a) Model-A, (b) Model-B, (c) Model-C, (d) Model-D, (e) Model-E.

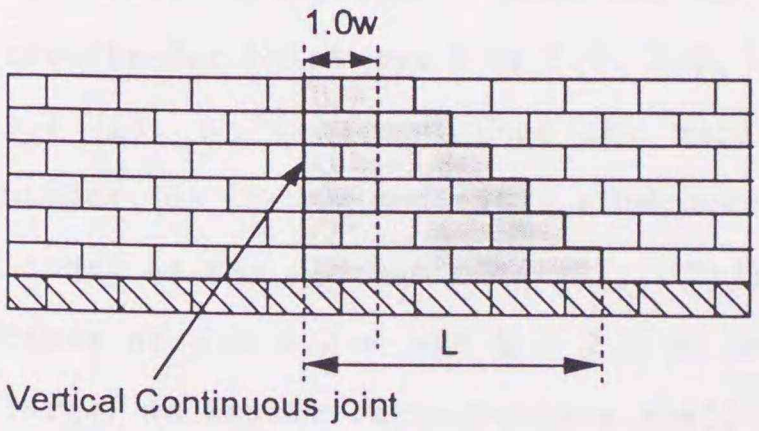

(a) Position of vertical continuous joint: X=2.0m (r=2.0, w=2.0)

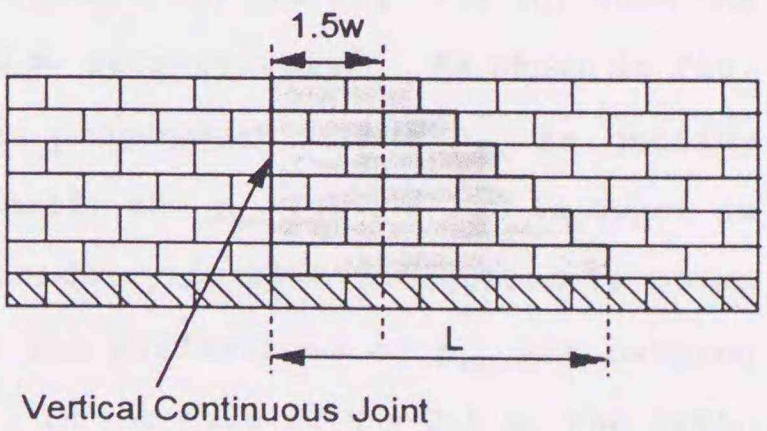

(b) Position of vertical continuous joint: X=3.0m (r=2.0, w=2.0)

Figs. 3.3 (a),(b). EPS model fill which have vertical continuous joint and r = 2.0; (a) vertical continuous joint set at X=1.0w, (b) vertical continuous joint set at X=1.5w.

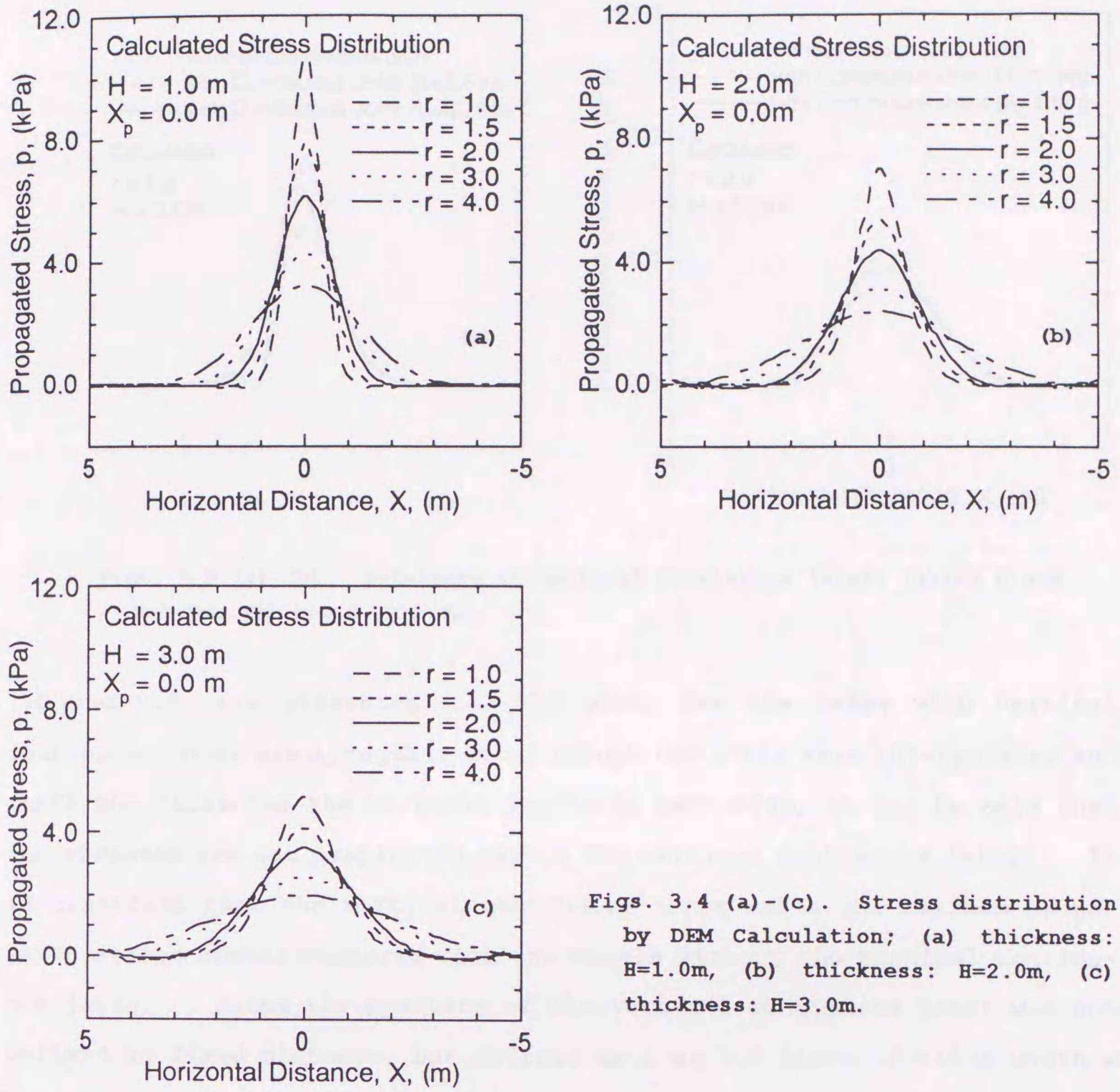

Figs. 3.4 (a)-(c). Stress distribution by DEM Calculation; (a) thickness: H=1.0m, (b) thickness: H=2.0m, (c) thickness: H=3.0m.

stress was not continuous, the plots were interpolated with spline of trinomial expression. Fig. 3.4 (a), Fig. 3.4 (b) and Fig. 3.4 (c) show the results for thickness H of 3.0, 2.0, 1.0 m, respectively. As shown in Fig. 3.4 (a), it is found that the maximum propagated stress p_{max} is getting higher, as the aspect ratio r becomes small; the p_{max} for r = 1.0 is twice as larger as the p_{max} for r = 4.0. This tendency is also recognized in other cases of H = 1.0 m and H = 2.0 m, but the differences of p_{max} are getting large, as aspect ratio becomes small. In the case of H = 2.0 m, the ratio of p_{max} for r = 1.0 to p_{max} for r = 4.0 is over three times, and in the case of H = 1.0 m, the ratio is about 3.7 times.

Shown in Figs. 3.5 (a), (b) is the influence of vertical continuous joint; the calculated stress distributions of H = 3.0 m, whose r values are

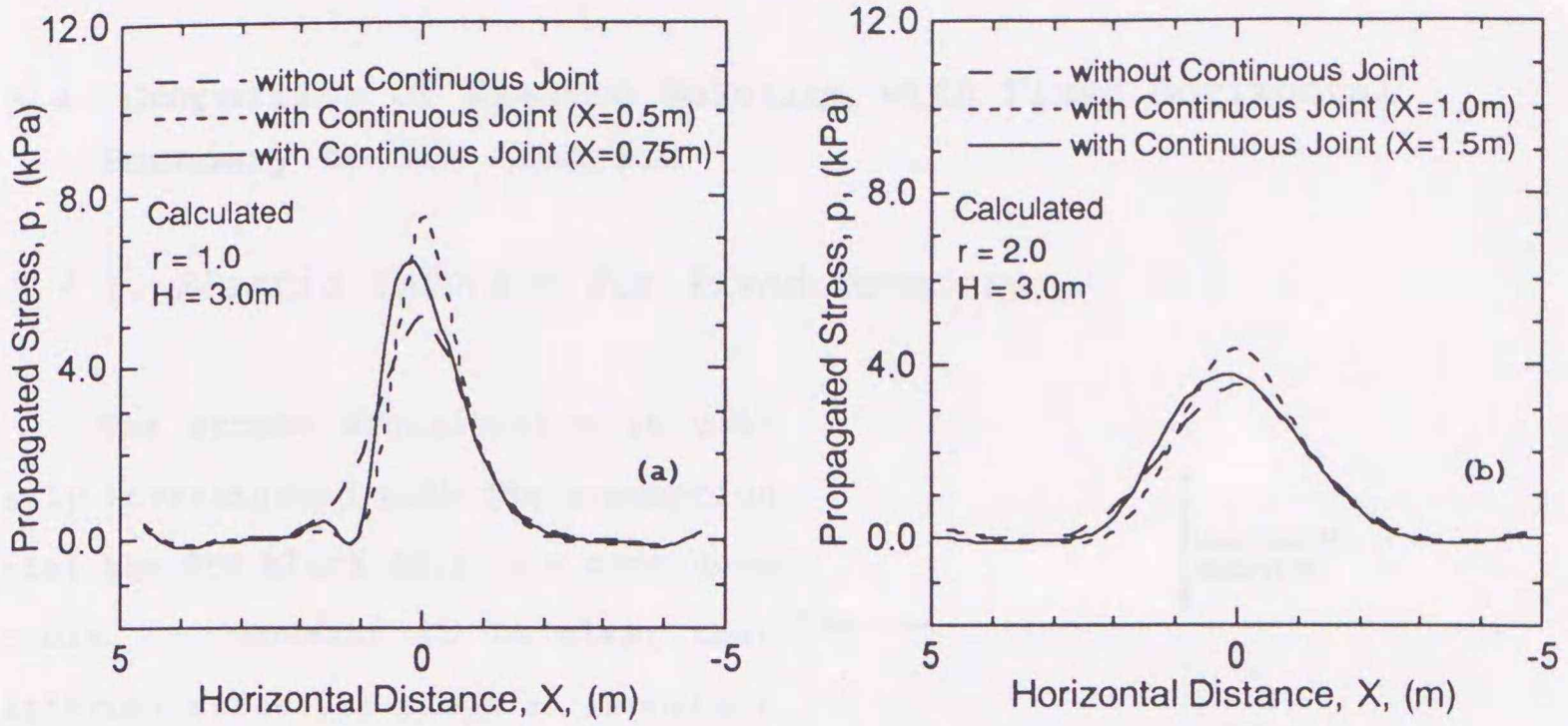

Figs. 3.5 (a),(b). Infulence of vertical continuous joint; (a) r=1.0 and H=3.0m, (b) r=2.0, H=3.0m.

1.0 and 2.0, are presented. The plots for the cases with vertical continuous joint are irregular form; though the plots were interpolated and shift the fills has the vertical joints in left side, it can be said that the stresses are not propagated beyond the vertical continuous joint. It is clarified that the vertical continuous joint makes the maximum propagated stress higher compared with the models without the vertical continuous joint. Since the position of the vertical continuous joint was not defined as fixed distance, but defined as 1 or 1.5 times of block width w from center of EPS model fill, as the aspect ratio r is getting larger, the distance from the center becomes long; the influence of the vertical continuous joint become small.

It was found by DEM calculation that the maximum propagated stress and the stress distribution is dominated by the aspect ratio and the structural length of distribution L.

3.4. Comparison of Elastic Solution with Fixed Horizontal Boundary to DEM Analysis

3.4.1. Elastic Solution for Fixed Boundary

The stress distribution is usually investigated with the assumption that the EPS block fill is a continuum media. However it is clear that internal structure plays an important role in EPS block fills, and the aspect ratio r of EPS block which constitutes the EPS block fill is a main parameter; therefore, not elastic analysis but DEM analysis can express this feature. The EPS model fills employed in this study have fixed boundary at bottom blocks line, and it is expected that the results of elastic solution with fixed boundary gives higher stress than the case without fixed boundary, but the amount of increments and the applicability to EPS block fill are not cleared. In the following, to examine the applicability of elasticity solution, the elastic solution with fixed boundary was derived. This solution is equivalent to the expression by Boussinesq, when the depth of fixed boundary becomes infinity.

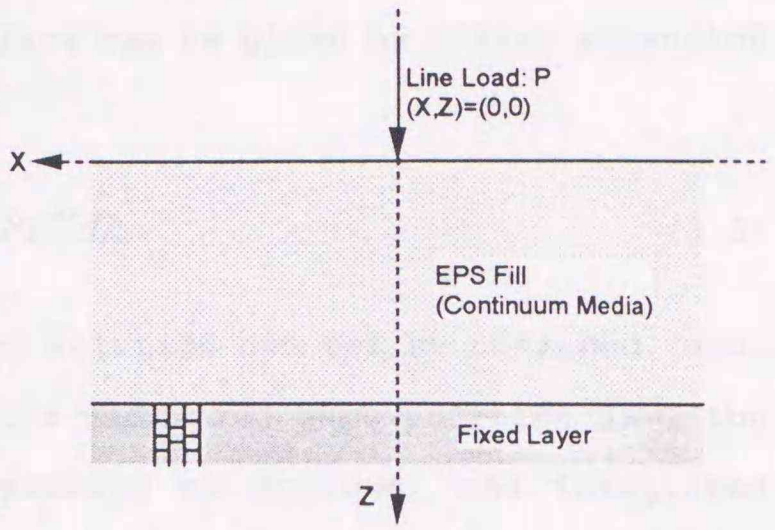

Fig. 3.6. EPS fill assumed as a continuum media with fixed boundary

In the situation shown in Fig. 3.6, according to linear elastic theory, the stress - strain relationship in plane stress condition is expressed by

$$\begin{cases} \sigma_z = -(B+G)\dfrac{\partial u_z}{\partial z} - (B-G)\dfrac{\partial u_x}{\partial x} \\ \sigma_x = -(B+G)\dfrac{\partial u_x}{\partial x} - (B-G)\dfrac{\partial u_z}{\partial z} \\ \tau_{zx} = -G\left(\dfrac{\partial u_z}{\partial x} + \dfrac{\partial u_x}{\partial z}\right) \end{cases} \tag{3.1}$$

where B is bulk modulus of EPS and G is shear modulus of EPS.

The equation of motion is as follows.

$$\begin{cases} \dfrac{\partial \sigma_z}{\partial z} + \dfrac{\partial \tau_{zx}}{\partial x} = 0 \\ \dfrac{\partial \sigma_x}{\partial x} + \dfrac{\partial \tau_{zx}}{\partial z} = 0 \end{cases} \tag{3.2}$$

The line load distribution on surface can be given by series expansion of Dirac delta function;

$$\sigma_z = \frac{1}{\pi} \int_0^\infty P e^{-\lambda x} d\lambda \tag{3.3}$$

but its mathematical expression of solution can not be obtained, and, therefore, by using the linearity of the media and superposition law, the boundary condition at surface is expressed as follows, and integrated numerically later.

$$\sigma_z = e^{-i\lambda x} \quad (z = 0) \tag{3.4}$$

From above boundary condition, the displacement functions are also given by

$$\begin{cases} u_z = U_z(z) e^{-i\lambda x} \\ u_x = U_x(z) e^{-i\lambda x} \end{cases} \tag{3.5}$$

When Eq. (3.5) was substituted for Eq. (3.2), and then the characteristic equation was solved using differential operator D, the solution of D = $\pm \lambda$ is obtained. Then the general expression of Eq. (3.5) is shown as follows.

$$\begin{cases} U_z(z) = a_1 e^{\lambda z} + a_2 e^{-\lambda z} a_3 \lambda z e^{\lambda z} + a_4 \lambda z e^{-\lambda z} \\ U_x(z) = b_1 e^{\lambda z} + b_2 e^{-\lambda z} b_3 \lambda z e^{\lambda z} + b_4 \lambda z e^{-\lambda z} \end{cases} \tag{3.6}$$

Eq. (3.5) and (3.6) were substituted to Eq. (3.2), and the obtained equation was solved as the identical equation of z.

Then the relationship shown in the following obtained and the number of unknown parameters was reduced to 4; a_1 - a_4.

$$\begin{cases} b_1 = -ia_1 - i\dfrac{B+2G}{B}a_3 \\ b_2 = ia_2 - i\dfrac{B+2G}{B}a_4 \\ b_3 = -ia_3 \\ b_4 = ia_4 \end{cases} \tag{3.7}$$

where the boundary condition is as follows.

$$\begin{cases} u_x = u_z = 0 \quad (z = H) \\ \sigma_z = \dfrac{1}{\pi}\int_0^\infty P e^{-i\lambda x} d\lambda \quad (z = 0) \\ \tau_{zx} = 0 \quad (z = 0) \end{cases} \tag{3.8}$$

But the second boundary condition is changed as follows at first, and as mentioned in Eq. (3.4). These boundary conditions, Eq. (3.4), and Eq. (3.1) gave the unknown parameter, a_1 - a_4.

$$\begin{cases} a_1 = \dfrac{X_1}{X_2} \\ a_2 = a_1\dfrac{B+2G}{B} + a_3\dfrac{2G(B+2G)}{B^2} + \dfrac{B+G}{2\lambda BG} \\ a_3 = \dfrac{X_3}{X_2} \\ a_4 = 2a_1 + a_3\dfrac{B+2G}{B} + \dfrac{1}{2G\lambda} \end{cases} \tag{3.9}$$

where X_1, X_2 and X_3 are

$$\begin{cases} X_1 = -\left(1+e^{2H\lambda}\right)\left(B^2+3BG+2G^2\right) - 2BH\lambda e^{2H\lambda}\left(B+G+BH\lambda\right) \\ X_2 = 2G\lambda\left\{B\left(B+2G\right)\left(1+e^{2H\lambda}\right)^2 + 4\left(G^2+B^2H^2\lambda^2\right)e^{2H\lambda}\right\} \\ X_3 = B\left\{B\left(1+e^{2H\lambda}+2H\lambda e^{2H\lambda}\right)+2G\right\} \end{cases} \tag{3.10}$$

Then the normal stress and shear stress were expressed by

$$\begin{cases} \sigma_z = \dfrac{2G\lambda}{B} e^{-\lambda\left(ix+z\right)} X_4 \\ \sigma_x = \dfrac{2G\lambda}{B} e^{-\lambda\left(ix+z\right)} X_5 \\ \tau_{zx} = \dfrac{2G\lambda}{B} ie^{-\lambda\left(ix+z\right)} X_6 \end{cases} \tag{3.11}$$

where the constants X_3, X_4 and X_5 are

$$\begin{cases} X_4 = -a_1 Be^{2\lambda z} - a_2 B - a_3\left(G+B\lambda z\right)e^{2\lambda z} - a_4\left(G-B\lambda z\right) \\ X_5 = a_1 Be^{2\lambda z} - a_2 B + a_3\left(2B+G+B\lambda z\right)e^{2\lambda z} + a_4\left(2B+G-B\lambda z\right) \\ X_6 = a_1 Be^{2\lambda z} + a_2 B + a_3\left(B+G+B\lambda z\right)e^{2\lambda z} - a_4\left(B+G-B\lambda z\right) \end{cases} \tag{4.12}$$

Then this obtained each function was transformed and numerical integration was carried out, because the mathematical expression can not be obtained. The range of the integration was determined as from 0 π to 10 π; the influence of the range to the numerical integration can be almost reduced, with an accuracy of second order.

3.4.2 Comparison of Elastic Solution with Fixed Boundary and DEM Analysis

The comparison of the elastic solutions with and without fixed boundary is shown in Fig. 3.7, and the stress distributions of H = 1.0, 2.0, 3.0 m are also plotted. It is found that the maximum propagated stress of the calculation with fixed boundary is higher than without fixed boundary by twenty or thirty percent.

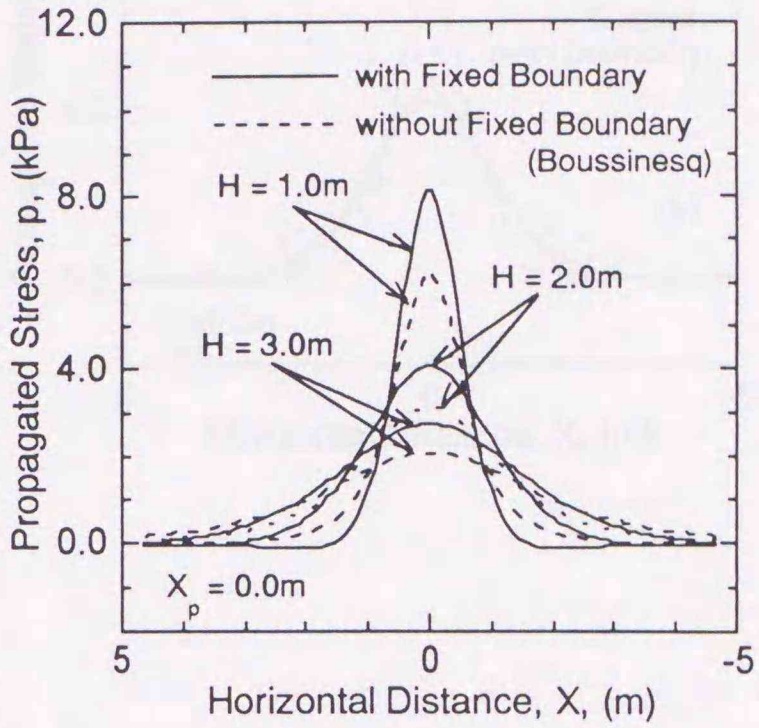

Fig. 3.7. Comparison of elastic solution with and without fixed bounday

Shown in Figs. 3.8 (a)-(c) give the comparison between the results of elastic solution with fixed boundary and DEM calculations, on the case of the EPS fill thickness H = 1.0, 2.0, 3.0 m.

In case of H = 1.0 m, only the models of r = 1.0 and 1.5 are gives higher maximum propagated stress p_{max} than the elastic solution, but in cases of H = 2.0 and 3.0 m, the model of r = 2.0 which is used in prototype generally also gives higher p_{max}. Shown in Fig. 3.9 is the relationship between the maximum propagated stress p_{max} and the EPS fill thickness H, it is found that when the thickness H is enough large, the elastic solution tends to underestimates p_{max}, though the elastic solution with fixed boundary gives twenty or thirty percent higher p_{max} than without fixed boundary as mentioned above.

It is able to conclude from these results that the elastic solution can not estimate the stress dispersion appropriately; even if the elastic solution with fixed boundary is given, the estimation is on risk side. On the other hand, it can be said that DEM can estimate the stress dispersion appropriately, since the applicability to EPS model fill has already confirmed in Chapter 2 and 3 of Part 2; however, the DEM calculation takes many computational cost even if it adopted the static solution. Then it is seemed that the appropriate estimation method of stress distribution in EPS block fill will be necessary.

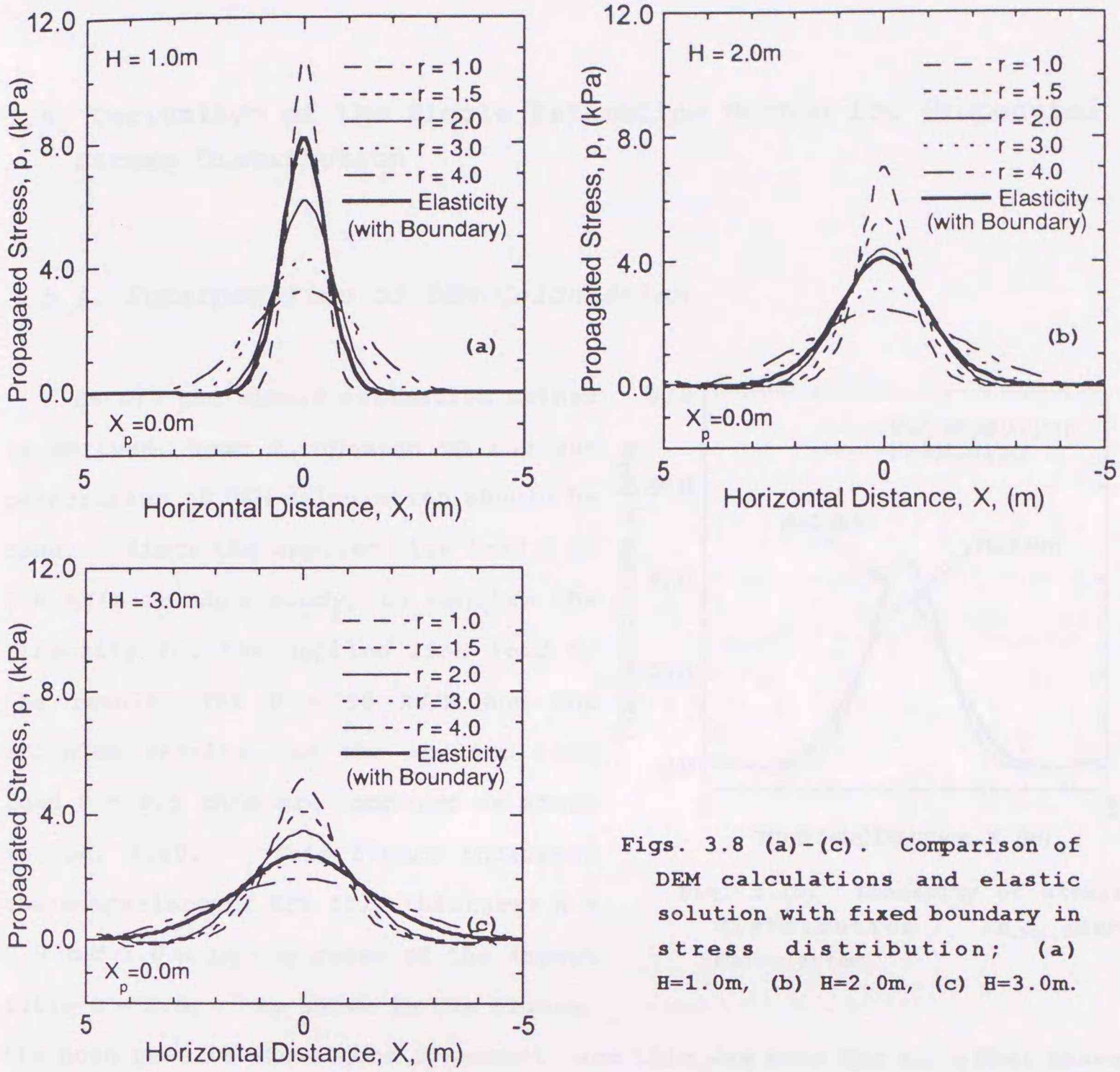

Figs. 3.8 (a)-(c). Comparison of DEM calculations and elastic solution with fixed boundary in stress distribution; (a) H=1.0m, (b) H=2.0m, (c) H=3.0m.

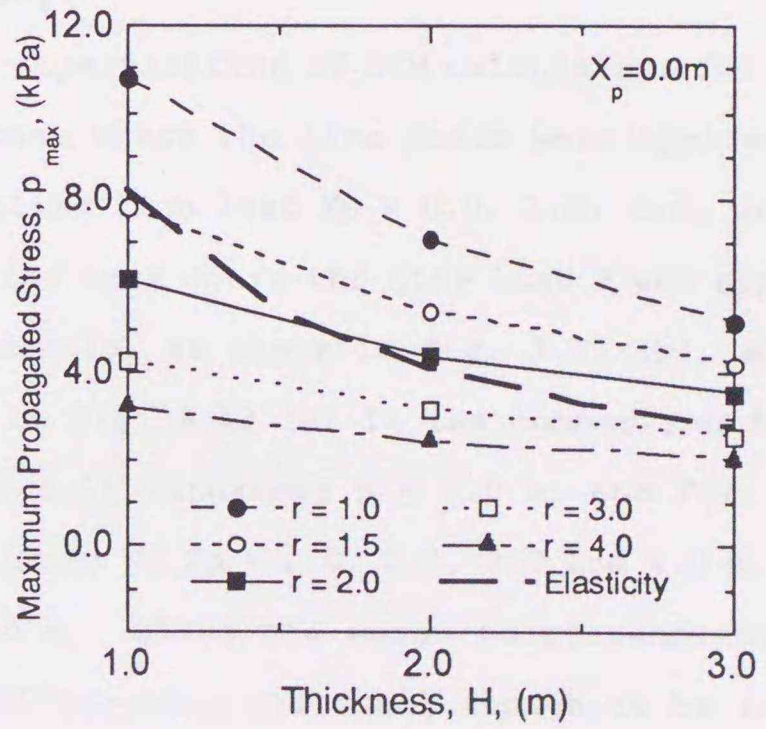

Figs. 3.9. Comparison of DEM calculations and elastic solution with fixed boundary in maximum propagated stress: p_{max}.

3.5. Derivation of the Simple Estimation Method for Propagated Stress Distribution

3.5.1. Superposition of DEM Calculation

Before the simple estimation method is derived, some discussion on the superposition of DEM calculation should be done. Since the applied line load P is 9.8 kN/m in this study, to confirm the linearity for the applied line load P, the results for P = 98 kN/m and the decupled results for the applied line load P = 9.8 kN/m are compared as shown in Fig. 3.10. This figure indicates the comparison of EPS fill thickness H = 2.0 and 3.0 m in the cases of the aspect ratio r = 2.0. As shown in the figure, the both results shows good agreement, and this was same for all other cases with similar accuracy.

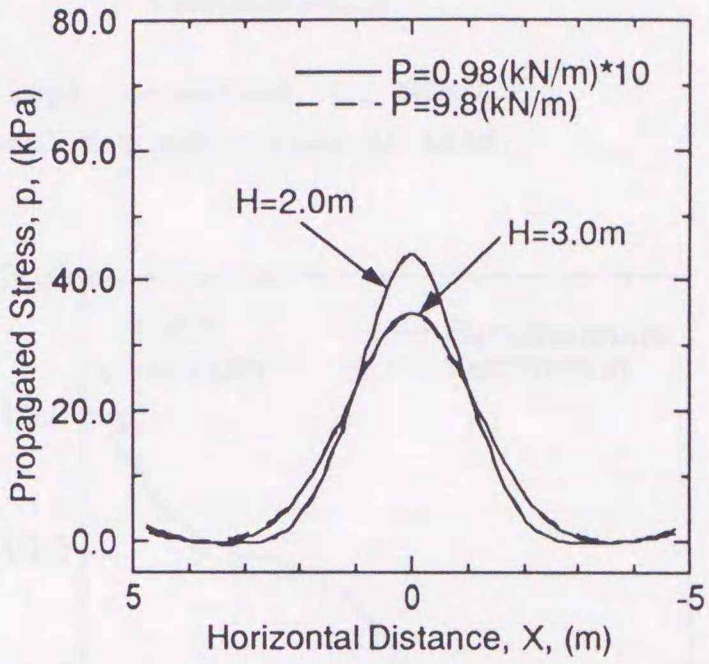

Fig. 3.10. Linearity of stress distribution in $_{r=2.0}$DEM Calculation.

To confirm the superposition of DEM calculation for the plural applying line loads P, the case where the line loads were applied simultaneously at the position of applied line load Xp = 0.0, 1.0, 2.0, and 3.0 m as shown in Fig. 3.11 (a), and the case where the line load P was applied Xp = 0.0, 1.0, 2.0, 3.0 m independently, as shown in Fig. 3.11 (b), are compared in Fig. 3.12 (a). Shown in Fig. 3.12 (a) is the comparison for the aspect ratio r = 2.0 and the EPS fill thickness H = 3.0 m, and Fig. 3.12 (b) shows the comparison for the cases of Xp = 1.0, 2.0, 3.0 and 4.0 m. Though the case, r = 2.0 and H = 3.0 m, gives the worst correspondence compared with the other models, the differences are small enough to be accepted.

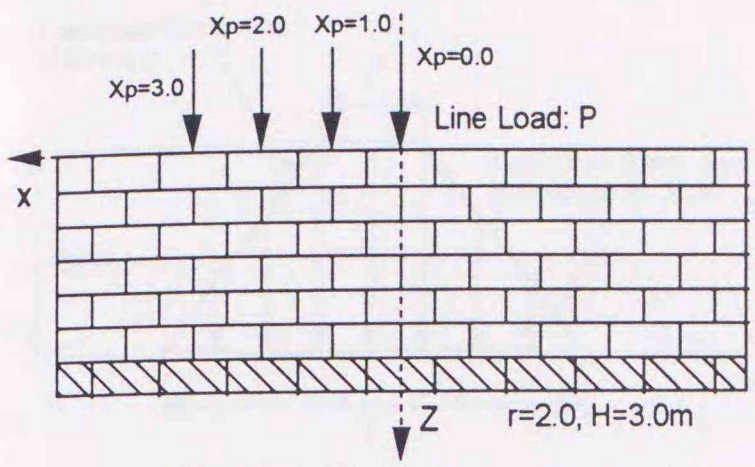

(b) Applying line load: P simultaneously

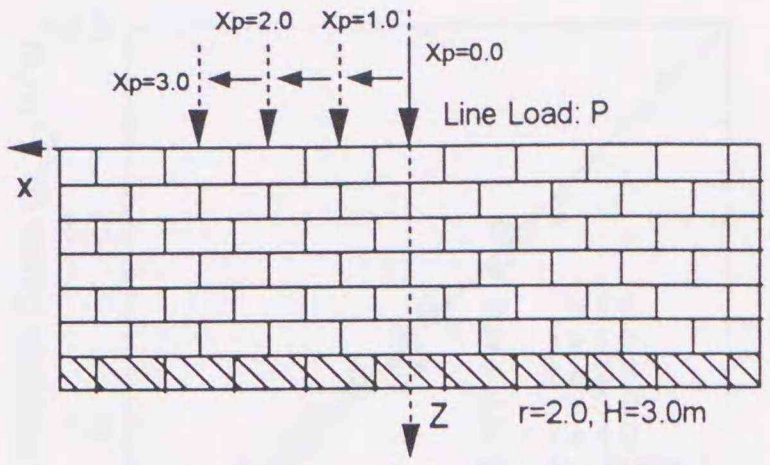

(b) Applying line load: P independently

Figs. 3.11 (a), (b). Diffrences of applying method; (a) model for simultaneous load apply, (b) model for summation of load.

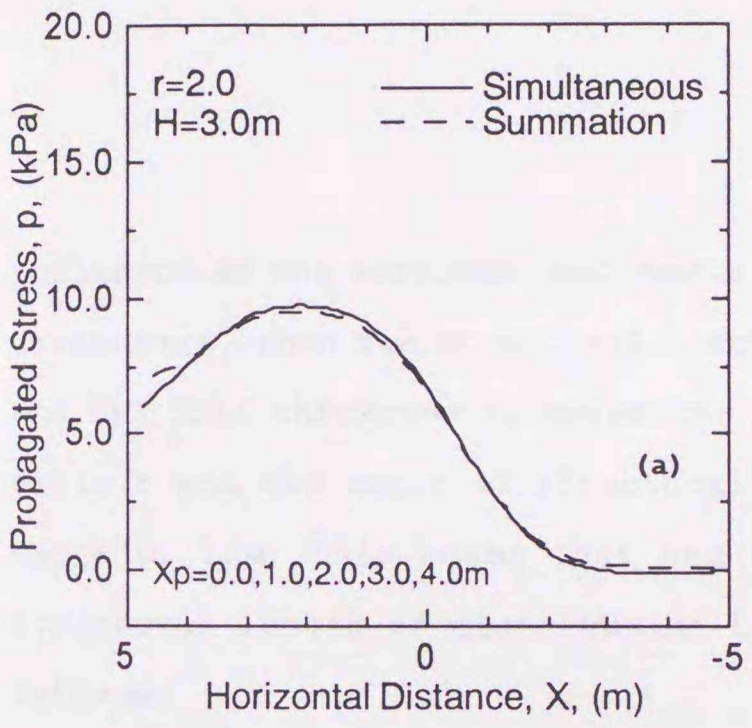

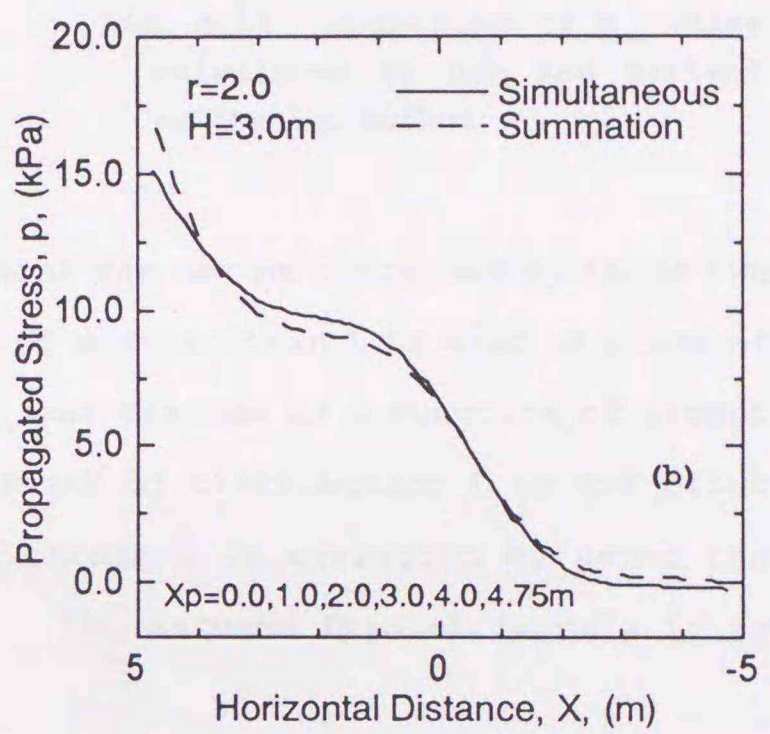

Figs. 3.12 (a), (b). Superposition of DEM calculation for plural line load:P; (a) Xp=0.0, 1.0, 2.0, 3.0m, (b) Xp=0.0, 1.0, 2.0, 3.0, 4.0m.

3.5.2. Derivation of the Simple Estimation Method for Propagated Stress Distribution

It is clear that the stress distribution properties due to line load is controlled by the aspect ratio and the EPS fill thickness from the results explained in previous sections. A simple estimation method of the stress distribution is presented in the following.

First, the maximum propagated stress p_{max} is estimated, and then the distribution form is estimated on the assumption that the stress distribution can be approximated as trapezoidal, as shown in Fig. 3.13. But the

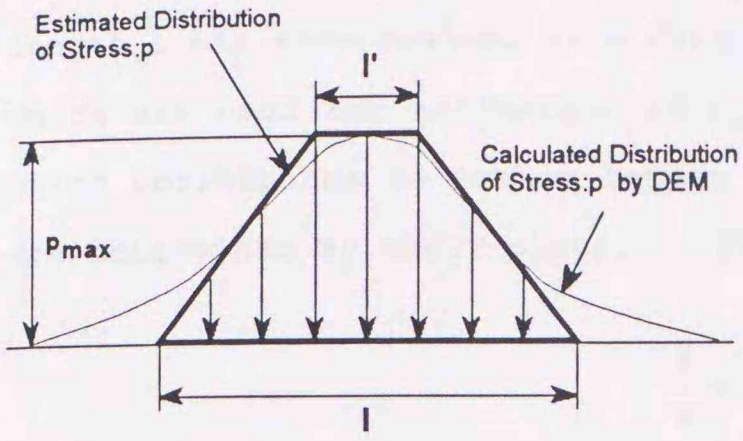

Fig. 3.13. Assumption of trapezoidal stress distribution.

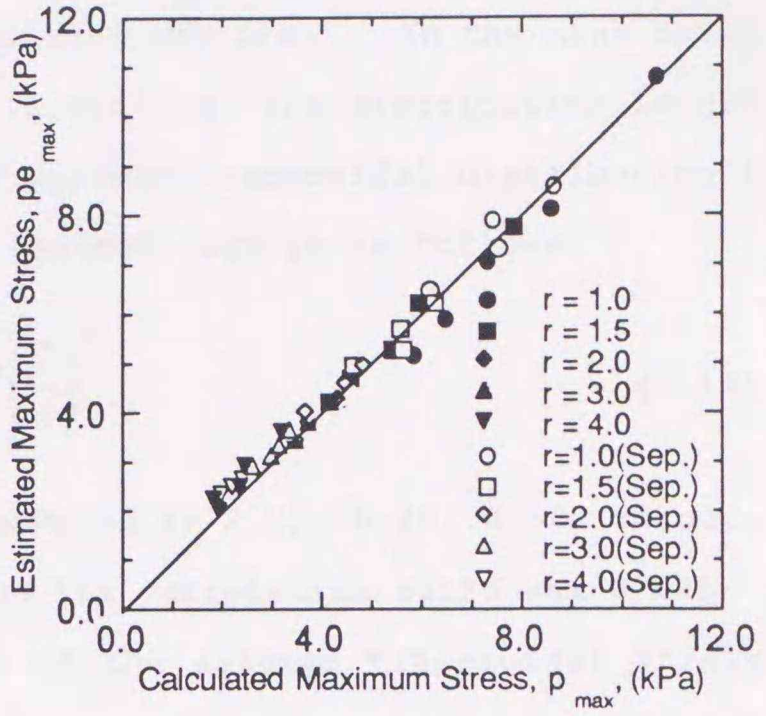

Fig. 3.14. Comparison of p_{max} value calculated by DEM and derived estimation method.

influence of the vertical continuous joint can not be expressed by these two parameters, then the structural length of distribution L is used in place of the EPS fill thickness H, parameter p_{max} was assumed as a function of aspect ratio r and the ratio of structural length of distribution L to EPS block width w, L/w; this means that the thickness H is corrected by using the structural length of distribution L. The assumed form of formula is as follows.

$$\frac{wp_{\max}}{P} = ar^b\left(\frac{L}{w}\right)^c \qquad (3.14)$$

The constants a, b and c were determined by using least square method from the calculation results of nine cases out of forty five cases; the nine cases are the models which have aspect ratio r = 1.0, 2.0, 4.0 and thickness H = 1.0, 2.0, 3.0 m without the vertical continuous joint. From the least square operation a = 0.8, b = 0.20, and c = -0.55 were obtained, and the correlation ratio was 0.992, and the comparison of the estimated p_{max} with the calculated p_{max} by DEM is shown in Fig. 3.14 including the other cases not used in the least square method. The differences between the estimated and calculation values are within 10 %.

Then the bottom length l of assumed trapezoidal stress distribution in Fig. 3.13 was determined by means of similar method as p_{max}; the bottom

length l was also assumed as a function of r and L/w. In the nine cases which are used for estimation of p_{max} in fitting, the distribution length which corresponds to bottom length of assumed trapezoidal distribution l was determined by their plots. The assumed form is as follows.

$$\frac{l}{w} = dr^{e}\left(\frac{L}{w}\right)^{f} \tag{3.14}$$

The constant d, e and f were determined as 2.2, -0.20, 0.50, respectively, by the least square method, and its correlation ratio was 0.997.

Finally, the top member's length of the assumed trapezoidal stress distribution l' in Fig. 3.12 was determined; this top member's length l' can be obtained from follow equation on the assumption that the area of the trapezoid equals the applied line load P.

$$l' = 2\frac{P}{p_{\max}} - l \tag{3.15}$$

The comparison of the stress distributions by the estimation method with DEM calculation gives in Fig. 3.15 (a)-(e); solid lines are for the derived estimation method and the broken curves are for DEM calculation. In Fig. 3.15 (a)- e) the aspect ratio r is different in the figures, and the estimated results for the EPS fill thickness H = 1.0 and 3.0 m are plotted in the same figure. Good agreement of the form of stress distribution as well as the maximum propagated stress p_{max} can be recognized.

In Fig. 3.16 (a)-(e), the comparison between the simple estimation method and DEM calculation for the models with vertical continuous joint at each aspect ratio r; the models of the EPS fill thickness H = 3.0 m and the position of vertical continuous joint X = 1.0 w are plotted. As shown in those figures, even in the case with vertical continuous joint, the derived simple estimation method gives good agreement with DEM calculations.

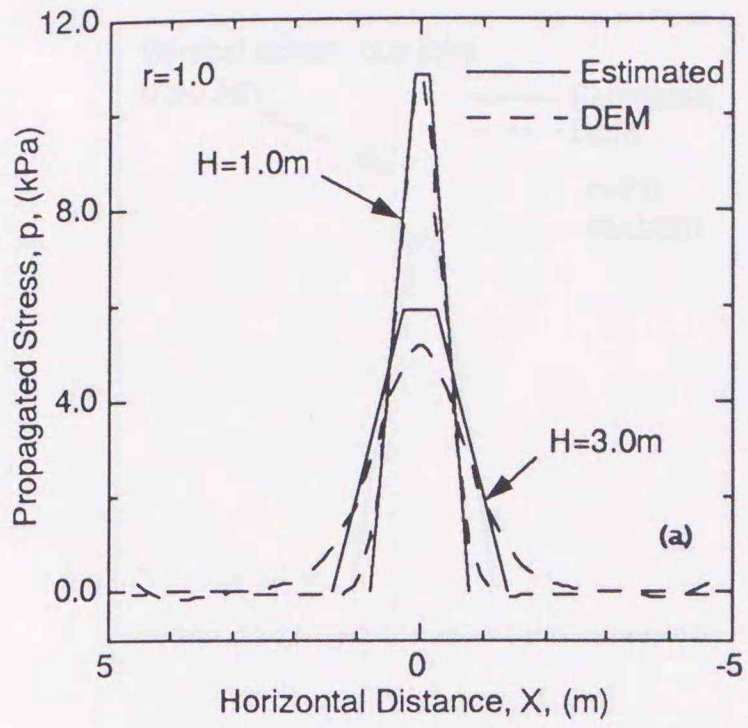

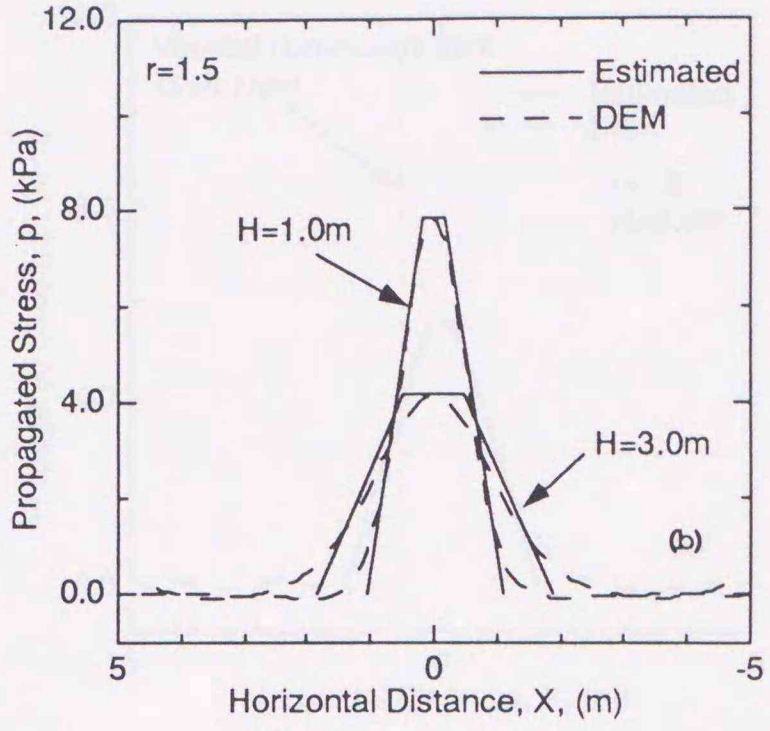

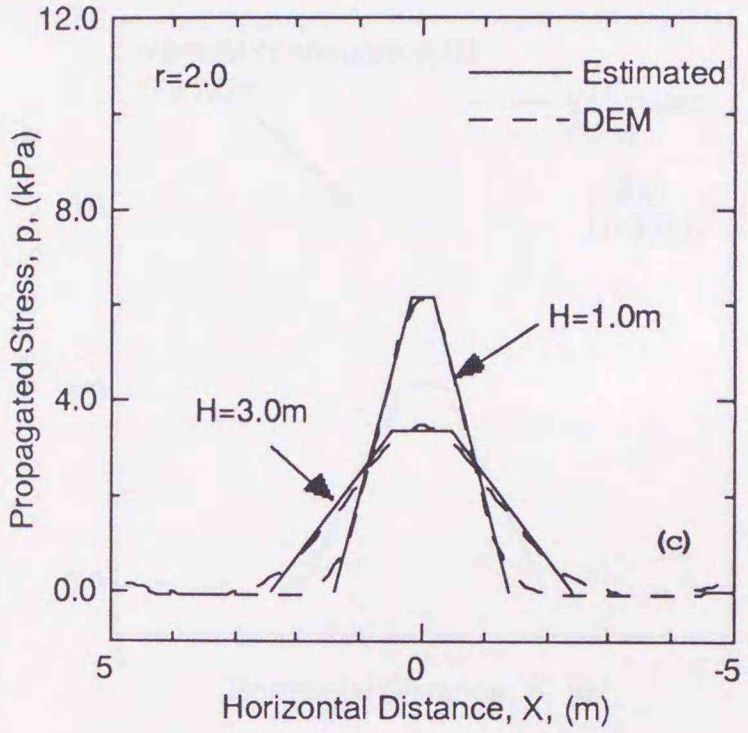

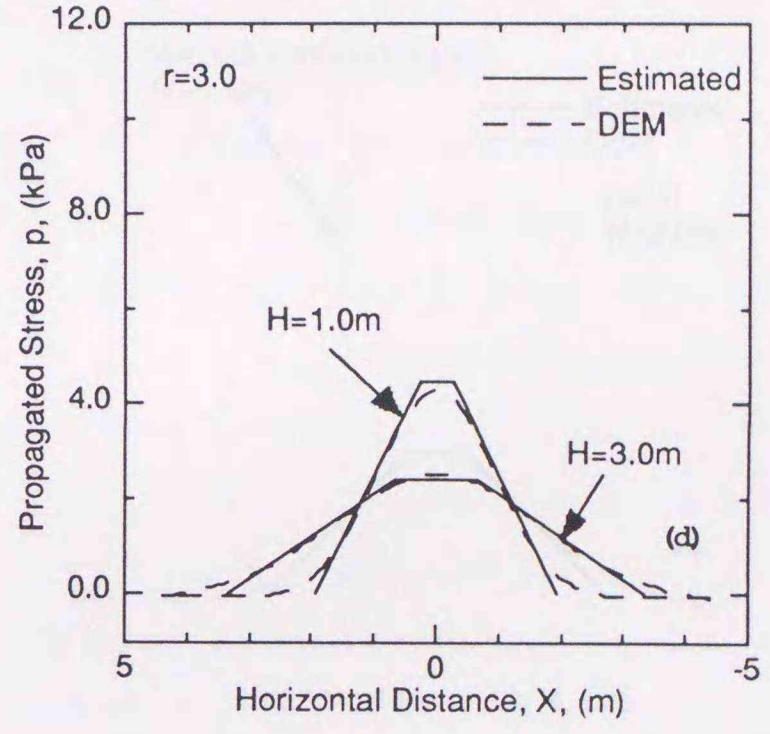

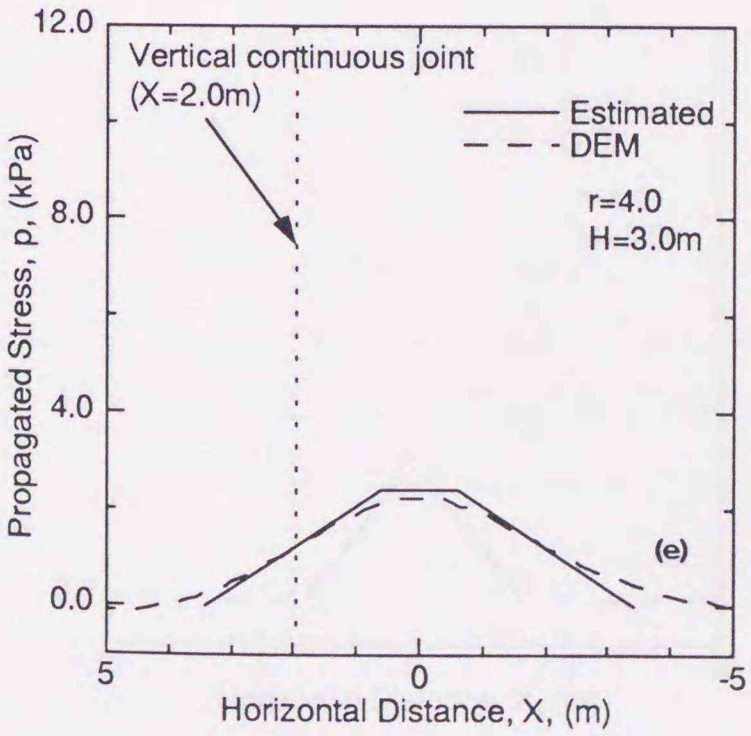

Figs. 3.15 (a)-(e). Comparison of the stress distributions by derived estimation method and DEM calculation(without vertical continuous joint); (a) Model-A, (b) Model-B, (c) Model-C, (d) Model-D, (e) Model-E.

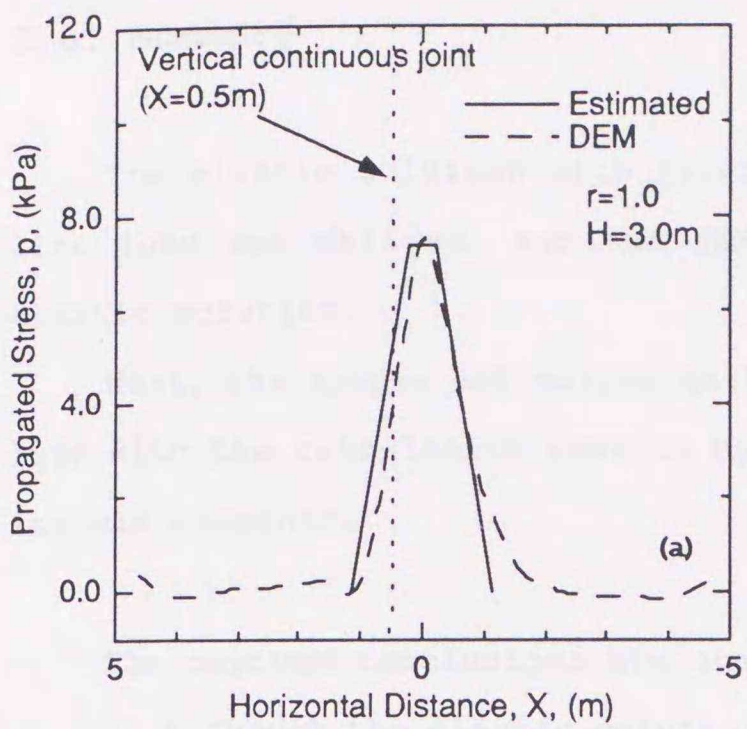

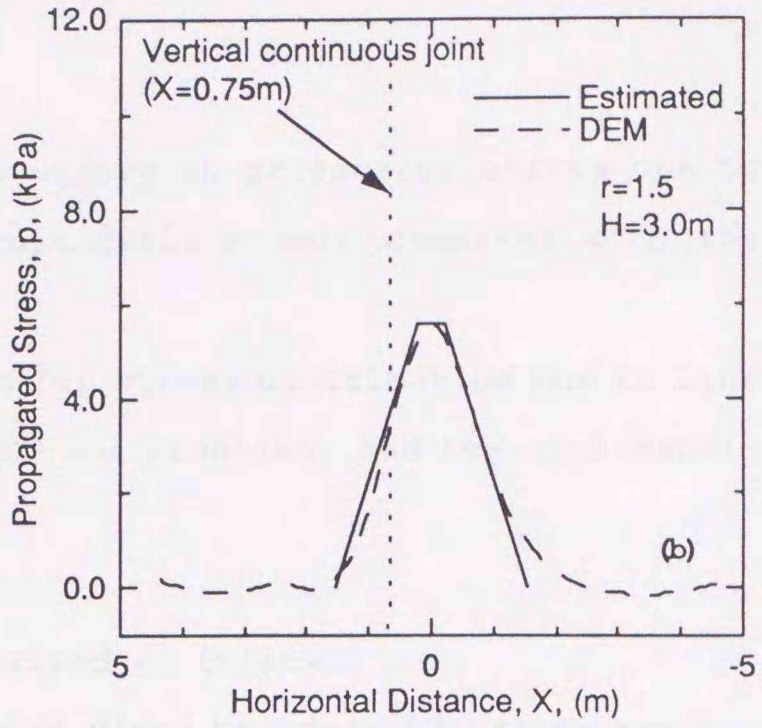

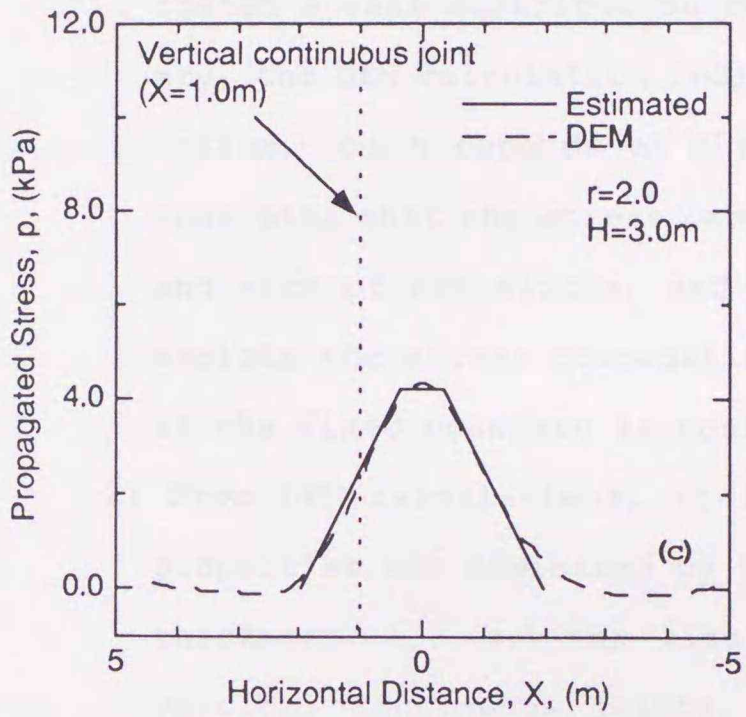

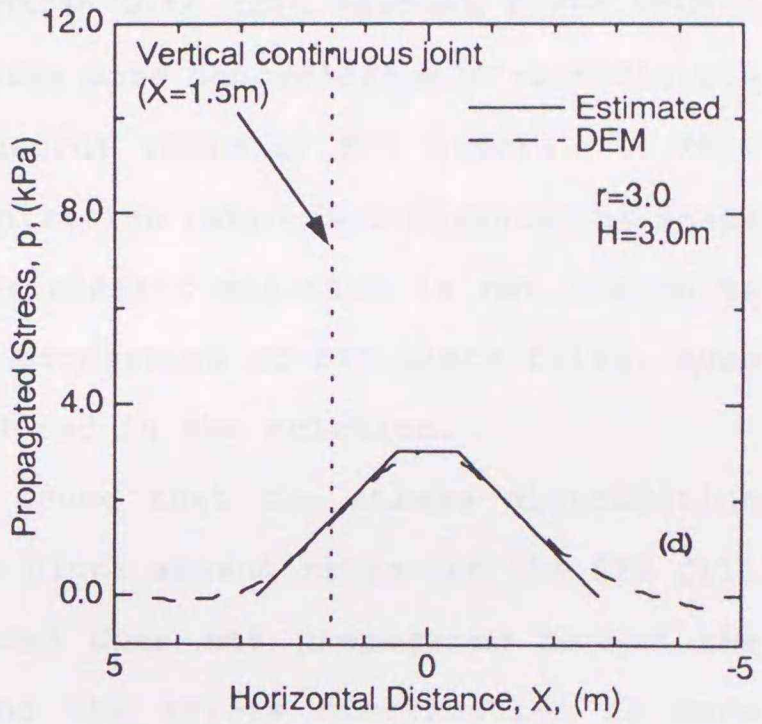

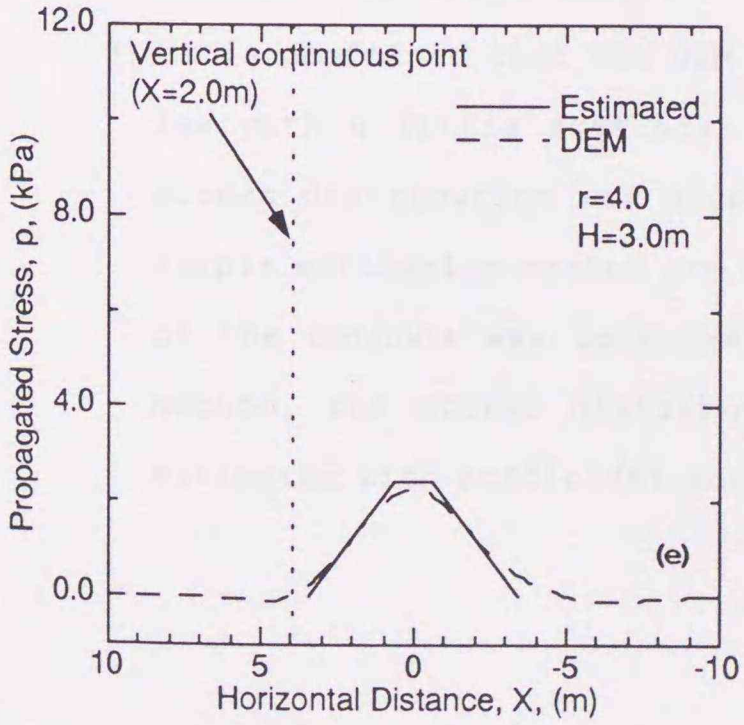

Figs. 3.15 (a)-(e). Comparison of the stress distributions by derived estimation method and DEM calculation(with vertical continuous joint); (a) Model-A, (b) Model-B, (c) Model-C, (d) Model-D, (e) Model-E.

3.6. Summary

The elastic solution with fixed boundary in propagated stress due to line load was derived, and the DEM calculations were compared with the elastic solution.

Next, the simple estimation method for stress distribution due to line load with the calculation results by DEM was proposed, and its applicability was examined.

The derived conclusions are summarized as follows;

1) Although the elastic solution with fixed boundary indicates concentrated stress distribution compared with that without fixed boundary, the DEM calculation indicates more concentrated stress distribution, which depends on the aspect ratio of EPS blocks. This indicates that the stress concentration ratio is influenced by shape and size of EPS blocks, and the elastic solution is not enough to explain the stress propagation properties of EPS block fills, even if the fixed boundary is considered in the solution.
2) From DEM calculations, it is found that the stress distribution properties are dominated by the block aspect ratio and the EPS fill thickness. And the line load does not propagated beyond the vertical continuous joints, and the stress distribution is more concerned in these cases.
3) It is confirmed that the DEM calculations follows the superposition law with a little scatters; the simple estimation method for the stress distribution was proposed. In the comparison between the simple estimation method and DEM calculation, the good applicability of the methods was confirmed. By using this simple estimation method, the stress distribution due to applied line load can be estimated with sufficient accuracy without large calculation by DEM.

Chapter 4. Stress Concentration Properties in EPS Fill subjected to Differential Settlement of Foundation

4.1. Objectives

When the EPS block fill is constructed on an unstable ground or culvert stiff structures, it is expected that the foundation of EPS fill is subjected to a kind of differential settlement. In this situation the internal structure of EPS block fill may be easily disturbed, and as a results, the stress propagation properties will be changed, and then the stress concentration will occur.

In this Chapter the stress concentration characteristics of uniform overburden pressure and line load are investigated for the idealized EPS fill subjected to differential settlement by DEM calculations.

4.2. Simplified EPS Fill

One of idealized EPS fills with uniform surcharge q = 9.8 kPa is presented in Fig. 4.1 and where EPS block aspect ratio r = 2.0 and the fill thickness H = 3.0 m as defined in Chapter 4.

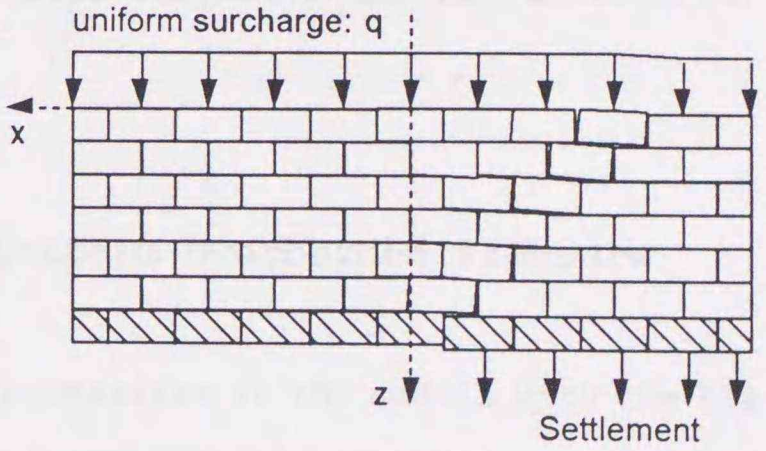

Fig. 4.1. EPS block fills subjected to differential settlement.

Initially, all the numerical model fills of EPS blocks were applied the uniform surcharge q, and the shaded bottom fixed blocks shown in Fig. 4.1 were assumed as a foundation of the EPS block fills. Then a settlement u was applied to the right half of the fixed bottom blocks as shown in Fig. 4.1. The other analyzed models in this chapter are the fill thickness of H = 1.0, 2.0, and 3.0 m, and block aspect ratio r = 1.0, 1.5, 2.0, 3.0 and 4.0; the prepared model fills are

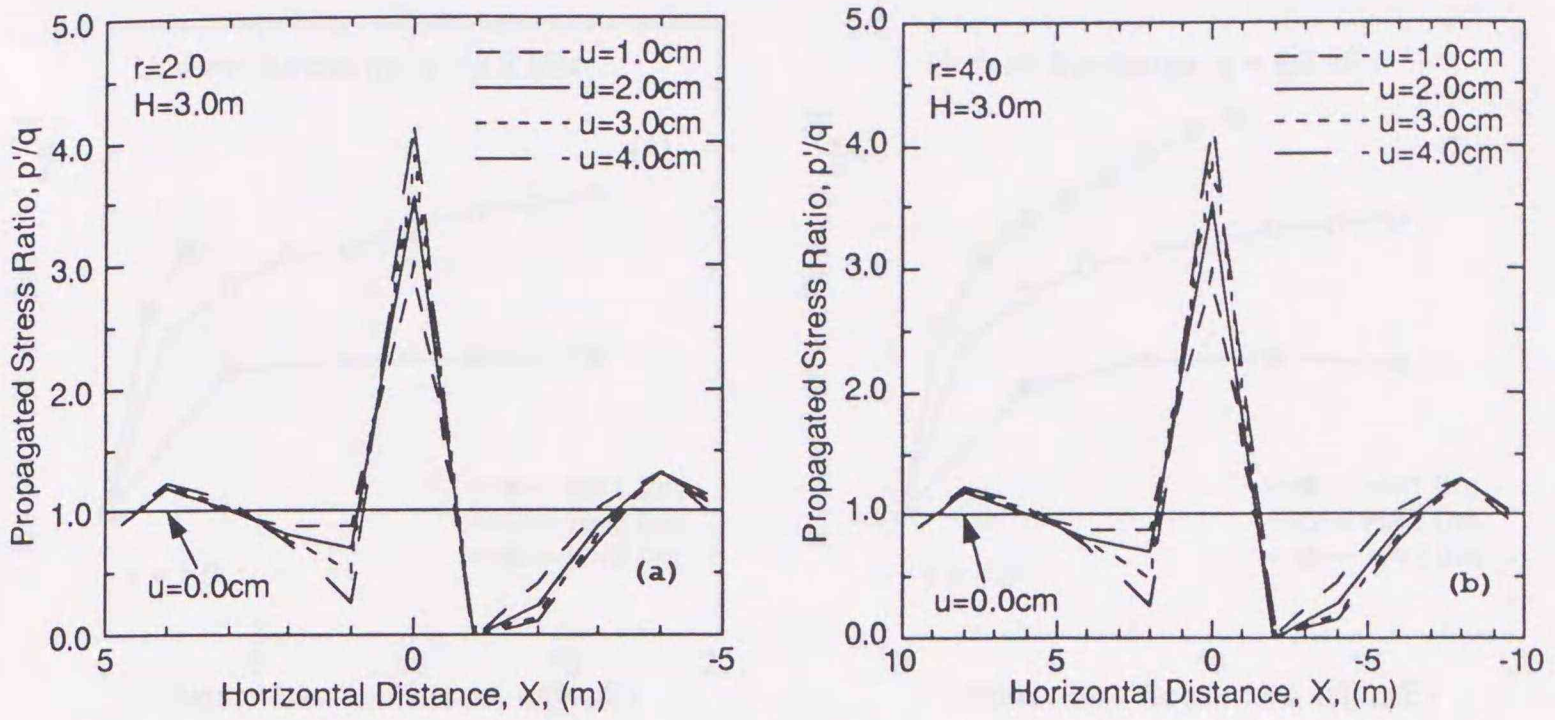

Figs. 4.2 (a), (b). Stress concentration of uniform surcharge in EPS fill subjected to differential settlement; (a) Model-C, (b) Model-E

fifteen in total, and the models with vertical continuous joint are not analyzed here. The maximum amount of applied settlement u were 2.0 cm for the model of H = 1.0 m, and 4.0 cm for the model of H = 2.0 and 3.0 m. However the model of r = 1.0 and H = 3.0 m could not be analyzed in case of the settlement u over u = 1.0 cm, because the calculation was not converged within allowed time by the calculation center of Hokkaido University.

In this chapter, the effects of steel fasteners are not considered, either.

4.3. Stress Concentration under Uniform Overburden Pressure

The change in stress distribution properties in the models with the EPS block aspect ratio of r = 2.0 and r = 4.0 and EPS fill thickness of H = 3.0 m, are indicated in Figs. 4.2 (a), (b). The plots of the stress distributions were not interpolated as in Chapter 4, because the stress distributions are no longer continuous as shown in Figs. 4.2 (a), (b). The ordinate is the ratio of the changed propagated stress p' to the initial surcharge q, and the abscissa is the horizontal distance X of EPS fill. As shown in Figs. 4.2 (a), (b), the stress was concentrated at the bottom - center fixed block which is at boundary of settled and not settled blocks, while the stress on adjacent two blocks decreases. This properties were

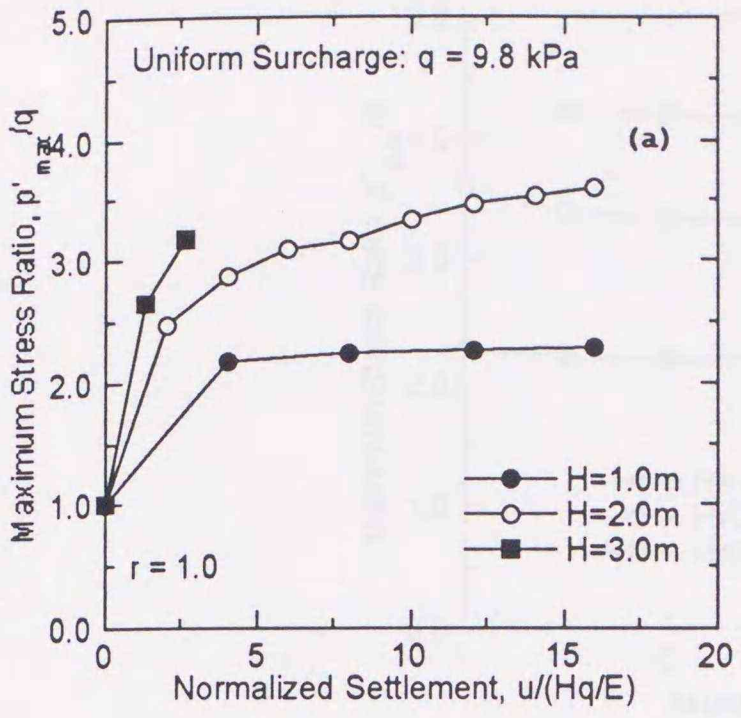

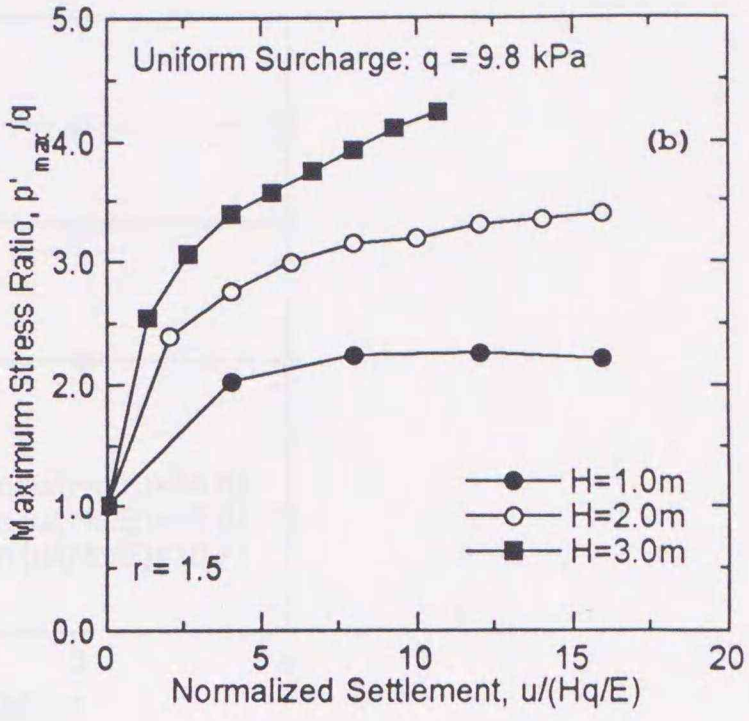

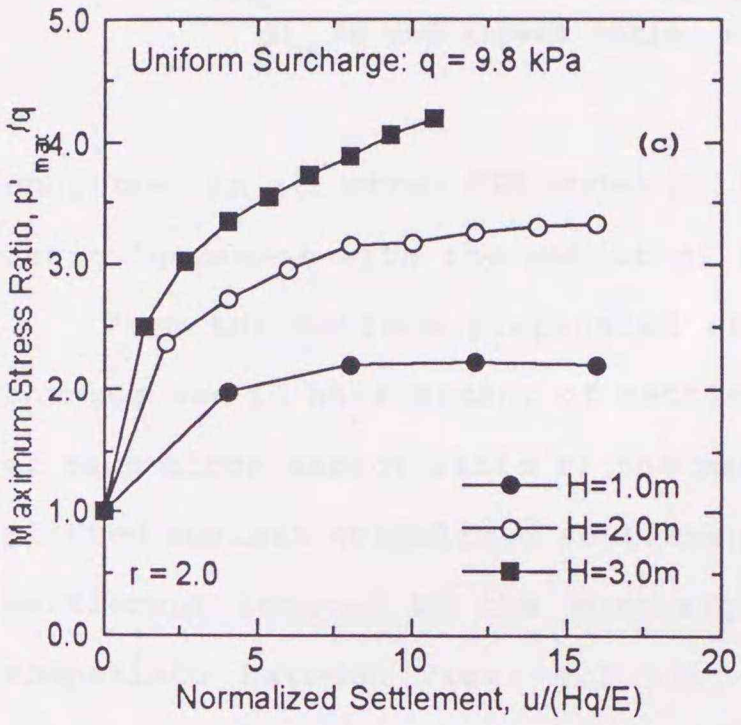

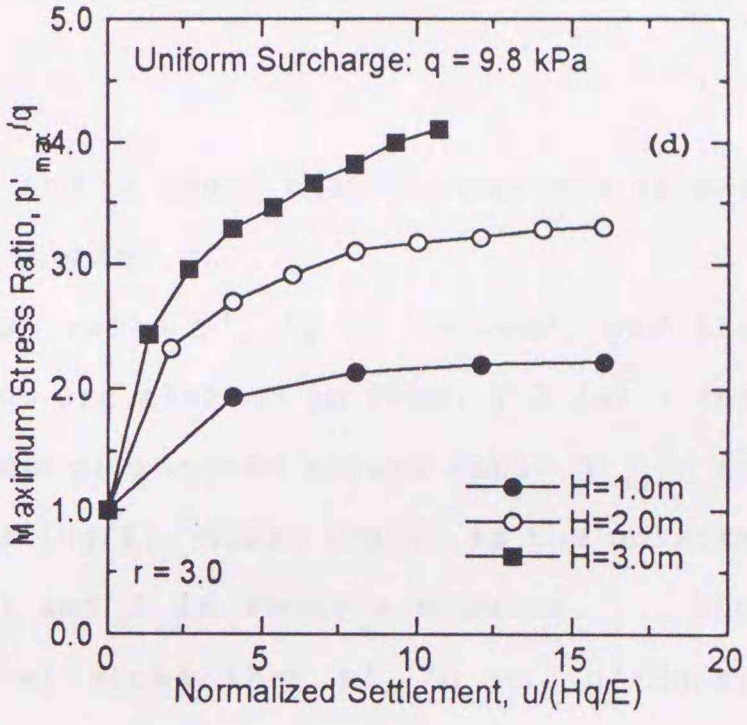

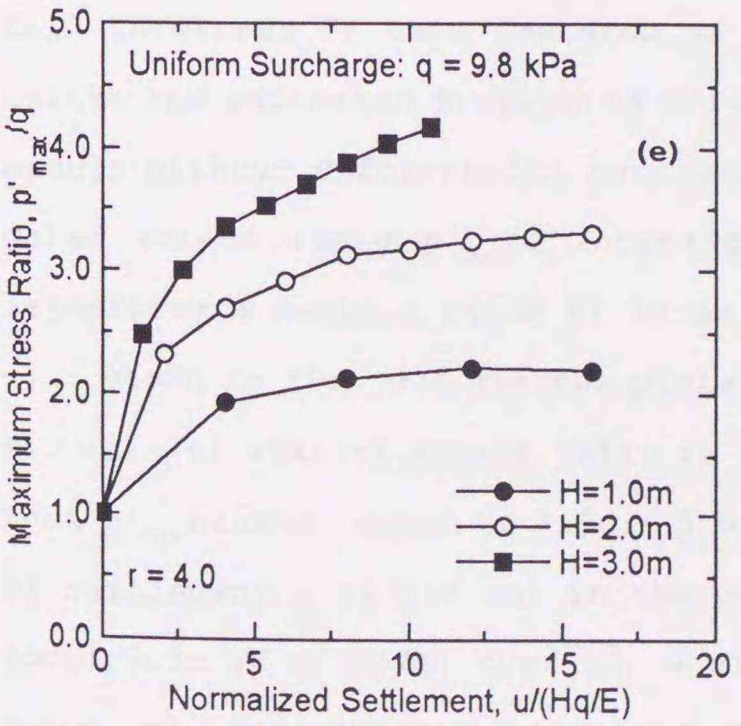

Figs. 4.3 (a)-(e). The relationship of maximum stress propagation ratio at bottom - center block and normalized settlement; (a) Model-A, (b) Model-B, (c) Model-C, (d) Model-D, (e) Model-E

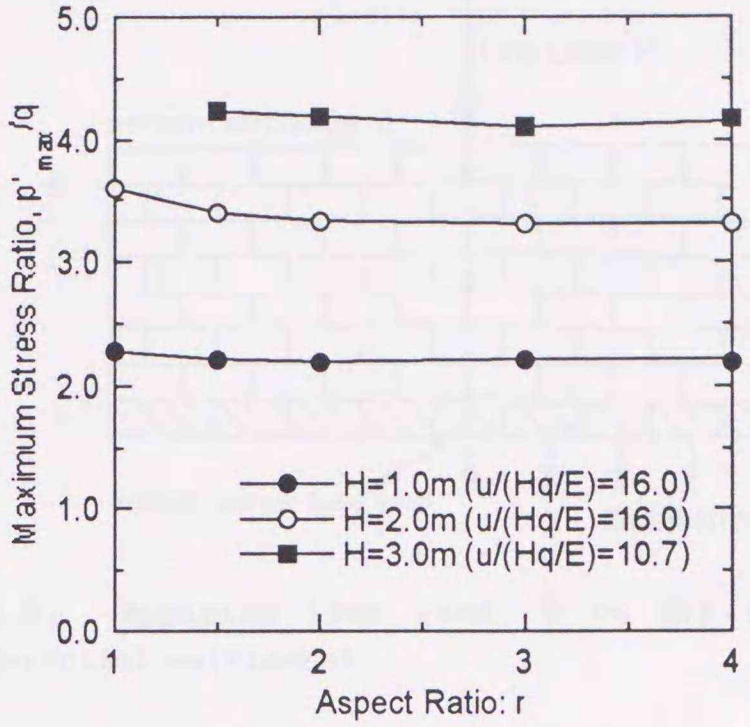

Fig. 4.4. The relationship of maximum stress propagation ratio: p'_{max}/q and aspect ratio: r.

confirmed in all other EPS model fills, and it seems that the maximum stress ratio increases with the amount of settlement u.

Then the maximum propagated stress ratio p'_{max}/q is focused, and its changes due to enlargement of settlement are plotted in Figs. 4.3 (a) - (e) at each block aspect ratio r; the maximum propagated stress ratio p'_{max}/q is plotted against normalized settlement u/(Hq/E), where (Hq/E) is the uniform settlement induced by the surcharge q and E is Young's modulus. The comparison between Figs. 4.3 (a) - (e) shows that p'_{max}/q vs. u/(Hq/E) relationship is hardly dependent on aspect ratio r, but is dependent on EPS fill thickness H; this features of independence on the aspect ratio r is unlike the indicated propagated stress character due to line load P for the models without differential settlement in Chapter 4. The maximum propagated stress ratio p'_{max}/q increases with differential settlement u and asymptotes a certain value at large u/(Hq/E).

Shown in Fig. 4.4 are the plots of p'_{max}/q at maximum u/(Hq/E) in Figs. 4.3 (a)-(e) against aspect ratio r; in the case of H = 3.0 m, it is expected that p'_{max} becomes equal to 4.5q - 5.0q at u(Hq/E) over 10, where the amount of settlement u is 4.0 cm, in the case of H = 2.0 m, p'_{max} becomes equal to about 3.3q at u/(Hq/E) over 12, where u = 3.0 cm. And in the case of H = 3.0 m, p'_{max} is converged to about 2.2q at u/(Hq/E) over 8, where u = 1.0 cm; when these amounts of settlement u is divided by their fill thickness H, the

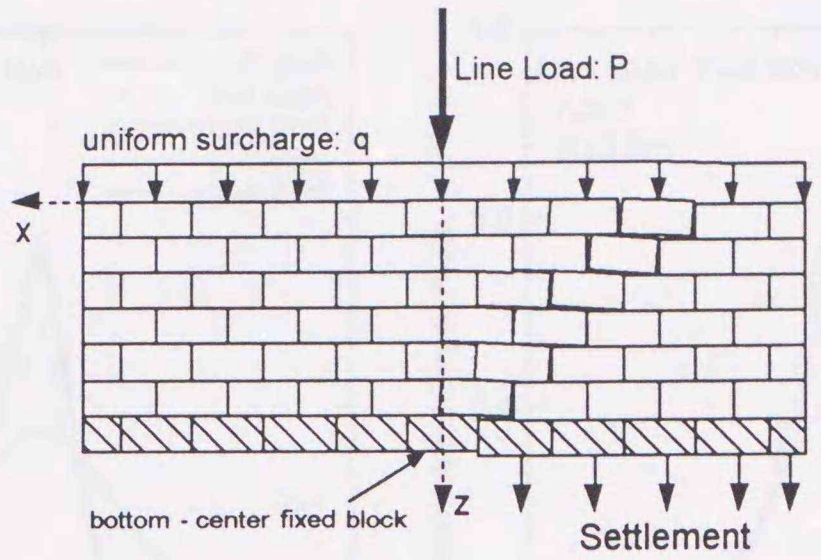

Fig. 4.5. Applying line load: P to EPS fill subjected to differential settlement.

value of (u/H) are 0.01, 0.0015, 0.0013, for H = 1.0, 2.0 and 3.0 m, respectively. It should be noted that the significant stress concentration more than several times of surcharge q must be easily induced by small differential settlement of foundation. In all the cases, when the amount of settlement u comes to 0.5 cm, the p'_{max} is over twice of initial surcharge q.

4.4. Stress Concentration under Line Load

To investigate the stress propagation characteristics of line load for the EPS fills subjected to differential settlement of its foundation, the line load P = 9.8 kN/m was applied to the EPS fills with differential settlement at each amount of settlement, at the center of EPS fill, as shown in Fig. 4.5. The amount of settlement u is dependent on fill thickness H and same as introduced in "4.3. Stress Concentration under Uniform Overburden Pressure"; in the case of H = 1.0 m, the maximum amount of settlement u is 2.0 cm, and in cases of H = 2.0 and 3.0 m, u is up to 4.0 cm except for the fill of r = 1.0. The propagated stress p is only due to line load P; the stress concentration of uniform surcharge q at initial condition was subtracted from the total stress distribution after applying line load P.

The stress concentration of line load P is presented in Figs. 4.6 (a), (b), the results are for the fills of H = 3.0 m, and r = 1.0, and 3.0. In

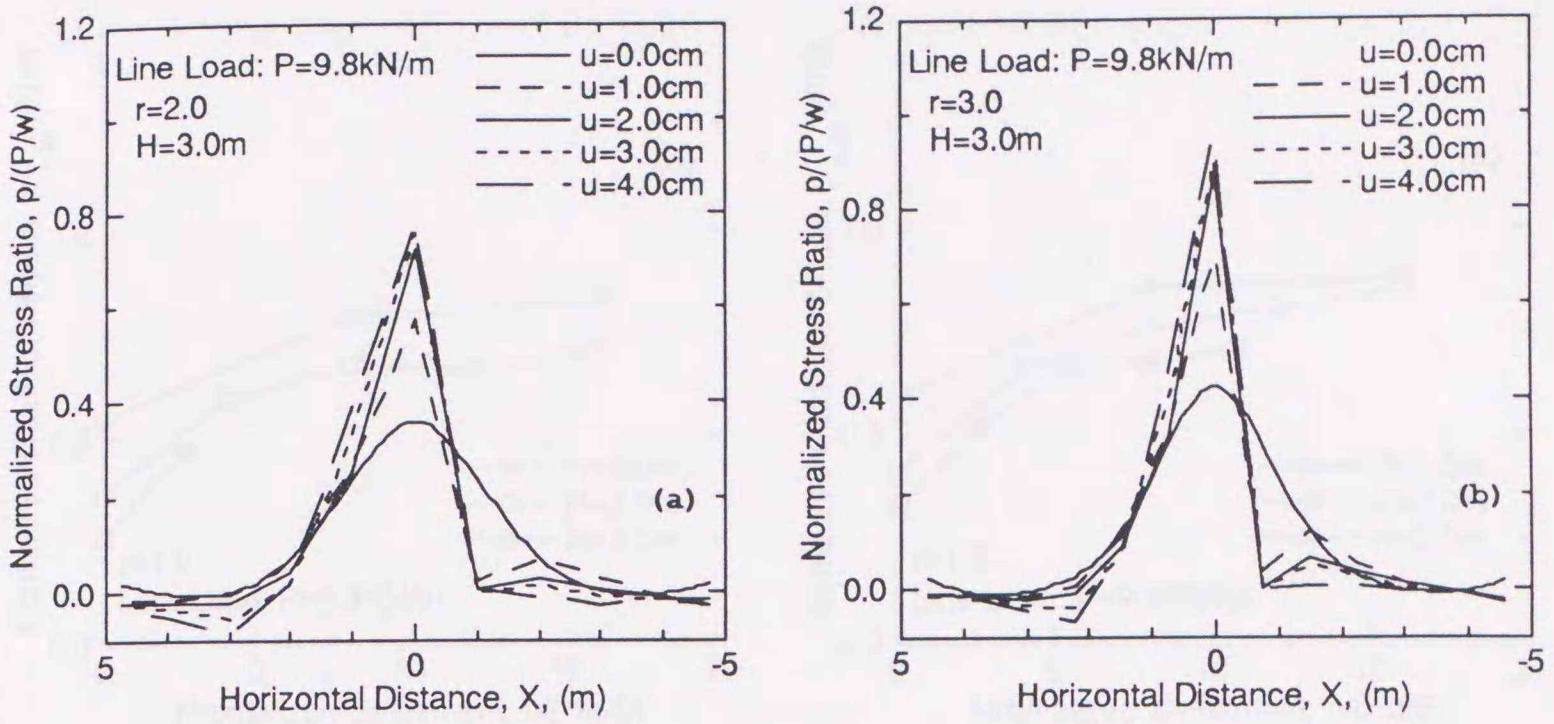

Figs. 4.6 (a), (b). Stress concentration of line load in EPS fill subjected to differential settlement; (a) Model-C, (b) Model-D

these figures the plots are not interpolated for the mentioned reason in 4.3. of Chapter 4, except for the result of u = 0.0 cm. The normalized propagated stress p/(P/w) is taken in the ordinates, and the horizontal distance X is taken in abscissas. As shown in Figs. 4.6 (a), (b) the stress p due to line load P is scarcely propagated to the right fixed blocks which were settled, and almost concentrates to the bottom - center fixed block which is just below the applied line load P (X = 0.0 m). The maximum propagated stress increases with an increase in the settlement u; this feature is same as the characteristics of stress distribution for uniform overburden pressure discussed in 4.3. of Chapter 4.

Then in Figs. 4.7 (a) - (e), the maximum normalized stress p/(P/w) is plotted against the normalized settlement u/(Hq/E) as described in 4.3. of Chapter 4. Although p/(P/w) increases with settlement u, unlike the characteristics of stress concentration of uniform surcharge q due to differential settlement, the dependency on fill thickness H is reduced largely. As the characteristics of stress concentration of uniform surcharge q due to differential settlement, the rise of the normalized maximum stress ratio p/(P/w) is converged at the normalized settlement u/(Hq/E) over 8 in all cases.

The maximum propagated stress ratio p/(P/w) at applied maximum normalized settlement u_{max}/(Hq/E) is plotted against the aspect ratio r in Fig.

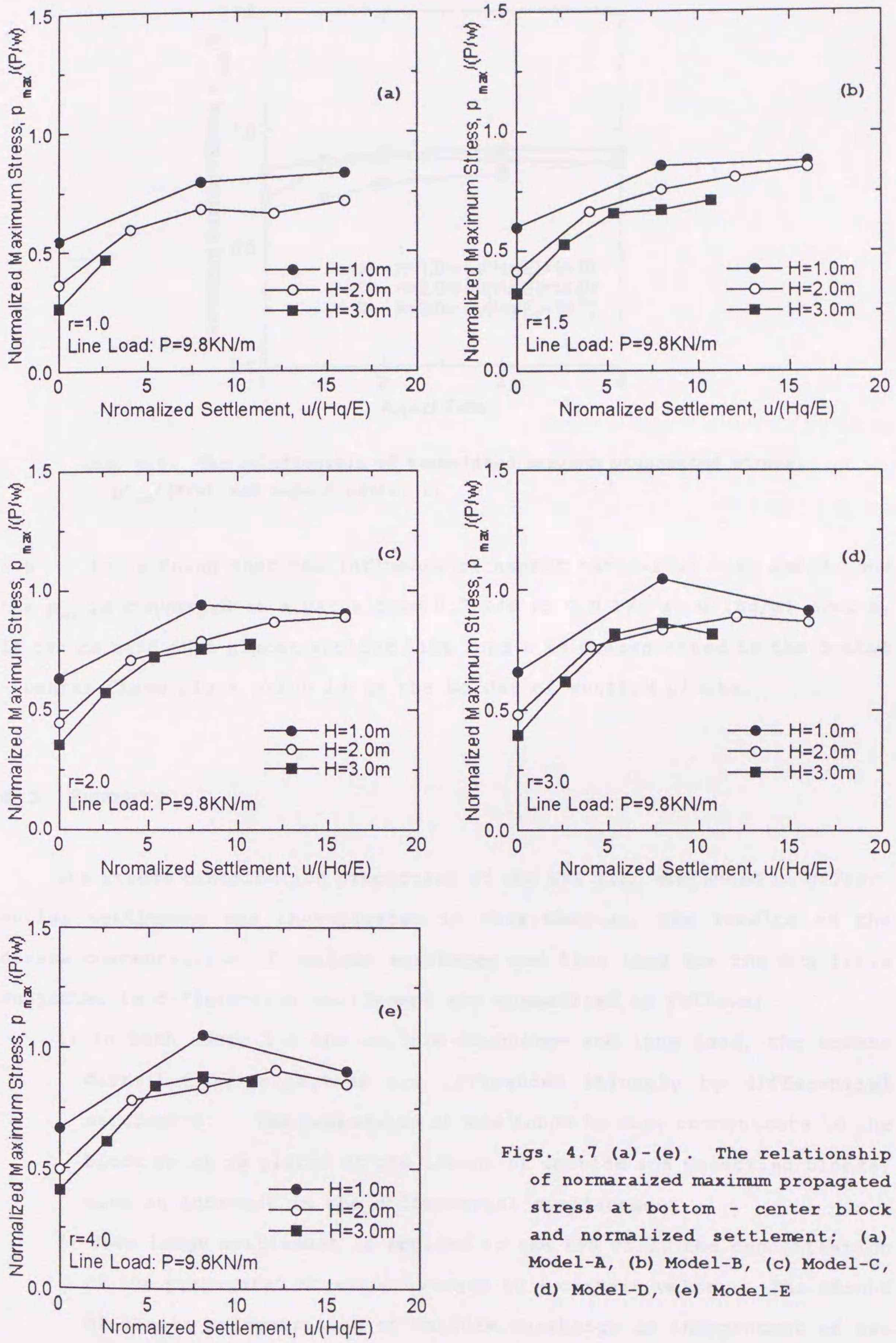

Figs. 4.7 (a)-(e). The relationship of normaraized maximum propagated stress at bottom - center block and normalized settlement; (a) Model-A, (b) Model-B, (c) Model-C, (d) Model-D, (e) Model-E

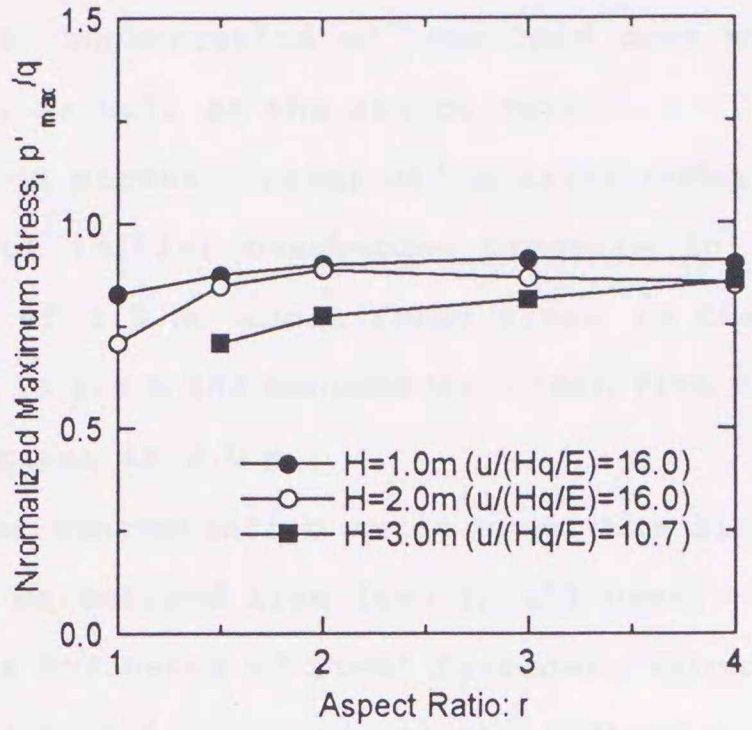

Fig. 4.8. The relationship of normalized maximum propagated stress: $p'_{max}/(P/w)$ and aspect ratio: r.

4.8. It is found that the influence of aspect ratio r is also small, and the p_{max} is converged to a value from 0.7 P/w to 0.9 P/w at u/(Hq/E) over 8. It can be said that almost applied line load P is concentrated to the bottom - center fixed block which is in the border of settled blocks.

4.5. Summary

The stress distribution properties of the EPS fill subjected to differential settlement was investigated in this Chapter, the results of the stress concentration of uniform surcharge and line load for the EPS fills subjected to differential settlement are summarized as follows;

1) In both cases for the uniform surcharge and line load, the stress distribution properties are influenced strongly by differential settlement. The propagated stress tends to more concentrate to the block which is placed at the border of settled and unsettled blocks, with an increase in the differential displacement.
2) When large settlement is applied to the EPS fill, the concentration of the propagated stress converges to a certain value. The amount of stress concentration of uniform surcharge is independent of aspect ratio, but dependent on fill thickness. On the other hand,

the stress concentration of line load does not depend on the fill thickness, as well as the aspect ratio.

3) The maximum stress concentration ratio under uniform surcharge is about twice initial overburden pressure in the case of the fill thickness of 1.0 m, about three times in the case which the fill thickness is 2.0 m and becomes more than five times in case which the fill thickness is 3.0 m.

4) The stress concentration ratio under the line load is from 0.7 to 0.9 times normalized line load in all cases.

5) Though the influence of steel fasteners which fix EPS blocks is not considered in this section, if the fasteners are installed and the EPS fill is subjected to differential settlement, it can easily be expected that the stress concentration of uniform surcharge will be increased.

Chapter 5. Control of Load Distribution Using Irregular EPS Blocks

5.1. Objectives

In view of the results presented in the previous chapters, it is clear that the internal structures formed by EPS blocks takes a very important role in load propagation properties in EPS block fills. The aim of this Chapter is to investigate whether the load distribution can be controlled by the variation of the internal structures through the model tests. To prepare the EPS block fills with different internal structures, EPS model fills were built up with the EPS blocks of trapezoidal and parallelogram section as well as with rectangular EPS blocks. And the internal structure were controlled so that the direction of joint between EPS blocks leaned toward selected directions.

5.2. Model Fill and Irregular EPS Blocks Used for Model Test

The EPS blocks used in a series of model tests are shown in Figs. 5.1 (a)-(d); Shown in Figs. 5.1 (a), (b) and (c) are blocks of trapezoidal section, and in Fig. 5.1 (d) the block with parallelogram section is shown, the degree of corner is about 67° as shown in Fig. 5.1 (a). These EPS blocks were cut in laboratory from Type-A block shown in Fig. 1.2 (a) of Chapter 1, a guide device shown in Figs. 5.2 (a), (b) were used and the accuracy of cutting was within ± 1.0 mm. The density of irregular EPS blocks and its Young's modulus and Poisson's ratio are 20.0 kg/m^3, 7.84 MPa and 0.01, respectively, and they are same as rectangular blocks used in Chapter 1.

The prepared model fills are shown in Figs. 5.3 (a)-(d) and Figs. 5.4 (a)-(d); The symmetrical model fills which have same silhouettes as symmetrical model fills in Chapter 1 are shown in Figs. 5.3, and the asymmetri-

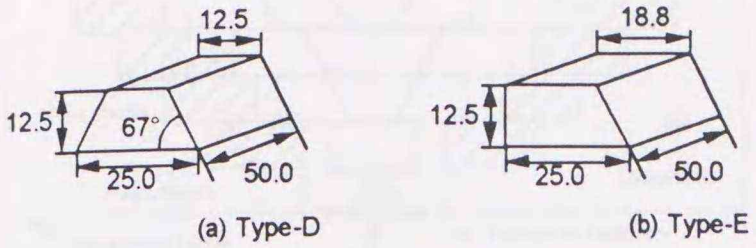

Figs. 5.1 (a)-(d). Not rectangular EPS blocks used in laboratory tests; (a) Type-D, (b) Type-E, (c) Type-F, (d) Type-G.

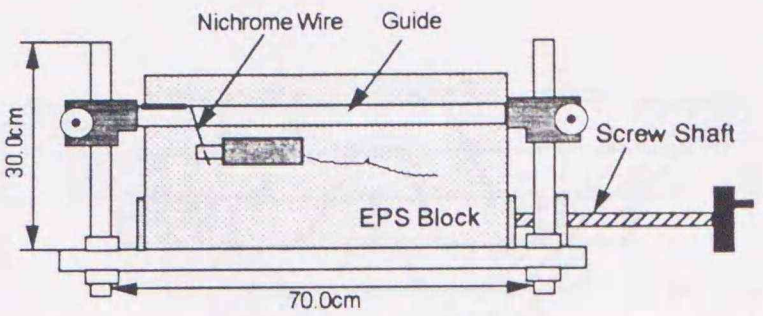

(a) Side view.

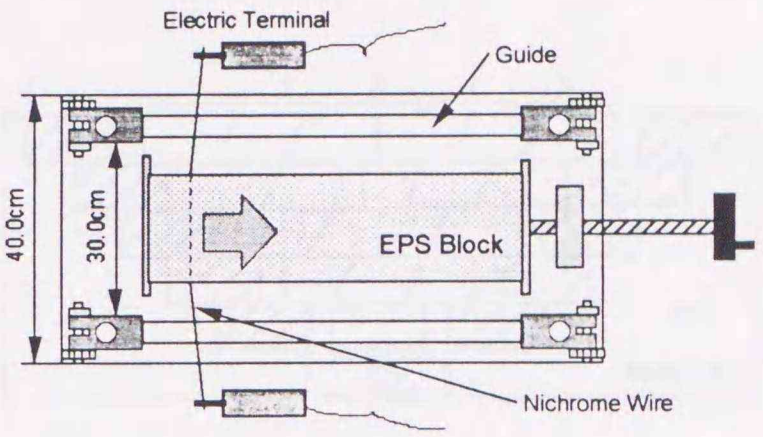

(a) Over view.

Figs. 5.2 (a),(b). Cutting guid device; (a) side view, (b) over view.

cal model fills which have same silhouettes as asymmetrical model fills in Chapter 1 are shown in Figs. 5.4. In symmetrical model fills, the name of model was appended the suffix 's' which is the first letter of 'symmetrical' like 'Model-As'. Model-As and Model-A have the centralized joint where the direction of joints are inclined toward the bottom-center block placed on the supporting plate of the bottom jack, and inversely Model-Bs and Model-B have spread out joint which the joints directions are spread out toward bottom of EPS fill chevron like. Model-Cs and Model-C have the direction of joints toward right down, and Model-Ds and Model-D have the joint directions toward left down.

The solid circles points out the positions of steel fasteners same as described in Chapter 1, and single fastener was set. The fasteners were installed only in Model-As and Model-A which have the centralized joint, and Model-Bs and Model-B which have the spread out joint. The steel plates whose weight is 22 kg each introduced in Chapter 1 were used for uniform overburden pressure of 1.7 kPa and for single static load of 215.6 N; the static load was moved at the each loading point on the surface of EPS

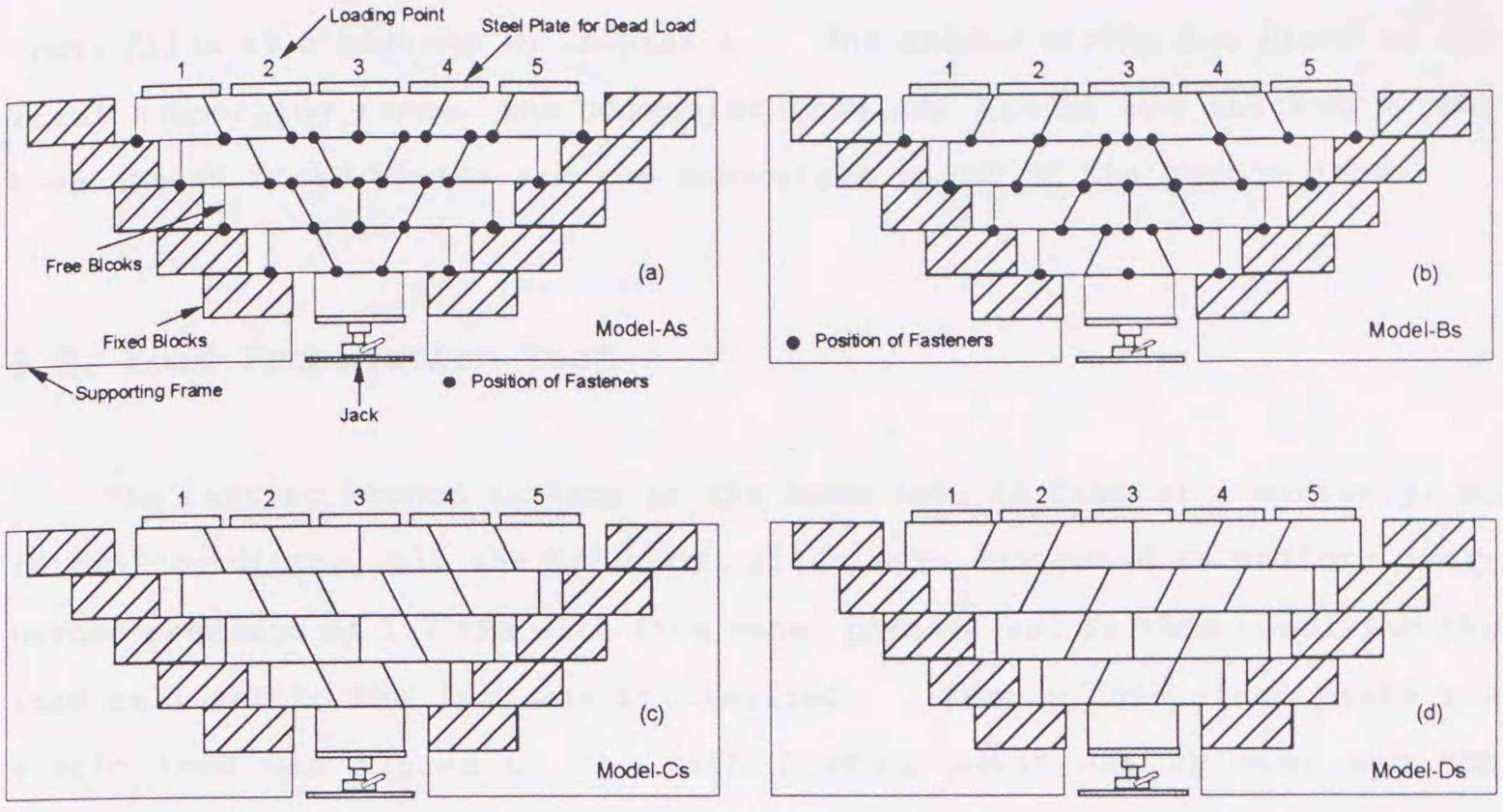

Figs. 5.3 (a)-(d). Prepared EPS model fills of symmetrical pattern; (a) Model-As, (b) Model-Bs, (c) Model-Cs, (d) Model-Ds

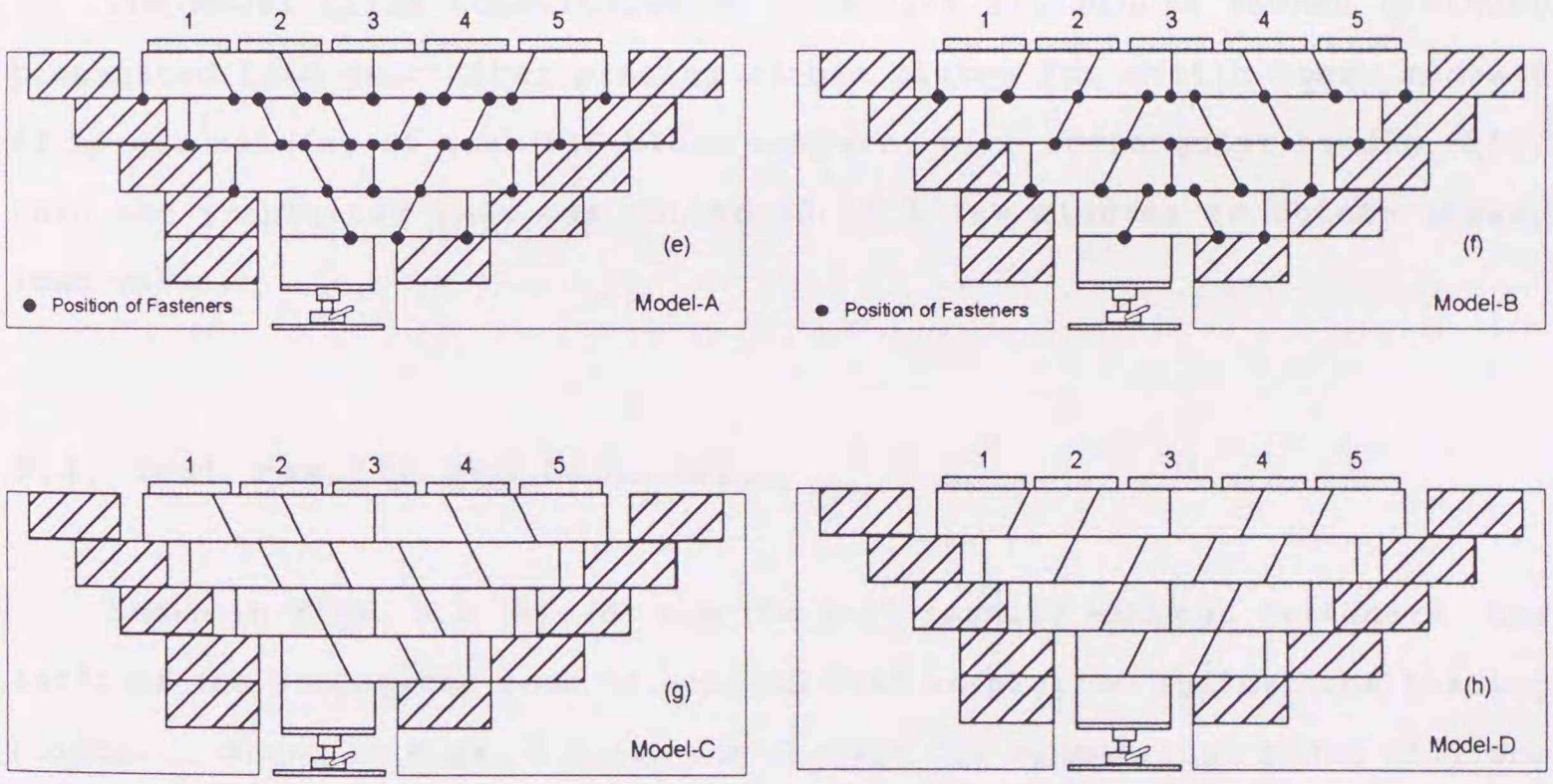

Figs. 5.4 (a)-(d). Prepared EPS model fills of asymmetrical pattern; (a) Model-A, (b) Model-B, (c) Model-C, (d) Model-D

model fills as explained in Chapter 1. The shaded blocks are fixed on the steel supporting frame, the irregular free EPS blocks are stacked up between these fixed blocks and the supporting plate of the bottom jack.

5.3. Load Propagation Test

The testing method is same as the described in Chapter 1 entirely; at initial condition, all the EPS model fills were subjected to uniform overburden pressure of 1.7 kPa with five steel plates, and in this condition the load cell set to the jack was initialized. Then single steel plate for static load was placed on the each loading point one by one, and the propagated load was measured at the bottom jack by load cell.

In Chapter 1, the load propagation test were carried out at two conditions; without and with distortion of EPS fill. In this Chapter, however, only the case of the model fill without distortion was carried out.

The model fills constituted of irregular EPS blocks showed unsteady propagated load just after placing single plates for static load, because of larger sliding of each EPS block compared with rectangular blocks fill, then the propagated load was monitored in a few minutes to obtain steady load value.

5.4. Test results and Discussion

Shown in Figs. 5.5 (a)-(d) are the test results without fasteners; the ratio of the propagated load to applied load is plotted against the loading points. Shown in Figs. 5.5 (a) and (b) are for symmetrical model fill and shown in Figs. 5.5 (c) and (d) are for asymmetrical model fill, the results for model fills constituted of only rectangular blocks are also shown; the rectangular block fill for symmetrical pattern is shown in Fig. 5.6 (a) and for asymmetrical pattern is shown in Fig. 5.6 (b), they are Model-A and Model-C in Chapter 1.

As shown in Fig. 5.5 (a), the influence of joint direction is found between the centralized joint and spread out joint in symmetrical model

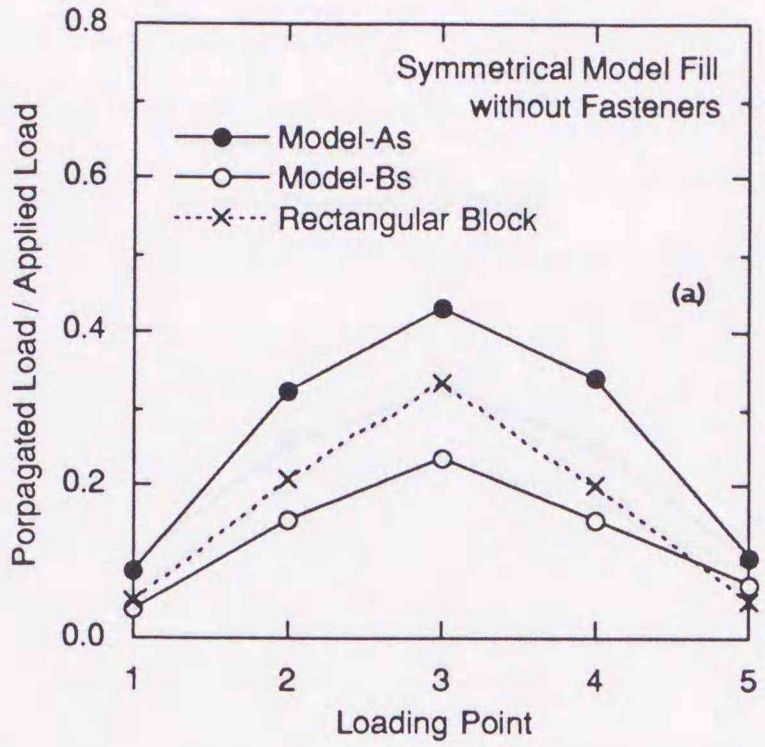

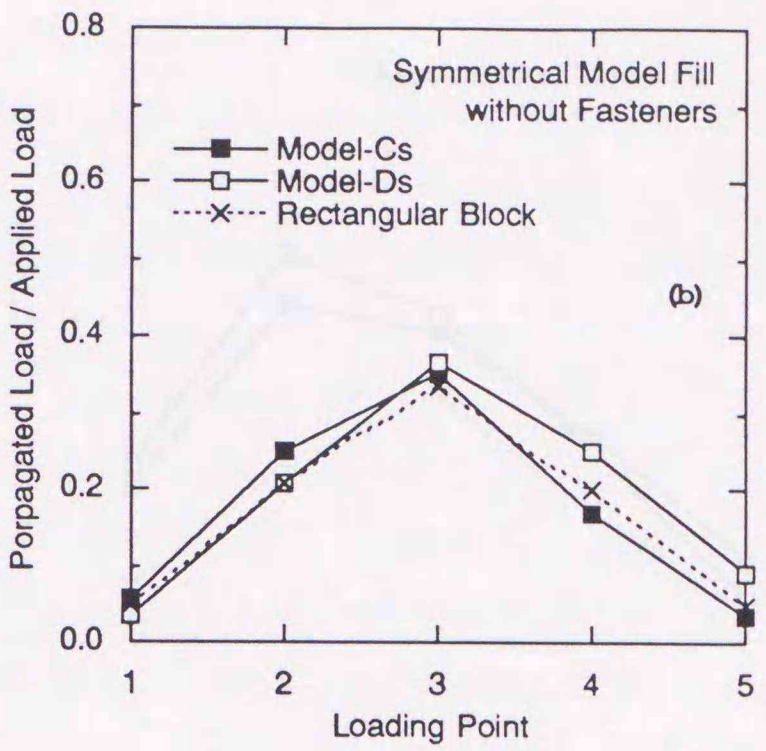

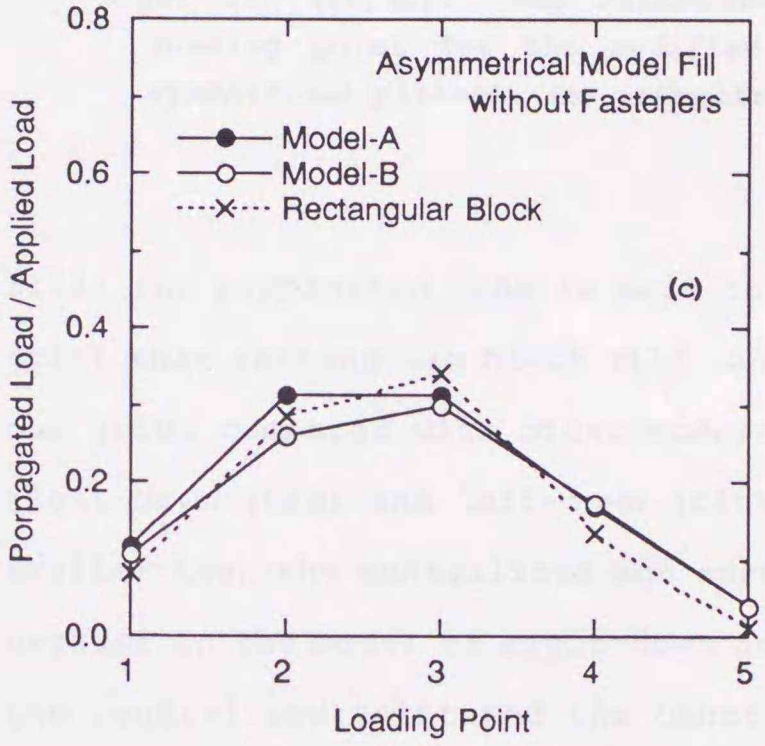

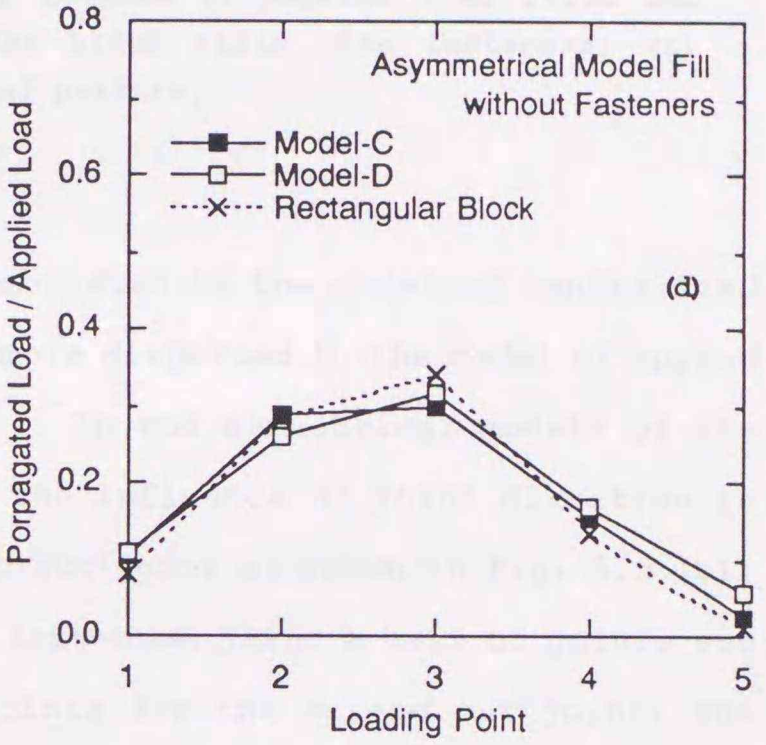

Figs. 5.5 (a)-(d). The relationship between propagated load ratio and loading point for the modified EPS block fills without fasners; (a) Model-As, (b) Model-Bs, (c) Model-Cs, (d) Model-Ds.

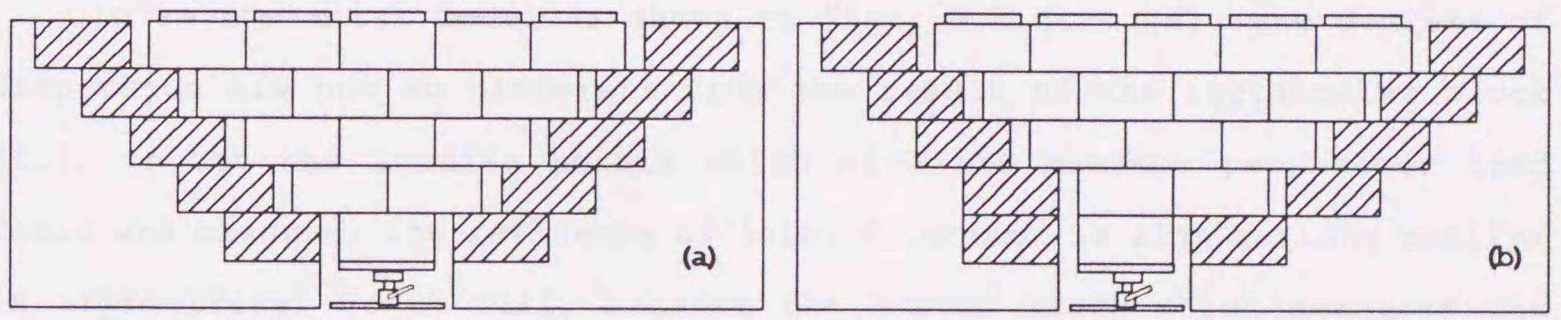

Figs. 5.6 (a),(b). EPS model fills constituted of rectangular blocks; (a) symmetrical pattern, (b) asymmetrical pattern.

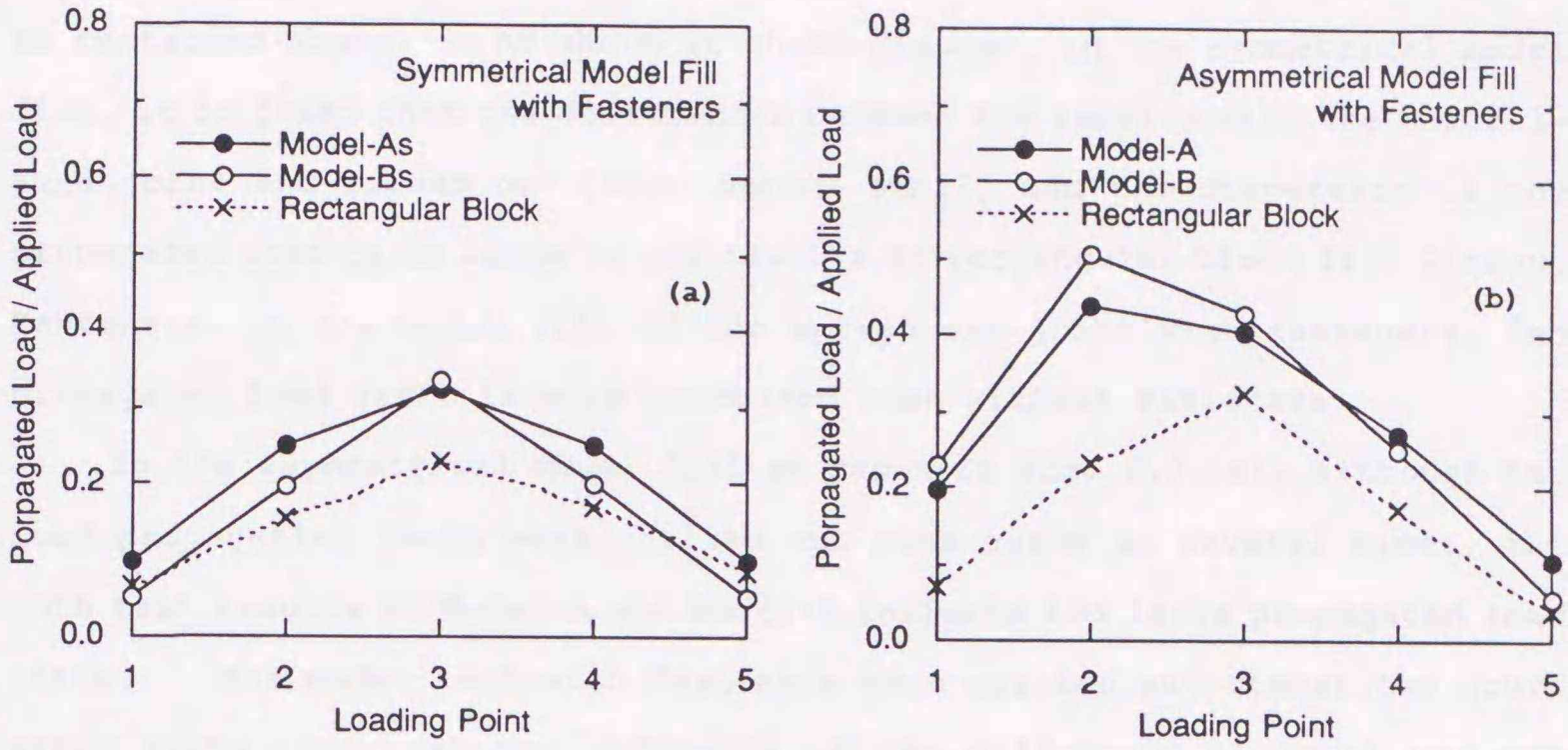

Figs. 5.7 (a),(b). The relashonship between propagated load ratio and loading point for the modified EPS block fills with fasteners; (a) symmetrical pattern, (b) asymmetrical pattern.

fill; the propagated load is more concentrated in the model of centralized joint than rectangular block fill, and more dispersed in the model of spread out joint compared with other models. In the symmetrical models of the right-down joint and left-down joint, the influence of joint direction is smaller than the centralized and spread out joint as shown in Fig. 5.5 (b), because in the model of right-down and left-down joint a half of joints are the centralized joint and the other joints are the spread out joint; the influence are cancelled each other. The degree of dispersion is almost same with rectangular block fill, but the difference of joint direction between the right and the left of the model fills is recognized clearly in Fig. 5.5 (b).

In asymmetrical model as shown in Figs. 5.5 (c), (d), the degrees of dispersion are not so different from the result of the rectangular block fill, though the loading points which give the maximum propagated load ratio are changed; the influence of joint direction is also getting smaller in asymmetrical model fill, because the bottom block which measures the propagated load is slid to left.

Shown in Figs. 5.7 (a), (b) are the results with fasteners; the model test with fasteners were carried out in Model-As and Model-A which have the centralized joint and Model-Bs and Model-B which have the spread out joint

as mentioned above. As shown in those figures, in the symmetrical model fill, it is found that the differences between the results with the centralized joint and spread out joint become small, and the dispersion of the propagated load is as large as the results of rectangular block fill without fasteners; in the model fill of the spread out joint with fasteners, the propagated load ratio is more concerned than without fasteners.

In the asymmetrical model fill as shown in Fig. 5.7 (b), although the load propagation tests were carried out over again in several times, the both test results of Model-A and Model-B indicate too large propagated load ratio. The model test with fasteners were carried out utmost two hours after installing, and the influence of the difference in level was not disappeared, because the irregular EPS block has sharp corner. But it should be noted that these facts which the fasteners don't always work for dispersion of propagated load, as shown in the Model-Bs, -A and -B, though in the Model-A and Model-B, the leaving time might be not enough.

Anyway it seems that the load propagation properties can be controlled by changing the direction of joints.

5.5. Comparison of Numerical Analysis with Model Test

The comparisons of numerical analysis with model test are shown in Figs. 5.8 (a)-(d) and Figs. 5.9 (a)-(d); these figures, Figs. 5.8 (a)-(d) and Figs. 5.9 (a)-(d), indicate the results of the symmetrical model fills and asymmetrical model fills, respectively, and both results are for models without fasteners.

The FEM code adopted in the present study can be dealt with only continuum media, then the difference of internal structures between Model-As and -A which have the centralized joint and Model-Bs and -B which have the spread out joint and so on. For this reason, the two types of FEM mesh for these model fills were prepared; one is for symmetrical model fills and the other is for asymmetrical model fills. On the other hand, DEM can take account of the influence of the joint direction; in comparison of the results from the symmetrical model fill which has the centralized joint (Model-As) and the symmetrical model fill which has the spread out joint

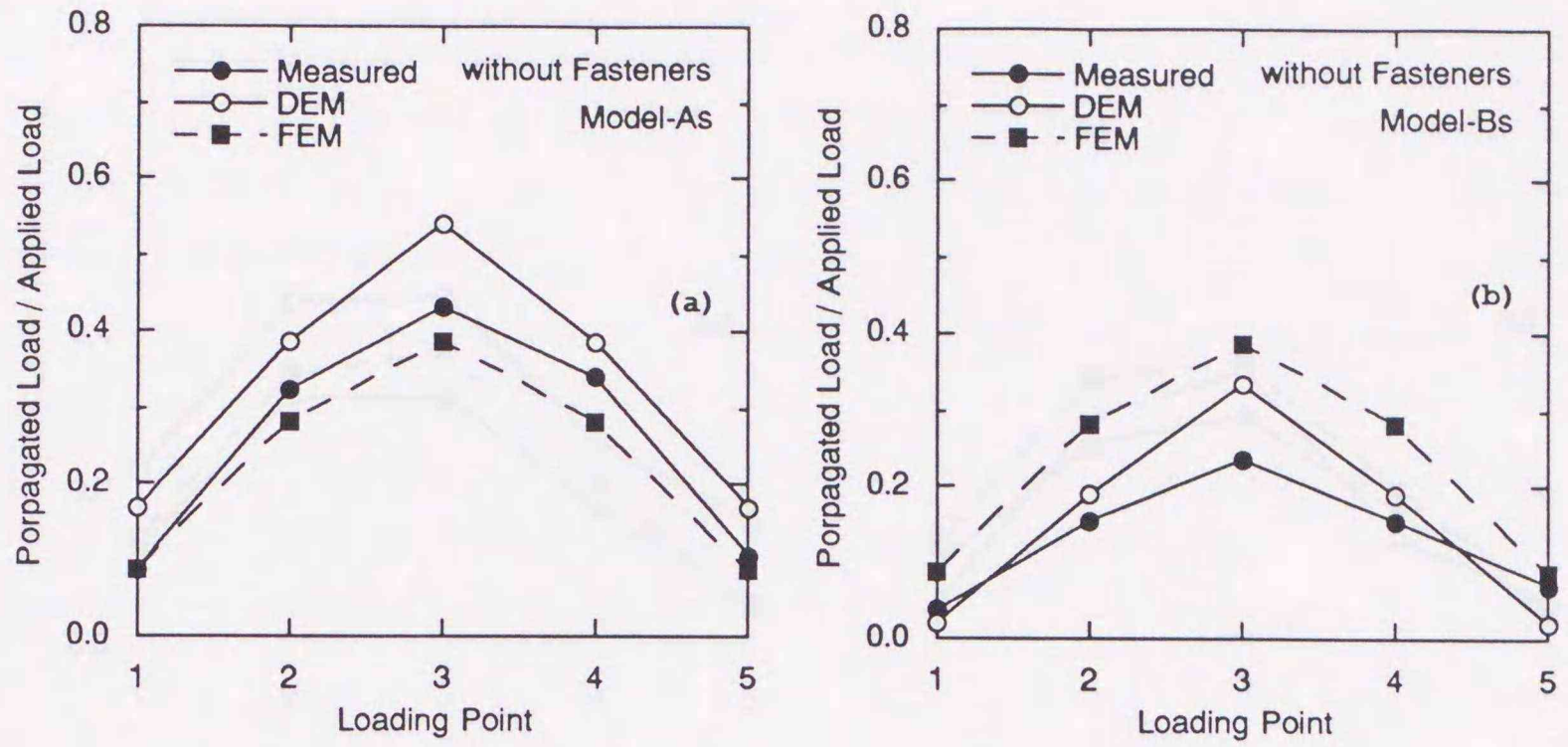

Figs. 5.8 (a)-(d). The comparison between numerical analysis and model tests of symmetrical pattern; (a) Model-As, (b) Model-Bs, (c) Model-Cs, (d) Model-Ds.

(Model-Bs), even in DEM analysis, the propagated load ratio is more concerned in Model-As than in Model-Bs. Moreover the results from the models of the right-down joint (Model-Cs) and the left-down joint (Model-Ds) are also expressed by DEM. It seems, however, that the results of DEM analysis overstate these influences of the internal structures to some extent, as

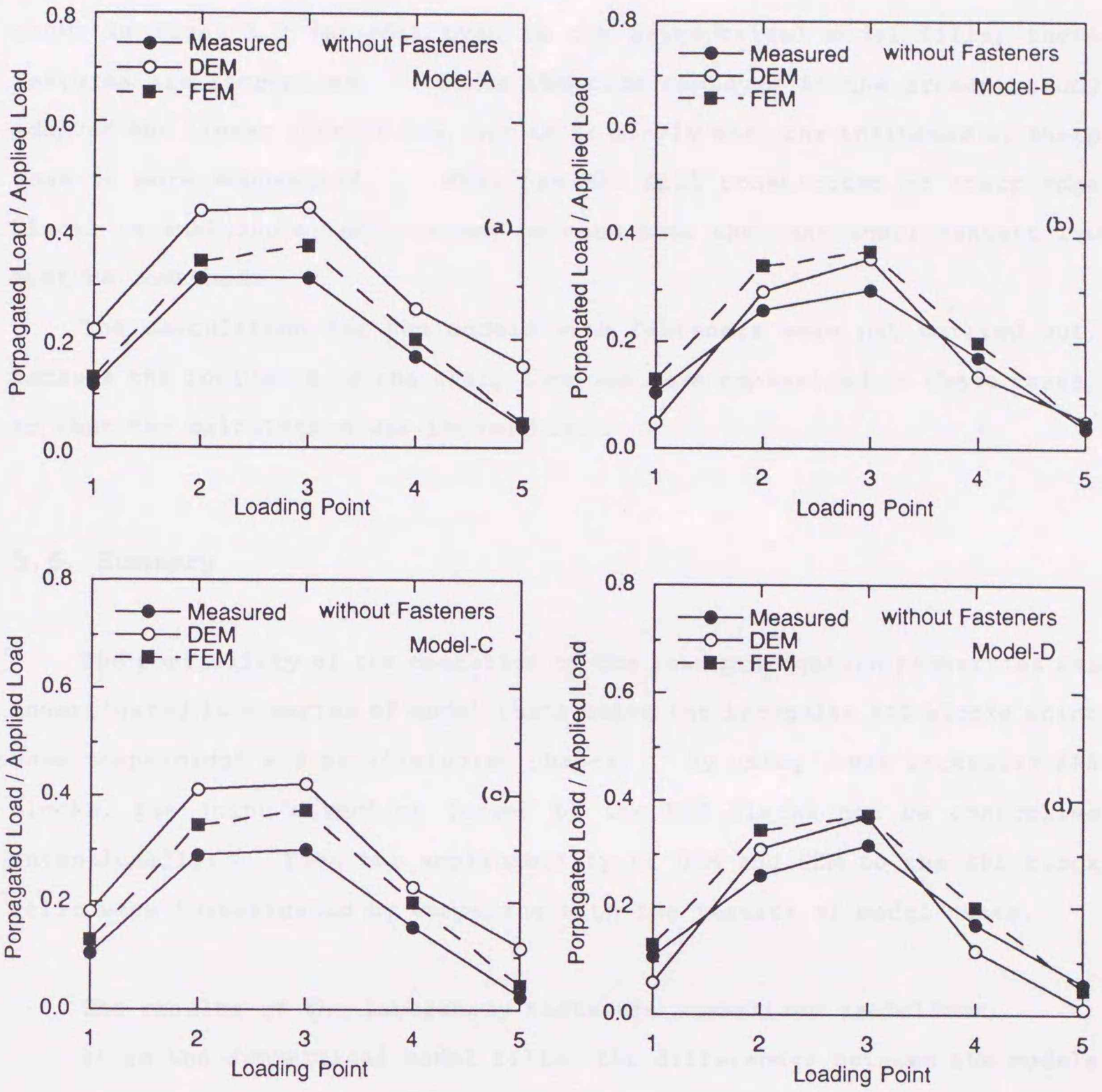

Figs. 5.9 (a)-(d). The comparison between numerical analysis and model tests of asymmetrical pattern; (a) Model-A, (b) Model-B, (c) Model-C, (d) Model-D.

shown in Figs. 5.9 (a)-(d); even in the asymmetrical model fills, these features are recognized. Since DEM code employed in the present study adopted the linear contact law, and it is likely that the influence of sharp edge is more emphasized. When the EPS fill constituted of sharp edge blocks is analyzed by DEM, it may be need that the non-linear contact law must be combined.

The calculation for the models with fasteners were not carried out, because the influence of the sharp edge was more emphasized in these cases, so that the calculation was impossible.

5.6. Summary

The possibility of the operation of the load propagation properties was investigated in a series of model tests using the irregular EPS blocks which have trapezoidal and parallelogram shapes. By using these irregular EPS blocks, the joint direction formed by the EPS blocks can be controlled intentionally. Then the applicability of DEM and FEM to the EPS block fills were investigated by comparing with the results of model tests.

The results of the laboratory tests are summarized as follows;

1) In the symmetrical model fills, the differences between the models with centralized joints and with spread out joints become small by installing fasteners. But the degree of the dispersion is same as the rectangular block fill's, the result of the models with spread out joints shows more concentrated load propagation than without fasteners.
2) The influences of the right-down joint and the left-down joint are relatively small in symmetrical model fills, they are similar to the cases without fasteners.
3) In asymmetrical model fills with fasteners the propagated load tend to concentrate, it seems that the fasteners are not effective always work, so that the applied load is dispersed.
4) In the symmetrical model fills, the differences between the models with centralized joints and with spread out joints become small by

installing fasteners. But the degree of the dispersion is same as the rectangular block fill's, the result of the models with spread out joints shows more concentrated load propagation than without fasteners.

5) The influences of the right-down joint and the left-down joint are relatively small in symmetrical model fills, they are similar to the cases without fasteners.

6) In asymmetrical model fills with fasteners the propagated load tends to concentrate, it seems that the fasteners are not effective always work, so that the applied load is dispersed.

The results of the comparison of the numerical analysis with the laboratory tests without fasteners are summarized as follows;

1) Since FEM employed in the present study cannot take account of the internal structures, the influence of the joint direction cannot be explained by FEM as a matter of course.

2) DEM can explained the differences due to the variation of the joint direction; however the results of calculation overestimates the influences to some extent. The major cause is that the static DEM employed in the present study assumed linear contact law even for sharp corners of EPS blocks.

Part 3. Dynamic Behavior of EPS Block Fill

Chapter 1. Experimental Investigation of Vibration Properties of EPS Fill

1.1. Prepared EPS Model Fill and Shaking Device for Vibration Test

Six EPS model fills were prepared for a series of vibration tests as shown in Figs. 1.1 (a)-(f); Model-A, Model-B1 and Model-C1 have same silhouettes of 1.0 × 2.0 × 0.5 m, Model-A is one continuum EPS block, Model-B1 is composed of five big EPS blocks which are 0.5 × 1.0 × 0.5 m or 0.5 × 0.5 × 0.5 m. And Model-C1 is composed of sixty eight EPS blocks which are 0.125 × 0.25 × 0.5 m or 0.125 × 0.125 × 0.5 m. Model-B2, Model-C2 and Model-C3 were prepared to investigate the influence of height or width of the whole EPS model fills; the height of Model-C2 is a half of Model-C1, Model-C3 is reduced the width to a half of Model-C2, and Model-B2 is model fill removed the two EPS blocks in top both sides of Model-B1. Especially Model-B2 was prepared to investigate the influence of collision with adjacent EPS blocks.

The solid circles on each model fill shown in Figs. 1.1 (a)-(f), indicates the position of accelerometers, each accelerometer is added the channel number in that figures. Although some solid circles are painted on front surface of EPS block, all the accelerometers were placed at middle of depth as shown in Fig. 1.2. The installation method of accelerometers to EPS blocks is shown in Fig. 1.2, accelerometers enclosed by vinyl tape were set into the trench on EPS block surface; the accelerometers were fixed in the trenches by using vinyl tape.

The accelerometer of Ch 5 in Model-C3 was installed to measure the vertical acceleration, other accelerometers measured horizontal acceleration. In all model fills, Ch 1 accelerometer is set up to the shaking table, the measured acceleration is assumed as a input acceleration wave. This Ch 1 accelerometer is named 'Base' and top-center accelerometer (Ch 3 in almost model fills) is 'Center' in the following figures. As the same

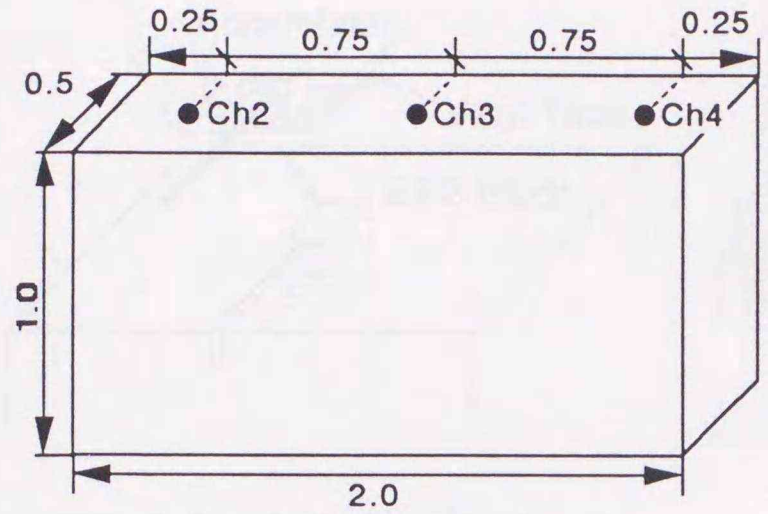

(a) Model-A

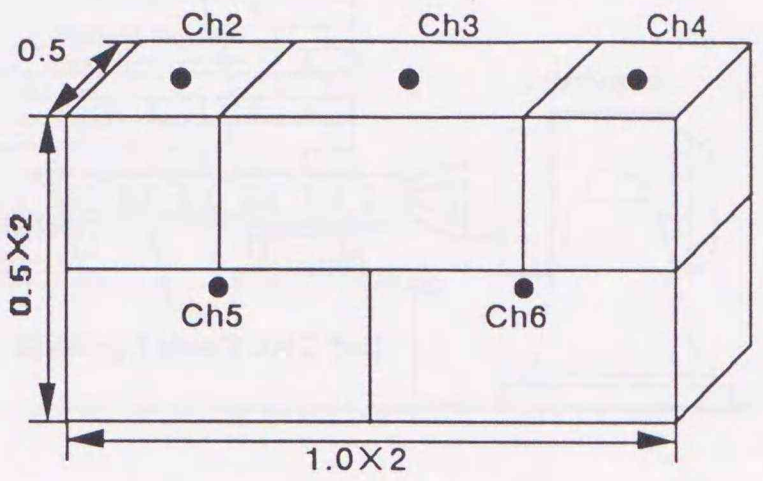

(b) Model-B1

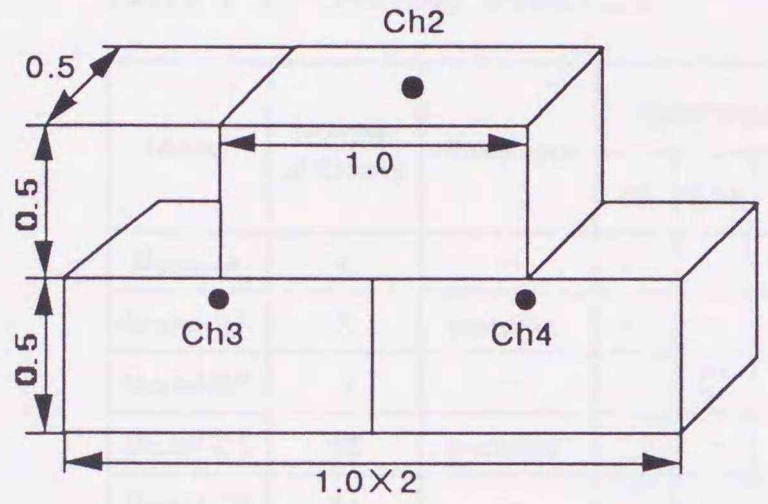

(c) Model-B2

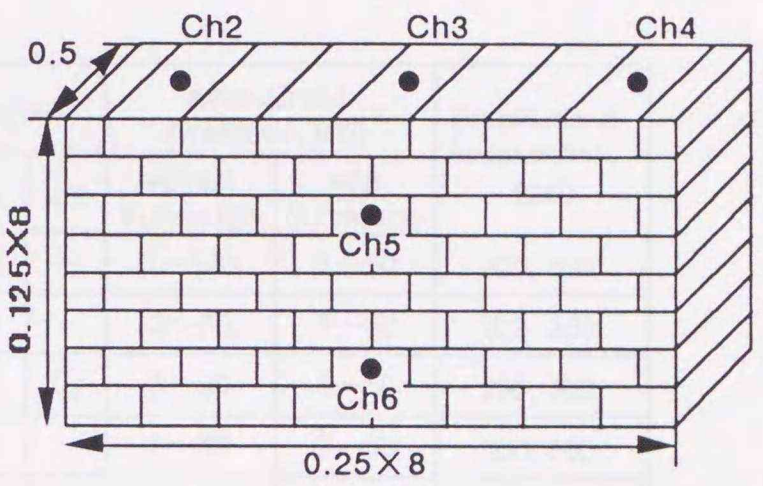

(d) Model-C1

Unit: mm

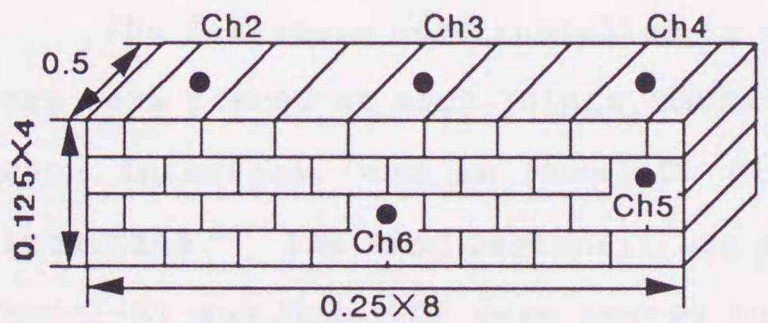

(e) Model-C2

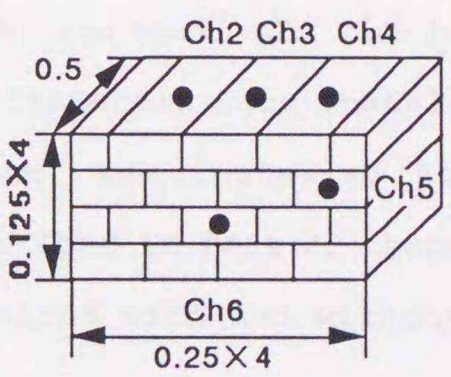

(f) Model-C3

Figs. 1.1 (a)-(f). Preparation EPS model fills; (a) Model-A, (b) Model-B1, (c) Model-B2, (d) Model-C1, (e) Model-C2, (f) Model-C3.

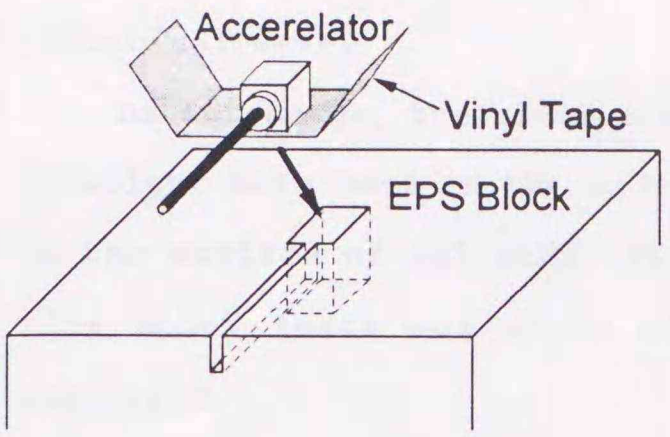

Fig. 1.2. Installation of Accelerometer.

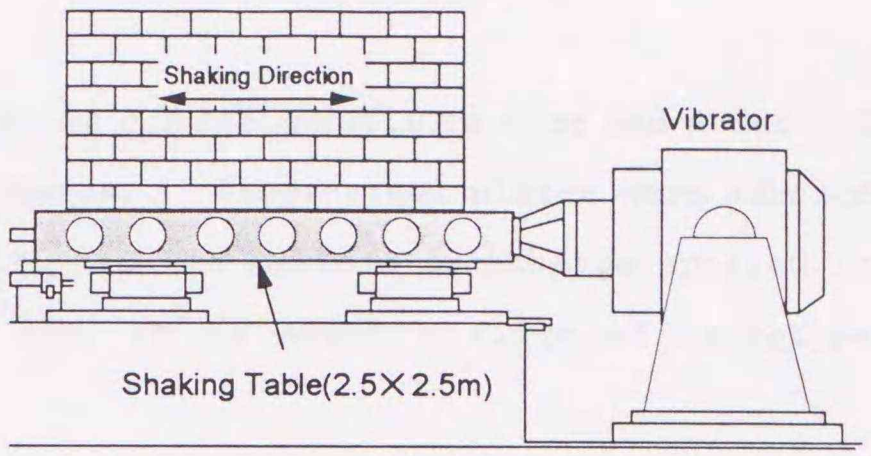

Fig. 1.3. Shaking Device.

Table 1.1. Testing condition.

Model	Number of Blocks	Fasteners	Surcharge, (kPa)				Aimed Input Amplitude, (Hz)		Amplitude of Acceleration, (gal)
			0.0	0.55	1.1	2.2	without Surcharge	with Surcharge	
Model-A	1	—	○	—	○	—	3～140	3～50	200, 300
Model-B1	5	installed	○	—	○	—	3～80	3～50	200, 300
Model-B2	3	—	○	○	○	○	3～80	3～50	200, 300
Model-C1	68	installed	○	—	○	—	3～50	3～50	200, 300
Model-C2	34	—	○	○	○	—	3～60	3～50	200, 300
Model-C3	18	—	○	○	○	○	3～80	3～50	200, 300

way, accelerometers of Ch 2 and Ch 4 were named 'Left' and 'Right', respectively, and 'Middle' and 'Bottom' mean the accelerometers of Ch 5 and Ch 6.

The fasteners were installed in only Model-B1 and Model-C1, the fasteners were placed at each joints, in Model-B1 two fasteners were installed at each interface, and in Model-C1 single fastener was installed at each interface. The used fasteners are same as described in Part 2, Chapter 2. Model-B1 and Model-C1 were tested in the conditions with and without fasteners.

Shown in Fig. 1.3 is shaking device used for vibration tests. The horizontal shaking table is square of 2.5 m, the capable frequency of input acceleration wave is from 0.01 to 3 MHz, and maximum acceleration amplitude is 2.8 G without surcharge or testing materials. The shaking table can support structure of 10 ton weight. The shaking direction is right and left direction in Fig. 1.3. The input acceleration wave was designated

sinusoidal wave.

As surcharge, the steel plates of 0.7×25.0×50.0 cm size and about 7.0 kg weight were used in the model tests. These steel plates were adhered on the surface of EPS model fills, and the maximum suracharge applied in this model tests was about 10 kPa, it is about a fifth of prototype surcharge.

2.2. Testing Condition and Arranging Method of Test Results

The model tests have four parameters: the shape of EPS model fills, surcharge, fasteners and amplitude of acceleration wave; the total test cases were forty two. And for the forty two cases, the vibration tests were performed to gain the amplification ratios under various frequency of input acceleration wave. The testing conditions are shown in Table. 1.1.

The input acceleration wave was used sinusoidal wave, and the preliminary tests were carried out to obtain appropriate amplitude ratio or transfer function. The increment of input wave frequency was 2 Hz around the resonant frequency, and from 5 to 10 Hz in other frequency region. The amplitudes of input acceleration wave were 200 and 300 gal.

Shown in Figs. 1.4 (a), (b) are input acceleration wave and the acceleration wave measured at the Center accelerometer (Ch 3), in Model-B1 and Model-C1; the aimed frequency and amplitude of acceleration were 20 Hz and 300 gal, respectively. In both results, surcharge was 1.1 kPa and fasteners were not installed. As shown in Figs. 1.4 (a), (b), the frequency of the input wave was smaller than 20 Hz, and this tendency was recognized in all tests; this tendency would be the propertie of shaking table and vibrator used in the present study. Then the true frequency of input wave was obtained by FFT analysis as explained below. On the other hand, the acceleration wave amplitude would have enough accuracy.

The results of FFT analysis for above two model fills are shown in Figs. 1.5 (a), (b), respectively, and it is found that all the EPS blocks vibrated in a manner of forced vibration not free vibration. This feature was also confirmed in all model tests.

The sampling was for twenty five seconds in total for all vibration

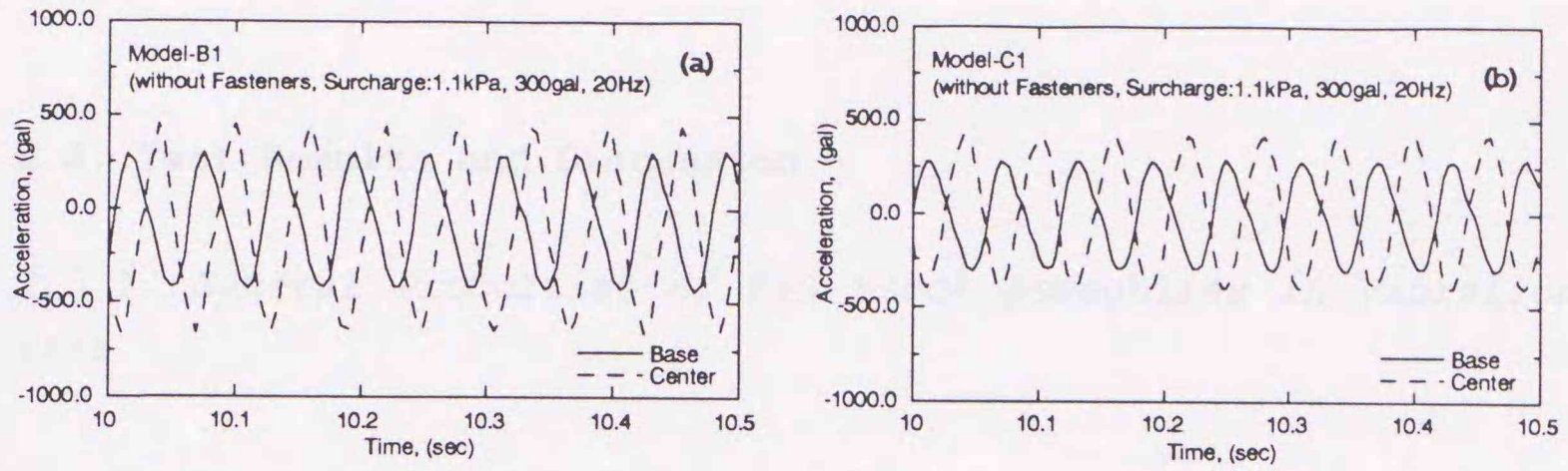

Figs. 1.4.(a),(b). Measured acceleration waves (input wave frequency : 20 Hz, input acceleration amplitude: 300 gal, surcharge: 1.1 kPa); (a) Model-B1, (b) model-C1.

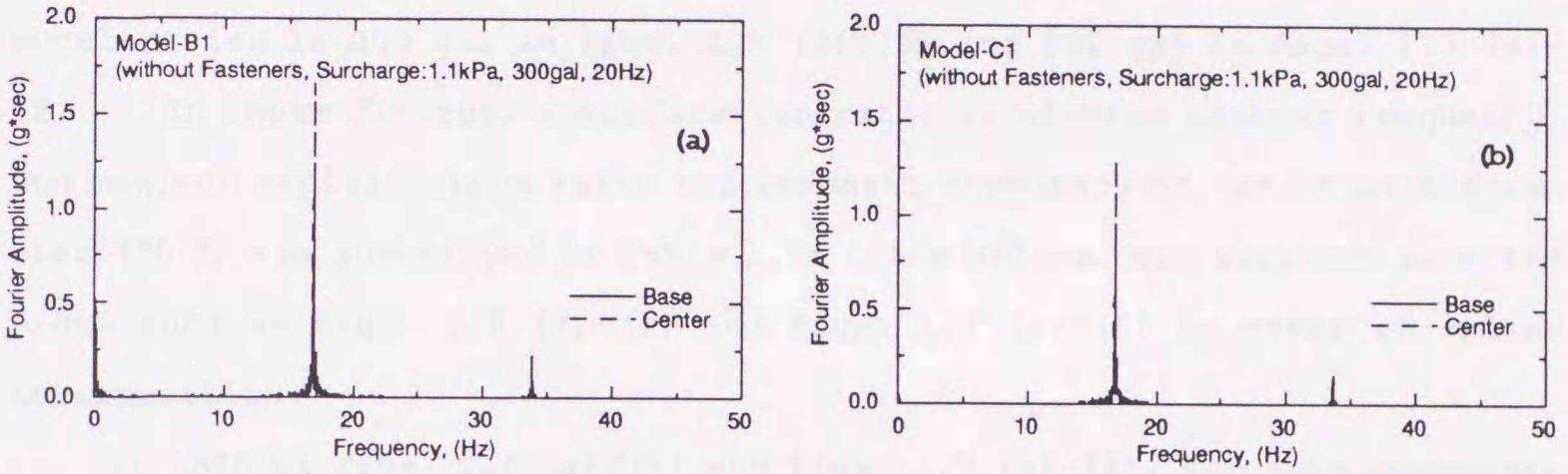

Figs. 1.5.(a),(b). The results of FFT analysis (input wave frequency : 20 Hz, input acceleration amplitude: 300 gal, surcharge: 1.1 kPa); (a) Model-B1, (b) Model-C1.

tests, the measured data for fifteen seconds in steady state of the applied acceleration wave were adopted as the data to be analyzed. The interval of sampling was changed for each frequency of the input wave, so that sampling frequency was more than ten times of aimed input frequency; in the cases shown in Figs. 1.4 (a), (b) and Figs. 1.5 (a), (b), the sampling frequency was 300 Hz.

To obtain amplification ratio (or transfer function), the maximum Fourier amplitude of each accelerometer set up to EPS blocks was divide by the maximum Fourier amplitude of input acceleration wave.

2.3. Test Results and Discussion

2.3.1. General Properties of EPS Block Assemblies in Vibration Test

At first, the behaviors of model fills without fasteners are discussed to investigate the vibration properties of EPS block assemblies, and then the influence of fasteners are discussed. Shown in Figs. 1.6 (a)-(f) and Figs. 1.7 (a)-(f) indicate the resonant properties for the six model fills whose surcharge is 1.1 kPa in common. And the amplitude of input acceleration is 200 gal in Figs. 1.6 (a)-(f) and 300 gal in Figs. 1.7 (a)-(f). In those figures, amplification ratio is plotted against frequency, and maximum amplification ratio and resonant frequency of Center accelerometer (Ch 3) are summarized in Table 1.2; those values were obtained from the plots such as Figs. 1.6 (a)-(f) and Figs. 1.7 (a)-(f) by means of spline interpolation.

In both of Figs. 1.6 (a)-(f) and Figs. 1.7 (a)-(f), the accelerometers near surface of EPS fills show higher amplification ratio than others, this tendency is similar to the behavior of elastic body.

2.3.2. The Influence of Acceleration Intensity

The amplification ratio of model fills applied 300 gal shown in Figs. 1.7 (a)-(f) is smaller than amplification of 200 gal shown in Figs. 1.6 (a)-(f) except for Model-A. It suggests that the inertia force in shaking by 300 gal becomes large compared with the friction force between EPS block layer. In fact, the amplification ratio in flat part of the plots, the slippage of EPS blocks were recognized. As shown in Figs. 1.6 (a)-(f), Figs. 1.7 (a)-(f) and Table 1.2, the resonant frequency of acceleration amplitude of 300 gal is seemed to be slightly small compared with results in 200 gal, the overall stiffness of EPS fill is likely to decrease. As the reasons of this decreasing of shear resistance, it would be said that EPS fills are disturbed by slippage of individual EPS blocks, and the area of

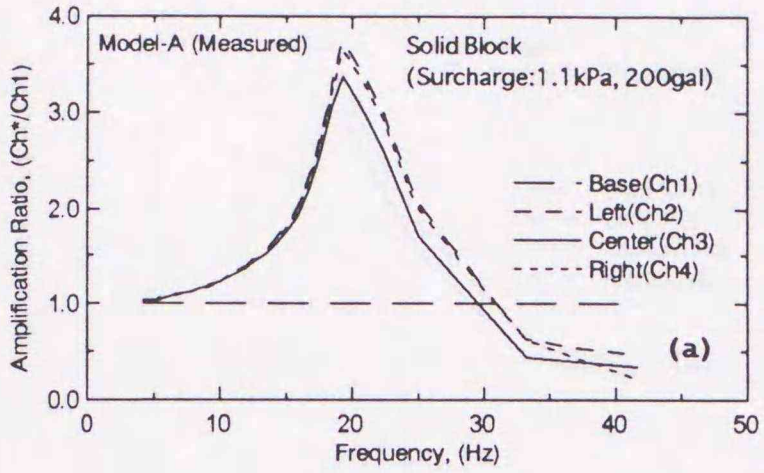

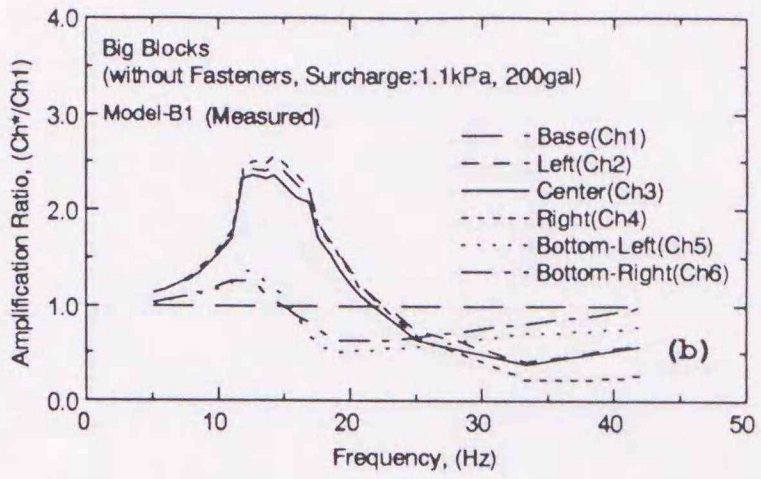

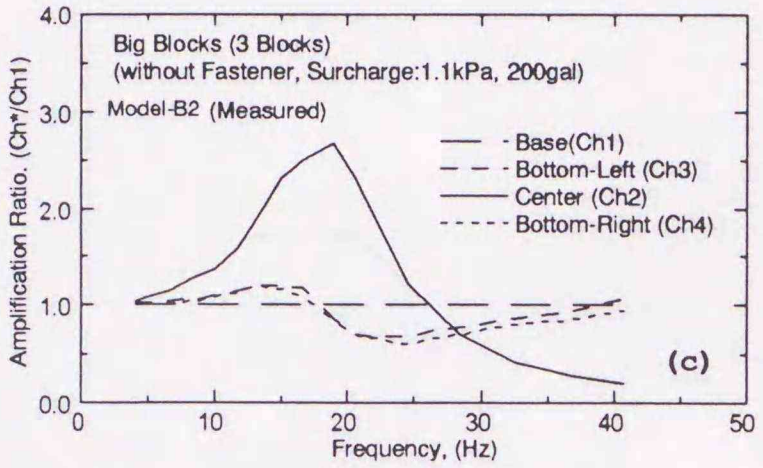

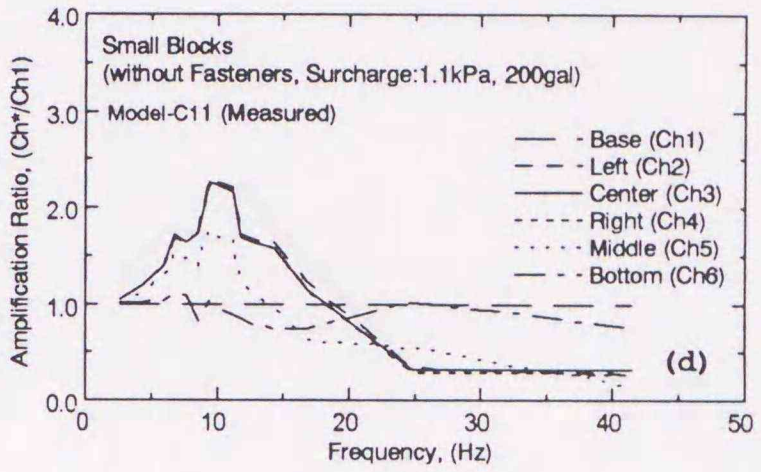

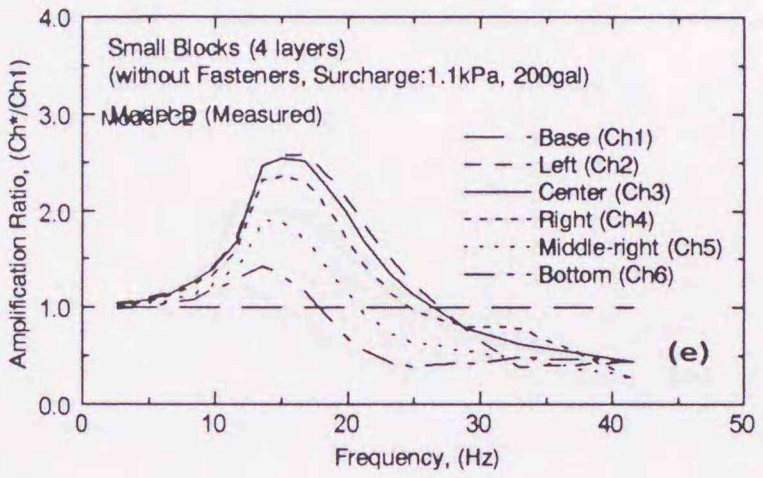

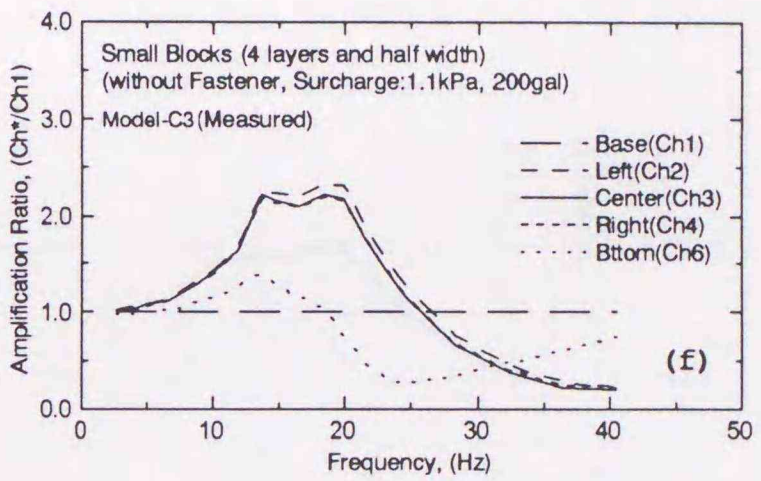

Figs. 1.6(a)-(f). The relationships between amplification ratio and frequency (without fasteners, surcharge is 1.1 kPa, applied acceleration amplitude is 200gal); (a) Model-A, (b) Model-B1, (c) Model-B2, (d) Model-C1, (e) Model-C2, (f) Model-C3.

contact is decreased by rotation of individual EPS blocks during vibration and then the friction resistance is getting small. From Table 1.2, in the case without fasteners, it is found that these tendencies are recognized.

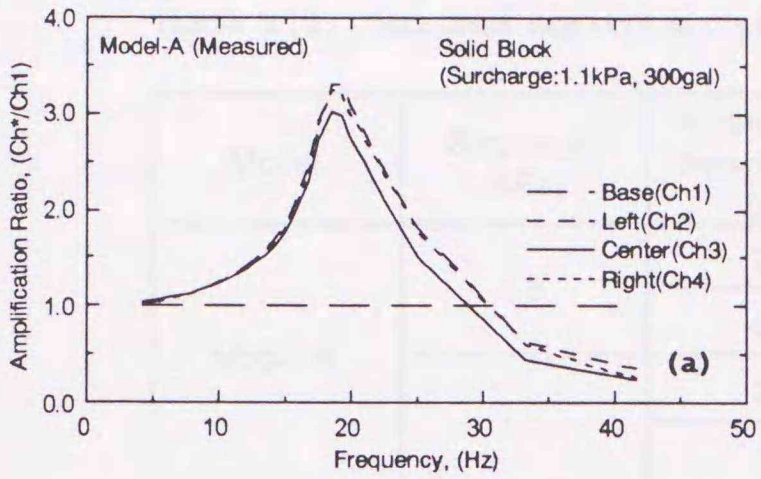

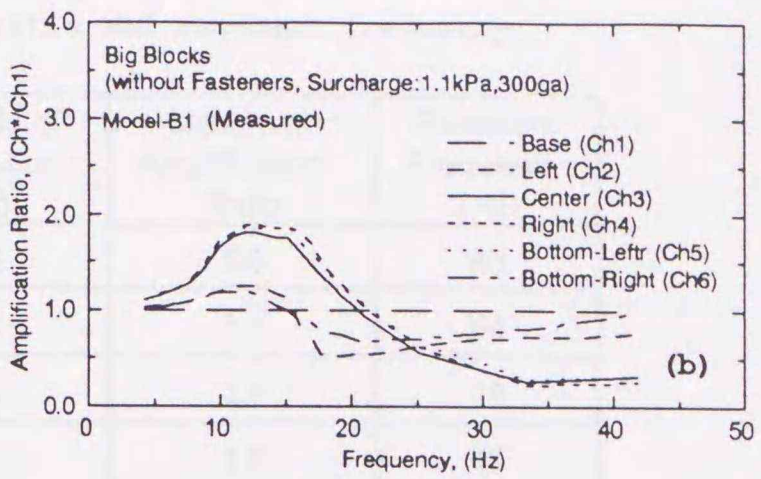

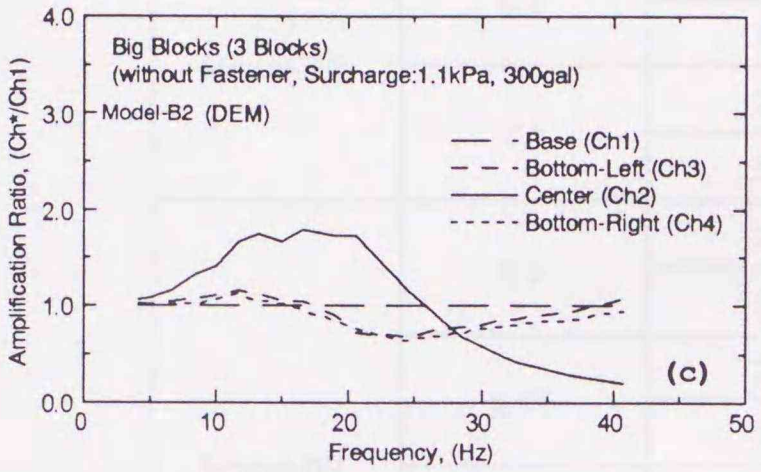

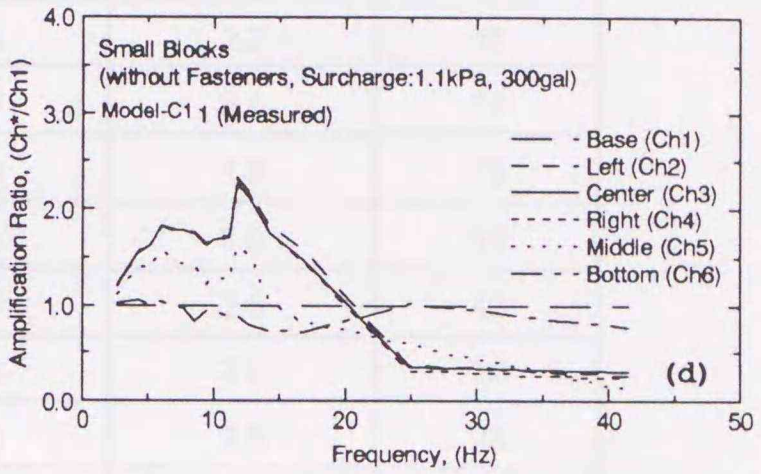

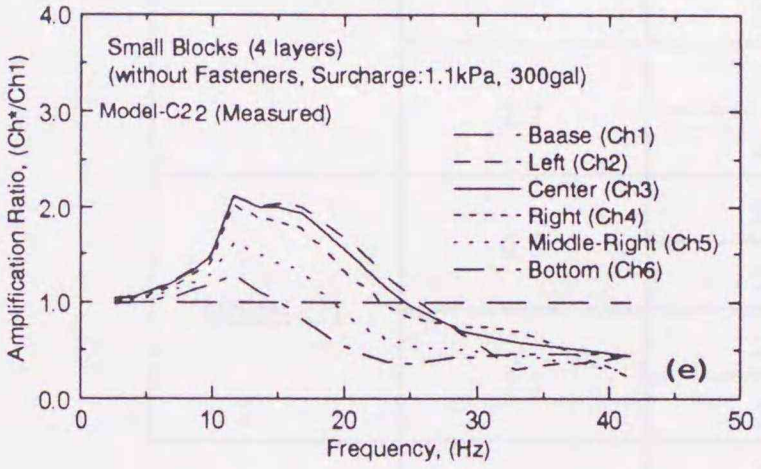

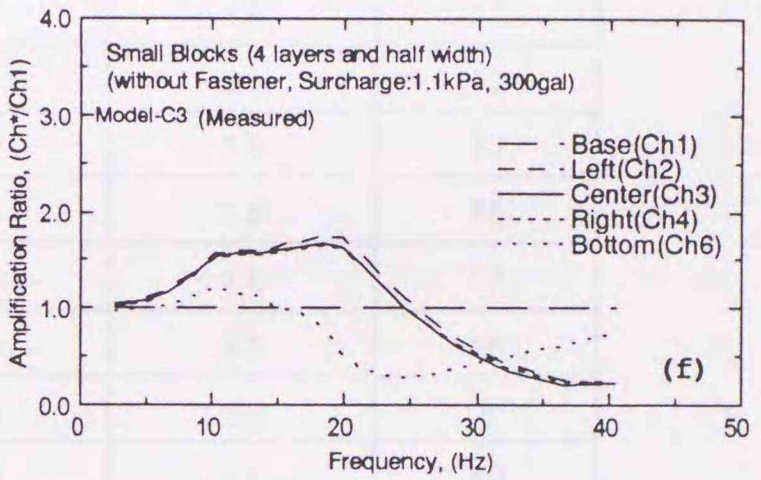

Figs. 1.7(a)-(f). The relationships between amplification ratio and frequency (without fasteners, surcharge is 1.1 kPa, applied acceleration amplitude is 300gal); (a) Model-A, (b) Model-B1, (c) Model-B2, (d) Model-C1, (e) Model-C2, (f) Model-C3.

2.3.3. The Influence of Number of EPS Blocks and Surcharge

Model-A, Model-B1 and Model-C1 have same silhouette, but the resonant frequency and maximum amplification ratio are getting small with an increase in the number of blocks or a decrease in size even in same surcharge condition as shown in Table 1.2. This corresponds to the decreasing of stiffness, and the amplification ratio is also getting small, as the EPS

Table 1.2. Maximum amplification ratio and resonant frequency.

Model	Surcharge (kPa)	Amplitude of Acceleration (gal)	Maximum Amplification Ratio	Resonant Frequency (Hz)
Model-A	0.0	200	5.0	83
		300	5.3	84
	1.1	200	3.4	19
		300	3.0	19
Model-B1	0.0	200	2.6	44
		300	2.2	45
	1.1	200	2.4	14
		300	1.8	13
Model-B2	0.0	200	3.0	50
		300	2.5	42
	0.55	200	2.9	22
		300	2.0	22
	1.1	200	2.7	18
		300	1.8	17
	2.2	200	2.5	12
		300	1.8	11
Model-C1	0.0	200	2.5	19
		300	1.8	17
	1.1	200	2.3	10
		300	2.0	9
Model-C2	0.0	200	2.0	40
		300	1.9	40
	0.55	200	2.6	19
		300	2.0	16
	1.1	200	2.6	16
		300	2.1	14
Model-C3	0.0	200	2.2	48
		300	1.8	47
	0.55	200	2.5	19
		300	1.9	17
	1.1	200	2.3	17
		300	1.7	16
	2.2	200	2.2	14
		300	1.7	13

blocks gain in number. The reasons of this tendency would be also that the collision due to the rotation of individual blocks during vibration, and the degree of disturbance is getting large with an increase of number of blocks.

As the surcharge is getting large, the resonant frequency become small except for Model-A, this feature is also similar to elastic body. In Model-B2 this tendency is likely to be small, because in Model-B2 the number of blocks was only a few, it seems that the influence of the number of blocks or test error is larger than the surcharge influence. Although it is reported that the overall stiffness of EPS fill is getting large with increasing of surcharge in previous study[17], it is difficult to confirm it without the basis stiffness. This influence will be discussed in Chapter 2 of this Part in detail.

Another influence of surcharge is shown in the comparison of Center accelerometer with Left and Right accelerometer which installed near the end of EPS model fills. The amplification ratios against frequency of Model-C1 without surcharge are shown in Figs. 1.8 (a), (b). The amplification ratio of Center accelerometer is 10 or 20 percent smaller than Right and Left accelerometer, and this tendency was recognized in all model fills. The movement of top center block would be restricted by the collision against adjacent blocks in horizontal direction, because in case with surcharge the differences between Center accelerometer and Left and Right accelerometers are getting small. The effect of adhesion of steel plate and the increase in confining stress, both would have decreased the influence of the collisions. These collision would be occurred by the rocking of individual EPS blocks during vibration mainly.

2.3.4. The influence of Height and Width of EPS Fill

Compared the results among Model-C1, Model-C2 and Model-C3 under surcharge of 1.1 kPa, the resonant frequency of Model-C1 is 10.4 Hz and the resonant frequencies of Model-C2 and Model-C3 are 16.3 and 16.9 Hz, respectively. This result was against our prediction. In the prospects, the highest resonant frequency would be obtained in Model-C2 whose height is a

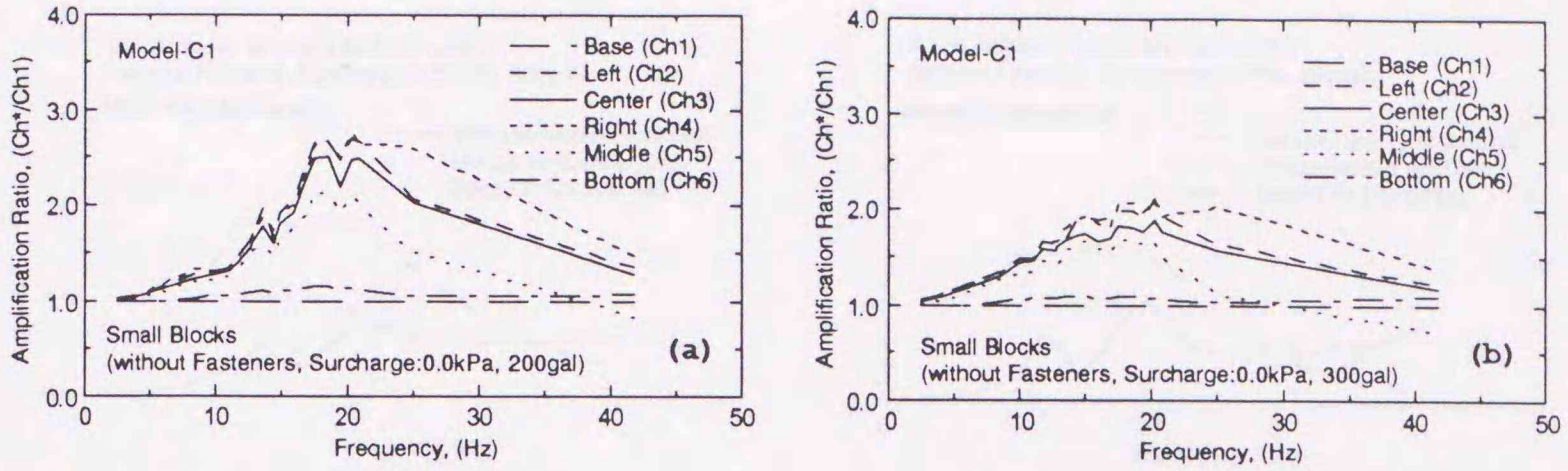

Figs. 1.8 (a), (b). The rerationship between aAmplification ratio and frequency in Model-C1 wihtout surcharge; (a) acceleration of 200gal, (b) acceleration of 300gal.

half of Model-C1, and the resonant frequency of Model-C3 would be smaller than Model-C2, because the width of Model-C3 is a half of Model-C2. But the resonant frequencies of Model-C2 and Model-C3 were almost same in fact. The reason of this small influence of width would be that the block number of Model-C3 is a half of Model-C2. The influences of the width and number of blocks would be canceled each other.

2.3.5. Properties of Rocking Vibration

Shown in Fig. 1.9 (a)-(c) shows the amplification ratio against the frequency obtained from the Middle-Right accelerometer placed to measure the vertical acceleration in Model-C2. The resulsts of the cases where the surecharges were 0.55, 1.1, 2.2 kPa and the acceleration amplitude is 300 gal, are plotted in Fig. 1.9 (a)-(c), respectively. The amplification ratios at Center accelerometer (Ch 3) are plotted at the same time.

From the plots for the Center accelerometer, it is found that the amnplification ratio of vertical acceleration is getting large at the both ends of the trapezoidal plots which shows the slippage of EPS blocks. And in the case where the surcharge is 2.2 kPa, the amplification ratio of vertical acceleration is larger than horizontal input acceleration, it shows that the rocking vibration is progressed. Moreover the amplification ratio of vertical acceleration is converged to 0.5 at high frequency area, and then over 40 Hz, the vibration mode is seemed to trans to second vibration mode.

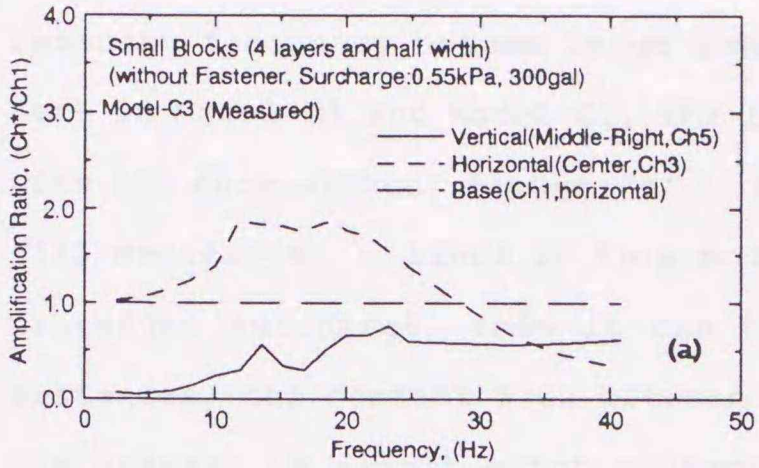

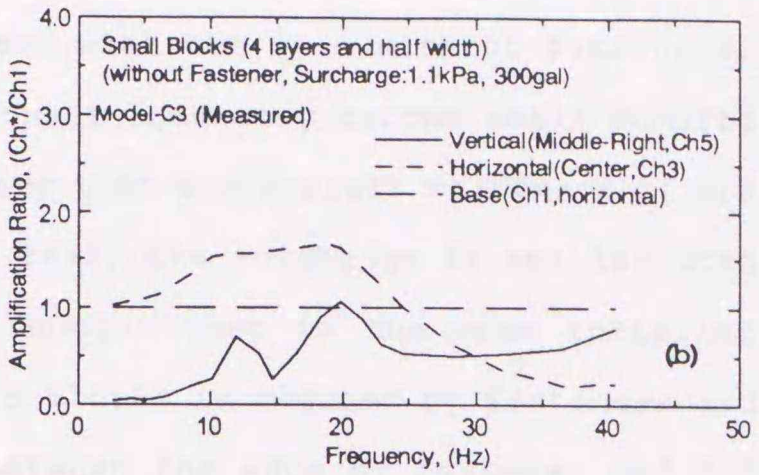

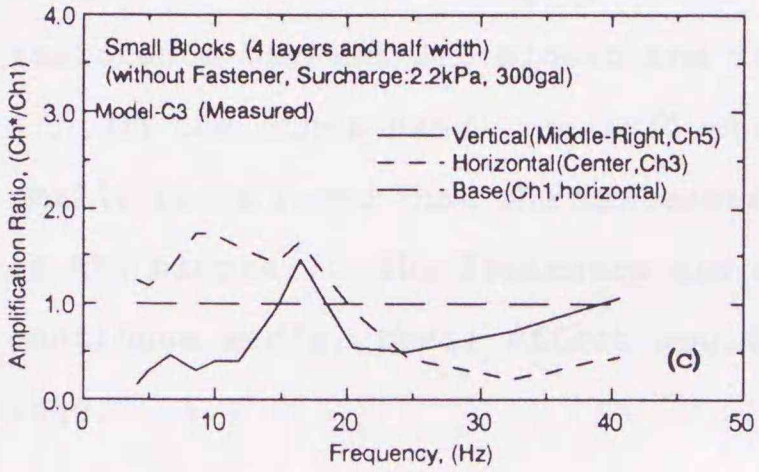

Figs. 1.9(a)-(c). Infuluence of Locking vibration in Model-F; surcharges are (a) 0.55 kPa, (b) 1.1 kPa, (c) 2.2 kPa.

Table 1.3. Maximum Amplification Ratio and resonant frequency for models with fasteners.

Model	Surcharge (kPa)	Amplitude of Acceleration (gal)	Maximum Amplification Ratio	Resonant Frequency (Hz)
Model-B1	0.0	200	2.3	30
		300	2.4	30
	1.1	200	2.3	13
		300	2.2	13
Model-C1	0.0	200	2.9	14
		300	2.8	14
	1.1	200	2.2	7
		300	2.0	6

2.3.6. The influence of Fasteners

In Table 1.3, maximum amplification ratio and resonant frequency obtained from plots for Model-B1 and Model-C1; the influence of applied acceleration amplitude is likely to become small compared with the model fills without fasteners. Although, in prospects, it was expected that the

resonant frequency became large compared with the case without fasteners, both in Model-B1 and Model-C1, the resonant frequency become small comared with the case without fasteners, it means that the overall stiffness of EPS fill decreases. Since in this model test, the surcharge is smaller than prototype surcharge, then it can be thought that in the case installed fasteners, the contact area between EPS blocks is reduced by fasteners and the contact is almost point contact between the edge of fastener and EPS blocks. The vibration properties would be dominated only by the shearing resistance between EPS blocks and fasteners.

On the other hand, the influence of magnitude of acceleration become small, it is found that the fasteners are available to restrain the slippage of EPS blocks. The fasteners are not enough to attempt the EPS fill as a continuum media, their effect would be restricted in restaining of slippage.

2.4. Summary

The vibration properties of EPS block fills are investigated in various conditions. The results are summarized as follows:

1) The vibration properties of EPS block fill is influenced by the number of EPS blocks which consist of the EPS block fill. As the number of EPS blocks become large, the overall stiffness of EPS fills is decreased and the amplification ratio is getting small; the collision between EPS blocks and slippage at the interfaces makes damping high and degree of disturbance large.
2) The overall stiffness of EPS fill is also decreased, as the applied acceleration amplitude becomes large.
3) It is found that the rocking vibration of whole EPS fill is progressed over prediction, and this influence must be considered into analysis of EPS fill.
4) The increas in overall stiffness of EPS fills can not be expected in case with fasteners, at least in small surcharge of present model tests. But the fasteners are available for preventing slippage of EPS blocks.

Chapter 2. Analytical Investigation of Vibration Properties of EPS Block Fill

2.1. General Remarks

To investigate the vibration properties of EPS block fill, model shaking table tests and the comparison between three analysis methods from elastic theory were performed. Simple estimation methods of natural period proposed by EDO was derived by modifying the elastic beam method, the continuous stratified layer model and the stratified layer model considered horizontal spring and slip element between EPS block layers were adopted in the present study. The result of model tests, however, showed that the resonant frequency depends on the number of EPS blocks or the size of EPS blocks. Since the three analysis methods from elastic theory can not express this type of feature as long as the same values of parameters such as shear modulus is adopted, the back analysis of vibration properties with the three analysis methods were done to examine the surcharge dependency of overall stiffness of EPS block fill.

The aim of this chapter is to investigate the applicability of three analysis methods and to clarify the vibration properties of EPS block fills by means of back analysis in detail. Moreover the dynamic DEM calculations were carried out and its applicability to the vibration properties of EPS block fill was investigated.

2.2. Analysis Methods Based on Elastic Theory

2.1.1. Simple Estimation Methods for Natural Period

EDO (EPS Construction method Development Organization, 1993) proposed a simple estimation method based on the elastic beam theory to obtain the natural period. Although the details are introduced in RIPW (Research Institute of Public Works, 1991), this method was obtained by modifying the

elastic beam method, and took into account of the influences of shear force and moment due to rocking vibration; the natural period can be obtained by following equation.

$$T_{EDO} = 2\pi\sqrt{\frac{mL}{Eab}\left(4\left(\frac{L}{a}\right)^2 + 1 + \frac{12}{5}(1+\upsilon)\right)} \quad , f_{EDO} = \frac{1}{T_{EDO}} \tag{2.1.1}$$

Where m is concentrated mass, E is Young's modulus, ν is Poisson's ratio, L is height of EPS block fill, a is width of EPS block fill and b is depth of EPS block fill, as shown in Fig. 2.1.

2.1.2. Continuous Stratified Layer Model

In the stratified ground as shown in Fig. 2.2 (a), the momentum equation of homogeneous ground is expressed as follows:

$$\rho_i \frac{\partial^2 u_i}{\partial t^2} = G_i \frac{\partial^2 u_i}{\partial z^2} + \eta_i \frac{\partial}{\partial t}\left(\frac{\partial^2 u_i}{\partial z^2}\right) \tag{2.1.2}$$

Where u_i is horizontal displacement of layer i, ρ_i is density of layer i, G_i is shear modulus of layer i and η_i is damping coefficient of layer i.

Since it would be thought that the EPS fill was vibrated in harmonic motion, the horizontal displacement $u_i(z,t)$ under the vibration with angular velocity ω is expressed as follows:

$$u_i(z,t) = U_i(z)\cdot e^{i\omega t} \tag{2.1.3}$$

When Eq. (2.1.3) is substituted for Eq. (2.1.2), and the complex shear modulus $G_i^* = G_i + i\omega\eta_i = G_i(1+2ih)$, where h is damping ratio, is employed, Eq. (2.1.2) is formed into the second order ordinary differential equation on $u_i(z)$ as follows:

$$\omega^2\rho_i u_i + G_i^* \frac{\partial^2 u_i}{\partial z^2} = 0 \tag{2.1.4}$$

The following relationship is substituted for Equ. (2.1.4).

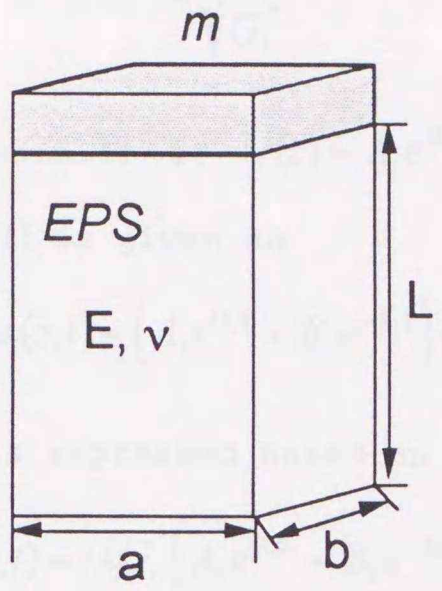

Fig. 2.1. EPS block fill assmued as a elastic beam.

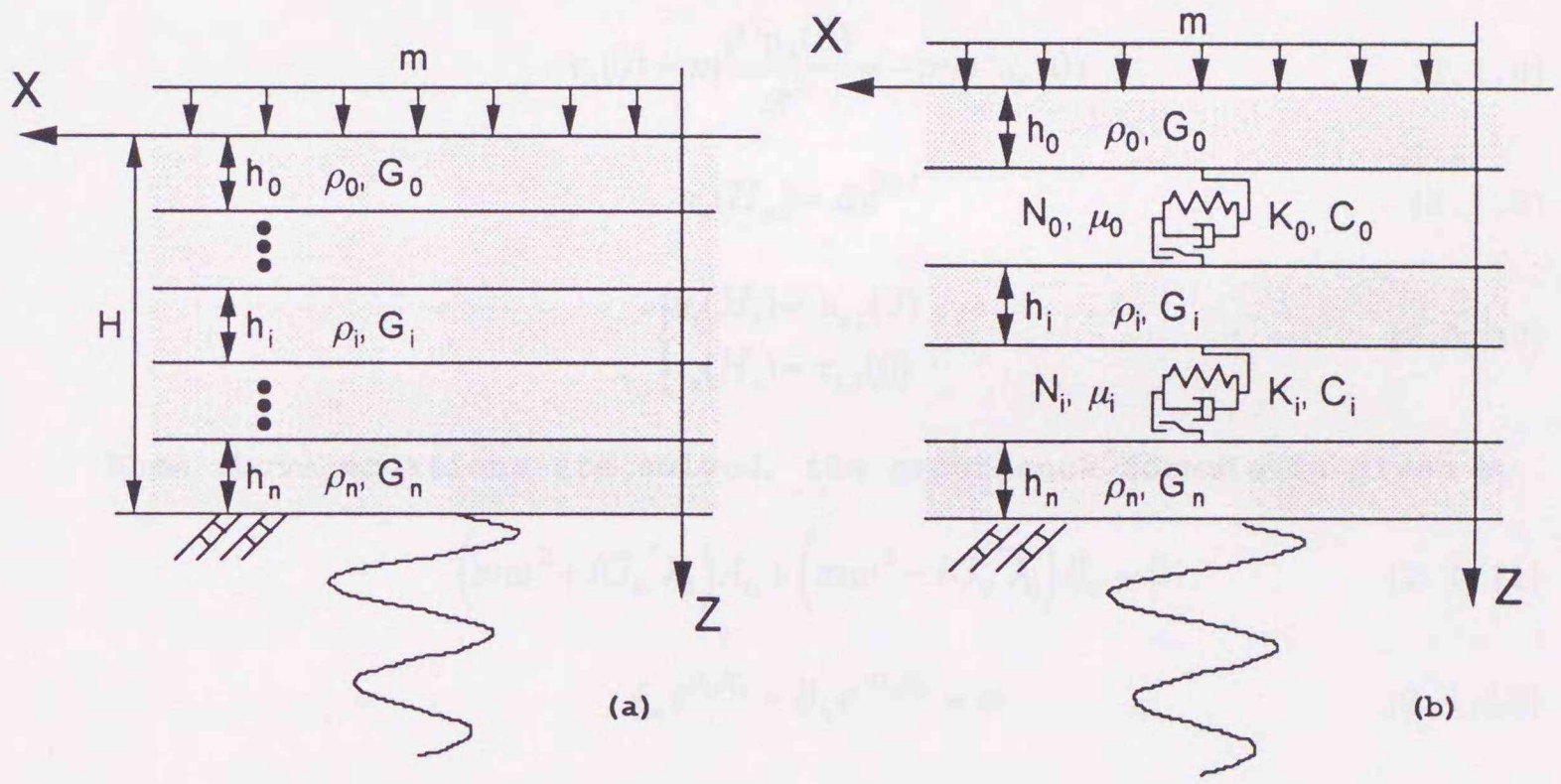

Fig. 2.2 (a), (b). EPS block fill assumed as a muti-layered ground; (a) interfaces between EPS block layers without element, (b) interfaces between EPS block layers with slip, spring and dashpot elements.

$$\lambda_i = \omega\sqrt{\frac{\rho_i}{G_i^*}} \tag{2.1.5}$$

Then the solution of Eq. (2.1.4) is $U(z) = A_i e^{i\lambda_i z} + B_i e^{-i\lambda_i z}$ obviously, the horizontal displacement $u_i(z,t)$ is given as

$$u_i(z,t) = \left(A_i e^{i\lambda_i z} + B_i e^{-i\lambda_i z}\right) e^{i\omega t} \tag{2.1.6}$$

Shearing stress $\tau_i(z,t)$ is expressed based on $\tau_i(z) = G_i^* \gamma_i$ as follows.

$$\tau_i(z,t) = i\lambda_i G_i^* \left(A_i e^{i\lambda_i z_i} - B_i e^{-i\lambda_i z}\right) e^{i\omega t} \tag{2.1.7}$$

The thickness of layer i is defined as H_i, and the condition of harmonic motion is followed in each layer. The boundary conditions are given as follows.

$$\tau_0(0) = m\frac{\partial^2 u_0(0)}{\partial t^2} = -m\omega^2 u_0(0) \tag{2.1.8}$$

$$u_n(H_n) = a e^{i\omega t} \tag{2.1.9}$$

$$\begin{cases} u_i(H_i) = u_{i+1}(0) \\ \tau_i(H_i) = \tau_{i+1}(0) \end{cases} \tag{2.1.10}$$

When above equations are solved, the recurrence formula is given by

$$\left(m\omega^2 + iG_0^*\lambda_0\right)A_0 + \left(m\omega^2 - iG_0^*\lambda_0\right)B_0 = 0 \tag{2.1.11}$$

$$A_n e^{i\lambda_n H_n} + B_n e^{-i\lambda_n H_n} = a \tag{2.1.12}$$

$$\begin{cases} A_{i+1} = \frac{1}{2}A_i\left(1+\alpha_i\right)e^{i\lambda_i H_i} + \frac{1}{2}B_i\left(1-\alpha_i\right)e^{-i\lambda_i H_i} \\ B_{i+1} = \frac{1}{2}A_i\left(1-\alpha_i\right)e^{i\lambda_i H_i} + \frac{1}{2}B_i\left(1+\alpha_i\right)e^{-i\lambda_i H_i} \end{cases} \tag{2.1.13}$$

Where ,

$$\alpha_i = \frac{G_i^*\lambda_i}{G_{i+1}^*\lambda_{i+1}} \tag{2.1.14}$$

By using Eq. (2.1.11), Eq. (2.1.12), Eq. (2.1.13), the amplification ratio for selected layer n is obtained. When the mechanical properties

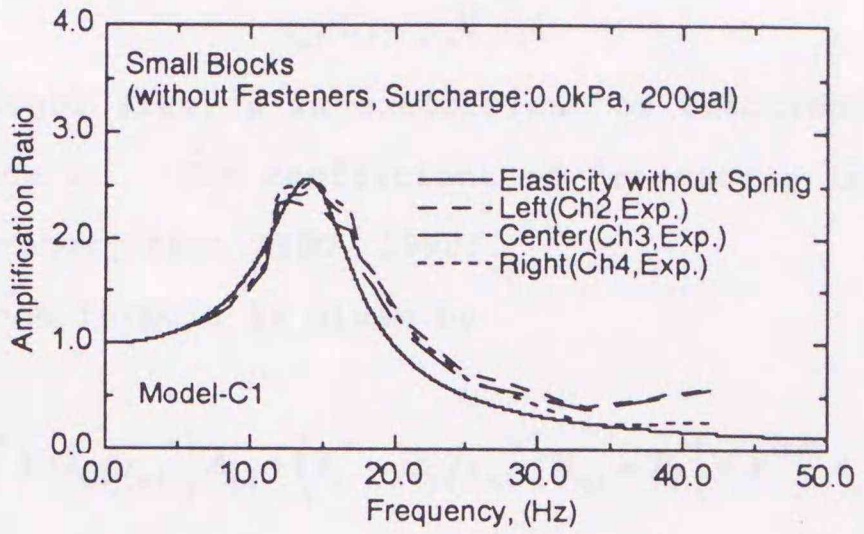

Fig. 2.3. Example of back analysis with Method 2 (Model-C1).

are uniform, the amplification ratio of surface is expressed as follows using the overall height of EPS fill H.

$$R_0 = e^{i\lambda H} + \left(1 - e^{2i\lambda H}\right) \frac{\left(iG^*\lambda - m\omega^2\right)e^{i\lambda H}}{m\omega^2\left(1 - e^{2i\lambda H}\right) + iG^*\lambda\left(1 + e^{2i\lambda H}\right)} \tag{2.1.15}$$

The example of back analysis is shown in Fig. 2.3.

2.1.3. Stratified Layer Model with Joints between Layers

To take account of slippage between EPS layers, the joint composed of tangential spring, slip and dashpot elements were employed at interface between EPS block layers in the continuous stratified layer model, as shown in Fig. 2.2 (b).

The boundary condition of Eq. (2.1.10) was changed to

$$\begin{cases} \tau_i(H_i) = \tau_{i+1}(0) \\ \tau_{i+1}(0) = -k_i \Delta\left(u_{i+1}(0) - u_i(H_i)\right) + C_i \Delta\left(\dot{u}_{i+1}(0) - \dot{u}_i(H_i)\right) \end{cases} \tag{2.1.16}$$

and when the following equation is satisfied,

$$\tau_{i+1}(0) * A > F_{t,i} = \mu_i N_i \tag{2.1.17}$$

shear stress $\tau_i(z,t)$ is given by

$$\tau_{i+1}(0) = \mu_f N_i / A \tag{2.1.18}$$

where A is sectional area, μ is coefficient of friction and N_i is normal force at interface i. The coefficient of friction μ is 0.64, which was measured in laboratory test (EDO, 1990).

The recurrence formula is given by

$$\begin{cases} \left(k_i^* + i\lambda_{i+1} G_{i+1}^*\right) A_{i+1} + \left(k_i^* - i\lambda_{i+1} G_{i+1}^*\right) B_{i+1} = k_i^* \left(A_i e^{i\lambda_i H_i} + B_i e^{-i\lambda_i H_i}\right) \\ A_{i+1} - B_{i+1} = \dfrac{G_i^* \lambda_i}{G_{i+1}^* \lambda_{i+1}} \left(A_i e^{i\lambda_i H_i} - B_i e^{-i\lambda_i H_i}\right) \end{cases} \tag{2.2.19}$$

where $k_i^* = k_i + i\omega C_i = k_i(1 + 2ih_k)$.

In the back analysis the shear modulus G was fixed to 2.5 MPa/m, and the stiffness of shearing spring was varied parametrically; although only Young's modulus was given by the laboratory test (EDO, 1990), the shear modulus was estimated from the Young's modulus by using following relationship,

$$G = \frac{E}{2(1+\nu)} \tag{2.2.20}$$

where ν is Poisson's ratio of 0.01.

The damping coefficient was determined so as to give good agreement in amplification ratio.

2.2. Back Analysis of Vibration Behaviors of EPS Block Fill

2.2.1. Back Analysis of Model Fills without Fasteners

The obtained shear modulus and stiffness of spring by back analysis are shown in Table 2.1. Since the modified elastic beam model can give only Young's modulus, the shear modulus was obtained by means of Eq. (2.2.20). In the continuous stratified layer model and the stratified layer model with joint, the shear modulus and stiffness of spring were assumed constant through the whole EPS block fills. From the results of the vibration

Table 2.1. Shear modulus and stiffness of spring obtained from back analysis of elasticity solutions.

Model	Surcharge (kPa)	Fasteners ○ :installed ×:not installed	Shear Modulus ($MN/m^2/m$)		Stiffness of Spring (MN/m/m)
			modified elastic beam model	continuous stratified layer model	stratified layer model with joint
Model-A	0.0	—	—	2.20	—
	1.1	—	3.73	1.80	—
Model-B1	0.0	×	—	0.60	0.98
		○	—	0.29	0.42
	1.1	×	1.87	0.90	1.50
		○	1.45	0.70	1.00
Model-B2	0.0	×	—	0.80	1.45
	0.55	×	0.86	1.30	3.10
	1.1	×	1.05	1.50	4.10
	2.2	×	1.01	1.40	3.70
Model-C1	0.0	×	—	0.12	0.90
	0.55	○	—	0.063	0.46
	1.1	×	1.04	0.50	4.60
	2.2	○	0.52	0.25	2.00
Model-C2	0.0	×	—	0.12	0.80
	0.55	×	0.69	0.40	2.90
	1.1	×	1.06	0.60	5.00
Model-C3	0.0	×	—	0.18	1.23
	0.55	×	0.93	0.45	3.30
	1.1	×	1.38	0.65	5.30
	2.2	×	1.94	0.90	9.00

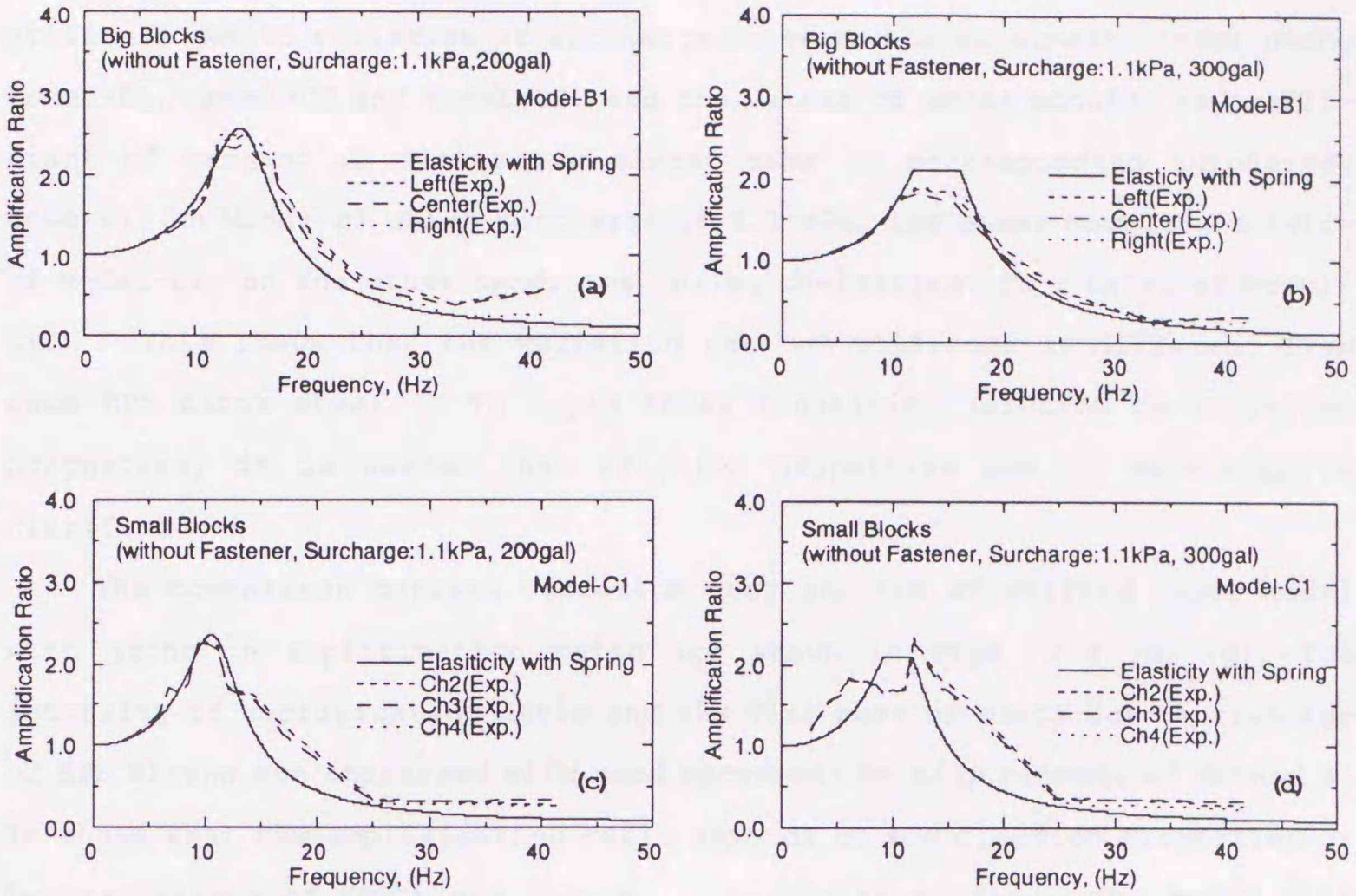

Figs. 2.4 (a)-(d). Comparisopn between amplification ratio obtained from back analysis of Method 3 and vibration tests; (a) Model-B1, 200gal, (b) Model-B1, 300gal, (c) Model-C1, 200ga, (d) Model-C1, 300gal.

tests, since it was found that the influence of magnitude of applied acceleration was not so large, the back analysis was carried out only for the case of 200 gal. And since the results of the modified elastic beam model were shown only for comparison, in the following discussion, the continuous stratified layer model and the stratified layer model with joint are concerned.

If the EPS model fills can be assumed as a continuum media, same shear modulus must be obtained from back analysis in same model fill; however, in all back analysis method the shear modulus or stiffness of spring tends to become large with increasing of surcharge except for Model-B2 which has only three EPS blocks, as shown in Table. 2.1. The increasing rate of

stiffness due to variation of surcharge is seemed to be almost linear among Model-C1, Model-C2 and Model-C3, and the values of shear modulus or coefficient of tangential spring are almost same in corresponding surcharge. However, in Model-B1 which surcharge is 1.1 kPa, the shear modulus is twice of Model-C1, on the other hand, the spring coefficient is a third of Model-C1. This shows that the variation rate of stiffness is different from each EPS block size. To apply these elasticity solution to vibration properties, it is needed that friction properties due to surcharge is clarified.

The comparison between vibration test and the stratified layer model with joint in amplification ratio are shown in Figs. 2.4 (a)-(d); the intensity of amplification ratio and the flat part of plots due to slippage of EPS blocks are expressed with good agreement by slip element of Method 3. It shows that the amplification ratio depends on the friction properties of between strata of EPS block layers. In the stratified layer model with joint, the friction coefficient was 0.64 which was measured in laboratory[4] as mentioned above.

2.2.2. Back Analysis of Model Fills with Fasteners

In Part 1, Chapter 1 the element tests were carried out to examined the shearing resistance between EPS block and fastener. From the test results the stiffness of spring is given 0.125 - 0.15 MN/m per single fastener. Since the depth of EPS block was 0.5 m in model test, the obtained stiffness of spring was doubled. In Model-B1, four fasteners were used at one interface of EPS block layers, and in Model-C1, 7.6 fasteners were used at single interface in average, then the stiffness of spring at single interface are calculated as $0.125 \times 2 \times 4 = 1.0$, and $0.125 \times 2 \times 7.6 = 1.9$ (MN/m), respectively. These values are almost same as the stiffness of spring obtained by the stratified layer model with joint (Method 3); they are 1.0 and 2.0 MN/m. In the case with fasteners, the vibration properties depends on the shearing resistance between EPS blocks and fasteners.

2.3. Comparison between the Results of Vibration Tests and DEM Calculation

The dynamic DEM adopted non-linear contact law in normal direction, however, from the results of preliminary calculations, it was found that the influence of surcharge could not explain. Then the stiffness of tangential spring was varied in proportion to overlap length; the overlap length of 0.5 × 1.0 × 0.5 size blocks used in Model-B1 and Model-B2 due to 1.1 kPa surcharge was assumed as a reference from preliminary calculations. In DEM calculations, the acceleration waves were applied to bottom EPS blocks, and when the surcharge was applied to EPS block fill, the density of the top blocks were increased so as to equal to surcharge condition. Each EPS block is treated as a rigid body and the deformation due to shear force is not considered in DEM. However, if the wavelength of input acceleration wave is longer enough than the height of single EPS block, the EPS block can be assumed as a rigid body. The case which gives the shortest wavelength and the largest block height is Model-B1; the frequency of input acceleration wave is 70 Hz and the block height is 0.5 m. When the shear modulus for EPS is used the value of 2.5 MPa, the wavelength becomes 5.1 m; it is about ten times of block height. In prototype, the block height is usually 0.5 m, the assumption of rigid body seemed to be acceptable.

The example of the input acceleration wave and calculated acceleration of top center block are plotted in Fig. 2.5 (a), (b). The acceleration was increased gradually in the both end of applying vibration, and the applied wave number was about ten without the both end.

The calculated amplification ratios are plotted against the frequency in Fig. 2.6, Fig. 2.7 and Figs. 2.8 (a)-(c), Figs. 2.9 (a)-(c): for Model-B1, Model-C1 and Model-B2 and Model-C3, respectively. And the results of model tests are shown in those figures. As shown in these figures, the amplification ratio and the influence of slippage as well as the resonant frequency are presented with good agreement by the dynamic DEM calculation. The influence of the number of EPS blocks is also explained by the dynamic DEM used same parameters; the difference in the results of Model-B1 and Model-C1 which have same silhouette is presented with good agreement. Moreover, by using the stress dependency of tangential spring coefficient,

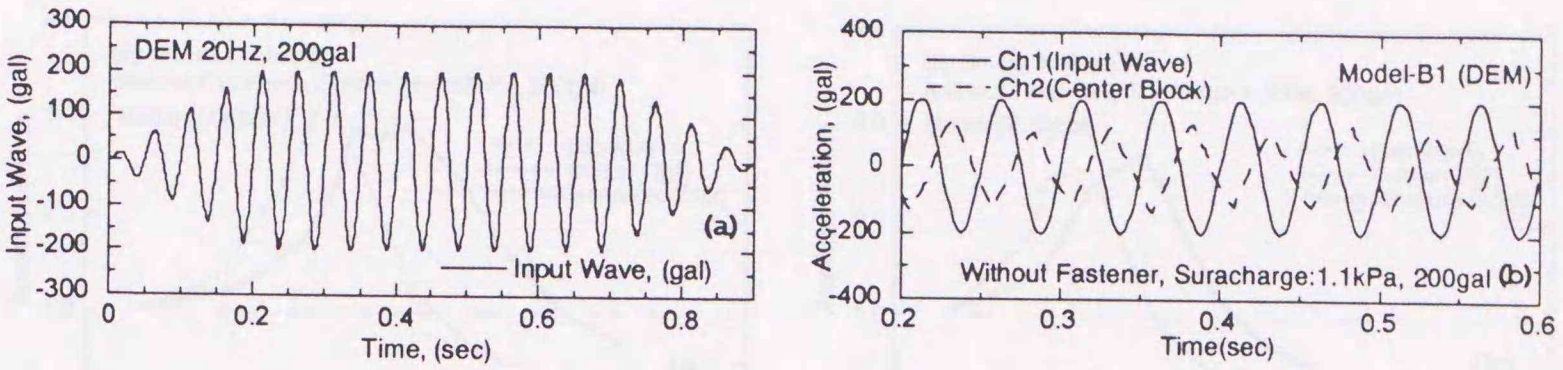

Figs. 2.5 (a),(b). Input acceleration wave and calculated acceleration during shaking; (a) input acceleration wave, (b) measeured acceleration.

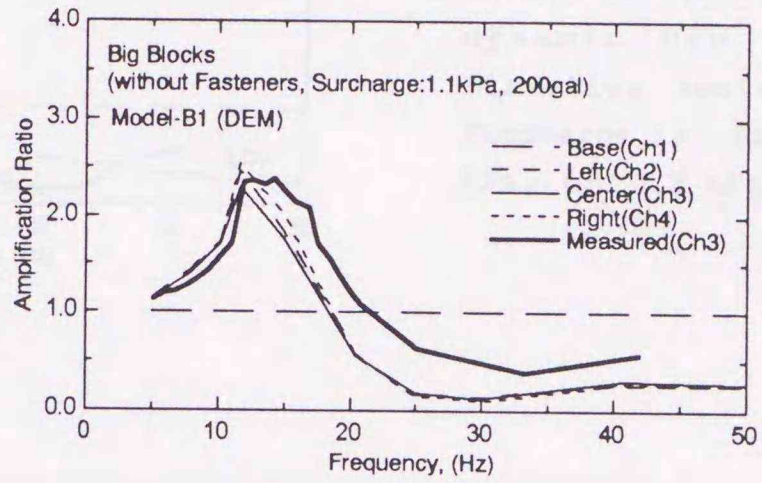

Fig. 2.6. Comparison between amplification ratio calculated by DEM and examined in laboratory (Model-B1, 200gal, surcharge is 1.1 kPa).

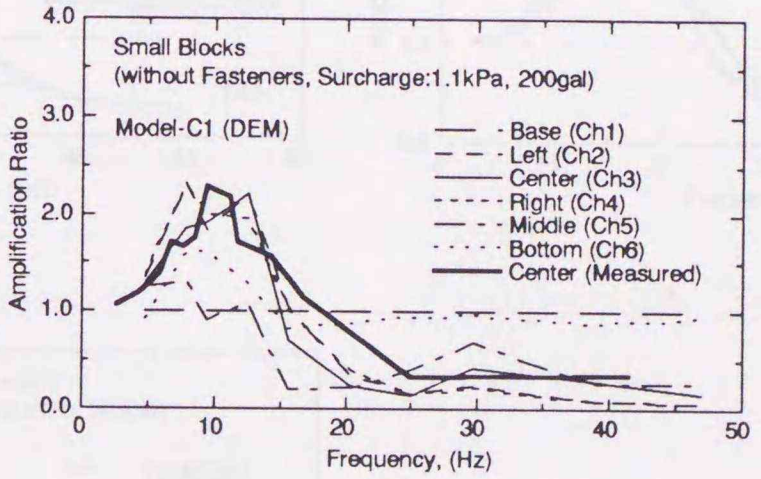

Fig. 2.7. Comparison between amplification ratio calculated by DEM and examined in laboratory (Model-C1, 200gal, surcharge is 1.1 kPa).

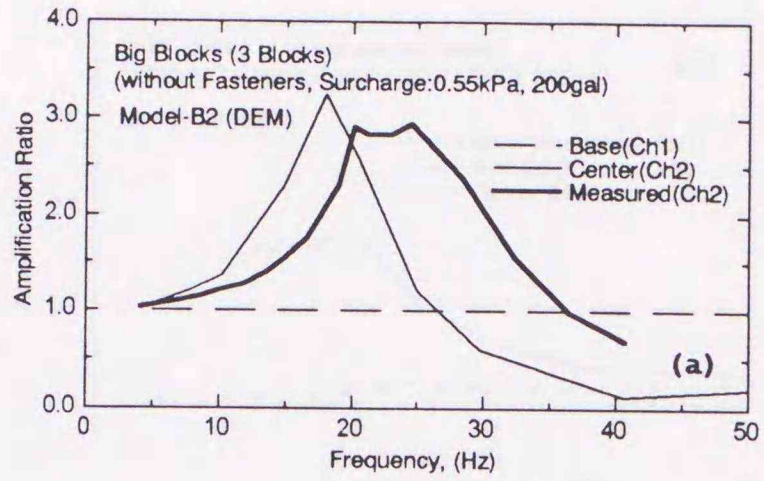

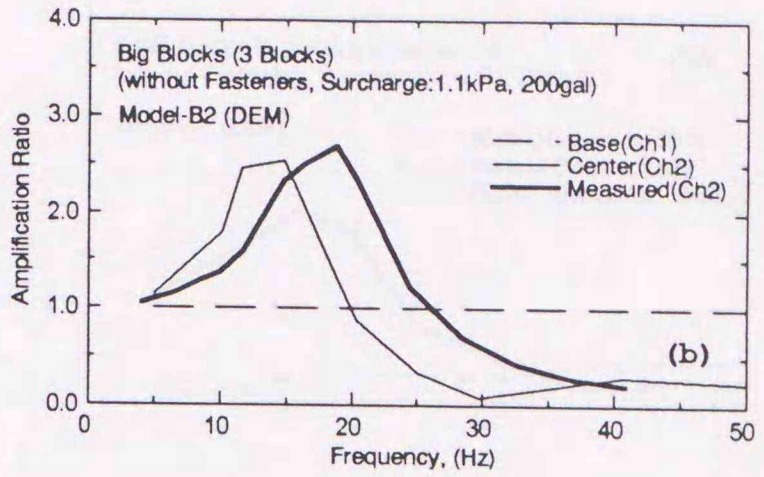

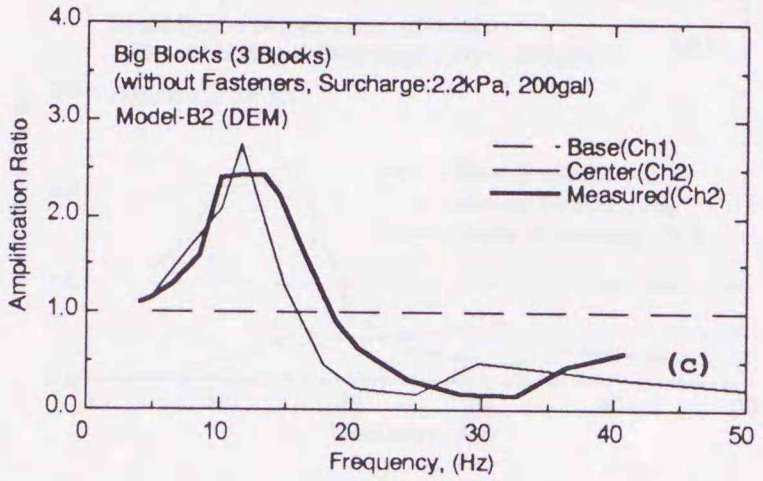

Figs. 2.8 (a)-(c). Comparison between dynamic DEM calculation and vibration tests in Model-B2 and Surcharge is; (a) 0.55 kPa, (b) 1.1 kPa, (c) 2.2 kPa.

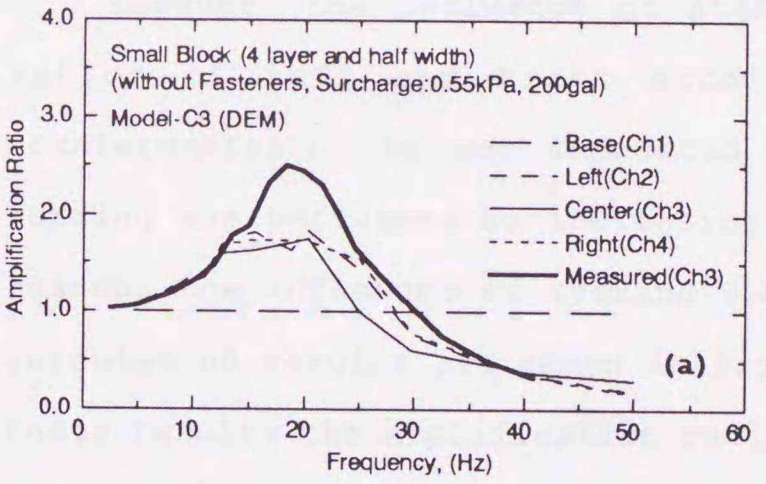

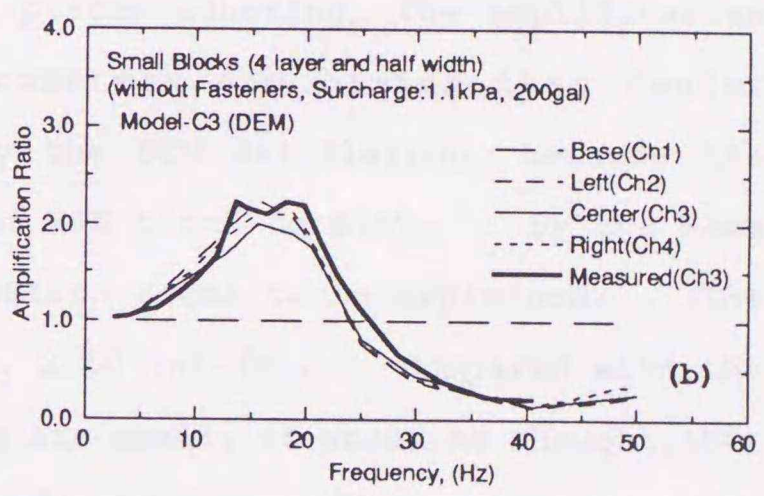

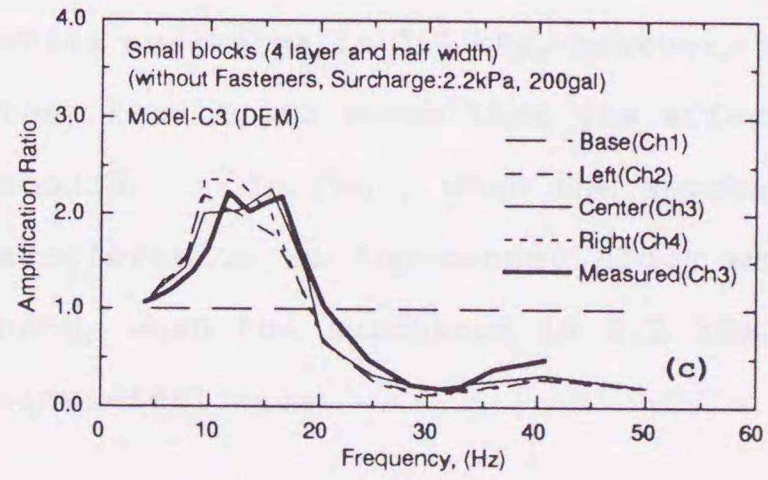

Figs. 2.9 (a)-(c). Comparison between dynamic DEM calculation and vibration tests in Model-C3 and Surcharge is; (a) 0.55 kPa, (b) 1.1 kPa, (c) 2.2 kPa.

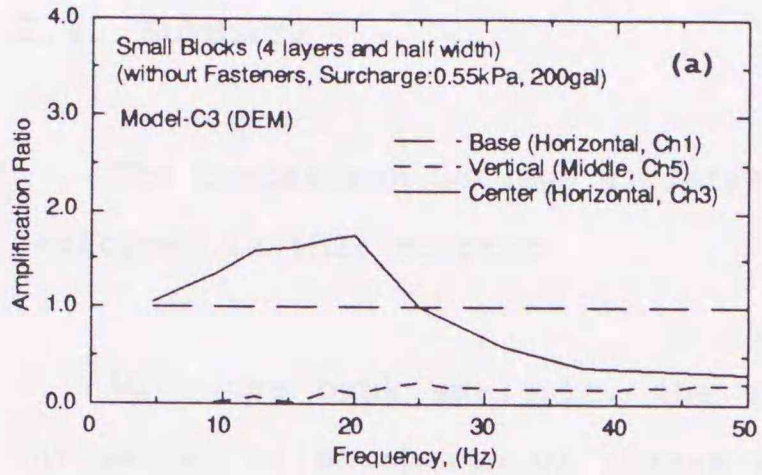

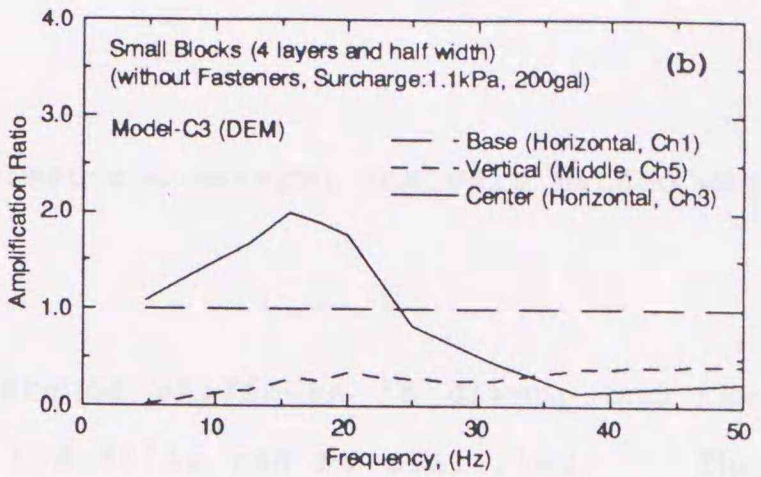

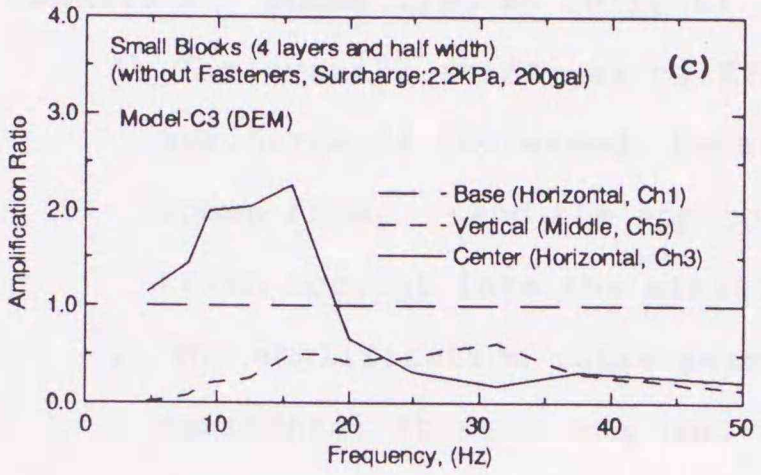

Figs. 2.10 (a)-(c). Influence of locking vibration in Model-C3 by DEM, Surcharge is; (a) 0.55 kPa, (b) 1.1 kPa, (c) 2.2 kPa.

it is found that the influence of surcharge would be explained with single stress dependency law of tangential spring coefficient.

However, the influence of steel plates adhering, the amplification ratios of Left and Right accelerometers are higher than Center accelerometer's, is not indicated by the DEM calculation, because the loading was performed by increasing of EPS block density. By the same reason, the influence of rocking vibration seems to be explained. The calculation results are shown in Figs. 2.10 (a)-(c). Compared with the tests results the amplification ratios are small, it would be thought that the confining for whole EPS fill was small and the overall rocking vibraion of EPS fill was restricted in the dynamic DEM calculations. In Model-C3 where surcharge is 2.2 kPa, however, the amplification ratio is close to the test result, it seems that the effect of confining due to surcharge works enough. In fact, when the surcharge was small, the plots of vertical acceleration at top-center block was not sinusoidal wave; on the other hand, when the surcharge is 2.2 kPa, the vertical acceleration was clear sinusoidal wave.

2.4. Summary

The comparison between vibration test and several analysis method was performed in this chapter.

With the back analysis, the reference stiffness is given, and the influences of surcharge or shapes of EPS fills can be clarified. The results are summarized as follows;

1) The overall stiffness of EPS block fill is getting large, as the surcharge is increased, because the contact between EPS blocks becomes firm. And the appropriate stiffness increasing law must be taken account into the elasticity solutions.
2) The amplification ratio seems to be influenced by slippage between horizontal stratum composed of EPS blocks strongly, the stratified layer model with joint can express the amplification ratio of model tests with good agreement. The coefficient of friction is 0.64 which was determined by laboratory test of EPS Construction Method Development Organization. Moreover the influence of fasteners are expressed by the stratified layer model with joint and tangential spring which uses the stiffness of tangential spring determined by shearing resistance tests.

The comparison between vibration tests and dynamic DEM calculation. The results are summarized as follows;

1) Since the dynamic DEM takes the influence of collision between EPS blocks, rocking and slippage of individual EPS blocks, then the stress dependency of overall stiffness of EPS block fill due to the number of EPS blocks is expressed with same parameters appropriately.
2) To consider the stress dependency of overall stiffness, the stiffness of tangential spring was varied linearly in the dynamic DEM. As the result, the influence of surcharge in model tests can be expressed with same stress dependency law of tangential spring coefficient.

It would be said that dynamic DEM calculation suggests some modification methods concerned on the stress dependency of overall stiffness of EPS block fill in the analysis methods based on elasticity solution.

Part 4. Conclusion

Chapter 1. Load Propagation and Deformation Characteristics of EPS Fill and Applicability of Static DEM

1.1. Load Propagation Characteristics of EPS Block Fill

To investigate the applicability of the static DEM, EPS block fills were concerned in the present study, the load propagation characteristics of EPS block fill were examined by a series model tests. The observed load propagation properties were compared with the results of numerical analyses.

The results of the laboratory tests are summarized as follows:

1) The EPS block fills behaved as a typical discrete media, the load propagation characteristics are largely influenced by their internal structures formed with the arrangement of EPS blocks. The load propagation intensity and the loading point which gives maximum propagated load, were changed with the difference in their internal structures; it was emphasized especially between the model fills with and without vertical continuous joints.
2) The effect of fastener on load propagation properties was recognized just after the application of loads; however, the effect was restricted and the improvement of load propagation properties was diminished under static loading condition or long term lading condition. The EPS model fill which was left for three days after installing fasteners, behaved as the model fill's without fasteners.
3) The load propagation of the EPS block fills which are subjected to distortion behaved in rather different manner with the EPS block fills without the distortion; even the slight distortion as 1.0 cm for the fill with 62.5 cm in height changed strongly the load propagation properties, and even if the disturbance of the EPS block fill is slightly and notable load concentration was recognized.

The results of the comparison of the numerical analysis and the laboratory tests are summarized as follows:

1) DEM shows enough applicability to the EPS block fills in various situation of the model fills; the effects of arrangement of EPS blocks, installation of fasteners and distortion can be explained by the static DEM.
2) FEM could be applied only to the EPS block fill bounded with adhesive agents which behaved as a continuum media. Even in the case with fasteners, the FEM adopted in the present study could not explain the load propagation properties.

1.2. Deformation Characteristics of EPS Fill

The applicability of static DEM to large deformation problem of EPS block fill were investigated; the motion of individual EPS blocks and reaction force at bottom EPS block fills during forced deformation were analyzed. The deformation tests of EPS model fills were performed in laboratory, and then the observed deformation behaviors were compared with the simulation by numerical calculations.

The results of the laboratory tests are summarized as follows;

1) When the vertical upward displacement was applied to the bottom EPS block fill, the EPS model fills were disturbed; even with small displacements the significant gaps which was enough to separate EPS blocks and the reaction load was became constant. With the large displacement some blocks were observed slide. The large displacement caused by the sliding was not recovered even when the vertical displacement was restored.
2) In the range of small displacement less than 5 mm, the relationship between the ratio of reaction and the vertical displacement was rather linear; however, after the initiation of gaps between blocks the reaction force became rather constant or fluctuated.
3) The model fills which had the vertical continuous joints gave

relatively small reaction compared with other model fills, because their fill bodies were separated at early step of vertical displacement.

The results of the comparison of the numerical analysis with the laboratory tests are summarized as follows;

1) Since the FEM adopted in the present study considers no slip or joint elements, the deformation is concentrated at the bottom EPS block unacceptably in the simulation, and the relationship between the reaction ratio and vertical displacement showed only linearity.
2) DEM treats the EPS blocks as individual elements, and can take the slide of side and gaps between EPS blocks. The simulation by DEM is in good agreement quantitatively with the measured behaviors, in the relationships between reaction and vertical displacement.

1.3. Estimation Method of Propagated Stress Distribution in EPS Fill

As the applicability of DEM to EPS block fills were confirmed in previous sections, the derivation of simple estimation method of propagated stress distribution through EPS fill body was attempted for prototype EPS block fills. But in geotechnical field, the elastic solution of propagated stress is usually used such as Boussinesq's solution which the ground is assumed as a elastic half-space model. If the elastic solution can express the stress concentration in EPS block fill, the numerical calculations are not needed. Then the elastic solution with fixed boundary in propagated stress due to line load was derived, and the DEM calculations were compared with the elastic solution with fixed boundary at first.

Next, the simple estimation method for stress distribution due to line load with the calculation results by DEM was proposed, and its applicability was examined.

The derived conclusions are summarized as follows;

1) Although the elastic solution with fixed boundary indicates concen-

trated stress distribution compared with that without fixed boundary, the DEM calculation indicates more concentrated stress distribution, which depends on the aspect ratio of EPS blocks. This indicates that the stress concentration ratio is influenced by shape and size of EPS blocks, and the elastic solution is not enough to explain the stress propagation properties of EPS block fills, even if the fixed boundary is considered in the solution.

2) From DEM calculations, it is found that the stress distribution properties are dominated by the block aspect ratio and the EPS fill thickness. And the line load does not propagated beyond the vertical continuous joints, and the stress distribution is more concerned in these cases.

3) It is confirmed that the DEM calculations follows the superposition law with a little scatters; the simple estimation method for the stress distribution was proposed. In the comparison between the simple estimation method and DEM calculation, the good applicability of the methods was confirmed. By using this simple estimation method, the stress distribution due to applied line load can be estimated with sufficient accuracy without large calculation by the static DEM.

1.4. Stress Concentration Properties in EPS Fill subjected to Differential Settlement of Foundation

The EPS block fill is constructed on soft unstable ground generally, so it is expected easily that the EPS fill is subjected to differential settlement of its foundation. Then the stress concentration properties of the prototype size EPS fill subjected to differential settlement was investigated by DEM calculations, the results of the stress concentration of uniform surcharge and line load for the EPS fills subjected to differential settlement are summarized as follows:

1) In both cases for the uniform surcharge and line load, the stress distribution properties are influenced strongly by differential settlement. The propagated stress tends to more concentrate to the

block which is placed at the border of settled and unsettled blocks, with an increase in the differential displacement.

2) When large settlement is applied to the EPS fill, the concentration of the propagated stress converges to a certain value. The amount of stress concentration of uniform surcharge is independent of aspect ratio, but dependent on fill thickness. On the other hand, the stress concentration of line load does not depend on the fill thickness, as well as the aspect ratio.

3) The maximum stress concentration ratio under uniform surcharge is about twice initial overburden pressure in the case of the fill thickness of 1.0 m, about three times in the case which the fill thickness is 2.0 m and becomes more than five times in case which the fill thickness is 3.0 m.

4) The stress concentration ratio under the line load is from 0.7 to 0.9 times normalized line load in all cases.

5) Though the influence of steel fasteners which fix EPS blocks is not considered in this section, if the fasteners are installed and the EPS fill is subjected to differential settlement, it can easily be expected that the stress concentration of uniform surcharge will be increased.

1.5. Control of Load Distribution Using Irregular EPS Blocks

The importance of internal structures formed by individual EPS blocks made clear through the model tests and numerical analyses in previous sections. The possibility of the operation of the load propagation properties was investigated in a series of model tests using the irregular EPS blocks which have trapezoidal and parallelogram shapes. By using these irregular EPS blocks, the joint direction formed by EPS blocks can be controlled intentionally. Then the applicability of DEM and FEM to the EPS block fills were investigated by comparing with the results of model tests.

The results of the laboratory tests are summarized as follows;

1) In the symmetrical model fills, the differences between the models with centralized joints and with spread out joints become small by installing fasteners. But the degree of the dispersion is same as the rectangular block fill's, the result of the models with spread out joints shows more concentrated load propagation than without fasteners.
2) The influences of the right-down joint and the left-down joint are relatively small in symmetrical model fills, they are similar to the cases without fasteners.
3) In asymmetrical model fills with fasteners the propagated load tend to concentrate, it seems that the fasteners are not effective always work, so that the applied load is dispersed.
4) In the symmetrical model fills, the differences between the models with centralized joints and with spread out joints become small by installing fasteners. But the degree of the dispersion is same as the rectangular block fill's, the result of the models with spread out joints shows more concentrated load propagation than without fasteners.
5) The influences of the right-down joint and the left-down joint are relatively small in symmetrical model fills, they are similar to the cases without fasteners.
6) In asymmetrical model fills with fasteners the propagated load tends to concentrate, it seems that the fasteners are not effective always work, so that the applied load is dispersed.

The results of the comparison of the numerical analysis with the laboratory tests without fasteners are summarized as follows;

1) Since FEM employed in the present study cannot take account of the internal structures, the influence of the joint direction cannot be explained by FEM as a matter of course.
2) DEM can explained the differences due to the variation of the joint direction; however the results of calculation overestimates the influences to some extent. The major cause is that the static DEM employed in the present study assumed linear contact law even for sharp corners of EPS blocks.

Chapter 2. Vibration Characteristics of EPS Fill and Applicability of Dynamic DEM

2.1. Experimental Investigation of Vibration properties of EPS Block Fill

The vibration properties of EPS block fills are investigated in various conditions. The results are summarized as follows:

1) The vibration properties of EPS block fill is influenced by the number of EPS blocks which consist of the EPS block fill. As the number of EPS blocks become large, the overall stiffness of EPS fills is decreased and the amplification ratio is getting small; the collision between EPS blocks and slippage at the interfaces makes damping high and degree of disturbance large.
2) The overall stiffness of EPS fill is also decreased, as the applied acceleration amplitude becomes large.
3) It is found that the rocking vibration of whole EPS fill is progressed over prediction, and this influence must be considered into analysis of EPS fill.
4) The increase in overall stiffness of EPS fills can not be expected in case with fasteners, at least in small surcharge of present model tests. But the fasteners are available for preventing slippage of EPS blocks.

2.2. Back Analysis of Vibration Tests Based on Elastic Theory and DEM Calculation

The comparison between vibration tests and three analysis methods from elasticity solution was performed in this chapter; the modified elastic beam method, the continuous stratified layer model and the stratified layer model with joint. Since these elasticity solutions can not express the influence of the number of EPS blocks, even in the stratified layer model with joint, the number of horizontal EPS blocks can not be taken account. Then these elastic solutions were used for back analysis of the stiffness of whole EPS fill.

To investigate the applicability of the dynamic DEM to vibration behavior of EPS block fill, the comparison between the vibration tests and DEM calculations was also carried out.

With the back analysis, the reference stiffness is given, and the influences of surcharge or shapes of EPS fills can be clarified. The results are summarized as follows;

1) The overall stiffness of EPS block fill is getting large, as the surcharge is increased, because the contact between EPS blocks becomes firm. And the appropriate stiffness increasing law must be taken account into the elasticity solutions.
2) The amplification ratio seems to be influenced by slippage between horizontal stratum composed of EPS blocks strongly, the stratified layer model with joint can express the amplification ratio of model tests with good agreement. The coefficient of friction is 0.64 which was determined by laboratory test of EPS Construction Method Development Organization. Moreover the influence of fasteners are expressed by the stratified layer model with joint and tangential spring which uses the stiffness of tangential spring determined by shearing resistance tests.

The comparison between vibration tests and dynamic DEM calculation. The results are summarized as follows;

1) Since the dynamic DEM takes the influence of collision between EPS blocks, rocking and slippage of individual EPS blocks, then the stress dependency of overall stiffness of EPS block fill due to the

number of EPS blocks is expressed with same parameters appropriately.

2) To consider the stress dependency of overall stiffness, the stiffness of tangential spring was varied linearly in the dynamic DEM. As the result, the influence of surcharge in model tests can be expressed with same stress dependency law of tangential spring coefficient.

It would be said that dynamic DEM calculation suggests some modification methods concerned on the stress dependency of overall stiffness of EPS block fill in the analysis methods based on elasticity solution.

Acknowledgment

The author is grateful to Professor Shousuke Toki and Associate Professor Kinya Miura of Hokkaido University for their continual guidance and encouragement from his being undergraduate student and their critical reading of this manuscript. And the author would like to express his gratitude to Professor Toshiyuki Mitachi for his giving many valuable advice and suggestions. And the author expresses his gratitude to Messrs. Yutaka Kudo and Migitoshi Nishimura for their guidance and support.

In load propagation tests of this manuscript, most of experimental devices, materials and site were offered from the Civil Engineering Research Institute of Hokkaido Development Bureau, especially Messrs. Shigeyuki Noto, Junichi Nishikawa and Yasuaki Matsuda offered convenience and gave valuable advice. The author wishes to express his gratitude for their support.

The author is also grateful to Mr. Yasuhiko Sasaki, who is in Structural Mechanics Group of Hokkaido University, for his giving kind guidance in operating the shaking device.

It should be emphasized that the present study has been supported by the students and graduates of GeoMechanics Group of Hokkaido University, Messrs. Hiroshi Tsujino, Kazunari Inoue, Takaaki Kita and Takashi Nakajima who supported in the major part of the experiments in the present study, and Messrs. Noboru Higashihira, Nobuhide Kato, Masaki Nishimura and Tamio Kanou who supported partly. And Messrs. Eiji Kohama and Masaaki Nagasawa, Yukitomo Tsubokawa, Kazuma Harada and Hideki Narumi helped in preparing and printing this manuscript. The author wishes to express his appreciate of their support. Especially, the author would like to express a deep sense of his gratitude to Dr. Kenichi Maeda for his giving valuable advice and discussions for the present study.

References

References

1) Cundall, P. A. (1971): "A computer model for simulation progressive, large-sca;e movement in block rock systems," Proc. of International Symposium on rock mechanics, Nancy 2, No. 8.

2) Cundall, P. A. and Strack, O. D. L. (1979): "A discrete numerical model for granular assemblies," Geotechnique, Vol. 29, No. 1, pp. 47-65.

3) EPS Construction method Development Organization (EDO) (1993): "Expanded Poly-Styrole construction method," Riko-Tosho Co. Ltd., (in Japanese).

4) EPS Construction method Development Organization (EDO) (1990): "A mannual for mechanical properties of EPS material," EDO, (in Japanese).

5) Goto, K., Mochishita, T., Matsumura, A. and Mukai, I. (1989): "Seismic Stability of a Bank with Light-Weight Fills," Tsuchi-to-Kiso, Vol. 37, No. 2, pp. 37-42, (in Japanese).

6) Kishino, Y. (1989): "Investigation of quasi-static behavior of granular materials with a new simulation method," proc. of JSCE, No. 406, pp. 97-196, (in Japanese).

7) Miura, K. (1991): "On the Analytical Condition in DEM for Granular Materials," Proc. of 26 th annual meeting of JGS, pp. 513-516, (in Japanease).

8) Miura, K., Ueno, K. and Toki, S. (1991): "Simulation of cyclic mobility by DEM," Proc. of the 7th International Conference of Computer Method and Advances in Geomechanics, pp. 839-844.

9) Murata, O., Yasuda, Y., Tateyama, M. and Kikuchi, T. (1989): "Study on the cyclic loading test and the resonant test of the test embankment made by using EPS on the soft ground," Proc. of the 24th annual meeting of JGS, pp.53-56, (in Japanese).

10) Noto, S., Nishikawa, J., Matsuda, Y. and Miura, K. (1992): "Model Tests on Earth Pressure Reduction Using EPS for Structures Under Roads'" Proc. of the 27th annual meeting of JGS, pp. 2503-2506, (in Japanese).

11) Reserch Institute of Public Works (1991): "Study on the earthquake proof of EPS fill'", Data of RIPW, No. 2946, (in Japanese).

12) Takahara, T. (1994): "A Study on the applicability of Distinct Element Method to the analysis of EPS block fill," master thesis, hokkaido

University, (in Japanese).

13) Takahara, T. and Miura, K. (1994): "Experimental and Analytical Study on the mechanical Characteristics of EPS fill," proc. of the Second Young Asian Geotechnical Engineers Conference, pp. 57-66.

14) Takahara, T., Miura, K. and Mastuda, Y. (1995): "Model Test and Numerical Analysis of Mechanical Behavior of EPS Embankment," Proc. of the 40 th JGS Symposium, pp. 207-213, (in Japanese).

15) Takahara, T., Miura, K. and Kita, T. (1995): "An Analysis of Mechanical behavior of EPS Embankment subjected to a Differntial Settlement," Proc. of the 40th JGS Symposium, pp. 199-206, (in Japanese).

16) Takahara, T. and Miura, K. (1996): "Analytical and Experimental Study on Load Propagation Characteristics of EPS Fill," Proc. of the Third Asian-Pacific Conference on Computational Mechanics, Vol. 2, pp. 1189-1194.

17) Tamura, J., Konagai, K., Unami, K. and Fukuzumi, R. (1989): "Study on the Dynamic Properties of EPS Block Structure （発泡スチロール（ＥＰＳ）ブロック構造体の動特性に関する基本的研究）," Proc. of the 44th annual meeting of JSCE, pp. 952-953, (in Japanese).

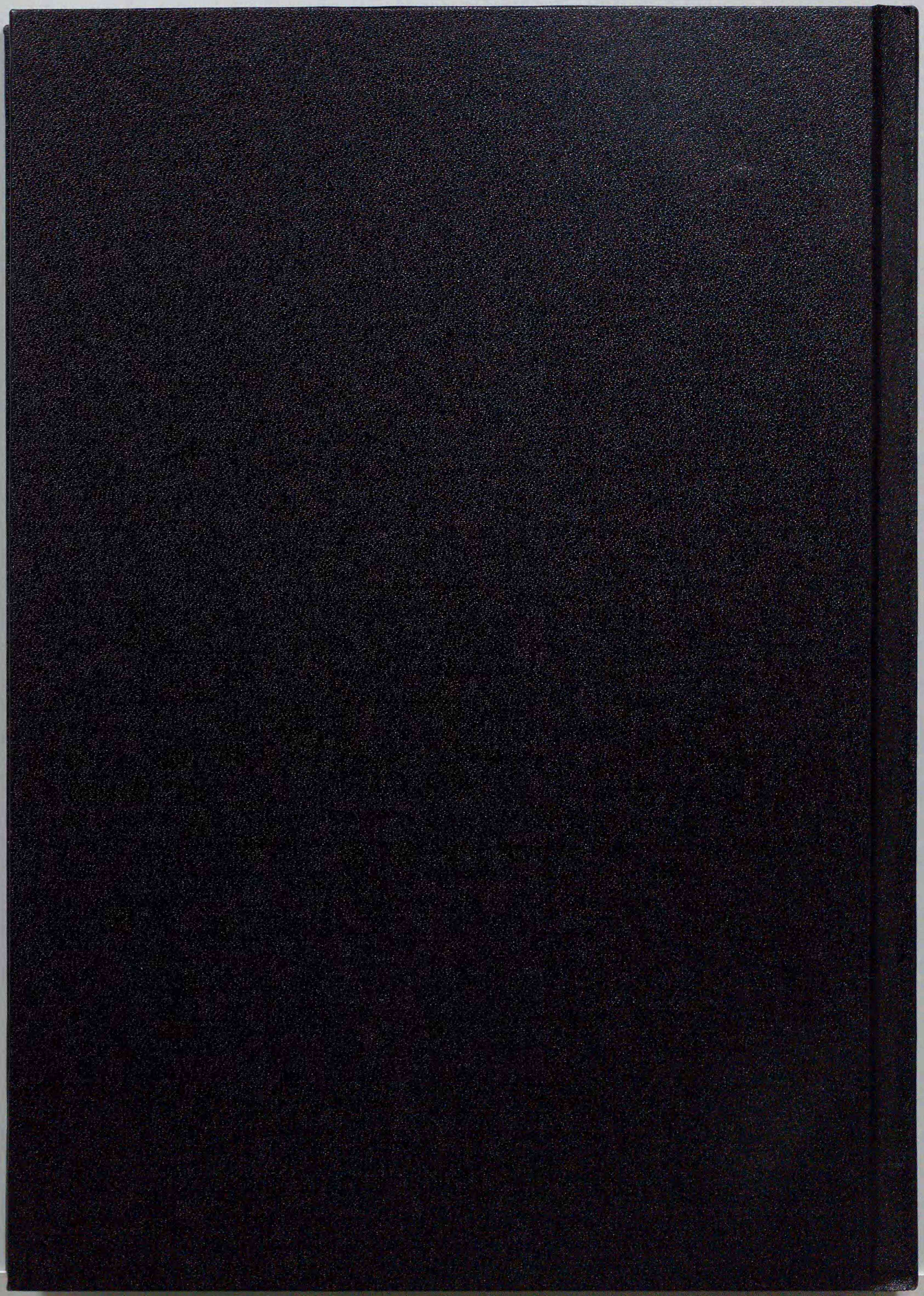

inches 1 2 3 4 5 6 7 8

cm 1 2 3 4 5 6 7 8 9 10 11 12 13 14 15 16 17 18 19

Kodak Color Control Patches

Blue Cyan Green Yellow Red Magenta White 3/Color Black

Kodak Gray Scale

C Y M

A 1 2 3 4 5 6 **M** 8 9 10 11 12 13 14 15 **B** 17 18 19